

THE UNIVERSITY OF CALGARY

Synchronous Machines Parameter Estimation Using Artificial Neural Networks

by

Mariano Calvo

A DISSERTATION

**SUBMITTED TO THE FACULTY OF GRADUATE STUDIES
IN PARTIAL FULFILLMENT OF THE REQUIREMENTS FOR THE
DEGREE OF DOCTOR OF PHILOSOPHY**

DEPARTMENT OF ELECTRICAL AND COMPUTER ENGINEERING

CALGARY, ALBERTA

APRIL, 2000

@ Mariano Calvo 2000



**National Library
of Canada**

**Acquisitions and
Bibliographic Services**

**395 Wellington Street
Ottawa ON K1A 0N4
Canada**

**Bibliothèque nationale
du Canada**

**Acquisitions et
services bibliographiques**

**395, rue Wellington
Ottawa ON K1A 0N4
Canada**

Your file Votre référence

Our file Notre référence

The author has granted a non-exclusive licence allowing the National Library of Canada to reproduce, loan, distribute or sell copies of this thesis in microform, paper or electronic formats.

The author retains ownership of the copyright in this thesis. Neither the thesis nor substantial extracts from it may be printed or otherwise reproduced without the author's permission.

L'auteur a accordé une licence non exclusive permettant à la Bibliothèque nationale du Canada de reproduire, prêter, distribuer ou vendre des copies de cette thèse sous la forme de microfiche/film, de reproduction sur papier ou sur format électronique.

L'auteur conserve la propriété du droit d'auteur qui protège cette thèse. Ni la thèse ni des extraits substantiels de celle-ci ne doivent être imprimés ou autrement reproduits sans son autorisation.

0-612-49485-3

Canada

ABSTRACT

Economic factors are constantly pushing the operation of power systems to their optimal capacity. For this to be possible, sophisticated models and accurate parameters of the electric components of the systems are required. This work presents an alternative approach that can be used to deal with the parameter estimation problem.

This thesis presents a new on-line based method to estimate the electric parameters of synchronous generators. The solution has been devised similar to that of solving a pattern recognition problem but in a manner which is an entirely new concept in the field.

The strategy is based on the following concept. A synchronous machine operating under different boundary conditions will have a unique response determined by its physical characteristics, which in mathematical terms are expressed by its electric parameters. Alternatively, given the behaviour of the synchronous generator, expressed in currents, voltages, and rotor position, it is possible to think of the existence of an inverse model that will be able to provide the parameters of the machine under consideration. This is a pattern classification problem.

The inverse model is obtained using a feedforward artificial neural network which has excellent properties as a pattern classifier. Artificial neural networks have been used in many areas of power systems, but this is the first time that they have been applied for parameter estimation purposes.

The proposed method has the capability to estimate all the electric parameters of a synchronous generator that govern its steady state and dynamic behaviour, including the saturation characteristics. The method has been extensively tested in a salient pole micro-alternator. On-line data from a round rotor generator has been used to successfully estimate the steady state characteristics of the synchronous machine and simulation studies have

confirmed that the proposed method can also be applied to estimate the dynamic characteristics of round rotor synchronous machines.

ACKNOWLEDGEMENTS

I would like to express my gratitude to my Supervisor, Dr. O.P. Malik, for having accepted me to pursue further academic studies, his guidance and encouragement through this project.

I would also like to thank Dr. O.P. Malik and The Department of Electrical And Computer Engineering of the University of Calgary for the partial financial support offered for this project.

I would like to thank Mr. Garwin Hancock, for his valuable help and assistance in developing the Data Acquisition System, and Mr. Patrick Walsh for his valuable technical help during the practical implementation of the tests.

I am also indebted to Professors A.O. Reda (UNLPAM, Arg.) and J. Feinstein (UNS Arg.) that through their academic attitude cultivated my desire to pursue further academic studies.

This work would not have been possible without the constant support from my parents and brother, to whom I will always be indebted.

To my Family:

Lara, Mariel, Martin, Manuel and Norma

who have shared the load of this work.

TABLE OF CONTENTS

APPROVAL PAGE	ii
ABSTRACT	iii
ACKNOWLEDGEMENTS	v
DEDICATION	vi
TABLE OF CONTENTS	vii
LIST OF TABLES	xiii
LIST OF FIGURES	xvi
LIST OF SYMBOLS	xix
LIST OF ABBREVIATIONS	xxii
CHAPTER 1	
PARAMETER ESTIMATION OF SYNCHRONOUS MACHINES	1
1.1 Introduction	1
1.2 The Parameter Estimation Problem	1
1.2.1 Accuracy of the Parameters	2
1.2.2 Consistency of the Parameters	5
1.2.3 Model Complexity Versus Accuracy of the Parameters	6
1.2.4 Economic Impact and Costs	6
1.3 Available Methods for Parameter Estimation	8
1.3.1 Slip Test	8
1.3.2 Short-Circuit Test	9
1.3.3 Load Rejection Tests	10
1.3.4 Frequency Response Tests	11
1.3.4.1 Standstill Frequency Response	11
1.3.4.2 On-line Frequency Response	13
1.3.5 Using the Reactance Operators	14
1.3.6 Analysis of Design Data	15
1.3.7 Other methods	15

1.4 Objectives	16
1.5 Thesis Contributions	17
1.6 Outline	18
CHAPTER 2	
SYNCHRONOUS MACHINE MODEL.....	20
2.1 Introduction.....	20
2.2 “a-b-c” Frame of Reference	20
2.3 “d-q-0” Frame of Reference	24
2.4 Operational and Standard Parameters.....	29
2.5 Saturation	33
2.6 Steady-State Analysis	39
2.6.1 Phasor Diagrams	39
2.6.2 Power Diagram	41
2.6.3 PQV Steady-State Solution.....	43
2.7 Transient-State Analysis	45
2.7.1 Integration of the Transient Equations.....	45
CHAPTER 3	
ARTIFICIAL NEURAL NETWORKS.....	47
3.1 Introduction.....	47
3.2 Model	48
3.2.1 Neuron Model	48
3.2.2 Artificial Neural Network Model	50
3.3 Learning Algorithms.....	52
3.3.1 Backpropagation	53
3.3.2 Conjugate Gradient Algorithms.....	55
3.3.3 Levenberg-Marquardt	56
3.4 Generalization	59
CHAPTER 4	
PROPOSED METHOD	64
4.1 Introduction.....	64

4.2 System Identification and Pattern Recognition	64
4.2.1 System Identification	64
4.2.2 Pattern Recognition.....	66
4.3 Parameter Estimation as a Pattern Recognition Problem	68
4.4 Proposed Method	70
4.4.1 Data Acquisition Stage	70
4.4.2 Learning Stage	72
4.4.3 Estimation Stage	76
4.4.4 Implementation	76
CHAPTER 5	
STEADY-STATE ANALYSIS	78
5.1 Introduction.....	78
5.2 Pattern Formation	78
5.3 Case Study: Salient Pole Micro-Generator.....	80
5.3.1 General Procedure and Pattern Formation.....	82
5.3.2 IfdPQ Case.....	88
5.3.3 IfPQ Case.....	94
5.4 Case Study: Round Rotor Generator	100
5.4.1 General Procedure and Pattern Formation.....	101
5.4.2 IfdPQ Case.....	104
5.4.3 IfPQ Case.....	109
5.5 Results Summary	114
CHAPTER 6	
TRANSIENT STATE ANALYSIS	115
6.1 Introduction.....	115
6.2 Boundary Conditions and Pattern Formation	115
6.2.1 Field Perturbations.....	115
6.2.2 System Perturbations	121
6.2.3 Pattern Formation	122
6.3 Data Acquisition System	122

6.4 Case Study: Salient Pole Micro-Generator	123
6.4.1 General Procedure and Pattern Formation	124
6.4.2 Estimation Results	129
6.5 Simulation Study: Round Rotor Generator.....	136
6.5.1 General Procedure and Pattern Formation.....	139
6.5.2 Estimation Results	141
6.6 Results Summary	144
CHAPTER 7	
CONCLUSIONS	145
7.1 Introduction.....	145
7.2 Conclusions.....	145
7.3 Future Work.....	149
REFERENCES	151
APPENDIX A	
STANDARD CHARACTERISTICS AND CIRCUIT PARAMETERS	161
A.1 Introduction.....	161
A.2 Exact Equivalence.....	161
A.2.1 Operational Equations of the SM.....	162
A.2.2 Transient and Subtransient Parameters.....	165
A.2.3 Circuit Parameters.....	166
A.2.3.1 Circuit Parameters Using The Short Circuit Current.....	170
A.2.3.2 Circuit Parameters Using The Field Resistance.....	171
A.2.4 Relationships Between Time Constants.....	173
A.2.4.1 Obtaining the Open Circuit Time Constants.....	173
A.2.4.2 Obtaining the Short Circuit Time Constants.....	174
A.3 Classical Approach	174
A.3.1 Standard Characteristics.....	175
A.3.2 Circuit Parameters.....	176
APPENDIX B	
CONSISTENCY CHECK OF THE STANDARD CHARACTERISTICS	177

B.1 Introduction	177
B.2 Data and Calculations	177
B.3 Consistency Check	187
B.4 Discussion	191
APPENDIX C	
PER UNIT SYSTEM	192
C.1 Introduction	192
C.2 Adopted Per Unit System	192
C.3 Normalized Field Magnitudes	193
APPENDIX D	
STEADY-STATE MEASUREMENTS	194
D.1 Introduction	194
D.2 Micro Alternator Characteristics	194
D.3 Operating Points	195
D.4 Open Circuit Characteristic	202
D.5 Armature and Field Resistances	203
APPENDIX E	
TURBO-GENERATOR STEADY-STATE DATA	204
E.1 Introduction	204
E.2 Turbo-Alternator Characteristics	204
E.3 Operating Points	205
E.4 Open Circuit Characteristic	208
APPENDIX F	
TRANSIENT STATE MEASUREMENTS	209
F.1 Introduction	209
F.2 Data Acquisition System	209
F.2.1 General Inputs/Outputs: CHA & CHB	210
F.2.2 External Interrupt Input Signal: CHC	211
F.3 Transient Measurements	214
F.3.1 General Setup	214

F.3.2 Measurements.....	215
--------------------------------	------------

LIST OF TABLES

Table 1-1: Manufacturer's and Adjusted Parameters for a 555 MVA Turbo-Alternator	2
Table 1-2: SSR Benchmark Results - Peak Values Comparison	5
Table 1-3: Definition of Generator Models of Varying Degrees of Complexity	7
Table 2-1: Fundamental Machine Parameters	29
Table 2-2: Standard Characteristics	32
Table 2-3: Phasor Definitions	40
Table 5-1: Typical SM Data	79
Table 5-2: Micro-Generator Ratings	81
Table 5-3: Training and Validation Points	82
Table 5-4: Root Set of Parameters and Ranges	83
Table 5-5: Boundary Conditions and Ranges	84
Table 5-6: Consideration of Noise	84
Table 5-7: Training Sets Characteristics	85
Table 5-8: ANNs Characteristics	85
Table 5-9: Training Parameters	86
Table 5-10: Best Performances Using VGroup1	90
Table 5-11: Best Performance Parameters Using VGroup1	90
Table 5-12: Performance Over VGroup2 with Parameters From VGroup1	90
Table 5-13: Best Performances Using VGroup2	92
Table 5-14: Best Performance Parameters Using VGroup2	92
Table 5-15: Best Performances Using VGroup1	95
Table 5-16: Best Performance Parameters Using VGroup1	96
Table 5-17: Performance Over VGroup2 Using Parameters From VGroup1	96
Table 5-18: Best Performances Using VGroup2	98
Table 5-19: Best Performance Parameters Using VGroup2	98
Table 5-20: Turbogenerator Ratings	100
Table 5-21: Training and Validation Points	101

Table 5-22: Root Set of Parameters and Ranges	102
Table 5-23: Boundary Conditions and Ranges	102
Table 5-24: Consideration of Noise	103
Table 5-25: Training Sets Characteristics	103
Table 5-26: ANNs Characteristics	103
Table 5-27: Best Performances Using VGroup1	106
Table 5-28: Best Performance Parameters Using VGroup1	106
Table 5-29: Performance Over VGroup2 with Parameters From VGroup1	106
Table 5-30: Best Performances Using VGroup2	107
Table 5-31: Best Performance Parameters Using VGroup2	108
Table 5-32: Best Performances Using VGroup1	110
Table 5-33: Best Performance Parameters Using VGroup1	111
Table 5-34: Performance Over VGroup2 Using Parameters From VGroup1	111
Table 5-35: Best Performances Using VGroup2	112
Table 5-36: Best Performance Parameters Using VGroup2	113
Table 6-1: Variations in the Transient and Subtransient Parameters	119
Table 6-2: Steady-State Parameters and Measurements	123
Table 6-3: Training and Validation Points	124
Table 6-4: Transient Parameters Range	125
Table 6-5: Training Set Characteristics	125
Table 6-6: Consideration of Noise	126
Table 6-7: ANNs Characteristics	126
Table 6-8: Training Parameters	127
Table 6-9: Best Performances	130
Table 6-10: Best Performance Parameters	130
Table 6-11: Performances Over VGroup	131
Table 6-12: Steady-State Parameters and Measurements	137
Table 6-13: Transient State Parameters of the Actual SM	137
Table 6-14: Training Group	139
Table 6-15: Transient Parameters Range	139

Table 6-16: Training Set Characteristics	140
Table 6-17: Consideration of Noise	140
Table 6-18: ANNs Characteristics	141
Table 6-19: Best Performances	142
Table 6-20: Best Performance Parameters	142
Table B-1: Machine Data and Calculations - (a)	180
Table B-2: Machine Data and Calculations - (b)	182
Table B-3: Machine Data and Calculations - (c)	184
Table B-4: Machine Data and Calculations - (d)	186
Table B-5: Consistency Check with 10% Margin of Error	189
Table B-6: Consistency Check Summary with 10% Margin of Error	190
Table B-7: Consistency Check Summary with 100% Margin of Error	190
Table C-1: Base Values	192
Table D-1: Micro-Alternator Ratings	194
Table D-2: Manufacturer's Data	195
Table D-3: Steady-State Operating Points	197
Table D-4: Open Circuit Measurements	202
Table D-5: Armature and Field Resistances	203
Table E-1: Turbo-Alternator Ratings	204
Table E-2: Manufacturer's Data	205
Table E-3: Steady-State Operating Points	205
Table F-1: Transient Measurements	216

LIST OF FIGURES

Figure 1-1: Response Curves for Transient Case 1-T[6]	4
Figure 2-1: "a-b-c" Model of the Synchronous Machine	21
Figure 2-2: "d-q-0" model of the synchronous machine	25
Figure 2-3: Direct axis equivalent circuit	27
Figure 2-4: Quadrature axis equivalent circuit	28
Figure 2-5: Saturation Effects at a Given Operating Point	34
Figure 2-6: Typical Saturation Curves	36
Figure 2-7: Mutual Inductance Error	36
Figure 2-8: New Saturation Function	37
Figure 2-9: Phasor Diagram of a Salient Pole Machine	40
Figure 2-10: Extended Phasor Diagram	41
Figure 2-11: Operating Chart of a Synchronous Generator	42
Figure 3-1: Schematic Drawings of a Neuron and the ANN Neuron Model	49
Figure 3-2: Structure of a Feedforward ANN	51
Figure 3-3: Rule Extraction and Generalization	60
Figure 3-4: Good Fit and Overfitting of Noisy Data	62
Figure 3-5: Cross-validation	63
Figure 4-1: System Identification Steps	65
Figure 4-2: Steps Involved in the Pattern Recognition Process	66
Figure 4-3: Direct Problem	68
Figure 4-4: Inverse Problem	69
Figure 4-5: Stages of the Proposed Estimation Method	71
Figure 5-1: Direct Axis Saturation (1-K _{sd})	79
Figure 5-2: Quadrature Axis Saturation (1-K _{sq})	80
Figure 5-3: Operating Points	81
Figure 5-4: Field Current Error for Try 3 Using VGroup1	89
Figure 5-5: Load Angle Error for Try 3 Using Vgroup1	89

Figure 5-6: Errors for P~0.66 pu Using VGroup1	91
Figure 5-7: Errors for P~0.87 pu Using VGroup1	91
Figure 5-8: Errors for P~0.66 pu Using VGroup2	93
Figure 5-9: Errors for P~0.87 pu Using VGroup2	93
Figure 5-10: Field Current Error for Try 1 Using VGroup1	95
Figure 5-11: Errors for P~0.66 pu Using VGroup1	97
Figure 5-12: Errors for P~0.87 pu Using VGroup1	97
Figure 5-13: Errors for P~0.66.pu Using VGroup2	99
Figure 5-14: Errors for P~0.87 pu Using VGroup2	99
Figure 5-15: Operating Points	100
Figure 5-16: Field Current Error for Try 4 Using VGroup1	105
Figure 5-17: Load Angle Error for Try 4 Using VGroup1	105
Figure 5-18: Errors Using VGroup1	107
Figure 5-19: Errors Using VGroup2	108
Figure 5-20: Field Current Error for Try 4 Using VGroup1	110
Figure 5-21: Errors Using VGroup1	112
Figure 5-22: Errors Using VGroup2	113
Figure 6-1: Direct Axis Currents	120
Figure 6-2: Quadrature Axis Currents	120
Figure 6-3: Estimated and Measured Currents Using the TGroup	132
Figure 6-4: Errors in the Currents Using the TGroup	133
Figure 6-5: Estimated and Measured Currents Using the VGroup	134
Figure 6-6: Errors in the Currents Using the VGroup	135
Figure 6-7: Simulation Circuit Schematic	136
Figure 6-8: LDIN10 Response	138
Figure 6-9: Time Varying Errors for Set 4	143
Figure A-1: Generic Equivalent Circuit	162
Figure A-2: Equivalent Circuit with Embedded Leakage Reactance	167
Figure A-3: Equivalent Circuit without the Mutual Inductance L12.	169
Figure A-4: Equivalent Circuits with Embedded and External Inductance L12	169

Figure D-1: Setup for the Steady-State Measurements196

Figure F-1: DAS Schematic Diagram210

Figure F-2: DAS User’s Guide212

Figure F-3: Setup for the Transient State Measurements215

Figure F-4: LDIN10 Measurements217

Figure F-5: LDIN67 Measurements218

LIST OF SYMBOLS

r_a	Armature resistance
l_a	Armature leakage inductance
L_{md}	Direct-axis magnetizing inductance
r_{fd}	Field resistance
l_{fd}	Field leakage inductance
r_{2d}	Direct axis damper resistance
l_{2d}	Direct axis damper leakage inductance
L_{f2d}	Direct axis field and damper winding leakage inductance
L_{mq}	Quadrature axis magnetizing inductance
r_{1q}	Quadrature axis damper resistance
l_{1q}	Quadrature axis damper leakage inductance
r_{2q}	Quadrature axis damper resistance
l_{2q}	Quadrature axis damper leakage inductance
L_d	Direct axis synchronous inductance
L_d'	Direct axis transient inductance
L_d''	Direct axis subtransient inductance
L_q	Quadrature axis synchronous inductance
L_q'	Quadrature axis transient inductance
L_q''	Quadrature axis subtransient inductance
T_{do}'	Direct axis transient open-circuit time constant
T_d'	Direct axis transient short-circuit time constant
T_{do}''	Direct axis subtransient open-circuit time constant

T_d''	Direct axis subtransient short-circuit time constant
T_{qo}'	Quadrature axis transient open-circuit time constant
T_q'	Quadrature axis transient short-circuit time constant
T_{qo}''	Quadrature axis subtransient open-circuit time constant
T_{qo}'''	Quadrature axis subtransient short-circuit time constant
λ	Flux linkage
p	d/dt operator or frequency domain of the Laplace transform
$L_d(p)$	Direct axis operational inductance
$L_q(p)$	Quadrature axis operational inductance
$G(p)$	Stator to field transfer function
K_{sd}, K_{sq}	Direct and quadrature axis saturation factors
S_d, S_q	Direct and quadrature axis saturation functions
$S_{1d}, S_{2d}, S_{1q}, S_{2q}$	Magnitudes of the saturation functions for an open circuit voltage of 1.0 and 1.2 pu, respectively
A_d, B_d, V_{od}, V_{zd}	Direct and quadrature axis saturation constants used to define the saturation functions
A_q, B_q, V_{oq}, V_{zq}	
S	Complex power
P	Active power
Q	Reactive power
V, I	Armature rms voltage and current
I_{fno}	Field current that in absence of saturation would produce a rated open circuit terminal voltage
δ	Load angle
ϕ	Power factor angle
η	Learning rate

α	Momentum parameter
c_i	Increasing learning rate factor
c_d	Decreasing learning rate factor

LIST OF ABBREVIATIONS

SM	Synchronous machine
SMs	Synchronous machines
SSR	Subsynchronous resonance
ANN	Artificial neural network
ANNs	Artificial neural networks
<i>d</i>	Direct
<i>q</i>	Quadrature
pu	Per-unit
ac	Alternating current
rms	Effective or root-mean-square value
SSFR	Standstill frequency response
OLFR	On-line frequency response
EMF	Electromotive force
TGroup	Training group
VGroup	Validation group
BC	Boundary condition
BCs	Boundary conditions
PQV	Boundary condition specified by the active and reactive power delivered by the synchronous machine and the terminal voltage
Mean	Mean value
StD	Standard deviation
Max	Maximum value

Perf	Performance index
PerfI	Field current performance index
Perf δ	Load angle performance index

CHAPTER 1

PARAMETER ESTIMATION OF SYNCHRONOUS MACHINES

1.1 Introduction

Parameter estimation has drawn the attention of the research community for many years and, from an engineering perspective, the topic can be considered far from over. In this chapter the question of why it is still necessary to perform tests on the actual synchronous machines (SMs) in order to obtain their parameters is discussed first. In the rest of the chapter, an overview of the methods available for parameter estimation is given, and the problems and advantages of each method are discussed. The focus is on the Standard ANSI/IEEE 115 [1].

1.2 The Parameter Estimation Problem

In this section some of the problems associated with parameter estimation of synchronous generators are discussed. They can be summarized as:

- Data that does not correspond to the physical machine.
- Consistency of the data.
- Systems analysis impact.
- Economic impact.

- Accuracy of data versus models.
- Costs associated with the measurements.

1.2.1 Accuracy of the Parameters

A comparison of the measured or adjusted parameters obtained using *standstill frequency response* tests with the data offered by the manufacturer for a 555 MVA turbo-generator unit is given in Table 1-1[2]. It can be seen that huge differences in the values of the parameters can be expected for any generating unit for which the parameters have not been adjusted.

Table 1-1: Manufacturer's and Adjusted Parameters for a 555 MVA Turbo-Alternator			
Constants	Manufacturer	Adjusted	Error(%)
L_d	1.970	1.810	8.840
L_d'	0.270	0.300	10.000
L_d''	0.175	0.217	19.355
L_q	1.867	1.760	6.080
L_q'	0.473	0.610	22.459
L_q''	0.213	0.254	16.142
l_a	0.160	0.160	0.000
T_{do}'	4.300	7.800	44.872
T_{do}''	0.031	0.022	40.909
T_{qo}'	0.560	0.900	37.778
T_{qo}''	0.061	0.074	17.568

An interesting point that follows is to analyse the effect that these errors can have on the actual behaviour of a synchronous generator. A numerical example can illustrate the problem.

The phenomenon of *subsynchronous resonance* (SSR) on alternating current power systems was first reported in the literature in 1937 [3] as strictly an electrical phenomenon. It was not until the early seventies, when two shaft failures occurred at the Mohave Generating Station in Southern Nevada, that the theory of interaction between a series compensated transmission system in electrical resonance, and a turbine-generator mechanical system in torsional mechanical resonance, was developed [4,5].

In order to be able to compare the results obtained using different techniques and models, the IEEE SSR Task Force developed a standard test case for SSR [6]. The plots of Figure 1-1 show the results of using the two sets of parameters in the first SSR benchmark model. The solid and dashed curves represent the responses obtained with the adjusted and manufacturer's parameters, respectively. Plots (a) and (b) show the voltage of the capacitor used to compensate the transmission line and the instantaneous current of the SM, both for phase 'A'. Plot (c) is the electrical torque and plots (d) and (e) are the mechanical shaft torques between the low pressure masses (LPA-LPB) and between the field and exciter masses. The curves for each of the variables are substantially different and the adjusted parameters show a much better response for this specific case. However, the opposite could be true as well. The attention should be focused on the uncertainty that inaccurate electric parameters can introduce in the results of studies where interactions with mechanical oscillations are involved.

A comparison of the peak values, as given in Table 1-2, shows that these kinds of discrepancies are unacceptable because they could hide potential damage to the turbine generator shaft or cause reduction of its life expectancy due to torsional fatigue. From a systems perspective, the overall stability can be seriously affected. This is also true out of the realm of the SSR problem [2].

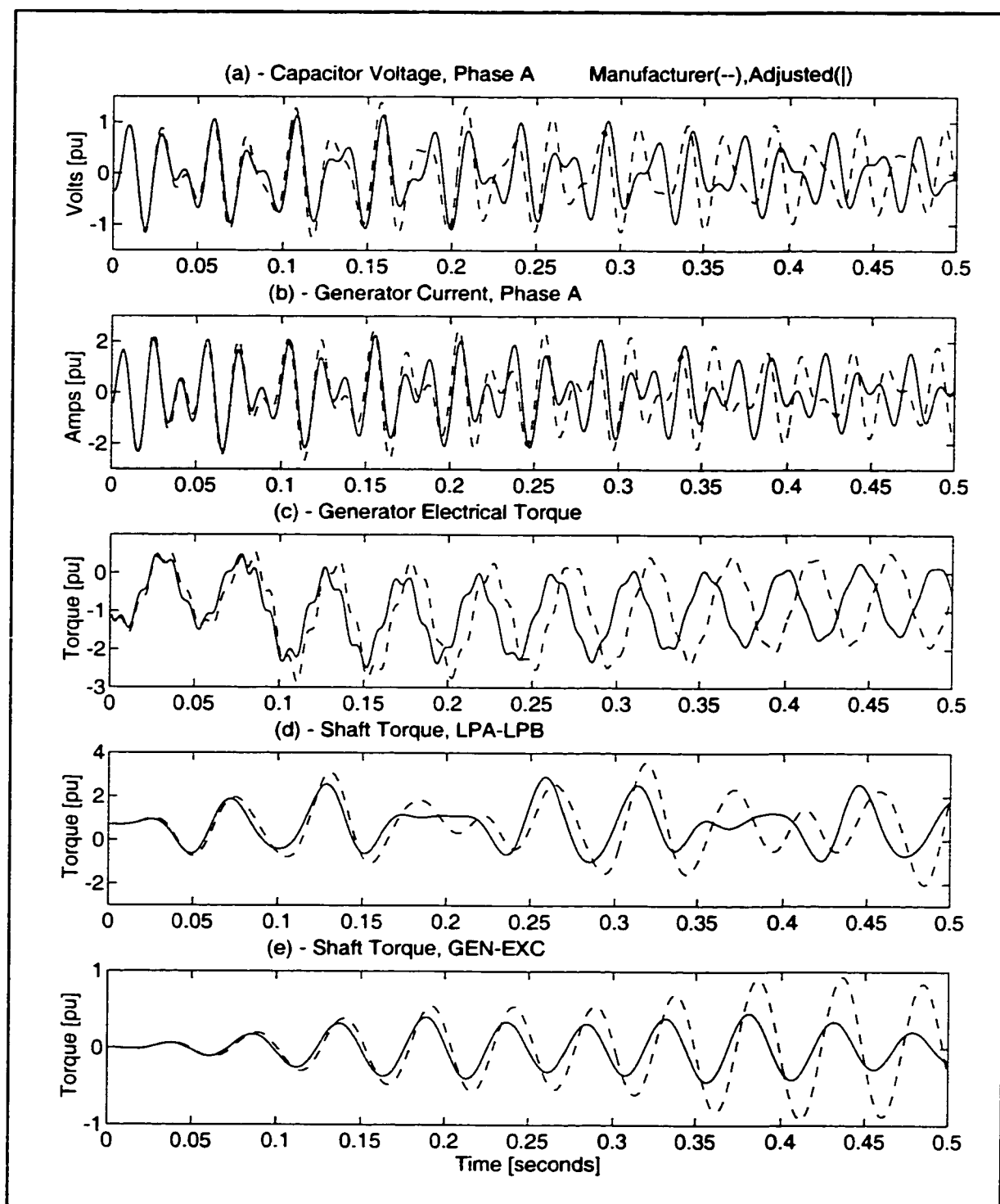


Figure 1-1: Response Curves for Transient Case 1-T[6]

Table 1-2: SSR Benchmark Results - Peak Values Comparison

Variable	Manufacturer	Adjusted	Error (%)
Capacitor Voltage, Phase A	1.40	1.14	22.37
Generator Current, Phase A	2.67	2.35	13.77
Generator Electrical Torque	2.87	2.49	15.45
Shaft Torque, LPA-LPB	3.58	2.91	23.24
Shaft Torque, GEN-EXC	0.93	0.46	103.69

1.2.2 Consistency of the Parameters

It is not necessary to perform actual measurements to put in doubt the accuracy of a given set of SM parameters. Appendix A presents an accurate transformation between circuit and standard parameters and this relationships are used in Appendix B to develop a consistency test. The foundation for this study is very simple: the data provided by the manufacturer, to be correct, should be consistent with the relationships derived from the mathematical model. If this is not so, it cannot be expected that the model will offer a good representation of the actual physical device.

The studies presented in Appendix B are conducted using data obtained from manufacturers. In one of the results, it is shown that only 45.0% of the overall data, or 55.0% and 35.0% for the d and q axis respectively, can be considered consistent with the model. These results are impressive and provide evidence, once again, of the lack of reliability of the provided data.

1.2.3 Model Complexity Versus Accuracy of the Parameters

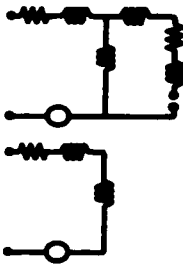
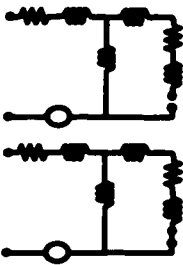
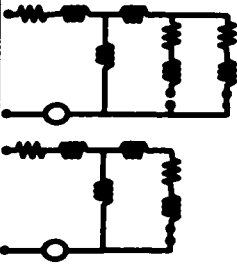
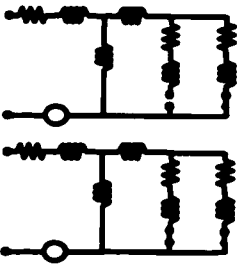
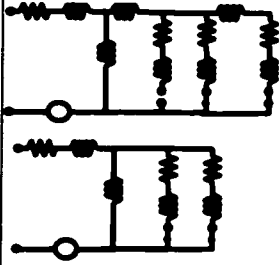
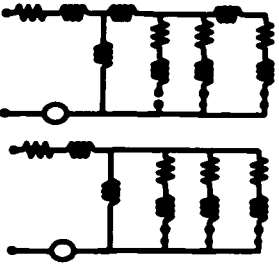
Over the years, the increase in *computing power* has made it possible to work with complex models. It is accepted, and intuitively expected, that with more accurate models better results will be obtained. Table 1-3 [7] shows the commonly accepted model for a synchronous machine with many of the possible variations of complexity according to how many damper windings are associated with each axis. According to this, it is expected that the best results will correspond to the model "3.3".

Surprisingly, studies conducted in the early seventies by the Northeast Power Coordinating Council [8] showed that, in general, in stability analysis it is more important to use accurate machine data than to use more elaborate machine models. In some of the studies, the less sophisticated models were even able to outperform the more accurate ones when both were supplied with inaccurate parameters.

1.2.4 Economic Impact and Costs

Having good parameters to complement complex models of the synchronous machines can have other benefits. In developing and applying more detailed saturation models [9,10], it was found that an economic benefit could be obtained from the increased capability to transmit power generated at a lower cost site. Obviously, in a deregulated environment, studies like this one can be extremely important.

The importance of having reliable data is related to the importance of the generator and the negative impact that bad data could have on the associated systems. Although some advances have been made on parameter estimation using constructive detailed information of the machines [11,12], the uncertainty associated with the parameters forces the electric utilities to perform actual tests on the generators when accurate data is required.

Table 1-3: Definition of Generator Models of Varying Degrees of Complexity				
Q Axis D Axis	No Equivalent Damper Circuit	One Equivalent Damper Circuit	Two Equivalent Damper Circuits	Three Equivalent Damper Circuits
Constant Flux Linkage	Model 0.0			
Field Circuit Only	Model 1.0 	Model 1.1 		
Field Circuit Plus One Equivalent Damper Winding		Model 2.1 	Model 2.2 	
Field Circuit Plus Two Equivalent Damper Winding			Model 3.2 	Model 3.3 

Performing tests on generators has its own related problems. The specialized equipment involved, the engineering costs of obtaining technical specialists and in some cases, the cost of having a generating unit not generating power, are some of the problems that

highlight the economic impact of performing tests on synchronous generators. It is not a surprise then that even today there is abundant work being done on this topic [1,13-15], almost three quarters of a century after the first publications in the area appeared [16,17].

1.3 Available Methods for Parameter Estimation

This section deals with the parameter estimation methods most widely used as well as some of the methods that have received considerable attention in the research community. The mathematical model of the synchronous generator is developed in the next chapter where all the background necessary to understand the specific parameters, that are referred to here, is given.

1.3.1 Slip Test

This test is part of the ANSI/IEEE Std 115-1995 [1]. The slip test is conducted by driving the rotor at a speed slightly different from the synchronous speed with the field open-circuited and the armature energized by a three-phase, rated frequency source. Steady-state analysis is valid because the slip is very small. It can be found [17] that the magnitude of the armature current is modulated between a maximum and a minimum value proportional to the inverse of X_q and X_d , respectively. Because of the limitations of the source, the applied voltage also varies inversely to the amount of the current being drawn from the voltage source. Then, X_d and X_q are finally obtained as:

$$X_d = \frac{V_{\max}}{I_{\min}} \quad ; \quad X_q = \frac{V_{\min}}{I_{\max}} \quad (1-1)$$

Although conceptually very simple, the implementation of this test is by no means trivial. For an accurate determination of the quadrature-axis synchronous reactance, it is difficult to maintain the speed constant when the slip is sufficiently small because the effects of the salient poles and the currents induced in the amortisseur windings produce a pulsating torque. Also, the induced voltage in the open field circuit may reach dangerous values when the slip is large.

1.3.2 Short-Circuit Test

The short-circuit test is probably the most well known test for parameter estimation. Its importance is not only due to the number of parameters that can be determined but also because it provides the theoretical background for the actual definitions of the standard parameters.

This test is based on equation (A-16) rewritten here for convenience and adapted for the direct axis:

$$\frac{1}{L_d(p)} = \frac{1}{L_d} + \left(\frac{1}{L_d} - \frac{1}{\bar{L}_d} \right) \frac{T_d' p}{(1 + T_d' p)} + \left(\frac{1}{\bar{L}_d} - \frac{1}{L_d} \right) \frac{T_d'' p}{(1 + T_d'' p)} \quad (1-2)$$

When a synchronous machine under no load is subjected to a sudden three-phase short-circuit, and assuming that the speed remains constant with a value of 1.0 per unit during the test, the armature current, in per unit, will be given by an expression of the form:

$$I(t) = E_o \left\{ \frac{1}{L_d} + \left(\frac{1}{L_d} - \frac{1}{\bar{L}_d} \right) e^{\frac{-t}{T_d'}} + \left(\frac{1}{\bar{L}_d} - \frac{1}{L_d} \right) e^{\frac{-t}{T_d''}} \right\} \quad (1-3)$$

where $I(t)$ is the ac rms short-circuit current, E_o is the ac rms voltage before the short-circuit, and t is the time in seconds measured from the instant of short circuit.

Because of the exponential terms involved, a graphical analysis allows the identification of both exponential terms and measurement of the direct axis transient and sub-transient short-circuit time constants. In a similar way, the direct axis transient and sub-transient reactances can be identified. Once the steady-state is reached, the direct axis reactance X_d can also be measured.

The above test also gives information of the direct axis open-circuit transient and sub-transient time constants [18,19] (see Appendix A) through the relationships

$$T'_{do} = \frac{L_d}{L'_d} T'_d \quad ; \quad T^-_{do} = \frac{L_d}{L^-_d} T^-_d \quad (1-4)$$

Improved methods of utilizing results from sudden short-circuit tests to determine more accurate d-axis parameters have been developed [20-22]. The most important feature of these methods is the utilization of rotor current measurements during the short-circuit tests to identify the field-circuit characteristics more accurately.

The main disadvantage associated with this test is the severe mechanical and electrical stress that is imposed on the machine. Although similar parameters are defined for the quadrature axis, this test does not provide any information about those parameters.

1.3.3 Load Rejection Tests

These tests are similar in approach to the sudden short-circuit tests in that the time responses of the machine variables following a sudden disturbance are measured to identify machine characteristics [23,24]. After certain initial conditions are set up, the response of

the machine to a load rejection is recorded. The initial conditions determine the axis on which the parameters are derived. In this way, with operating conditions arranged in such a way that the current is flowing only in the direct axis ($i_q=0$), the unit is tripped and the resulting terminal voltage and field current decay are used to extract parameters for the d-axis model. A similar test is performed with current flowing only in the quadrature axis ($i_d=0$) to obtain q-axis data.

These tests provide data for the direct and quadrature axes. However, they are somewhat difficult to conduct. For most machines, it is difficult or impossible to attain unsaturated conditions which certainly complicates the testing and the analysis of results [25].

1.3.4 Frequency Response Tests

Frequency response methods represent the state of the art in parameter estimation. Over the years, extensive work conducted by a wide range of research groups has given these tests a solid basis for their practical implementation that has even displaced the most conventional "short-circuit" approach.

1.3.4.1 Standstill Frequency Response

It is widely accepted that present day stability studies require both direct and quadrature axis synchronous machine characteristics. Alternative procedures that provide both direct and quadrature axis stability parameters are specified in the IEEE Std 115 [1], called the *Standstill Frequency Response* (SSFR) tests. Through these procedures it is possible to obtain the rates of change of stator or field quantities over a wide range of frequencies.

The theory behind these tests is given by equations (A-11) and (A-12) derived in Appendix A, rewritten here for each axis:

$$\begin{aligned}\Psi_d &= L_d(p)i_d + G(p)v_f \\ \Psi_q &= L_q(p)i_q\end{aligned}\tag{1-5}$$

Applying different boundary conditions, it is straightforward to obtain the following quantities.

- $Z_d(p)$ - The synchronous machine direct axis operational impedance. With the rotor short-circuited and aligned with the phases used to conduct the experiment, it is possible to obtain

$$Z_d(p) = \left. \frac{v_d}{i_d} \right|_{v_f = 0}\tag{1-6}$$

- $G(p)$ - The armature to field transfer function. $G(p)$ can be measured in two ways as shown in (1-7). The first expression can easily be derived from (1-5). The second one makes usage of the fact that the factor $G(p)$ is what relates the field current and direct axis current in expression (A-7).

$$G(p) = \left. \frac{v_d}{pv_f} \right|_{i_d = 0} \quad ; \quad pG(p) = \left. \frac{i_f}{i_d} \right|_{v_f = 0}\tag{1-7}$$

- $Z_q(p)$ -The synchronous machine quadrature axis operational impedance. With the rotor in quadrature to the phases used to conduct the experiment, it is possible to obtain:

$$Z_q(p) = \frac{v_q}{i_q}\tag{1-8}$$

All tests are conducted with the unit at rest (rotor stationary) and disconnected from the system, and with the stator excited by a low level source ($\pm 60\text{A}$, $\pm 20\text{V}$). The tests are performed over a range of frequencies that varies from a minimum at least one order of magnitude less than that corresponding to the transient open-circuit time constant of the generator, to a maximum that should be somewhere between two or three times the rated frequency of the generator.

Expressions (1-6) to (1-8) allow one to plot $L_d(p)$, $G(p)$ and $L_q(p)$ from where the polynomial representation of each value, as it is explicit in expressions (A-11) and (A-13) of Appendix A, can be found with a curve fitting process. This is an excellent feature of the method because it allows a very detailed representation of each axis just by adding more poles and zeroes to the model. This is equivalent to including more damping windings in the model [1]. On the other hand, this can be a relevant problem by itself because of the variety of different models that can be fitted according to how many mutual effects are considered. This has generated extensive discussions on the physical meaning of the models themselves [26,27].

There can be problems related to the lack of consideration of rotational effects because the damper windings may not form a good connection at standstill, and the extent to which rotation causes the slot wedges to form a low impedance path to the rotor is largely unknown [25,28].

This technique has been extensively tested [29-31]. First introduced as a *trial use* standard of the IEEE in 1983 [32], it was incorporated in the IEEE Std.115 in 1995 [1].

1.3.4.2 On-line Frequency Response

The *On-line Frequency Response* (OLFR) tests are a variation that tend to overcome the problems associated with the SSFR tests. Here, the machine is tested under the

same conditions as those under which the model is expected to perform, although over a restricted operating range. The machine can be operated near rated or at reduced load. The frequency response is obtained by applying sinusoidal signals to the excitation and measuring the steady-state changes in field voltage and current, rotor speed, terminal voltage and active and reactive power.

In this approach, the on-line frequency response of the power systems is first computed using estimated values for the parameters of the synchronous machine. Then, an iterative technique which attempts to minimize the differences between measured and computed responses at specified frequencies by adjusting the parameters of the machine model is applied. The dynamic behaviour of the power system is simulated with different degrees of modelling, the representations varying in detail according to the importance of the specific elements and influence on the tests.

On the studies carried out [28,31,33], this technique proved to complement the results of the SSFR tests for generators with actual damper windings.

On the other hand, what makes this technique so distinctive is probably its main drawback. To perform a test of this type on an operating unit connected to the system is an extremely delicate topic [25]. Also, this technique involves the simulation of both the machine and the system to which it is attached and it is not clear how uncertainties derived from the power system side could affect the estimation process.

1.3.5 Using the Reactance Operators

This method uses a hybrid approach, combining SSFR tests with short-circuit tests [34]. SSFR characteristics are used to fit the reactance operators $X_d(p)$ and $X_q(p)$ defined by expression (B-13). Once this is done, an exact transformation is used to obtain the circuit

parameters [35], where the mutual inductances of the direct axis are adjusted using the measured value of the field current following a short-circuit test.

Although no results showing the performance of the parameters have been provided, it is clear that this approach is able to incorporate the best qualities of both the SSFR procedures and the more conventional short circuit test.

1.3.6 Analysis of Design Data

Improved generator models developed from design information is not a new area [36]. More recent work, applying finite elements analysis seems to be a promising field of work [37]. Extensive work applying this technique to obtain steady-state solutions [12], frequency response characteristics [11] and to derive saturation functions [9] from design data, has shown good agreement with measured results.

More work needs to be done though, in order to prove the consistency of the method to any particular design. Also, the significance of the rotational effects and the effect of disturbance amplitude on the model require additional investigation [25].

1.3.7 Other methods

The amount of work that has been done developing new methods or improving existing ones is vast. This makes very difficult, if not impossible, the task of trying to summarize many of the approaches without understating them or being unfair to their importance. The intention has been to follow to some extent the standards [1,7,19], present important literature in the area [31,37] or developments that, in the author's opinion, repre-

sent a landmark [31,35] in the evolution of parameter estimation field. However, this does not mean that other works [15,38-47] cannot be more effective or even provide much better results than the ones mentioned here.

1.4 Objectives

The following are the main objectives of this dissertation.

To present an original on-line approach for synchronous machines (SMs) parameter estimation. From the introduction, it is clear that there are many very well tested choices when referring to off-line methods for parameter estimation. The same assertion is not valid for the on-line counterpart. The reasons are both technical and practical. There is agreement that an on-line method that retrieves information of the machine working under normal operating conditions has all the components required to get the best possible parameters for that machine. So far though, just a few approaches in the area have shown their viability. Working on-line is a problem by itself because it will always face practical restrictions and innumerable concerns about the possibility of undesirable side effects. To overcome this barrier, the idea is to present a method that is both conceptually clean and as non-intrusive as it can be when referring to on-line methods. To achieve this, the goal is to reformulate the parameter estimation problem as a pattern recognition problem. The idea is to offer a versatile method that can be adapted to many of the practical restrictions that can arise in any on-line application.

To develop an original, practical and viable application of Artificial Neural Networks (ANNs). The objective is to explore the ANN ability to

recognize patterns from on-line data in order to extract the parameters of the synchronous machines.

1.5 Thesis Contributions

This thesis makes the following main contributions:

- A new on-line based method for SMs parameter estimation is presented, introducing the estimation problem as a pattern recognition problem.
- A new application of ANNs has been developed being the first time that ANNs have been applied to parameter estimation of SMs.

Other contributions are:

- It is shown that field perturbations are not effective to fully excite the dynamics of the SMs, hence they impose a strong limitation on any method for parameter estimation that is based on these disturbances.
- A consistency check of the standard characteristics to analyse the validity of the parameters offered by the manufacturer.
- A deductive approach that shows the equivalence of the standard characteristics and circuit parameters has been developed. The procedure has been extended to consider the equivalence between the parameters when the field resistance is known.
- The classic representation of saturation has been redefined to avoid conflicts with the linear parameters.

- A general purpose data acquisition system to be able to measure on-line instantaneous variables from the SM has been developed.

1.6 Outline

This work is organized in seven chapters and six appendices with the following structure.

The first chapter presents an overview of the problem and some of the methods currently available for parameter estimation. The chapter ends with the objectives of this work and is complemented by the development of a consistency check for the standard characteristics obtained from manufacturers in Appendix B.

The model of the synchronous machine is described in Chapter 2 following a classical and conceptual approach. Appendix C offers a note on the adopted per unit system. An accurate transformation between circuit and standard parameters is presented in Appendix A.

Presented in Chapter 3 are the basics of Artificial Neural Networks with the different learning methods that have been applied during the development of this work.

Chapter 4 describes and formally presents the theory behind the proposed method.

The new method for parameter estimation is applied to obtain the steady-state parameters and saturation factors of synchronous generators in Chapter 5. Appendix D and Appendix E have the measurements done on a micro-generator and the data obtained from a turbo-alternator used in the studies.

In Chapter 6 presents the application of the proposed method to obtain the parameters that govern the transient behaviour of the synchronous machine. Appendix G gives an

overview of the data acquisition system developed to measure the *on-line* data and corresponding measurements.

Conclusions and suggestions for further work are given in Chapter 7.

CHAPTER 2

SYNCHRONOUS MACHINE MODEL

2.1 Introduction

The purpose of this chapter is to introduce the most common and well known model of the synchronous machine. The idea is to define the basic framework over which the parameter estimation will take place. This is just a summary of the topic that will present all the required concepts and useful extensions used in the following chapters. For a more comprehensive understanding of the topic, there are many introductory [25,48-50] and advanced [18,51,52] references that can be consulted.

2.2 “a-b-c” Frame of Reference

Figure 2-1 shows the model of the synchronous machine most closely related to the actual physical device. The stator circuits consist of three armature windings carrying alternating currents. The rotor has a field winding on the *direct* (d) axis connected to a source of direct current and windings, one on the d axis and two on the *quadrature* (q) axis, that represent the effects of the actual damper windings or the eddy currents in the iron.

Depending upon the nature of the studies involved and the specific physical design, more amortisseur circuits can be added to the direct and/or the quadrature axes to obtain a more accurate representation of the machine.

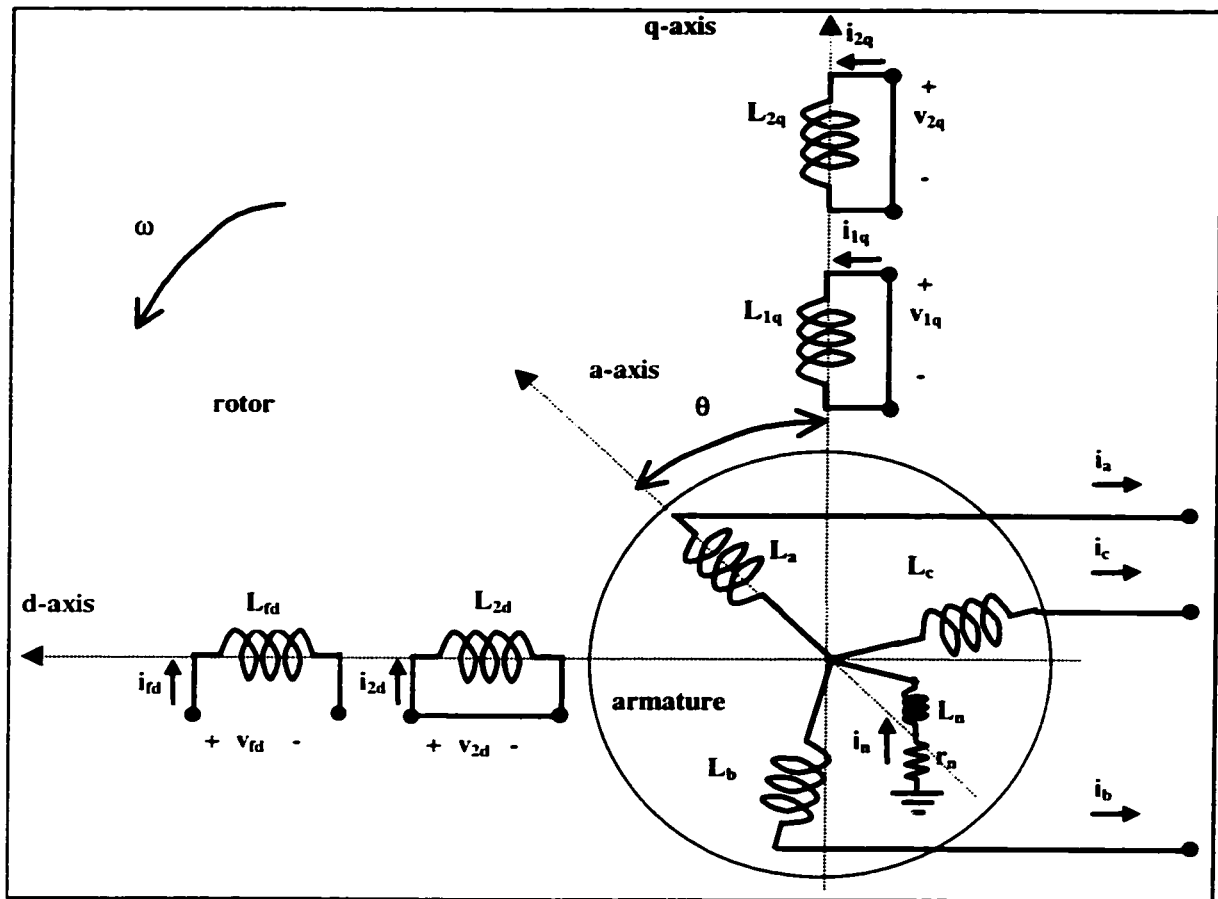


Figure 2-1: "a-b-c" Model of the Synchronous Machine

The assumptions behind this model are [25]:

- (a) The armature windings are sinusoidally distributed along the air-gap.
- (b) The stator slots cause no appreciable variation of the rotor circuit inductances with rotor position.
- (c) Magnetic hysteresis is negligible.
- (d) Magnetic saturation effects are neglected.

Assumption (d) is just for convenience in the analysis. Otherwise, one has to deal with non-linear coupled circuits. The effects are important and are discussed in section 2.5.

In a general form, the instantaneous terminal voltage v of any winding is given by a combination of the Ohm and Faraday's laws [52]

$$v = \pm ri \pm \frac{d\lambda}{dt} \quad (2-1)$$

where r is the winding resistance, λ its flux linkage, and i its current.

Then, the equations that relate the circuits of Figure 2-1 can be summarized in a matrix form as¹

$$\begin{bmatrix} v_a \\ v_b \\ v_c \\ \hline -v_{fd} \\ v_{2d}(=0) \\ v_{1q}(=0) \\ v_{2q}(=0) \end{bmatrix} = - \begin{bmatrix} r_a i_a \\ r_b i_b \\ r_c i_c \\ \hline r_{fd} i_{fd} \\ r_{2d} i_{2d} \\ r_{1q} i_{1q} \\ r_{2q} i_{2q} \end{bmatrix} - \frac{\partial}{\partial t} \begin{bmatrix} \lambda_a \\ \lambda_b \\ \lambda_c \\ \hline \lambda_{fd} \\ \lambda_{2d} \\ \lambda_{1q} \\ \lambda_{2q} \end{bmatrix} + \begin{bmatrix} \mathbf{V}_n \\ 0 \\ 0 \\ 0 \\ 0 \end{bmatrix} \quad (2-2)$$

where the *neutral* voltage is given by

$$\mathbf{V}_n = v_n \begin{bmatrix} 1 \\ 1 \\ 1 \end{bmatrix} = - (r_n + L_n p) \begin{bmatrix} 1 & 1 & 1 \\ 1 & 1 & 1 \\ 1 & 1 & 1 \end{bmatrix} \begin{bmatrix} i_a \\ i_b \\ i_c \end{bmatrix} \quad (2-3)$$

1. Throughout these developments and to avoid special considerations, all magnitudes and parameters are assumed to be in per-unit (pu) values. Refer to Appendix C for a note on the adopted per-unit system.

and the flux linkage equations for the seven circuits are

$$\begin{bmatrix} \lambda_a \\ \lambda_b \\ \lambda_c \\ \lambda_{fd} \\ \lambda_{2d} \\ \lambda_{1q} \\ \lambda_{2q} \end{bmatrix} = \begin{bmatrix} L_{aa} & L_{ab} & L_{ac} & L_{afd} & L_{a2d} & L_{a1q} & L_{a2q} \\ L_{ba} & L_{bb} & L_{bc} & L_{bfd} & L_{b2d} & L_{b1q} & L_{b2q} \\ L_{ca} & L_{cb} & L_{cc} & L_{cfd} & L_{c2d} & L_{c1q} & L_{c2q} \\ \hline L_{fda} & L_{fdb} & L_{fdc} & L_{fdfd} & L_{fd2d} & 0 & 0 \\ L_{2da} & L_{2db} & L_{2dc} & L_{2dfd} & L_{2d2d} & 0 & 0 \\ L_{1qa} & L_{1qb} & L_{1qc} & 0 & 0 & L_{1q1q} & L_{1q2q} \\ L_{2qa} & L_{2qb} & L_{2qc} & 0 & 0 & L_{2q1q} & L_{2q2q} \end{bmatrix} \begin{bmatrix} i_a \\ i_b \\ i_c \\ i_{fd} \\ i_{2d} \\ i_{1q} \\ i_{2q} \end{bmatrix} \quad (2-4)$$

The inductance matrix of equation (2-4) is composed of the variable terms ($f(\theta)$)

- Stator self-inductances: L_{aa} , L_{bb} , L_{cc} ;
- Stator mutual inductances: $L_{ab}(=L_{ba})$, $L_{bc}(=L_{cb})$, $L_{ca}(=L_{ac})$;
- Stator to rotor mutual inductances:
 - $L_{afd}(=L_{fda})$, $L_{bfd}(=L_{fdb})$, $L_{cfd}(=L_{fdc})$;
 - $L_{a2d}(=L_{2da})$, $L_{b2d}(=L_{2db})$, $L_{c2d}(=L_{2dc})$;
 - $L_{a1q}(=L_{1qa})$, $L_{b1q}(=L_{1qb})$, $L_{c1q}(=L_{1qc})$;
 - $L_{a2q}(=L_{2qa})$, $L_{b2q}(=L_{2qb})$, $L_{c2q}(=L_{2qc})$;

and the constant terms

- Rotor self-inductances: L_{fdfd} , L_{2d2d} , L_{1q1q} , L_{2q2q} ;
- Rotor mutual inductances: $L_{fd2d}(=L_{2dfd})$, $L_{1q2q}(=L_{2q1q})$.

The response of the electrical machine can be obtained by solving the matrix equation (2-2). However, the number of parameters which vary with the angle θ , which in turn

varies with time, introduces considerable complexity in solving machine and power system problems. This *time-varying* feature of the parameters is a major drawback of the model when considering the parameter estimation problem¹.

2.3 “d-q-0” Frame of Reference

The solution of the equations becomes much easier if the armature variables are transformed to new variables related to a frame of reference fixed to the field system. The transformation used is usually referred to as the Park transformation [53,54]. The Park transformation defines a new set of stator variables (currents, voltages, and flux linkages), obtained from the projection of the three-phase quantities on the direct and quadrature axes of the rotor, and a third variable corresponding to a stationary axis. The new variables with the frame of reference attached to the rotor are known as the d and q axis components. The third variable is proportional to the *zero sequence* component. This new model is represented in Figure 2-2.

The properties of the new stator windings are the same as those possessed by a commutator winding in which the current passes between a pair of brushes [18]:

- a current in the coil produces a field which is stationary in space;
- a voltage can be induced in the coil by the rotation of the moving element.

Although it is simple and straightforward to derive the equations that represent the circuit of Figure 2-2 [49], a more rigorous mathematical approach, using the Park transformation, also offers a direct solution.

1. In fact, there is no reference in the technical literature to any available method that estimates the parameters of the “a-b-c” model directly from tests.

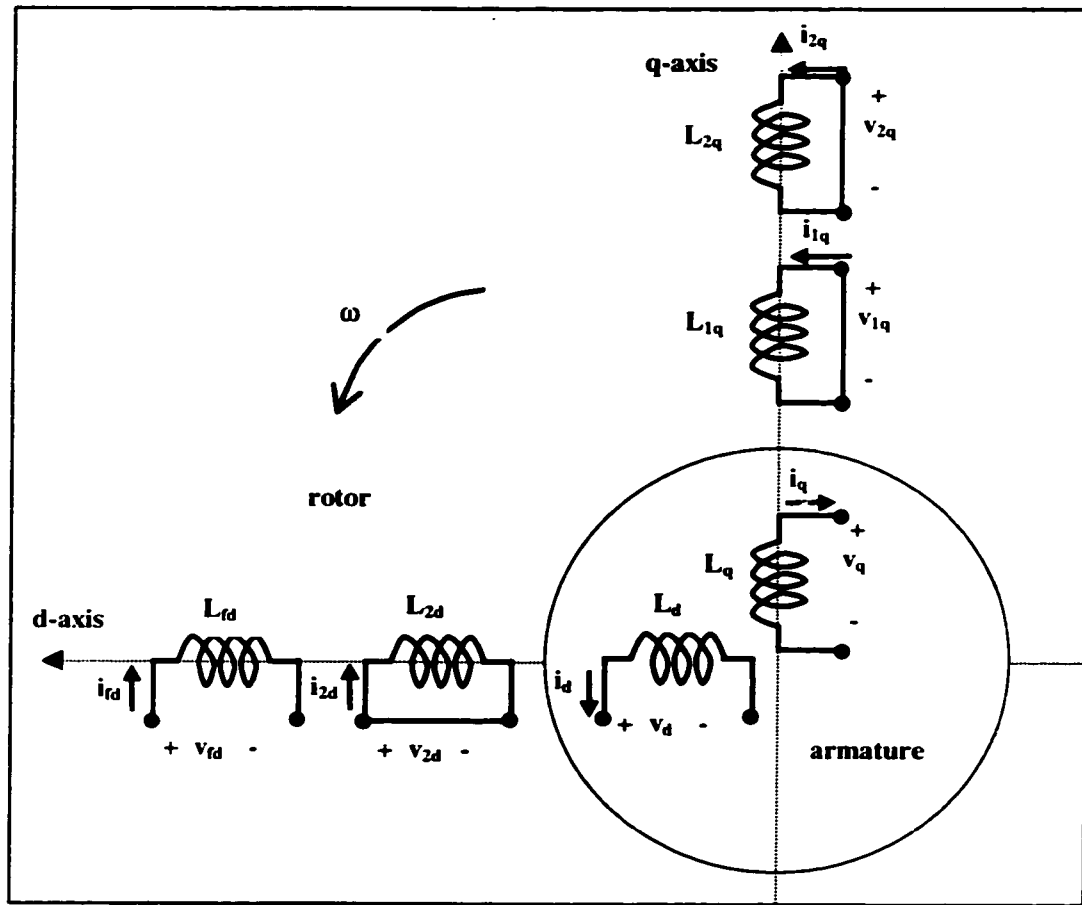


Figure 2-2: “d-q-0” model of the synchronous machine

The adopted Park transformation is defined as¹[48]:

$$\mathbf{P} = \sqrt{\frac{2}{3}} \begin{bmatrix} \cos(\theta) & \cos(\theta - 2\pi/3) & \cos(\theta + 2\pi/3) \\ \sin(\theta) & \sin(\theta - 2\pi/3) & \sin(\theta + 2\pi/3) \\ 1/\sqrt{2} & 1/\sqrt{2} & 1/\sqrt{2} \end{bmatrix} \quad (2-5)$$

1. With this particular definition, the transformation \mathbf{P} is orthogonal

Applying the transformation **P** to the stator variables of equation (2-2) it is possible to obtain the following set of equations for the direct and quadrature axes:

$$\begin{bmatrix} v_d \\ -v_{fd} \\ v_{2d} \\ v_q \\ v_{1q} \\ v_{2q} \end{bmatrix} = - \begin{bmatrix} r_a & 0 & 0 & \omega(L_{mq}+l_a) & \omega L_{mq} & \omega L_{mq} \\ 0 & r_{fd} & 0 & 0 & 0 & 0 \\ 0 & 0 & r_{2d} & 0 & 0 & 0 \\ -\omega(L_{md}+l_a) & -\omega L_{md} & -\omega L_{md} & r_a & 0 & 0 \\ 0 & 0 & 0 & 0 & r_{1q} & 0 \\ 0 & 0 & 0 & 0 & 0 & r_{2q} \end{bmatrix} \begin{bmatrix} i_d \\ i_{fd} \\ i_{2d} \\ i_q \\ i_{1q} \\ i_{2q} \end{bmatrix} - \frac{\partial}{\partial t} \begin{bmatrix} \lambda_d \\ \lambda_{fd} \\ \lambda_{2d} \\ \lambda_q \\ \lambda_{1q} \\ \lambda_{2q} \end{bmatrix} \quad (2-6)$$

where the fluxes are given by

$$\begin{bmatrix} \lambda_d \\ \lambda_{fd} \\ \lambda_{2d} \\ \lambda_q \\ \lambda_{1q} \\ \lambda_{2q} \end{bmatrix} = \begin{bmatrix} L_{md}+l_a & L_{md} & L_{md} & 0 & 0 & 0 \\ L_{md} & L_{md}+l_{fd} & L_{md} & 0 & 0 & 0 \\ L_{md} & L_{md} & L_{md}+l_{2d} & 0 & 0 & 0 \\ 0 & 0 & 0 & L_{mq}+l_q & L_{mq} & L_{mq} \\ 0 & 0 & 0 & L_{mq} & L_{mq}+l_{1q} & L_{mq} \\ 0 & 0 & 0 & L_{mq} & L_{mq} & L_{mq}+l_{2q} \end{bmatrix} \begin{bmatrix} i_d \\ i_{fd} \\ i_{2d} \\ i_q \\ i_{1q} \\ i_{2q} \end{bmatrix} \quad (2-7)$$

For the zero sequence the following equation is obtained:

$$v_o = -(r_a + 3r_n) i_o - (L_o + 3L_n) \frac{\partial i_o}{\partial t} \quad (2-8)$$

The effects of the transformation can now be fully appreciated: the terms of the inductance matrix of equation (2-7) are constants. Using the operator p defined as $p=d/dt$ [1]

and the corresponding self-inductances ($L_d=l_a+L_{md}$; $L_{fd}=l_{fd}+L_{md}+L_{f2d}$; ...), equations (2-6) and (2-7) can be rewritten in a more compact form as:

$$\begin{bmatrix} v_d \\ v_{fd} \\ v_{2d} \\ v_q \\ v_{1q} \\ v_{2q} \end{bmatrix} = - \begin{bmatrix} r_a + L_d p & L_{md} p & L_{md} p & \omega L_q & \omega L_{mq} & \omega L_{mq} \\ L_{md} p & r_{fd} + L_{fd} p & L_{md} p & 0 & 0 & 0 \\ L_{md} p & L_{md} p & r_{2d} + L_{2d} p & 0 & 0 & 0 \\ -\omega L_d & -\omega L_{md} & -\omega L_{md} & r_a + L_q p & L_{mq} p & L_{mq} p \\ 0 & 0 & 0 & L_{mq} p & r_{1q} + L_{1q} p & L_{mq} p \\ 0 & 0 & 0 & L_{mq} p & L_{mq} p & r_{2q} + L_{2q} p \end{bmatrix} \begin{bmatrix} i_d \\ i_{fd} \\ i_{2d} \\ i_2 \\ i_{1q} \\ i_{2q} \end{bmatrix} \quad (2-9)$$

Equation (2-9) can be represented by two circuits as shown in Figure 2-3 and Figure 2-4 for the direct and quadrature axes, respectively. The advantage of these equivalent circuits is that additional damper windings, to account for a more accurate representation of the rotor, can easily be incorporated in the model with the insertion of parallel branches to the existing damper windings.

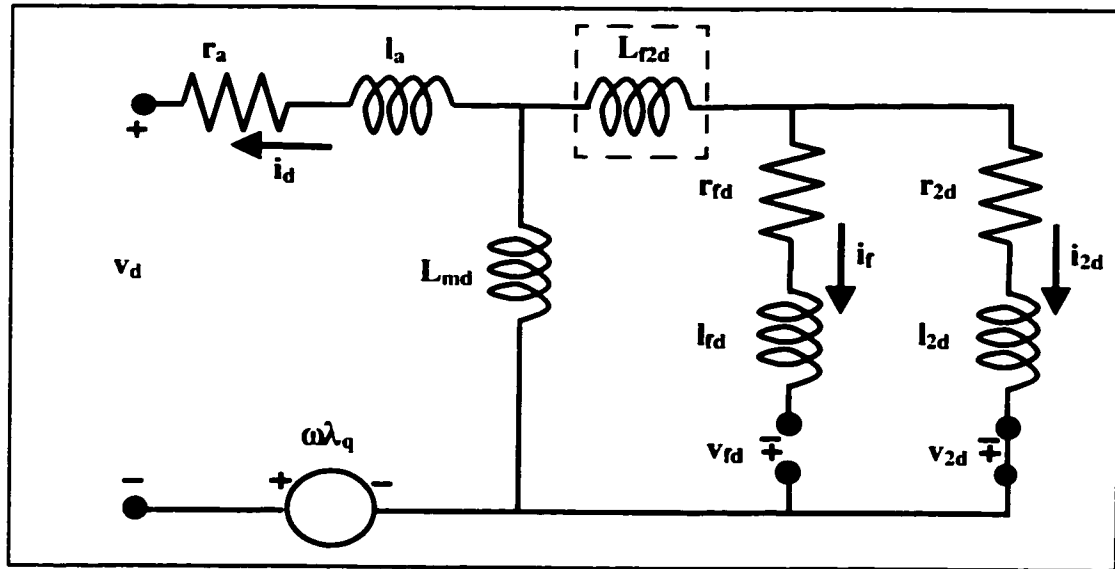


Figure 2-3: Direct axis equivalent circuit

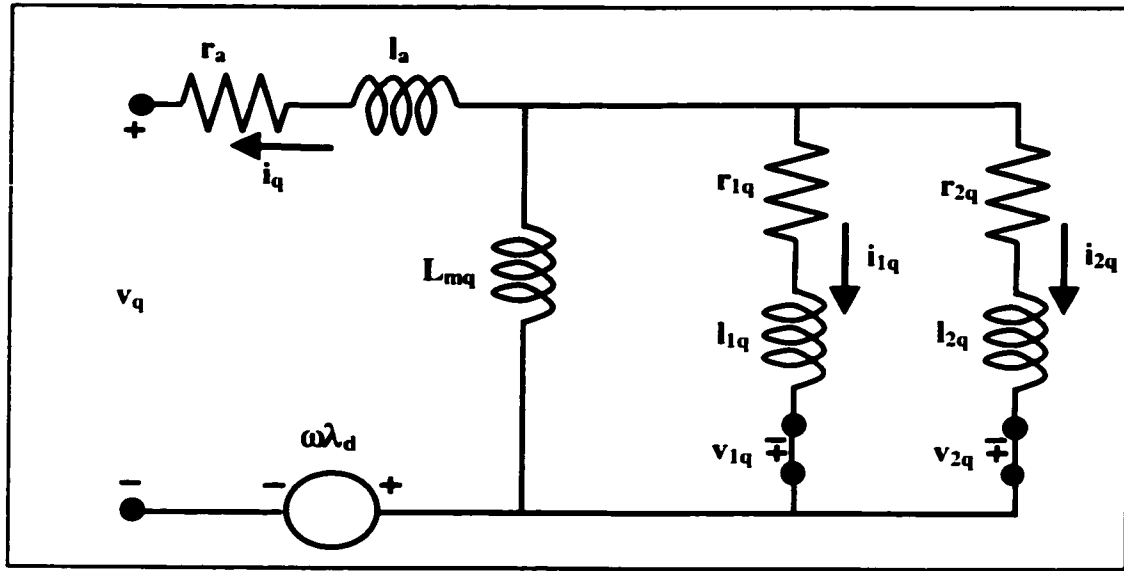


Figure 2-4: Quadrature axis equivalent circuit

This feature can also be extended to take into account physical aspects like considering unequal mutual inductances. It is very common in practice to assume that the mutual inductances between armature, field and damper windings are equal. Although this gives good results from the armature point of view [18], it can be the cause of considerable errors in determining the field current. It has been shown [55] that a more accurate value is obtained if an additional parameter is introduced in the equations to allow the mutual inductance between the field and damper windings to differ from the other two, as it has been done in Figure 2-3 with the insertion of L_{fd} .

The components of the circuits showed in Figure 2-3 and Figure 2-4 are known as the *fundamental machine parameters* and are summarized in Table 2-1.

Table 2-1: Fundamental Machine Parameters	
Constants	Definitions
r_a	Armature resistance
l_a	Armature leakage inductance
L_{md}	Direct axis magnetizing inductance
r_{fd}	Field resistance
l_{fd}	Field leakage inductance
r_{2d}	Direct axis damper resistance
l_{2d}	Direct axis damper leakage inductance
L_{f2d}	Direct axis field and damper winding leakage inductance
L_{mq}	Quadrature axis magnetizing inductance
r_{1q}	Quadrature axis damper resistance
l_{1q}	Quadrature axis damper leakage inductance
r_{2q}	Quadrature axis damper resistance
l_{2q}	Quadrature axis damper leakage inductance

2.4 Operational and Standard Parameters

When referring to the parameters of a SM, manufacturers do not offer the basic parameters identified by the elements of the d and q axis equivalent circuits of Figure 2-3 and Figure 2-4. Instead, these fundamental parameters are expressed in terms of derived parameters more closely related to what can be measured from the terminals of a machine under suitable test conditions.

Applying the Laplace transformation to equations (2-6) and (2-7) and solving for the direct and quadrature flux linkages, the following equations are obtained:

$$\begin{aligned}\lambda_d(p) &= G(p) v_{fd}(p) - L_d(p) i_d(p) \\ \lambda_q(p) &= -L_q(p) i_q(p)\end{aligned}\tag{2-10}$$

with the factors

- $L_d(p)$: d-axis operational inductance
- $L_q(p)$: q-axis operational inductance
- $G(p)$: stator to field transfer function

defined as

$$\begin{aligned}L_d(p) &= L_d \frac{(1 + pT_d') (1 + pT_d'')}{(1 + pT_{do}') (1 + pT_{do}'')} \\ L_q(p) &= L_q \frac{(1 + pT_q') (1 + pT_q'')}{(1 + sT_{qo}') (1 + sT_{qo}'')} \\ G(p) &= \frac{L_{md}}{r_{fd}} \frac{(1 + p \frac{l_{2d}}{r_{2d}})}{(1 + pT_{do}') (1 + pT_{do}'')}\end{aligned}\tag{2-11}$$

The general form of Equations (2-10) is valid for any number of rotor circuits or even if the rotor is considered as a distributed parameter system. The operational parameters defined in (2-11) are expressed as the ratio of polynomials in p , the order of which will depend upon the number of rotor circuits considered on each axis.

Under open-circuit conditions, from (2-10), the response is proportional to $G(p)$. But from the expression for $G(p)$, it is possible to conclude that the terminal voltage will respond to a change in the field voltage with time constants T_{do}' and T_{do}'' . Being always

valid that T_{do}' is bigger than T_{do}'' , they are referred to as the direct axis open-circuit transient and subtransient time constants respectively.

A similar analysis can be done for the short-circuit case. From (2-10), and assuming that the field voltage does not change, the currents for each axis will be proportional to the inverse of the respective operational inductance. The inverse of the direct axis operational inductance has poles defined by the time constants T_d' and T_d'' . Being always true that T_d' is bigger than T_d'' , they are referred to as the direct axis short-circuit transient and subtransient time constants.

Any response to a sudden perturbation has three well delimited periods defined by the subtransient and transient time constants. The magnitudes of the responses are modulated by the actual values of the operational parameters.

Applying a unit-step to $L_d(p)$, the initial value or direct axis subtransient inductance can be obtained as:

$$\tilde{L}_d = \lim_{p \rightarrow \infty} \{L_d(t)u(t)\} = \lim_{p \rightarrow \infty} \{pL_d(p)\frac{1}{p}\} = L_d \frac{T_d' T_d''}{T_{do}' T_{do}''} \quad (2-12)$$

After the subtransient period, the effect of the damper winding can be neglected, i.e: all the subtransient terms of $L_d(p)$ in (2-11) can be ignored. With this simplification, a similar analysis gives the direct axis transient inductance:

$$\dot{L}_d = \lim_{t \rightarrow 0} \{L_d(t)u(t)\} = \lim_{p \rightarrow \infty} \{sL_d(p)\frac{1}{p}\} = L_d \frac{T_d'}{T_{do}'} \quad (2-13)$$

Under steady-state conditions, after the subtransient and transient periods, the direct axis synchronous inductance can be obtained as:

$$L_d = \lim_{t \rightarrow \infty} \{L_d(t)u(t)\} = \lim_{s \rightarrow 0} \{pL_d(p)\frac{1}{p}\} = L_d \quad (2-14)$$

An analogous procedure can be used to obtain the corresponding definitions for the quadrature axis. Table 2-2 summarizes the derived parameters which, together with the armature resistance and leakage inductance, are the parameters offered by the manufacturer, better known as the *Standard Characteristics*.

Table 2-2: Standard Characteristics	
Constants	Definitions
L_d	Direct axis synchronous inductance
L_d'	Direct axis transient inductance
L_d''	Direct axis subtransient inductance
L_q	Quadrature axis synchronous inductance
L_q'	Quadrature axis transient inductance
L_q''	Quadrature axis subtransient inductance
T_{do}'	Direct axis transient open-circuit time constant
T_d'	Direct axis transient short-circuit time constant
T_{do}''	Direct axis subtransient open-circuit time constant
T_d''	Direct axis subtransient short-circuit time constant
T_{qo}'	Quadrature axis transient open-circuit time constant
T_q'	Quadrature axis transient short-circuit time constant
T_{qo}''	Quadrature axis subtransient open-circuit time constant
T_{qo}''	Quadrature axis subtransient short-circuit time constant

The standard characteristics are also important because of their direct physical meaning and the fact that possible numerical ranges can be associated to them, according to the type of machine and ratings involved [25,48,50]. However, the numerical solution of

the differential equations requires the knowledge of the circuit parameters. The relationship between both sets of parameters is not a trivial problem. In fact, until recently [35], there was no exact solution for this transformation. Presented in Appendix A is a rigorous mathematical approach that accounts for an exact equivalence between the circuit parameters and the standard characteristics, and also the simplified definitions derived from a classical approach.

2.5 Saturation

Saturation is the physical aspect that makes the model *non-linear*. *Off-line* parameter estimation techniques usually avoid the saturation problem, imposing boundary conditions for which the synchronous machine has a linear response. On the other hand, tests based on *on-line* data have to be prepared to solve the problem beforehand. There are many techniques to consider the saturation problem [9,13,14,25,48,56], of which the most common approach will be presented with some detail [25,48].

To represent the effects of saturation, the following assumptions are made [25]:

- (a) The leakage inductances are independent of saturation;
- (b) The leakage fluxes do not contribute to the iron saturation;
- (c) Saturation under load conditions is the same as under no-load conditions;
- (d) There is no magnetic coupling between the direct and quadrature axes.

With the above assumptions, saturation can be represented as:

$$\begin{aligned} L_{md} &= K_{sd} L_{mdu} \\ L_{mq} &= K_{sq} L_{mqu} \end{aligned} \tag{2-15}$$

where the sub-index u stands for the unsaturated values of the mutual inductances.

Assumption (c) means that the degree of saturation on the d axis can be determined from the open-circuit characteristic (OCC). From Figure 2-5 the following relationship is valid:

$$K_{sd} = \frac{V}{V_u} = \frac{i_{fu}}{i_f} = \frac{i_{fu}}{i_{fu} + \Delta i_f} = \frac{1}{1 + \frac{\Delta i_f}{i_{fu}}} \quad (2-16)$$

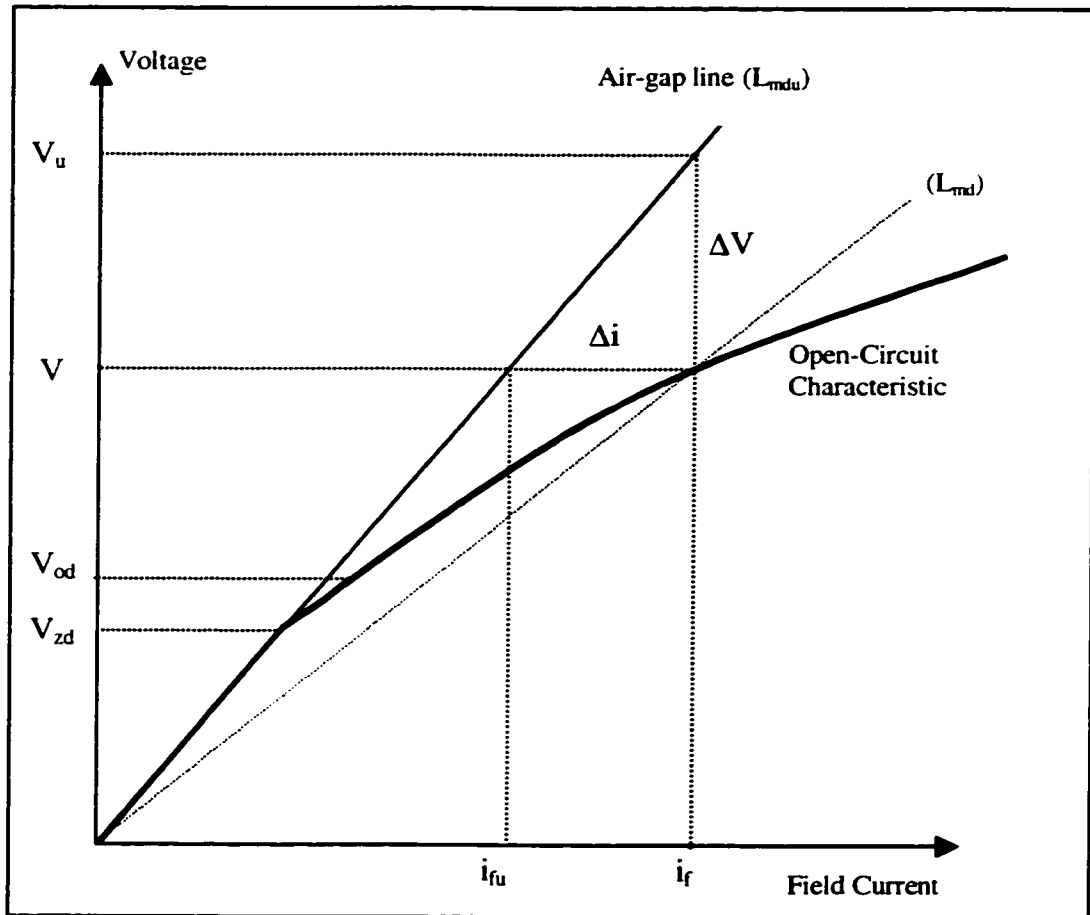


Figure 2-5: Saturation Effects at a Given Operating Point

Defining the factor [48]:

$$S_d = \frac{\Delta i_f}{i_{fu}} \quad (2-17)$$

the final expression for the saturation factor on the d-axis is:

$$K_{sd} = \frac{1}{1 + S_d} \quad (2-18)$$

For any practical purposes, it has been found that a good approximation for the factor S_d is given by the exponential:

$$S_d = A_d e^{B_d (V - V_{zd})} \quad (2-19)$$

where A_d and B_d are constants and V_{zd} is the adopted threshold value that defines the limit where saturation starts. It is worth to mention that comparable results are obtained if the field current variation Δi_f is approximated with an exponential function similar to (2-19) [25].

Although it has been stated [48,25] that the errors introduced by the value of the saturation function S_d at the threshold point V_{zd} are negligible, a little bit of investigation can show that this assertion is not necessarily true.

Figure 2-6 plots fifty saturation functions obtained from the saturation curves taken from [48], for which the threshold value is $V_{zd}=0.8$ pu. These plots have been obtained using a linear mutual inductance L_{md} of 1.7 pu.

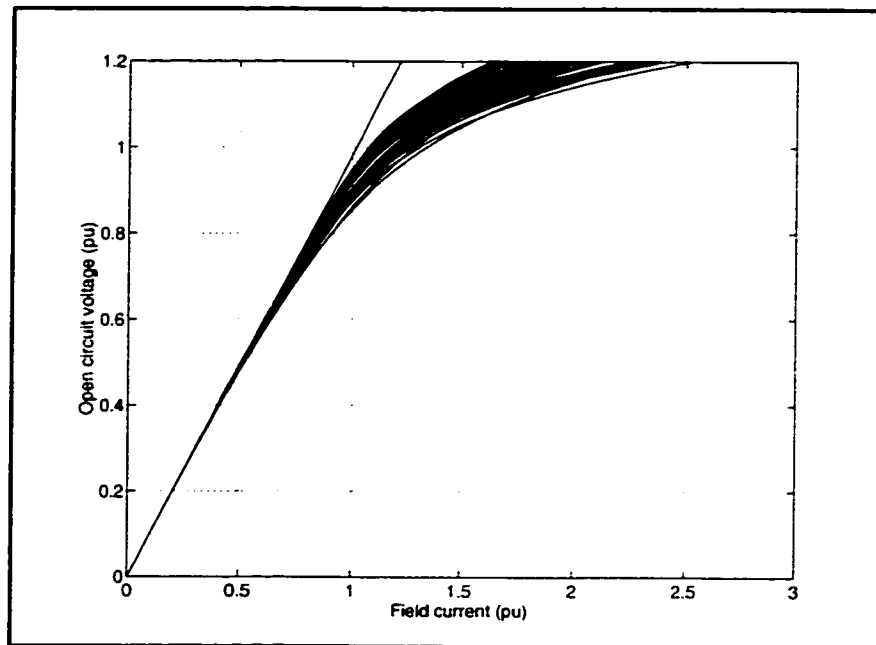


Figure 2-6: Typical Saturation Curves

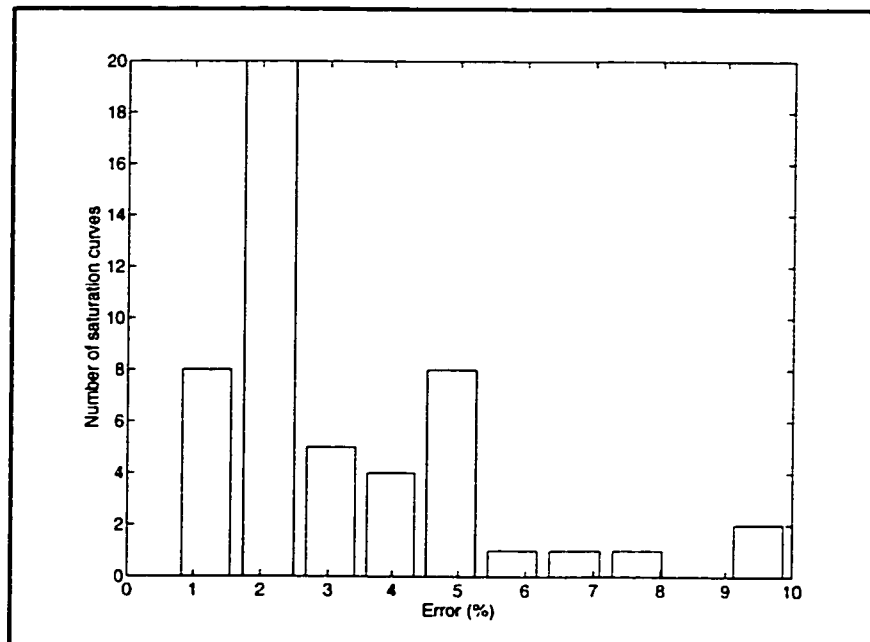


Figure 2-7: Mutual Inductance Error

One way of analysing the problem is through the differences in the field current at V_{zd} , where it can be observed that the errors can easily reach 5%. A more interesting approach is to approximate the saturation curve below the assumed threshold value V_{zd} by a straight line between the origin and the crossing point at V_{zd} (0.8). In fact, this represents a redefinition of the linear characteristic L_{md} . Figure 2-7 shows a histogram of the errors on L_{md} that are introduced by saturation when the overall model is supposed to be linear.

The saturation model has to be redefined in order to avoid these problems. Figure 2-8 offers a schematic of the solution.

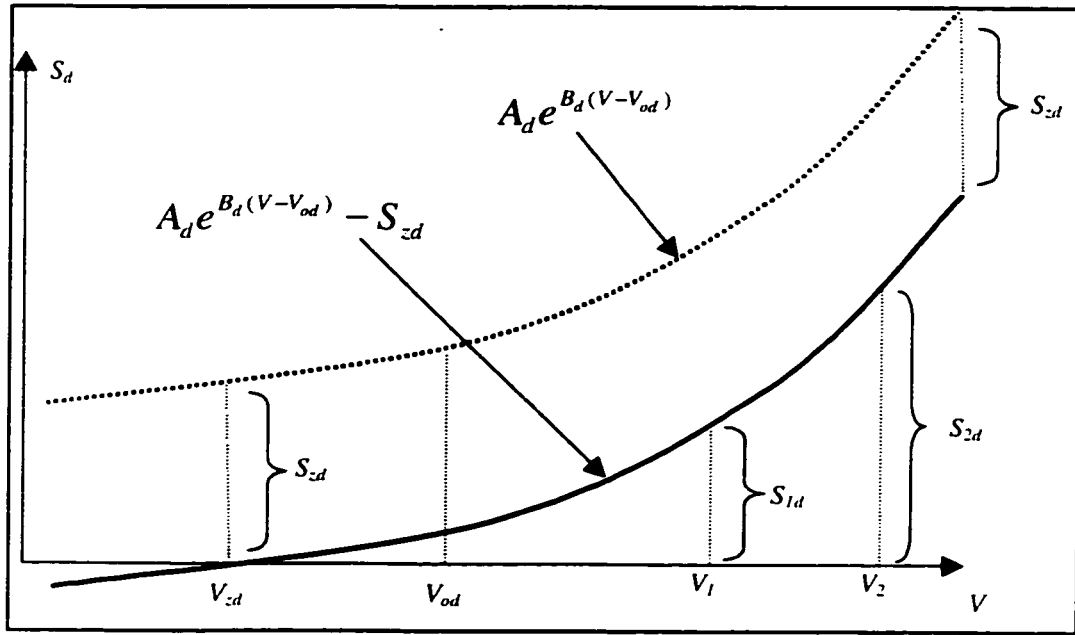


Figure 2-8: New Saturation Function

Given the values of saturation for two voltages V_1 and V_2 , and knowing the voltage V_{zd} , below which saturation is considered nil, it is possible to redefine saturation as per expression (2-20):

$$\begin{aligned}
S_{zd} &= A_d e^{B_d(V_{zd} - V_{od})} \\
S_d &= \begin{cases} A_d e^{B_d(V - V_{od})} - S_{zd} & , V \geq V_z \\ 0 & , V < V_z \end{cases} \quad (2-20)
\end{aligned}$$

where V_{od} is any adopted value. Then, saturation is defined when the set of constants $\{A_d, B_d, V_{zd}, V_{od}\}$ are known. The value of V used in the exponential function can be considered to be a function only of the direct axis air-gap flux linkages λ_{AGd} or computed as a function of the total air-gap flux linkage λ_{AGt} [57] as

$$\begin{aligned}
\lambda_{AGt} &= \sqrt{\lambda_{AGd}^2 + \lambda_{AGq}^2} \\
\lambda_{AGd} &= L_{md}(i_d + i_{fd} + i_{2d}) \\
\lambda_{AGq} &= L_{mq}(i_q + i_{1q} + i_{2q}) \quad (2-21)
\end{aligned}$$

Saturation for the quadrature axis is obtained in a similar way. For salient pole machines though, the saturation factor K_{sq} is usually considered equal to 1.0, due to the fact that the path for the flux is largely in air.

Although it has been found (see Appendix 5C of [19]) that different saturation curves, similar to the OCC, can be obtained according to the level of the active power involved, saturation will be considered to be independent of the active power, as per equation (2-20).

2.6 Steady-State Analysis

In steady-state, the currents are constant and the damper windings can be ignored in the analysis. With these considerations, equations (2-9) can be simplified as follows:

$$\begin{bmatrix} v_d \\ v_{fd} \\ \vdots \\ v_q \end{bmatrix} = \begin{bmatrix} r_a & 0 & \omega L_q \\ 0 & -r_{fd} & 0 \\ \vdots & \vdots & \vdots \\ -\omega L_d & -\omega L_{md} & r_a \end{bmatrix} \begin{bmatrix} i_d \\ i_{fd} \\ \vdots \\ i_q \end{bmatrix} \quad (2-22)$$

2.6.1 Phasor Diagrams

Using the inverse of the Park transformation (2-5), the instantaneous voltage of phase "a" can be solved in terms of the "dq" components as:

$$v_a = \sqrt{2/3} (v_d \cos(\theta) + v_q \sin(\theta)) \quad (2-23)$$

where by definition $\theta = \omega_o t + \delta + \pi/2$.

Substituting the direct and quadrature axis voltages from (2-22) in (2-23) and considering the definitions given in Table 2-3 [48], it is possible to obtain, after some manipulation, the following phasor equation:

$$\vec{E} = \vec{V} + r_a \vec{I} + jX_q \vec{I}_q + jX_d \vec{I}_d \quad (2-24)$$

Equation (2-24) can be summarized in the phasor diagram of Figure 2-9. In the case of a round rotor machine, where a generally accepted assumption is $X_d = X_q$, the diagram is just a simplified version of Figure 2-9.

Table 2-3: Phasor Definitions		
$I_d = \frac{i_d}{\sqrt{3}};$	$\vec{I}_d = I_d e^{j(\delta+90)}$	rms equivalent "d" and "q" axis currents and phasors
$I_q = \frac{i_q}{\sqrt{3}};$	$\vec{I}_q = I_q e^{j\delta}$	
$V_d = \frac{v_d}{\sqrt{3}};$	$\vec{V}_d = V_d e^{j(\delta+90)}$	rms equivalent "d" and "q" axis voltages and phasors
$V_q = \frac{v_q}{\sqrt{3}};$	$\vec{V}_q = V_q e^{j\delta}$	
$\vec{I} = I e^{j\phi}$	$= \vec{I}_q + \vec{I}_d$	stator current phasor
$\vec{V} = V e^{j0}$	$= \vec{V}_q + \vec{V}_d$	stator voltage phasor
$E = \frac{\omega_o L_{md} i_{fd}}{\sqrt{2}};$	$\vec{E} = E e^{j\delta}$	stator equivalent EMF corresponding to i_{fd}
δ	load angle (between \vec{E} and \vec{V})	
ϕ	power factor angle (between \vec{I} and \vec{V})	

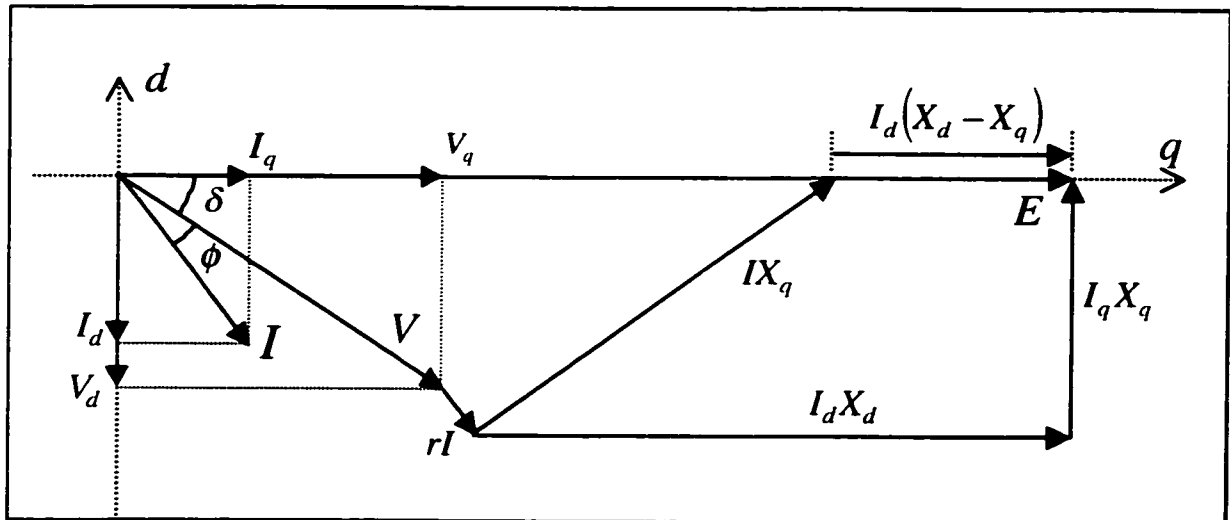


Figure 2-9: Phasor Diagram of a Salient Pole Machine

2.6.2 Power Diagram

From the diagram of Figure 2-9 it is easy to prove the geometric relationships shown in the *phasor diagram* of Figure 2-10 [58], where the resistive component has been neglected.

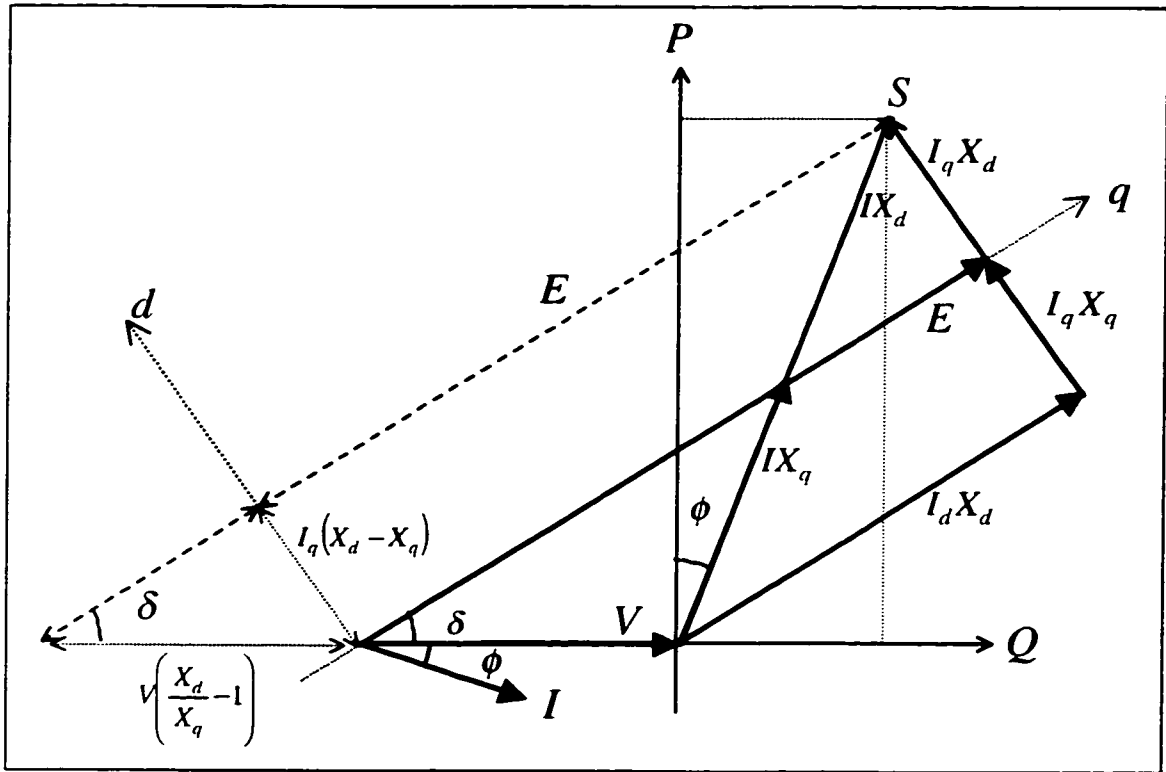


Figure 2-10: Extended Phasor Diagram

The complex output power of a synchronous machine is given by

$$\vec{S} = \vec{V} \vec{I}^* = P + jQ = VI(\cos\phi + j\sin\phi) \quad (2-25)$$

Multiplying the voltage vectors of Figure 2-10 by the magnitude V/X_d , the *voltage diagram* is transformed to a *power diagram*, where the point S will verify the relationship given in (2-25) for the complex power. This new diagram is conceptually very important because it offers a graphical image of the operating limits of the generator [58,59], as shown in Figure 2-11.

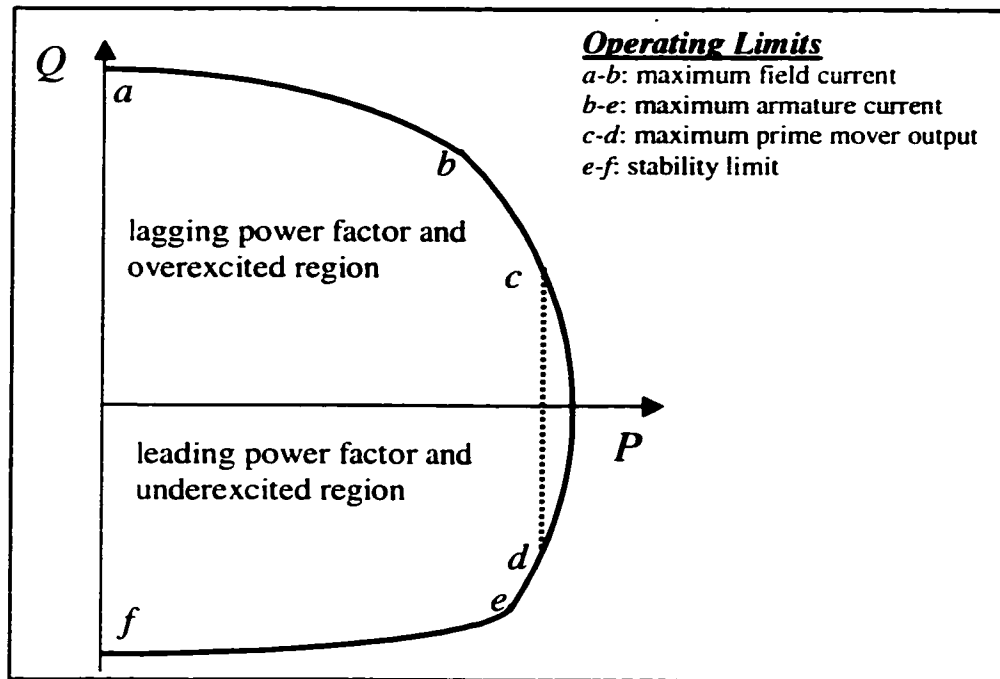


Figure 2-11: Operating Chart of a Synchronous Generator

From Figure 2-10, the terms $I \cos \phi$ and $I \sin \phi$ can be obtained as functions of E , V , X_d , X_q and δ . When these values are substituted in the complex equation (2-25), the following well known relationships can be verified:

$$\begin{aligned}
 P &= \frac{EV \sin \delta}{X_d} + \frac{V^2 \sin 2\delta}{2} \left(\frac{1}{X_q} - \frac{1}{X_d} \right) \\
 Q &= \frac{EV \cos \delta}{X_d} - \frac{V^2}{X_d} - \frac{V^2 (\sin \delta)^2}{2} \left(\frac{1}{X_q} - \frac{1}{X_d} \right)
 \end{aligned}
 \tag{2-26}$$

2.6.3 PQV Steady-State Solution

It is a common practice to specify the steady-state operating point of a synchronous machine as a function of some of the terminal quantities. Normally the active and reactive power together with the terminal voltage (P, Q and V) are the variables specified.

The rest of the variables are determined as follows.

- The terminal current I is obtained from the expression of the power ($S=VI$).
- The power factor angle ϕ is obtained from the equation for the power given in (2-25).
- If saturation is considered and it is evaluated as a function of the total air-gap flux as in expression (2-21), the iterative process described below can be avoided, obtaining the factor S_d directly from (2-20).
- The load angle δ is obtained from the following relationship derived from the phasor diagram of Figure 2-9:

$$\tan\delta = \frac{X_q I \cos\phi - rI \sin\phi}{V + rI \cos\phi + X_q I \sin\phi} \quad (2-27)$$

- The remaining machine quantities are obtained from the definitions given in Table 2-3 and considering the following expression from Figure 2-9:

$$E = V_q + rI_q - X_d I_d \quad (2-28)$$

- If saturation is not evaluated as a function of the total air-gap flux as in expression (2-21), an iterative process can be established.

(a) Assume no saturation ($K_{sd}=K_{sq}=1$).

(b) With these saturation factors, all the machine quantities can be obtained as explained in the previous steps.

(c) Obtain the fluxes for the new axis currents using the simplified version of equations (2-7) for the steady-state case.

(d) Get the new saturation factors for these fluxes using (2-20) and (2-18).

(e) Repeat from step (b) until the differences in the currents are negligible.

2.7 Transient-State Analysis

The full equations (2-9) have to be considered in this case. Using matrix notation, these equations can be rewritten in a compact form as:

$$\mathbf{v} = -\mathbf{R} \mathbf{i} - \mathbf{L} \frac{d\mathbf{i}}{dt} \quad (2-29)$$

Solving for the currents,

$$\frac{d\mathbf{i}}{dt} = -\mathbf{L}^{-1} \mathbf{R} \mathbf{i} - \mathbf{L}^{-1} \mathbf{v} \quad (2-30)$$

which can be recognized in the *state variable* form as:

$$\frac{d\mathbf{x}}{dt} = \mathbf{A} \mathbf{x} + \mathbf{B} \mathbf{u} = \mathbf{f}(\mathbf{x}, \mathbf{u}, t) \quad (2-31)$$

2.7.1 Integration of the Transient Equations

The integration of (2-31) gives:

$$\mathbf{x}(t_{n+1}) = \mathbf{x}(t_n) + \int_{t_n}^{t_{n+1}} \mathbf{f}(\mathbf{x}, \mathbf{u}, t) dt \quad (2-32)$$

Different numerical integration methods can be defined according to the way the integral part is approximated. The trapezoidal rule [60], which is extensively used to solve electromagnetic transient problems in power systems [61,62], takes the form:

$$\mathbf{x}_{n+1} = \mathbf{x}_n + \frac{h_n}{2} \left(\mathbf{f}(\mathbf{x}_n, \mathbf{u}_n, t_n) + \mathbf{f}(\mathbf{x}_{n+1}, \mathbf{u}_{n+1}, t_{n+1}) \right) \quad (2-33)$$

where h_n is the step size. Substituting the expression for the currents (2-30) and after some processing, the following expression is obtained:

$$\mathbf{i}_{n+1} = \left(\frac{2}{h_n} \mathbf{L}_{n+1} + \mathbf{R}_{n+1} \right)^{-1} \left(\mathbf{L}_{n+1} \left(\frac{2}{h_n} \mathbf{i}_n + \frac{d\mathbf{i}_n}{dt} \right) - \mathbf{v}_{n+1} \right) \quad (2-34)$$

If saturation is taken into consideration, an iterative approach, similar to that shown in section 2.6.3 but adapted for this particular case, should be followed. In terms of computation this is a very intensive process. Saturation affects the matrices \mathbf{R} and \mathbf{L} , which in turn, have to be re-evaluated in order to get the new currents that define new saturation factors and so on.

CHAPTER 3

ARTIFICIAL NEURAL NETWORKS

3.1 Introduction

Artificial Neural Networks (ANNs), represent an emerging technology rooted in many disciplines. Work on ANNs has been motivated right from its inception by the recognition that the brain computes in an entirely different way from the conventional digital computer. It would be desirable to have a tool that, like the brain, could be:

- Robust and fault tolerant;
- Flexible enough to adapt and learn from the environment;
- A reliable instrument while dealing with probabilistic, noisy or inconsistent information;
- Highly parallel;
- Small and compact.

To some extent, ANNs already share these features [63]. Moreover, this is the main reason to account for so many successful applications in different disciplines over the last few years, as in the hyphenation of words, sonar target recognition, car navigation, image compression, signal prediction and forecasting, speech and character recognition [63,64].

This chapter offers a brief introduction to the topic, specifically to multilayer perceptrons, discussing with some detail the training method known as backpropagation as

well as some extensions or alternative approaches that have been used during the development of this work.

3.2 Model

The ANN field has been largely motivated by the possibility of modelling networks of real neurons in the brain. From a neurophysiological point of view though, the models are extremely simplified and it would be misleading to think that the models offer an actual representation of the brain. However, they are an important and very valuable tool for understanding the internal complexity of the brain and for gaining insight into the principles of biological computation.

3.2.1 Neuron Model

Figure 3-1 shows a schematic drawing of a nerve cell and the counterpart model used for ANNs [63,64]. Arborescent ramifications of nerve fiber called dendrites, receiving ends of the cell, are connected to the cell body or soma. Extending from the cell body is a single long fiber called the axon, which also arborizes into the transmitting ends called synapses. The synapses form junctions with dendrites of other neurons forming a massive network of 10^{11} neurons [64]. This explains, in an oversimplified way, how information can be transmitted among neurons.

The ANN neuron model evokes this concept, as it can also be seen in Figure 3-1. Input signals are internally weighted, added and shifted with an appropriate bias. A transformation is applied to the result, which in turn is passed along as input for other neurons.

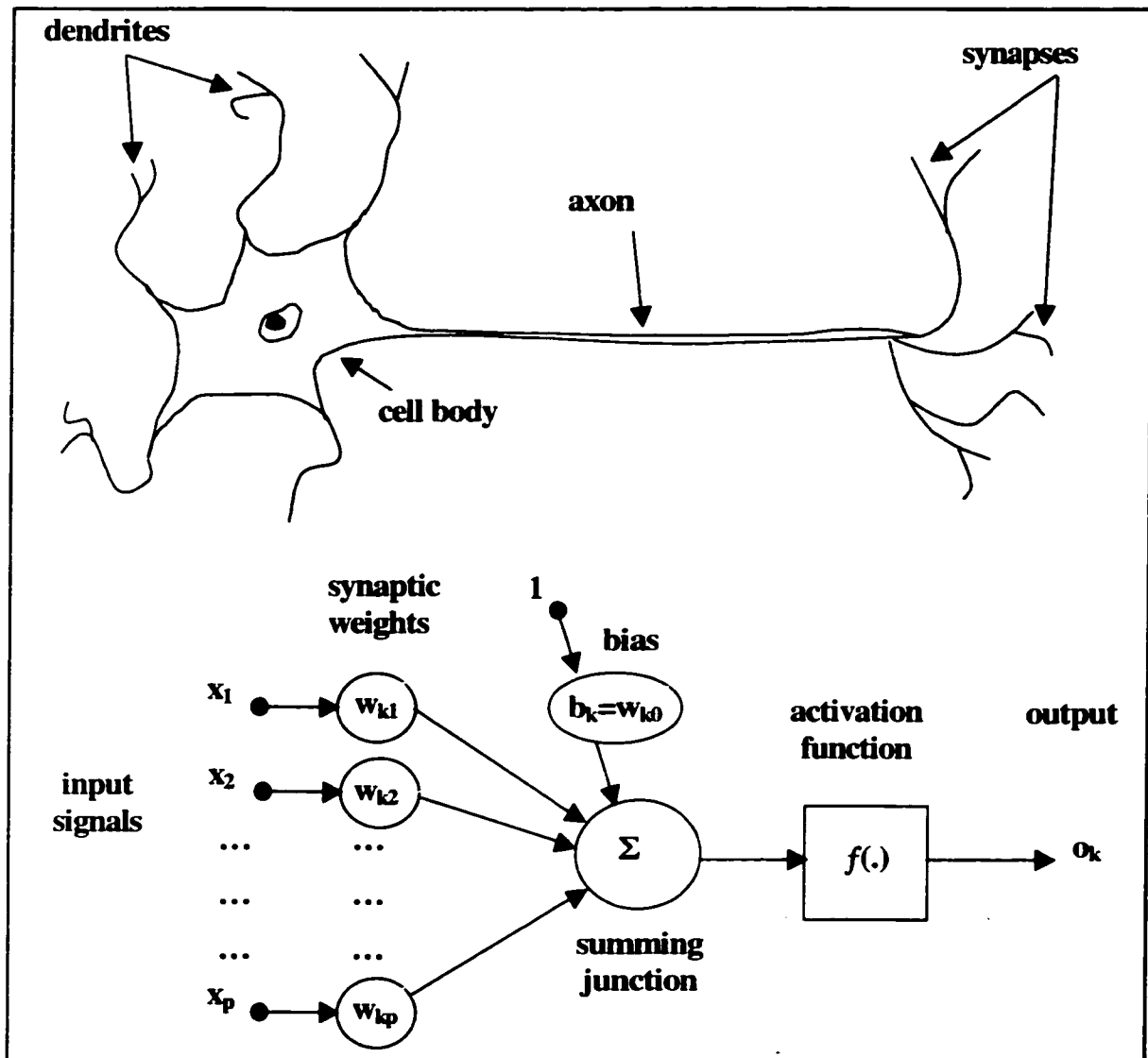


Figure 3-1: Schematic Drawings of a Neuron and the ANN Neuron Model

Being more specific in the functional details of the neuron model, three basic elements can be identified:

- (a) A set of connecting links characterized each by a weight. Each input signal to a specific connecting link is affected by its weight.

- (b) An adder for summing the input signals and the neuron's own bias. The bias has the effect of applying an affine transformation to all the input signals.
- (c) An activation function. In general, the main purpose of the activation function is to introduce a non-linearity to the model and to limit the permissible amplitude range of the output signal. Good examples of activation functions that have output ranges between $[0,1]$ and $[-1,1]$ are the logistic function and the hyperbolic tangent function as shown in equation (3-1).

$$f(x) = \frac{1}{1 + ae^{-x}} \quad ; \quad f(x) = \frac{e^x - e^{-x}}{e^x + e^{-x}} \quad (3-1)$$

However, it is important to consider that, in general, the shape of the functions has more impact on the speed of the learning process than on the ultimate power of the network [65].

It is worth noting that the model of the neuron presented here constitutes, by itself, the simplest form of an ANN. It can be used for the classification of a special type of patterns said to be linearly separable i.e., patterns that lie on opposite sides of a hyperplane. This interesting property, whose proof is better known as the *Perceptron Convergence Theorem*, gives an insight on how the association of several units into a more complex structure, can become a powerful pattern classifier.

3.2.2 Artificial Neural Network Model

The model that will be presented is the multilayer feedforward network. It consists of a set of neurons that are arranged into two or more layers: input layer, hidden layers and an output layer. A generic multilayer feedforward network is presented in Figure 3-2

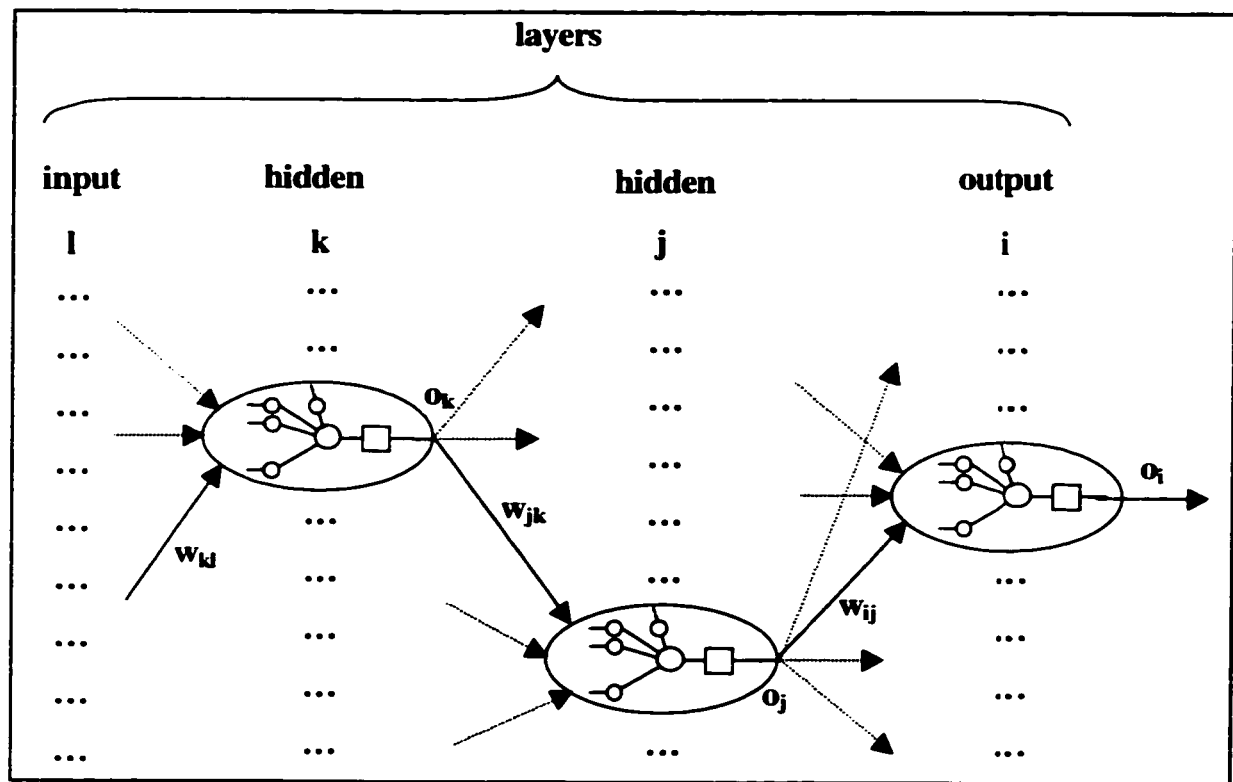


Figure 3-2: Structure of a Feedforward ANN

The neurons of the input layer do not perform any computation. They could be named identity neurons: the inputs to the network are the outputs of these neurons. For this reason, some authors do not consider the inputs as an actual layer of neurons.

The amount of hidden layers, in theory, is unlimited. However, one hidden layer is usually enough for most engineering problems, and two hidden layers cover the vast majority of them [65]. For example, the *Exclusive OR* (XOR) problem, a case of non linearly separable patterns that cannot be solved by a single perceptron¹ [63], only one hidden layer with two neurons is required.

1. The XOR problem is very important for historical reasons because it was used to put in doubt the computational capabilities of not only the perceptron but neural networks in general [66].

3.3 Learning Algorithms

In order to define a learning process, it is necessary to define a function to measure the errors. The most common *cost function* choice is the quadratic function:

$$E = \frac{1}{2} \sum_i (t_i - o_i)^2 = \frac{1}{2} \sum_i e_i^2 \quad (3-2)$$

where t_i is the expected target for neuron i .

This equation can be expanded for the generic feedforward neural network of Figure 3-2:

$$E = \frac{1}{2} \sum_i \left(t_i - f \left(\sum_j w_{ij} f \left(\sum_k w_{jk} f \left(\sum_l w_{kl} o_l \right) \right) \right) \right)^2 \quad (3-3)$$

Expression (3-3) is a continuous differentiable function of every weight, so, a gradient descent algorithm can be used to learn appropriate weights. The partial derivatives against the weight of an output layer neuron are given by:

$$\begin{aligned} \frac{\partial E}{\partial w_{ij}} &= \frac{\partial E}{\partial e_i} \frac{\partial e_i}{\partial o_i} \frac{\partial o_i}{\partial n_i} \frac{\partial n_i}{\partial w_{ij}} = \\ &= (t_i - o_i)(-1) f'(n_i) o_j = -\delta_i o_j \quad ; \quad \delta_i = (t_i - o_i) f'(n_i) \end{aligned} \quad (3-4)$$

When considering hidden layers, it can be seen that each neuron of the following layer offers a path for a specific weight to propagate to the output and, eventually, make a contribution to the overall error. Following the notation of Figure 3-2, each contribution will be given by:

$$\begin{aligned}
 \left(\frac{\partial E}{\partial w_{jk}} \right)_i &= \frac{\partial E}{\partial e_i} \frac{\partial e_i}{\partial o_i} \frac{\partial o_i}{\partial n_i} \frac{\partial n_i}{\partial o_j} \frac{\partial o_j}{\partial n_j} \frac{\partial n_j}{\partial w_{jk}} \\
 &= -\delta_i \quad w_{ij} f'(n_j) p_k
 \end{aligned} \tag{3-5}$$

Then, the gradient will be:

$$\begin{aligned}
 \frac{\partial E}{\partial w_{jk}} &= -\sum_i \delta_i w_{ij} f'(n_j) p_k \\
 &= -\delta_j o_k \quad ; \quad \delta_j = f'(n_j) \sum_i \delta_i w_{ij}
 \end{aligned} \tag{3-6}$$

Equations (3-4) and (3-6) offer the same compact formula to evaluate the gradient. The only difference is given in the way that the quantity δ is evaluated. Equation (3-6) is valid for all but the output layer, for which equation (3-4) is a particular case.

3.3.1 Backpropagation

With the knowledge of the partial derivatives, the weights of any neuron of the network can be updated using the gradient descent rule:

$$\Delta w_{ij} = -\eta \frac{\partial E}{\partial w_{ij}} \quad (3-7)$$

where the parameter η is called the learning rate.

This way of updating the weights is better known as the *backpropagation* algorithm [67]. This is just another name for the gradient descent algorithm, but of great practical importance in the form of the resulting update rules.

There are many problems associated with the backpropagation algorithm. One is the selection of the appropriate learning rate which can be influential in getting a very slow convergence rate or wild oscillations for small or big η . One of the solutions has been to add a *momentum* term, which gives each of the weights some inertia in the direction that they tend to change. This avoids oscillations and enforces changes in the direction of the average path to a minimum. This modification to the updating rule can be seen in equation (3-8), where α is the momentum parameter.

$$\Delta w_{ij}(t+1) = -\eta \frac{\partial E}{\partial w_{ij}} + \alpha \Delta w_{ij}(t) \quad (3-8)$$

The selection of the learning rate η can be a problem by itself. Furthermore, an excellent selection at one moment of the training process can give a poor performance later on. This problem can be solved by adapting the learning rate itself along the training process according to its performance [64]:

$$\eta = \eta + \Delta\eta \quad ; \quad \Delta\eta = \begin{cases} c_i \eta \rightarrow \Delta E < 0 \\ -c_d \eta \rightarrow \Delta E > 0 \end{cases} \quad (3-9)$$

where c_i and c_d are the increasing and decreasing factors respectively.

This rule can easily be combined with the previous one, zeroing the momentum factor whenever the learning rate is decreasing due to a bad step.

Either one of the improvements just mentioned, or certainly a combination of both, are a powerful and effective addition to the original algorithm.

3.3.2 Conjugate Gradient Algorithms

The *steepest descent method* updates the weights minimizing the error along a line in the gradient direction. After the line minimization, the new gradient direction is perpendicular to the old direction, and the method approaches the minimum following a zigzag path. The main reason for this is that the new directions will not necessarily keep the gradient perpendicular to the old directions, and this is responsible for the poor performance of the method.

The condition on a new search direction to avoid spoiling the previous minimization is that the new direction should keep the gradient perpendicular to the previous direction. Two directions that have this property are said to be conjugate. Then, the new direction should be a compromise between the gradient direction and the previous search direction, as stated in the following equation:

$$D(t+1) = -\nabla E(t+1) + \beta D(t) \quad (3-10)$$

An appropriate selection of the factor β will make this procedure a conjugate gradient method. The *Polak-Ribiere* rule [68] defines this factor as being:

$$\beta = \frac{(\nabla E(t+1) - \nabla E(t)) \bullet \nabla E(t+1)}{\nabla E(t) \bullet \nabla E(t)} \quad (3-11)$$

where “ \bullet ” denotes the scalar or dot product of the vectors. In fact, this will keep track of the directions, making the series mutually conjugate.

In general, conjugate gradient methods are an order of magnitude faster than the backpropagation algorithms [69].

3.3.3 Levenberg-Marquardt

The minimization of equation (3-2) is a nonlinear least-squares problem. For a training set of N number of presentations, it can be rewritten as:

$$E = \frac{1}{2} R' R \quad (3-12)$$

where the superscript “ t ” denotes the transposed vector. R is the vector formed with the outputs of the neural network:

$$\begin{aligned}
 R &= [R_1 \quad \cdots \quad R_n \quad \cdots \quad R_N]' \\
 R_n &= [e_{n,1} \quad \cdots \quad e_{n,i} \quad \cdots \quad e_{n,l}]'
 \end{aligned}
 \tag{3-13}$$

The first and second derivatives against the weights (gradient and Hessian matrix, respectively) can be obtained as:

$$\begin{aligned}
 \nabla E &= \sum_{n,i} e_{n,i} \cdot \nabla e_{n,i} \\
 &= J' R \quad ; \quad J = \begin{bmatrix} \cdots & \cdots & \cdots \\ \cdots & \frac{\partial e_{n,i}}{\partial w_w} & \cdots \\ \cdots & \cdots & \cdots \end{bmatrix}
 \end{aligned}
 \tag{3-14}$$

$$\begin{aligned}
 \nabla^2 E &= H = \sum_{n,i} (\nabla e_{n,i} \cdot \nabla e_{n,i}' + e_{n,i} \cdot \nabla^2 e_{n,i}) \\
 &= J' J + S \quad ; \quad S = \sum_{n,i} e_{n,i} \cdot \nabla^2 e_{n,i}
 \end{aligned}$$

where, the Jacobian matrix J and the matrix S which carries the second order information of $\nabla^2 E$ have been defined. The quadratic model of the cost function around a set of weights W_o is:

$$E = E_o + \nabla E_o \cdot (W - W_o) + \frac{1}{2} (W - W_o) \cdot H_o \cdot (W - W_o)
 \tag{3-15}$$

Differentiating (3-15), solving for the weights, and substituting the results from (3-14), the following expression is obtained:

$$\begin{aligned} W &= W_o - H_o^{-1} \nabla E_o \\ &= W_o - (J_o' J_o + S_o)^{-1} J_o' R_o \end{aligned} \quad (3-16)$$

This equation, used iteratively, is better known as the *Newton's method*. The main problem associated with this method is that it requires the second derivatives and, unless the departure point is close to the solution, it is numerically unstable [70].

An alternative approach comes from using the affine model of R around W_o :

$$R = R_o + J_o (W - W_o) \quad (3-17)$$

Since (3-17) is an over determined system of linear equations, the logical way to proceed is to choose the next iterate W , as the solution of the linear least-squares problem [70], given by

$$W = W_o - (J_o' J_o)^{-1} J_o' R_o \quad (3-18)$$

The method that uses (3-18) at each iteration is called the *Gauss-Newton method* where it can be seen that the only difference with the *Newton method* is given by the omission of the S_o matrix. The success of this method will be associated to the importance of this omission, having at most, the same convergency properties as the *Newton method*.

Of the many variants of the *Gauss-Newton method*, the most successful is the one that chooses the next set of weights by a trust region approach or, alternatively, that accepts

or discards a new set of weights according to its performance measured by the cost function. With these restrictions, the solution of (3-17) is

$$W = W_o - (J_o' J_o + \mu I)^{-1} J_o' R_o \quad (3-19)$$

This solution is known as the *Levenberg-Marquardt method*. In this procedure [68], every time a new set of records is accepted, μ is decreased by a constant factor. On the contrary, μ is increased if the set is rejected, and (3-19) is re-evaluated to obtain a new set which in turn, will be accepted or rejected by the same rules. The importance of the method is that it bounces between the *Gauss-Newton* method for small values of μ , and the gradient descent method when μ is large. The method is robust and very efficient [71]. However, depending upon the size of the ANN and amount of training samples, memory requirements can make it impractical for many applications.

3.4 Generalization

Generalization is the property that most of the practical applications of the ANNs try to take advantage of. Whenever a neural network is trained to recognize a rule (R), there is a universe (U) of possible input-output mappings, some of which will form part of the rule. After being trained using a training set (T) that is representative of the rule, a validation set (V) can be used to measure the performance of the neural network, i.e., its ability to generalize can be tested. This concept is illustrated in Figure 3-3 [64]. The network only knows about the training set, not the validation set or the rule. If the ANN is *trainable*, all the possible generalizations (G1, G2 and G3) will cover the training set. Performance over the training and validation sets measures memorization and generalization, respectively.

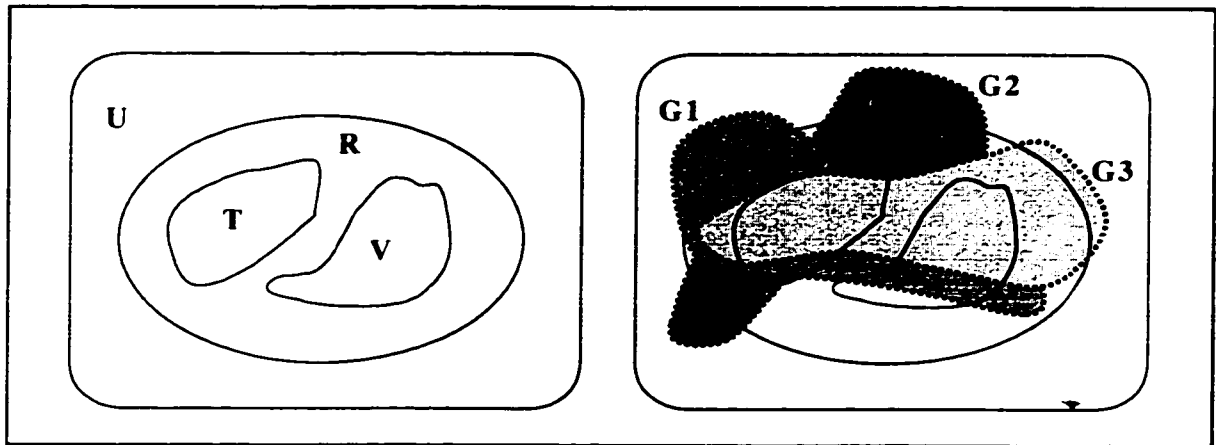


Figure 3-3: Rule Extraction and Generalization

It is interesting to gain some insight into the problem of how many possible generalizations can be obtained. Given a neural network with N input bits and one output bit, there are 2^N possible input presentations each of which might have either output value. Then there are 2^{2^N} possible mappings. Training the network with P distinct input presentations, only P out of 2^N entries of the truth table, leaves $2^{2^N - P}$ mappings consistent with the training set. Realistic numbers like $N=30$ and $P=1000$ give 2^{10^9} generalizations.

This incredible amount of possibilities is the main problem to overcome on any ANN application: how to ensure that the generalizations of the neural network will be the ones with a good overall performance. The answer lies in the nature of the rules that are specified. The information required to specify an arbitrary rule on N bits is 2^N bits, but N^k bits is enough to represent any reasonable rule, for some small k [64]. Also, the representation of most arbitrary rules would require an exponentially large number of hidden units, which is a practical limitation.

Some work has been done in order to obtain quantitative estimates of generalization, such as the average number of alternative generalization of a training set, the proba-

bility that the trained network will generate the right output for any input, or a measure of the worst case scenario.

One of the most important theoretical results about feedforward networks is that only one hidden layer is enough to approximate any continuous function [66], better known as the *universal approximation theorem*. Further work has been able to quantify the ability of the network to generalize to new data as a function of general factors like size of the training set, amount of hidden units, number of inputs and the target function itself; which in turn can lead to an optimization of the amount of hidden neurons. This is an existence theorem that has limited practical value though. In fact, the approximation becomes more manageable using an ANN with two hidden layers [63].

When considering the size of the training set for a valid generalization, a useful result has been obtained for the case of a neural network containing a single hidden layer and used as a binary classifier. Its simplified expression [63] is given by:

$$N > \frac{W}{\varepsilon} \quad (3-20)$$

where N is the required amount of samples used to train the network, W is the number of weights and the factor $\varepsilon/2$ is the maximum error permitted on the training set. This expression offers a worst case limit, therefore there can be a huge gap between this limit and what is actually required in practice, where the size is usually smaller.

As it can be seen, the theoretical background for a successful generalization lacks of a solid basis to give or generate specific rules to follow. The solution is a practical approach where the rules are based in cumulative experience in the field, hints from theoretical results, and the experience and common sense of the user.

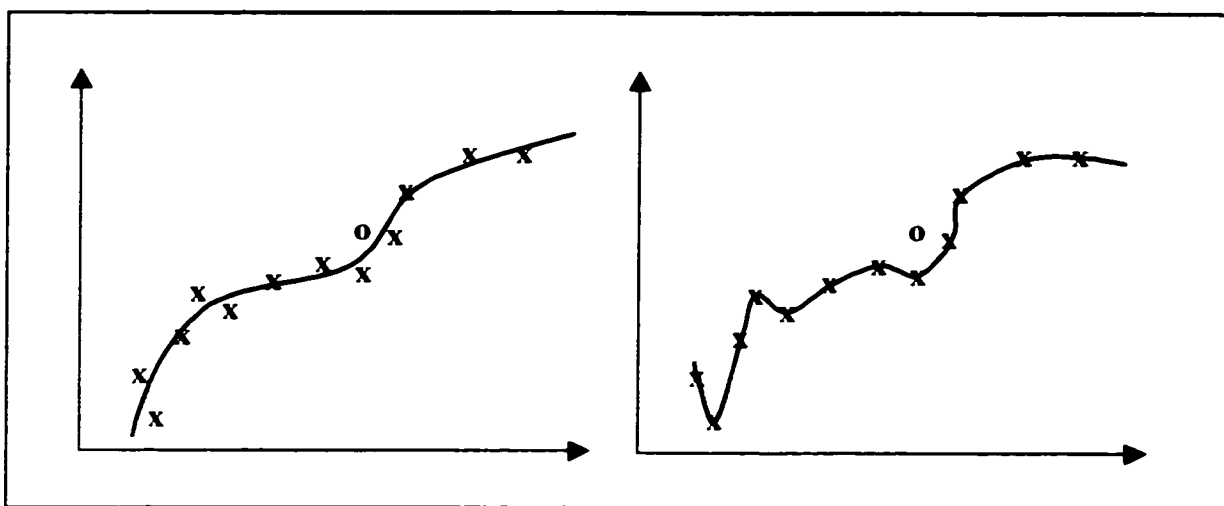


Figure 3-4: Good Fit and Overfitting of Noisy Data

For example, when dealing with the amount of hidden neurons, experience learned from statistics and curve-fitting indicates that too many hidden units can result in an overfitting of the training set due to the amount of free parameters. This situation is represented in Figure 3-4 where the effects of the overfitting can lead the ANN to learn certain specifics, like noise, not necessarily part of the pattern.

Nevertheless, this problem can be detected and avoided with the use of an adequate validation set in a technique called *cross-validation*, also borrowed from statistics. The idea is to check the error over the validation set while training the neural network. This concept is illustrated in Figure 3-5, where one complete presentation of the entire training set during the learning process is called an epoch. The first application of this technique is to tune the internal complexity of the ANN. But it can also be applied to determine when the training of a network should stop, to define the actual size of the training set or even inserted into the learning algorithm to define the learning rate according to the performance.

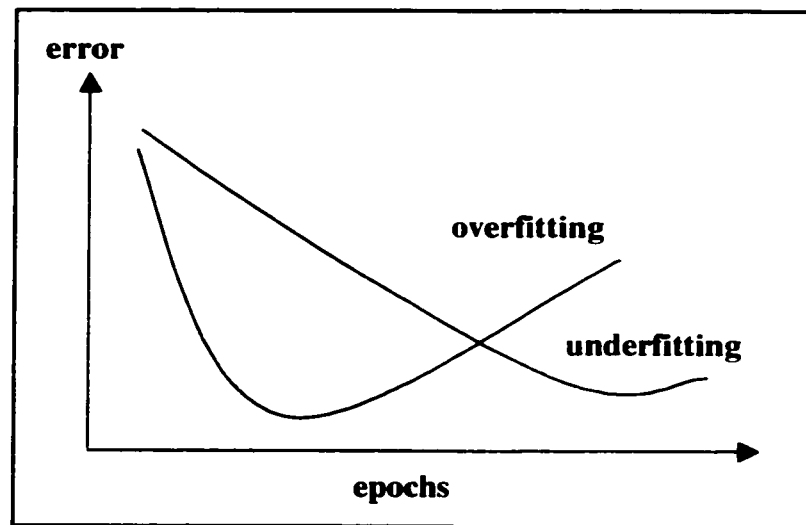


Figure 3-5: Cross-validation

Having said this, it is clear that any new engineering application of ANN represents both a challenge and a learning experience where the developer plays, in general, an important role in the success of the application.

CHAPTER 4

PROPOSED METHOD

4.1 Introduction

This chapter presents a new method for synchronous machines parameter estimation. The method is based on a pattern recognition approach, where the generalization properties of the ANNs play a fundamental role. Implementation details and particulars are left for the next two chapters where some case studies are presented

4.2 System Identification and Pattern Recognition

At this point, it is worth to clarify some general concepts related to system identification and pattern recognition, as they are useful to understand the relationships with parameter estimation in view of this work.

4.2.1 System Identification

Parameter estimation is commonly accepted as a fundamental step of the system identification process as shown in Figure 4-1 [72].

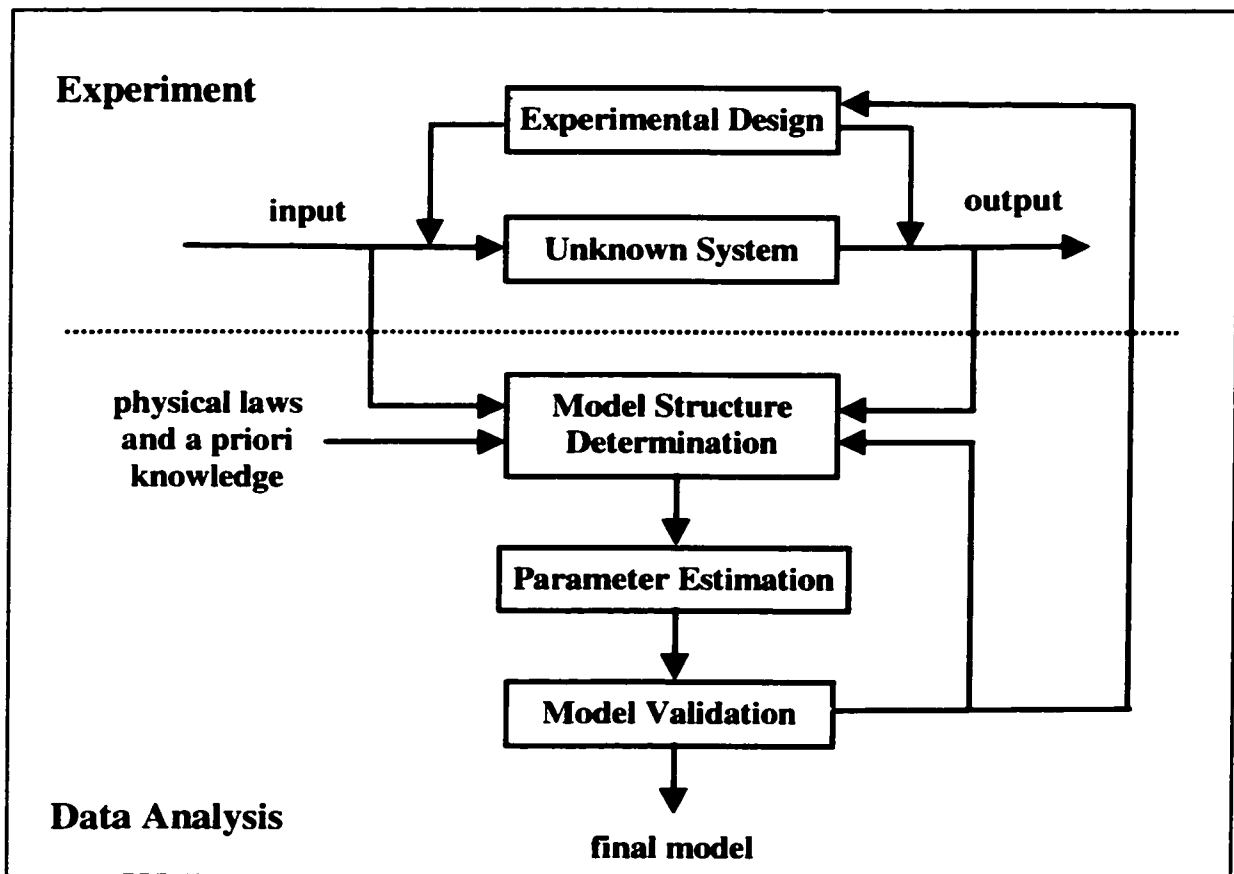


Figure 4-1: System Identification Steps

As it can be seen, system identification is a much broader concept that can be considered as dual to that of controlling a system [73]: a system can be controlled only if it is identified. The concept includes systems where it may not be possible to write mathematical equations that accurately describe the processes of interest. In general, in system identification problems or inverse problems, as they are also called, fundamental properties of a system are to be determined from observed behaviour of the system. The underlying theme is the relationship between the internal structure of a system and the observed output. The hidden features of the system are to be extracted from the experimental data.

4.2.2 Pattern Recognition

The problem of pattern recognition usually denotes the classification and/or description of a set of processes or events [74]. Figure 4-2 [75] offers a schematic of the steps involved in the pattern recognition process.

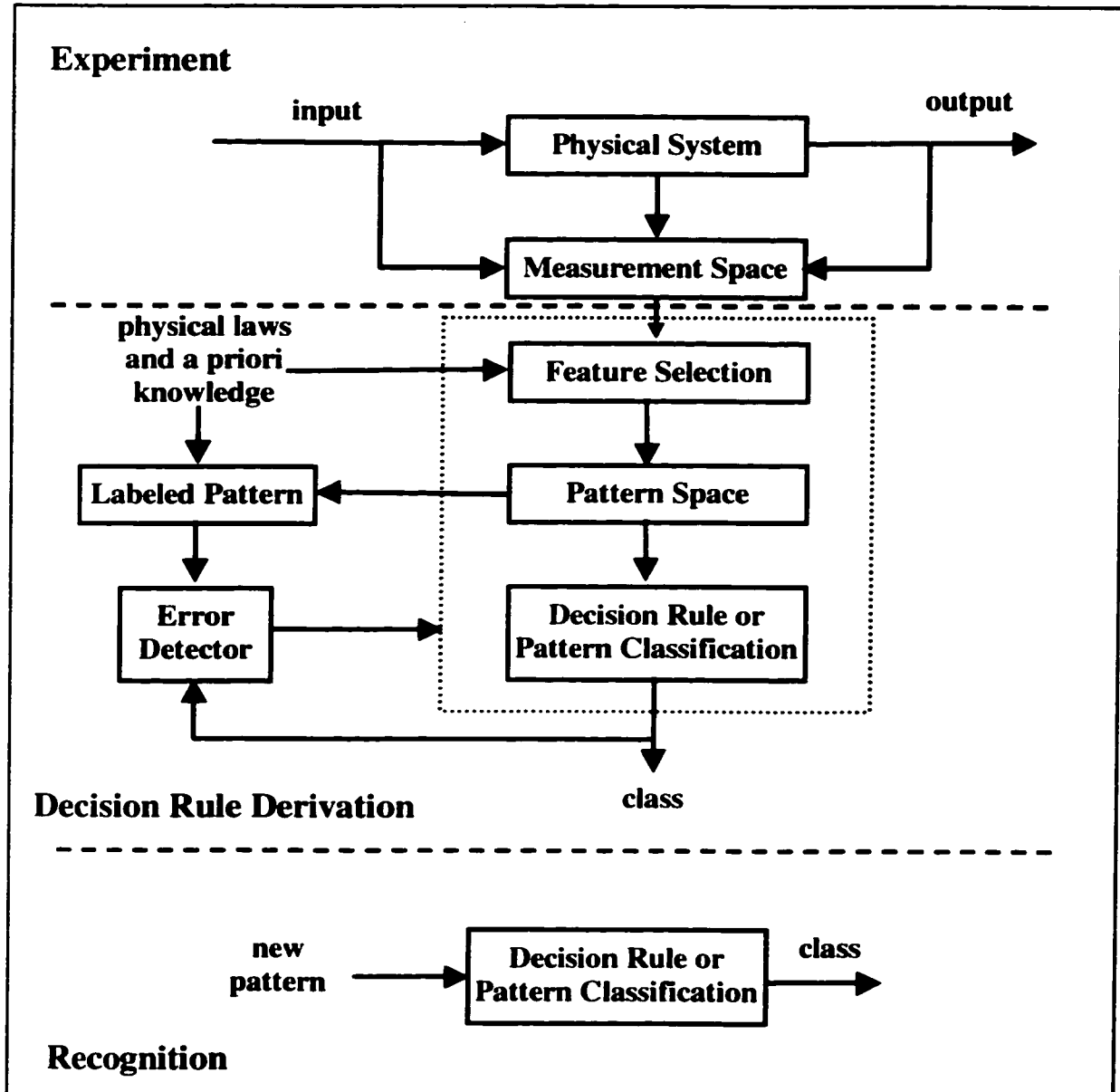


Figure 4-2: Steps Involved in the Pattern Recognition Process

Once all the required data is obtained, the development of a decision rule and using it are the two main stages of the pattern recognition process. While developing a decision rule, feature selection or preprocessing and pattern classification are the main aspects to consider. Feature selection is the process by which measurement characteristics are described by a set of numbers that become components of the pattern space.

Indeed, the goal is to reduce the dimensionality of the measurement space, which can also be considered a pattern space, extracting the unique characteristics of the problem. Finally, a decision rule must be derived in order to correctly classify the patterns. This is a learning process that, in the most simplified version, involves only feedback over the decision rule in order to reduce the classification errors. In general, the feedback will transcend this limit up to the feature selection phase, and could even reach the experimental stage, if the measurements are incomplete.

When applying this concept to the parameter estimation problem the classes are the possible sets of parameters. Therefore, the classification takes place over a continuous domain. Although this does not contradict any principle or premise of pattern recognition, its usage does not seem to be common in practice where the classification usually takes place over a discrete set of classes.

The similarities of the schematic of Figure 4-2 with any application of ANNs are remarkable. Actually, an ANN can be thought of as nothing but a highly complex tool for pattern recognition, where the feature extraction and decision rule are embedded into the structure of the neural network. There is abundant literature on the usage of ANN for pattern recognition purposes [76,77].

4.3 Parameter Estimation as a Pattern Recognition Problem

Synchronous machine parameter estimation can be considered as a pattern recognition problem. In this sense, it is useful to understand the direct and inverse problems involved in dealing with the SM model.

One SM under different operating conditions will have a unique response determined by its physical characteristics. Alternatively, a SM model provided with appropriate parameters and all the required variables to solve the mathematical equations (boundary conditions) can be used to estimate the behaviour of the physical system. How good the estimation is will depend on the accuracy of the model, its parameters, and the boundary conditions. A picture of the direct problem is represented in Figure 4-3.

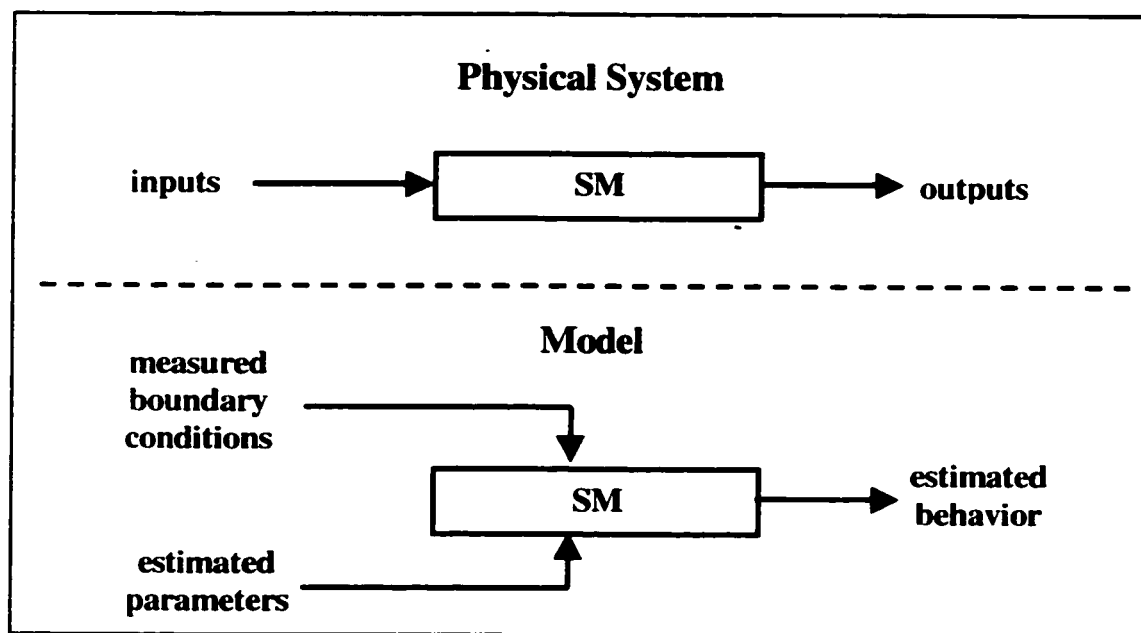


Figure 4-3: Direct Problem

It is possible to think, at least in theory, on the existence of an inverse model that when given the behaviour of the synchronous generator and the boundary conditions, could extract the fundamental characteristics of the model. Furthermore, for a fixed set of boundary conditions, the behaviour of the SM can be thought as a pattern that uniquely identifies its characteristics, i.e., the SM parameters. Then, given the pattern, it should be possible to obtain the parameters as shown at the bottom of Figure 4-4.

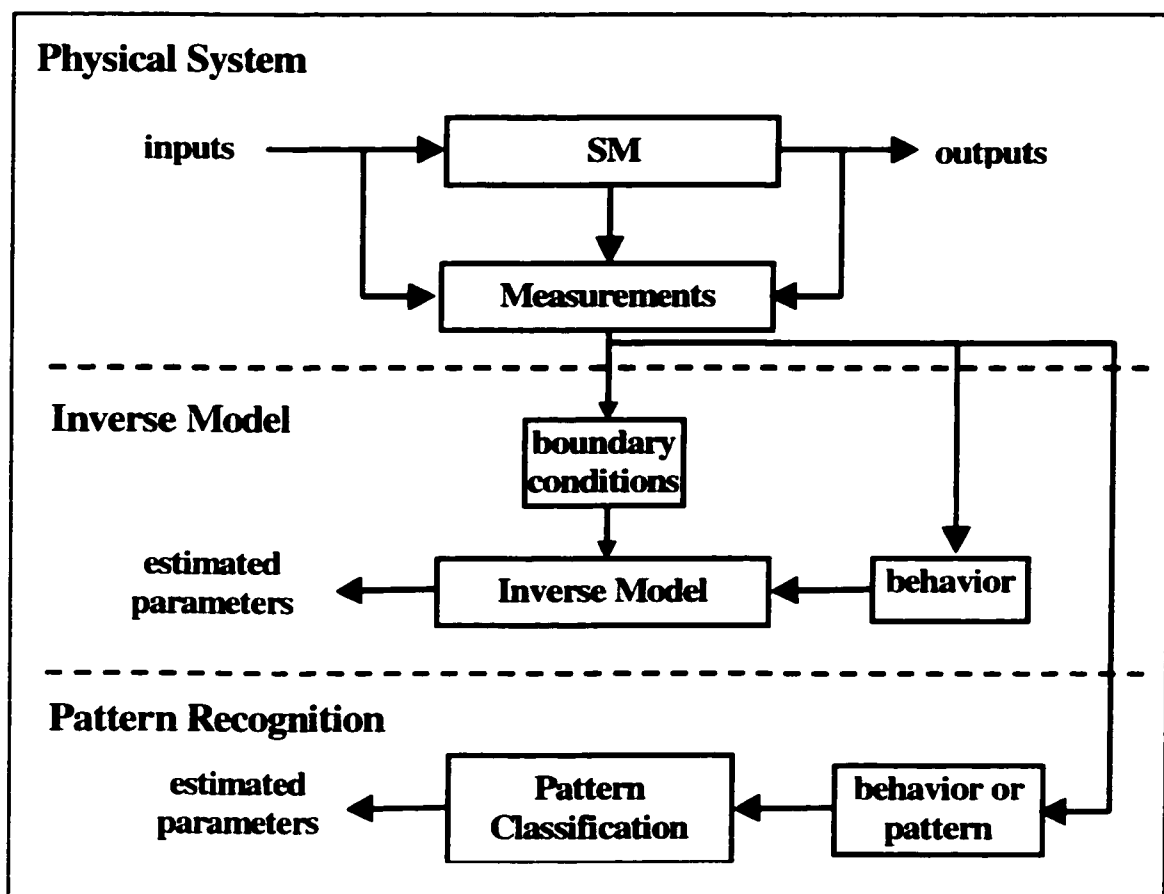


Figure 4-4: Inverse Problem

To explore the parameter estimation problem with a pattern recognition approach is the central idea behind this work

4.4 Proposed Method

Figure 4-5 presents the different stages involved in the new method, explained in more detail in the following sub-sections

4.4.1 Data Acquisition Stage

- (a) *A priori knowledge*. The data acquisition stage is a phase where all the field measurements take place. Basically, the main input is given by the previous knowledge about the problem. As a physical device, the generator has restrictions under which it should be operated. The restrictions are imposed both by its internal design as well as by system requirements. Indeed, it is not acceptable to impose any operating conditions on a synchronous machine without having an accurate idea of the outcome. Then, the previous knowledge restricts the amount of inputs.
- (b) *Inputs and Outputs*. The *Inputs* are the actual boundary conditions that are imposed. These can be actual variables on the machine, like field or armature voltages among others, or external events to the synchronous machine like perturbations on the system to which the generator is subjected.

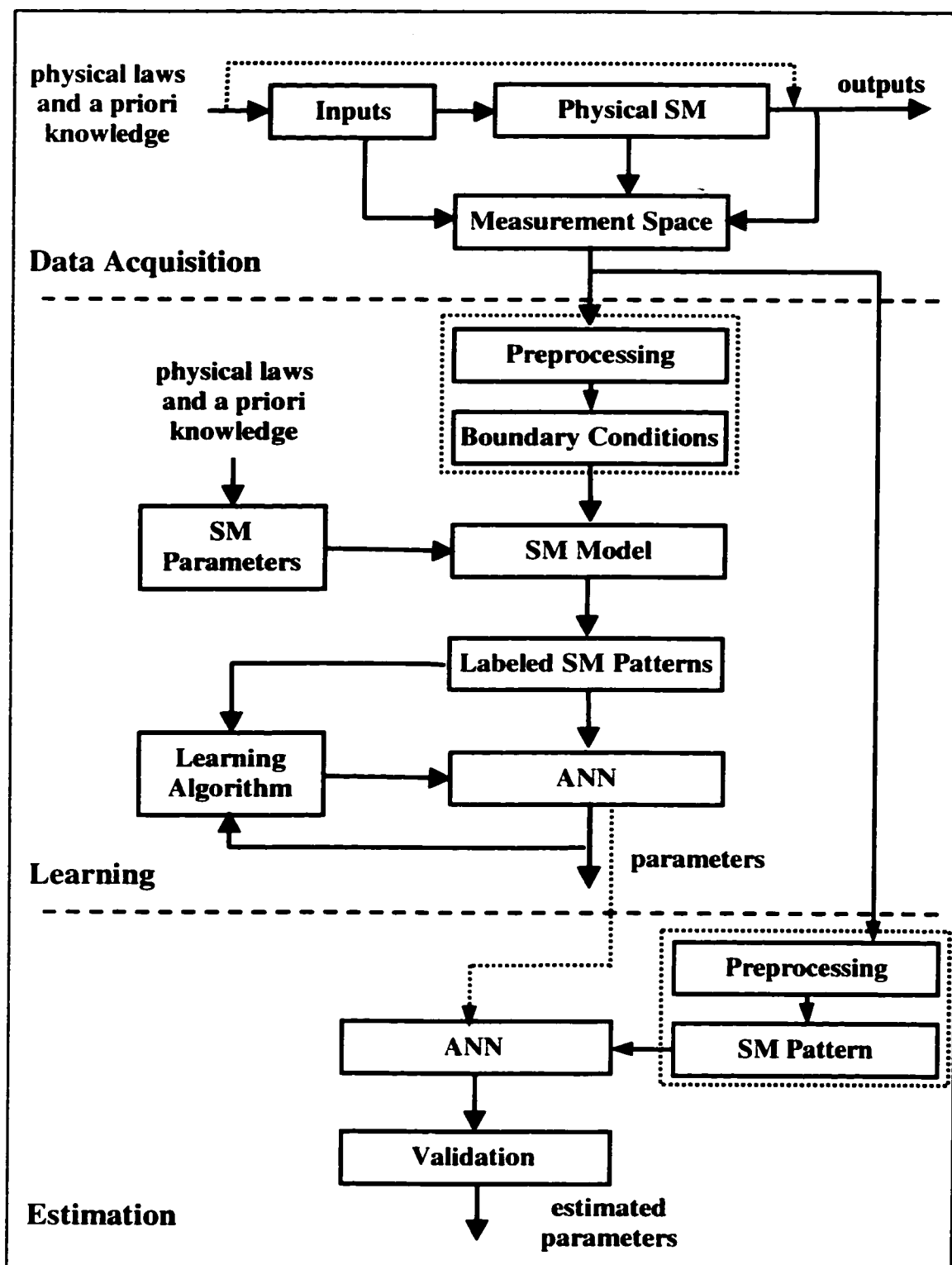


Figure 4-5: Stages of the Proposed Estimation Method

The *Outputs* are the results of fixing these variables or the consequences of the external events on the synchronous generator. How the synchronous generator reacts to specific inputs can be considered as being the outputs of the model.

In terms of measurable variables, there is no distinction between inputs and outputs. In fact, what can be considered as an input for one test, can be the output of another one.

- (c) *Measurement Space*. In essence, the measurement space is formed with the values of all the variables measured during the experiment. This should include the quantities that have been defined as essential to be able to proceed with the method at the learning and estimation stages, as well as the ones that will allow validation studies to be performed on the estimated parameters.

4.4.2 Learning Stage

- (a) *Boundary Conditions*. The measurements are the main input from the previous stage. In this sense, some preprocessing may be required to transform the raw values from the field in order to obtain adequate boundary conditions. Acceptable boundary conditions are those that can be used to solve the differential equations or mathematical model presented in Chapter 2, like the time varying voltages from transient conditions or *PQV* steady-state conditions.

It is important to note that the boundary conditions are fixed as a result of the experimental stage. In this sense, it is also reasonable to think that previous studies will result in requirements on these boundary conditions

that certainly will affect what is done on the field or in the experimental phase. This means that the estimation stage, probably for most cases, will be previously simulated in order to define the acceptable boundary conditions. All these studies will result in a priori knowledge that is actually an input of the previous stage.

- (b) *SM Parameters*. Another input, local to this stage, is the previous knowledge about the parameters of the synchronous machine that will, in turn, be used to generate a pool of possible SM parameters. The goal here is to generate a population of possible SMs, expecting that the actual SM will be included within the boundaries of this population. The parameters offered by the manufacturer should be considered, in most cases, as a good starting point. Other possibilities are the machine characteristics based on design, size, etc. A simple way to proceed is to delimit a possible range of variation for those parameters, and randomly generate sets of parameters within those ranges.
- (c) *SM Model*. Once the sets of possible parameters and the set of boundary conditions have been defined, the equations of the SM can be solved in a conventional way. It should be noted that each set of parameters has to be used for each boundary condition or vice-versa. Depending upon the size of these variables, this step can be very intensive in terms of computation and should receive appropriate consideration.
- (d) *Labeled SM Patterns*. From the solution of the machine model, variables can be extracted to form a pattern that will be representative of the behaviour of that particular set of parameters under different operating condi-

tions. To be more specific, each set of parameters or SM_j , will have a sub-pattern for each set of boundary conditions i of the form:

$$P_{ij} = [p_{1,ij} \quad \cdots \quad p_{n,ij} \quad \cdots \quad p_{N_i,ij}] \quad (4-1)$$

where p are the variables used to form the pattern and N_i is the number of variables used to form part of the pattern for this particular boundary condition.

If all the boundary conditions are considered, SM_j will have a pattern given by:

$$P_j = [P_{1j} \quad \cdots \quad P_{ij} \quad \cdots \quad P_{Ij}] \quad (4-2)$$

where I is the amount of boundary conditions.

When all the possible machines are considered, all the patterns can be represented using matrix notation as:

$$P = [P_1 \quad \cdots \quad P_j \quad \cdots \quad P_I] = \begin{bmatrix} \begin{bmatrix} P_{11} \\ \vdots \\ P_{i1} \\ \vdots \\ P_{I1} \end{bmatrix} & \cdots & \begin{bmatrix} P_{1j} \\ \vdots \\ P_{ij} \\ \vdots \\ P_{Ij} \end{bmatrix} & \cdots & \begin{bmatrix} P_{1I} \\ \vdots \\ P_{iI} \\ \vdots \\ P_{II} \end{bmatrix} \end{bmatrix} \quad (4-3)$$

In this stage, the sets of parameters or SMs that gave origin to the patterns (4-3) are known. Using the same notation, each pattern j will have a corresponding SM_j :

$$SM = [SM_1 \quad \dots \quad SM_j \quad \dots \quad SM_J] \quad (4-4)$$

Finally, (4-3) and (4-4) can be combined to form the matrix of labeled SM patterns LP :

$$LP = \begin{bmatrix} SM \\ P \end{bmatrix} = \begin{bmatrix} [SM_1] & \dots & [SM_j] & \dots & [SM_J] \\ [P_{11}] & & [P_{1j}] & & [P_{1J}] \\ \vdots & & \vdots & & \vdots \\ P_{i1} & \dots & P_{ij} & \dots & P_{iJ} \\ \vdots & & \vdots & & \vdots \\ P_{I1} & & P_{Ij} & & P_{IJ} \end{bmatrix} \quad (4-5)$$

(e) *ANN and Learning Algorithm.* Once all the patterns have been obtained, the goal is to use them to teach an ANN how to recognize the patterns and identify them with the corresponding set of parameters that represent each pattern.

Any learning algorithm from the ones presented in Chapter 3 can be used to train the ANN. In a very conventional way, the set of parameters obtained from the ANN will be compared to the parameters from the labeled pattern in order to get an error and so on. An alternative approach can consider a function of the parameters, like using them to form a new pattern under the same boundary conditions and just comparing the patterns.

After each iteration of the learning process, a tentative set of parameters can be obtained. Information of the actual generator can be used to check the validity of these parameters and determine which is the best set of parameters. In the end, the output of the training stage is a trained ANN that is able to produce a set of SM parameters when fed by a SM pattern with an acceptable error.

4.4.3 Estimation Stage

- (a) *SM Pattern*. The pattern for the actual SM should be obtained using the field measurements. Some preprocessing may be required in order to make this pattern similar to that of expression (4-2), for a generic machine j .
- (b) *ANN and Validation*. The trained network from the previous stage is fed with the pattern of the actual SM to obtain the parameters. In order to accept the parameters, proper validation studies on the estimated parameters are a necessary and very important final step. Eventually, more studies may be required which will materialize in proper adjustments into the learning stage.

4.4.4 Implementation

The method has been exposed in a general manner being open to many variants. Trying to define specific rules for the actual implementation can result in a very frustrating task due to the explosion on the amount of possible solutions.

Details of the approach followed here will be fully addressed in the next two chapters that are devoted to the practical implementation of the method to obtain the steady-state and dynamic parameters of synchronous generators.

CHAPTER 5

STEADY-STATE ANALYSIS

5.1 Introduction

This chapter accounts for the practical application of the proposed method to estimate the parameters of the SM responsible for its steady-state behaviour. The method will be applied to both a salient pole micro-alternator and a round rotor turbo-generator. Two studies will be presented for each type of SM corresponding to the cases when the load angle is considered a variable of the pattern or not. This chapter, as well as the next one, make use of all the theoretical background presented in the previous chapters.

5.2 Pattern Formation

In principle, any point in the capability region is a potential candidate to form part of the pattern that represents a specific machine. Considering a linear model, it is intuitive that having the points spread as much as possible within the capability range, will ensure to have a good representation for the pattern. In addition, the minimum amount of points required is, at least, the amount of parameters to be determined.

In theory, the extension of the analysis to consider saturation is straightforward if there are no restrictions on the amount of points that can be incorporated into the patterns. In practical terms though, the amount of inputs to the ANN should be kept under control,

in which case, the requirements on the points that will be part of the pattern increase substantially.

Figure 5-1 and Figure 5-2 plot the different levels of saturation, showed as percentage (out of one) for the direct and quadrature axis for the data given in Table 5-1.

Table 5-1: Typical SM Data		
Parameter	"d" axis	"q" axis
I_a	0.1550	0.1550
L_m	1.8580	1.7620
A	0.0719	0.2583
B	5.8312	2.8352
V_z	0.6356	0.4574
V_o	0.8000	0.6000

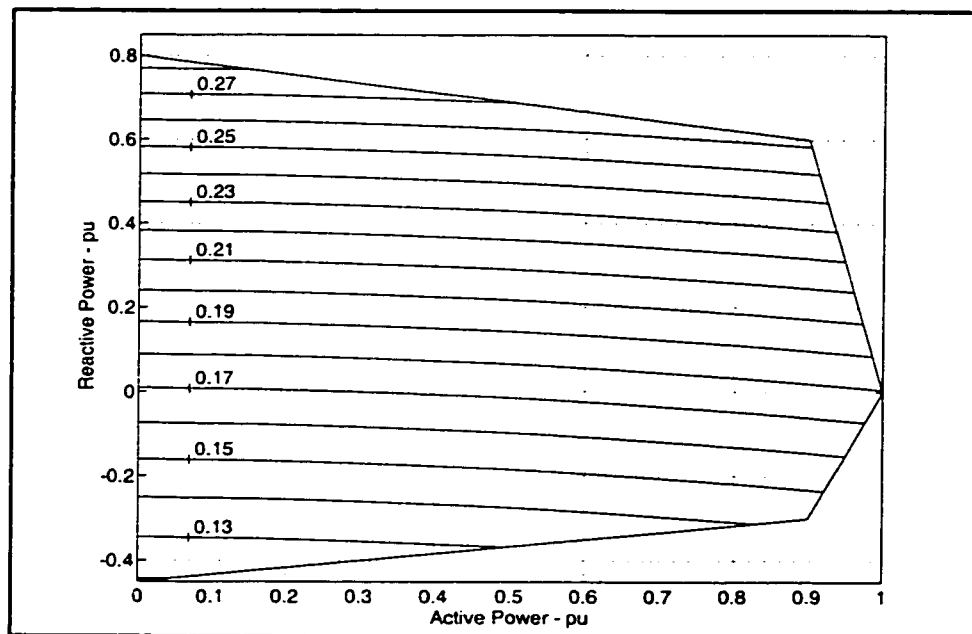


Figure 5-1: Direct Axis Saturation (1-Ksd)

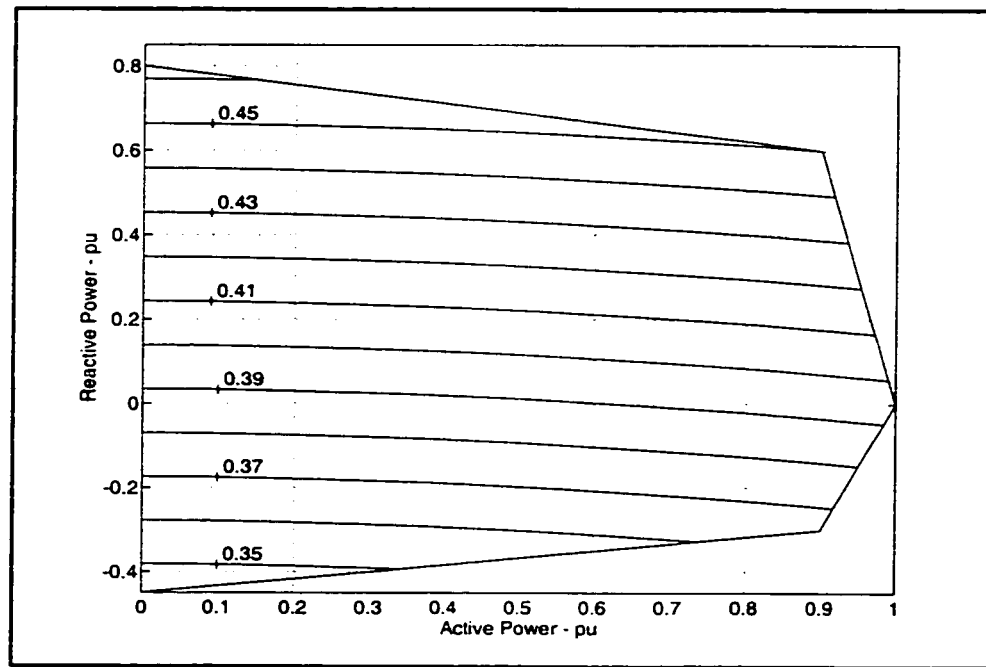


Figure 5-2: Quadrature Axis Saturation (1-Ksq)

From the figures it can be seen saturation has a strong correlation with the reactive power. Then, patterns formed with points that have a bigger variance over the reactive power component will carry much more information about the saturation characteristics of the SM. This observation is valid for both the direct and quadrature axes.

5.3 Case Study: Salient Pole Micro-Generator

Experimental studies have been carried out on a micro-generator with the ratings given in Table 5-2.

Table 5-2: Micro-Generator Ratings	
Characteristics	Values
Power	3.0 KVA
Voltage	220 V
Power Factor	0.8
Speed	1800 rpm
No. of poles	4

The set up for the tests as well as the measured data is contained in Appendix D. The operating points are summarized in Figure 5-3.

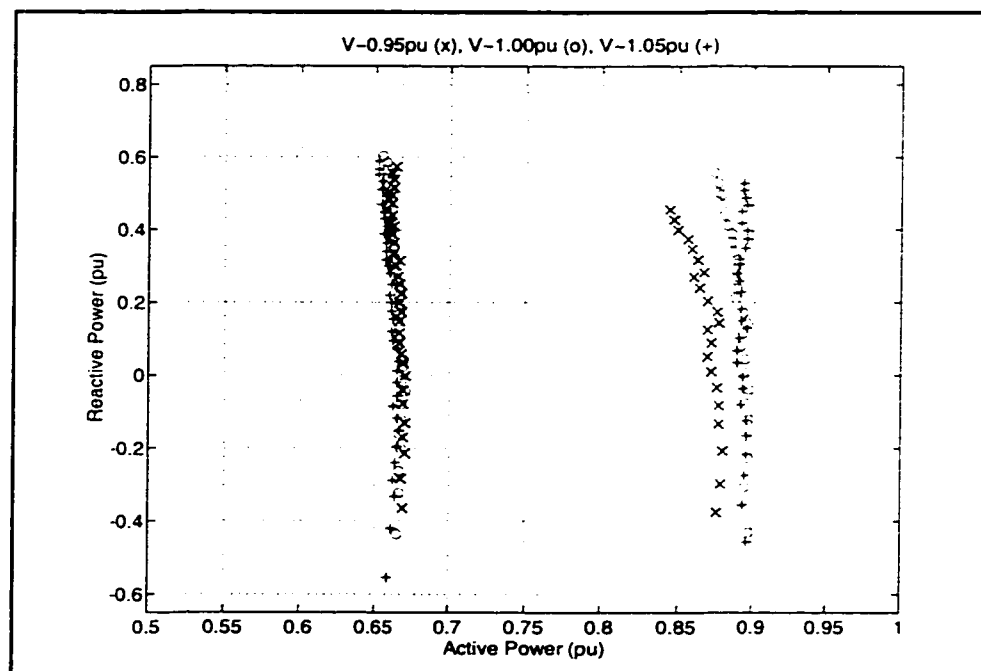


Figure 5-3: Operating Points

5.3.1 General Procedure and Pattern Formation

Table 5-3 shows some of the measured points of Appendix D selected to conduct the estimation studies. According to their usage, the points have been grouped as Training and Validation points

Table 5-3: Training and Validation Points			
Groups	PQV Operating Points		
	P(pu)	V(pu)	Point No (refer to Appendix D)
TGroup	~0.87	~1.00	25 29 34 38 40 43 46 48 49
	~0.65	~1.00	115 120 124 129 133 136 140 142 144
VGroup1 & VGroup2	~0.87	~1.00	24 28 32 36 39 42 45 47 49
	~0.65	~1.00	117 122 126 131 134 139 141 143 145
VGroup2	~0.87	~0.95	2 4 7 10 13 16 19 20 21
	~0.87	~1.05	53 56 61 64 68 70 74 76 77 78
	~0.65	~0.95	80 83 88 93 97 100 104 107 109 110
	~0.65	~1.05	148 152 156 161 165 169 172 176 178 180 181 182

The operating points specified in the *Training Group* TGroup will be used to generate the training set for the ANN. This means that the pattern of the actual SM will be formed by variables extracted from these operating points.

A population of possible SMs can be generated by imposing random variations within a specified range of a predetermined *root set* of parameters, as it is specified in Table 5-4.

Table 5-4: Root Set of Parameters and Ranges		
Parameter	Root Value ^a	Range ^b
L_{md}	2.0000	$L_{mdo} \pm 20\%$
L_{mq}	1.3000	$L_{mqo} \pm 20\%$
I_a	0.1100	$I_a \pm 40\%$
S_{1d}^c	0.0600	$S_{1do} \pm 40\%$
S_{2d}	0.1800	$S_{2do} \pm 20\%$
V_{zd}	0.6000	V_{zdo}
V_{od}	0.8000	V_{odo}
S_{1q}	0.0000	S_{q1o}
S_{2q}	0.0000	S_{q2o}
r_a	0.0167	r_{ao}
I_{fnv}^d	1.2077 (A)	I_{fnvo}

- a. Values are in pu unless otherwise specified.
- b. Variables with the final sub-index "o" refer to the root value.
- c. S_{1d} and S_{2d} are the values of the saturation function S_d specified for a voltage V of 1.0 and 1.2 pu respectively.
- d. I_{fnv} is the field current that in absence of saturation would produce a rated open circuit terminal voltage.

Each SM generated in this way will have a set of boundary conditions (BCs) associated with it. These BCs can, eventually, be the same for all the SMs, in which case the set is given by the PQV values of each of the operating points selected as part of the TGroup. Alternatively, variations can be imposed to these base values to generate a unique set of BCs for each SM. Table 5-5 shows the variations used during the studies.

Table 5-5: Boundary Conditions and Ranges		
TGroup Points	Variable	Range
Point "j" $\Rightarrow \{P_{oj}, Q_{oj}, V_{oj}\}$	P_j	$P_{oj} \pm 0.05 \text{ pu}$
	Q_j	$Q_{oj} \pm 0.05 \text{ pu}$
	V_j	V_{jo}

Once a set of BCs is defined, the model of the SM can be evaluated for that specific set of SM parameters and all the BCs. Only the field current (I_f), load angle (δ), active power (P), and reactive power (Q) will be considered as the possible variables to form part of the pattern, and different subcases will be contemplated according to which variables are used to form the pattern

When this is extended over the whole set of generated SMs, a training set for the ANN is obtained, like the one specified in equation (4-3) of the previous chapter. The pattern that characterizes the actual SM under consideration has to be formed with the corresponding variables extracted from the TGroup points from Table 5-3. The target set to train the ANN is given by the parameters of each of the generated SMs, in the form specified in equation (4-4).

Table 5-6: Consideration of Noise	
Variables	Noise
I_f	$\pm 0.5\%$ of I_{fnv}
δ	± 0.5 degrees
P	$\pm 0.0025 \text{ pu}$
Q	$\pm 0.0025 \text{ pu}$

The magnitudes obtained from the measurements are a combination of the actual signal under consideration, noise, and errors from the instruments involved in the tests. To consider these adverse effects into the studies, the variables that form the pattern are affected by noise, as per Table 5-6.

It is possible to define different training sets for the cases when the load angle δ is considered a variable of the pattern or not, with the characteristics defined in Table 5-7. The structures of the ANNs for each of the previous cases are specified in Table 5-8. The learning algorithm used to train the ANNs is the backpropagation method with adaptive learning rate and momentum, as presented in section 3.3.1, using the parameters specified in Table 5-9. Also, five training tries corresponding to different initial sets of weights will be shown..

Table 5-7: Training Sets Characteristics		
Attribute	Case	
	If δ PQ	IfPQ
No. of SMs	2500	
No. of BCs	18	
Variables per BC	I_f, δ, P, Q	I_f, P, Q
Targets per SM	$L_{md}, L_{mq}, I_a, S_{d1}, S_{d2}$	

Table 5-8: ANNs Characteristics		
Attribute	Case	
	If δ PQ	IfPQ
No. Inputs	72	54
No. Hidden 1	18	
No. Hidden 2	5	
No. Outputs	5	

Table 5-9: Training Parameters

Parameter	Value	Parameter	Value
η	0.01 ^a	c_i	1.05
α	0.90	c_d	0.70

a. Initial value.

After each epoch of the ANN training process, a presentation of the pattern corresponding to the actual machine will generate a set of parameters. When these parameters are evaluated for the BCs of a Validation Group of points, it is possible to quantify the performance of each set of parameters by comparing the calculated and measured variables. In order to analyse the importance of the validation group, two validation sets will be considered as specified in Table 5-3: one restricted to the same capability region of the TGroup, Validation Group 1 (VGroup1), and another covering a wider range of possible operating conditions, Validation Group 2 (VGroup2).

The variables that can be used to measure the errors are both the field current and the load angle. Given a set of parameters and the BCs of all the points that form a group, it is possible to form a pattern with the load angle and the field current obtained for each BC. The errors are defined as the differences between the *measured pattern* (*PM*) and the generated pattern (*PG*). Because of the different units involved, the errors are defined as follows. After epoch k , the errors in the currents are expressed as percentage as:

$$EI_k = [PGI_k - PMI] / PMI \cdot 100 [\%] = \begin{bmatrix} pgi_{1,k} / pmi_1 - 1 \\ \vdots \\ pgi_{i,k} / pmi_i - 1 \\ \vdots \\ pgi_{N,k} / pmi_N - 1 \end{bmatrix} 100 [\%] \quad (5-1)$$

where “/” denotes the quotients of the individual elements; pgi and pmi are the current components of the generated and measured patterns, respectively; and N_i is the number of components of the pattern. The load angle errors are given by the differences as:

$$E\delta_i = [PG\delta_k - PM\delta] [\text{degrees}] = \begin{bmatrix} pg\delta_{1,k} - pm\delta_1 \\ \vdots \\ pg\delta_{i,k} - pm\delta_i \\ \vdots \\ pg\delta_{N,k} - pm\delta_N \end{bmatrix} [\text{degrees}] \quad (5-2)$$

where the notation is similar to that used for equation (5-1).

Once the errors are obtained, it is possible to analyse the performance of each set of parameters by calculating the mean value (Mean), the standard deviation (StD), and the maximum value (Max) of the error by defining the following performance indexes:

$$PerfI_k = |Mean(EI_k)| + StD(EI_k) + Max(|EI_k|) \quad (5-3)$$

$$Perf\delta_k = |Mean(E\delta_k)| + StD(E\delta_k) + Max(|E\delta_k|)$$

These definitions have proven to be a very simple and effective way of obtaining a performance index that allows the comparison of different set of parameters: the best set of parameters will have its performance index closer to zero (0.0). Furthermore, when both the field current and load angle are compared simultaneously, a unified performance index can be obtained as the arithmetic sum of the individual performance indexes as:

$$Perf_k = PerfI\delta_k = PerfI_k + Perf\delta_k \quad (5-4)$$

5.3.2 If δ PQ Case

The training set defined in Table 5-7 is used to train the ANN defined in Table 5-8 for this specific case. The ANN is trained for five different initializations.

The error through the training process for Try 3 against the points from VGroup1 is plotted in Figure 5-4 and Figure 5-5 for the field current and load angle, respectively.

The best performance from each training process measured over the VGroup1 is summarized in Table 5-10 and the corresponding parameters are given in Table 5-11. Generalization can be tested by measuring the performance of the previous sets of parameters over the extended VGroup2 as it is done in Table 5-12. The errors generated by the parameters with the best performance index (Try 3) are plotted as functions of the voltages and active power in Figure 5-6 and Figure 5-7.

The improvements in the selection of the parameters using the VGroup2 can be seen in Table 5-13 and the corresponding sets of parameters in Table 5-14. The results are plotted in Figure 5-8 and Figure 5-9.

It can be said then that using the variables {If δ PQ} as components of the patterns, it is possible to obtain the parameters of the SM. Furthermore, using only a restricted set of points to make the selection, the parameters will have an excellent overall performance. When the performances of using VGroup1 (Table 5-12) and VGroup2 (Table 5-13) are compared, the gain of using an extended set of validation points to select the parameters is only marginal.

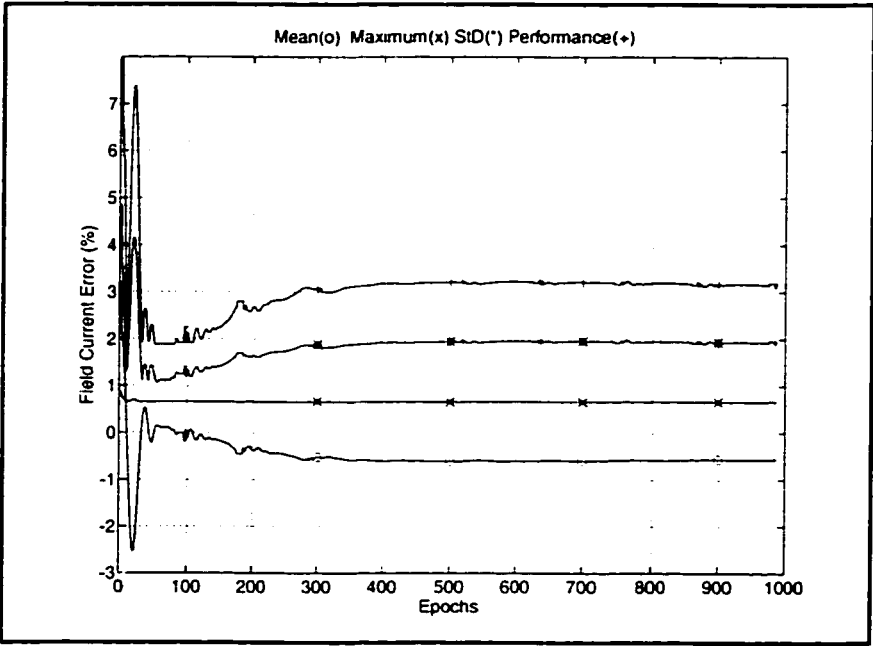


Figure 5-4: Field Current Error for Try 3 Using VGroup1

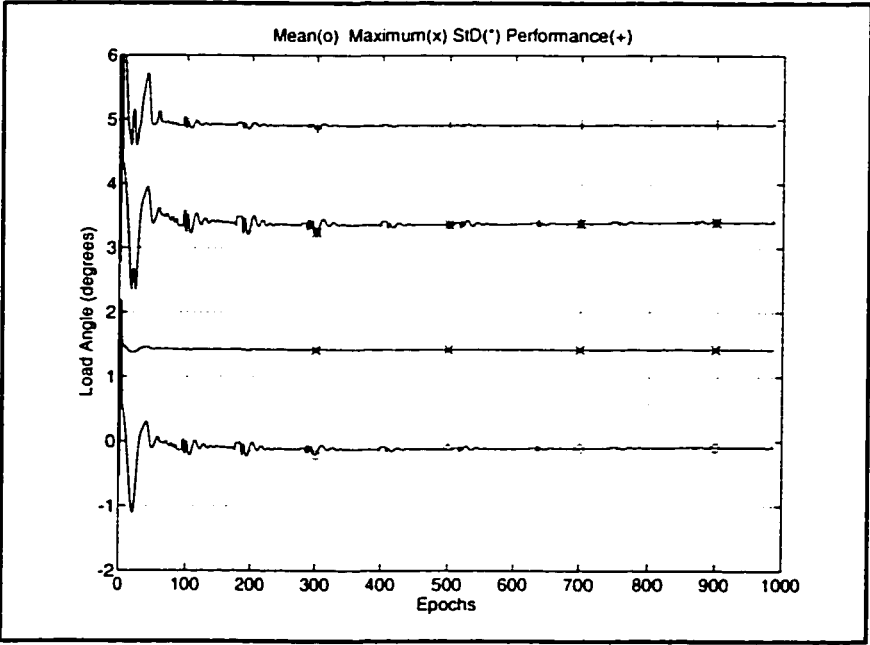


Figure 5-5: Load Angle Error for Try 3 Using Vgroup1

Table 5-10: Best Performances Using VGroup1

Try	Epoch	Perf	If Error (%)			δ Error (degrees)		
			Mean	StD	Max	Mean	StD	Max
1	34	6.849	0.17	0.68	1.11	-0.16	1.42	3.30
2	103	7.908	0.72	0.68	1.64	-0.21	1.41	3.24
3	106	6.780	0.07	0.67	1.18	-0.22	1.41	3.23
4	90	6.813	0.04	0.68	1.30	-0.36	1.40	3.03
5	45	6.782	0.18	0.70	1.22	-0.61	1.39	2.68

Table 5-11: Best Performance Parameters Using VGroup1

Try	L_{md}	L_{mq}	l_a	A_d	B_d
1	2.1600	1.4635	0.1116	0.0228	5.1830
2	2.1701	1.4628	0.1093	0.0323	4.4900
3	2.1476	1.4624	0.1094	0.0338	4.3660
4	2.1450	1.4462	0.1169	0.0267	4.9150
5	2.1584	1.4329	0.1150	0.0271	4.6868

Table 5-12: Performance Over VGroup2 with Parameters From VGroup1

Try	Perf VGroup1	Perf VGroup2	If Error (%)			δ Error (degrees)		
			Mean	StD	Max	Mean	StD	Max
1	6.849	8.896	-0.20	1.17	2.88	-0.01	1.33	3.30
2	7.908	8.420	0.35	1.15	2.30	-0.06	1.32	3.24
3	6.780	8.906	-0.30	1.11	2.88	-0.07	1.32	3.23
4	6.813	9.056	-0.32	1.13	3.05	-0.21	1.31	3.03
5	6.782	8.924	-0.20	1.21	3.08	-0.47	1.29	2.68

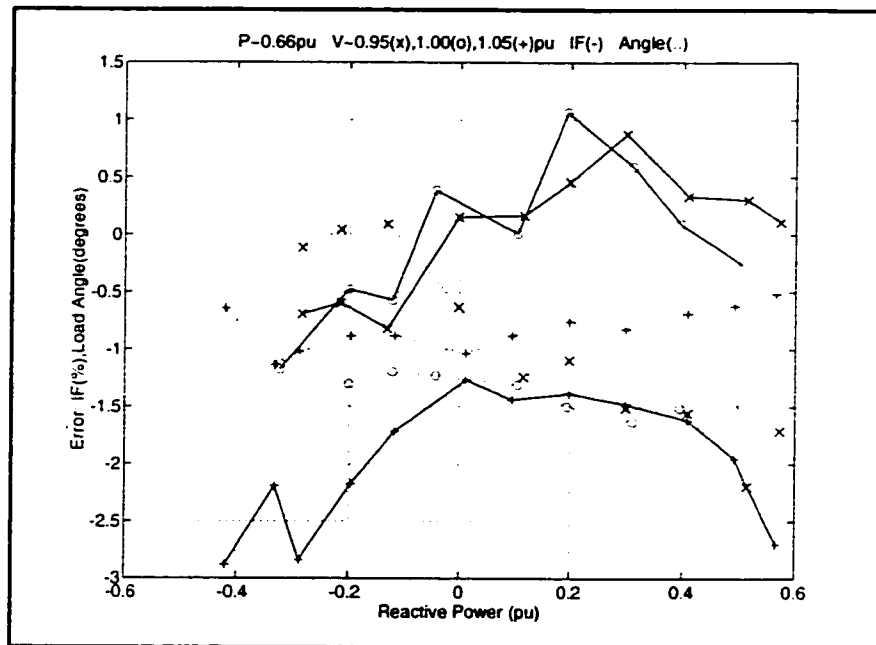


Figure 5-6: Errors for P~0.66 pu Using VGroup1

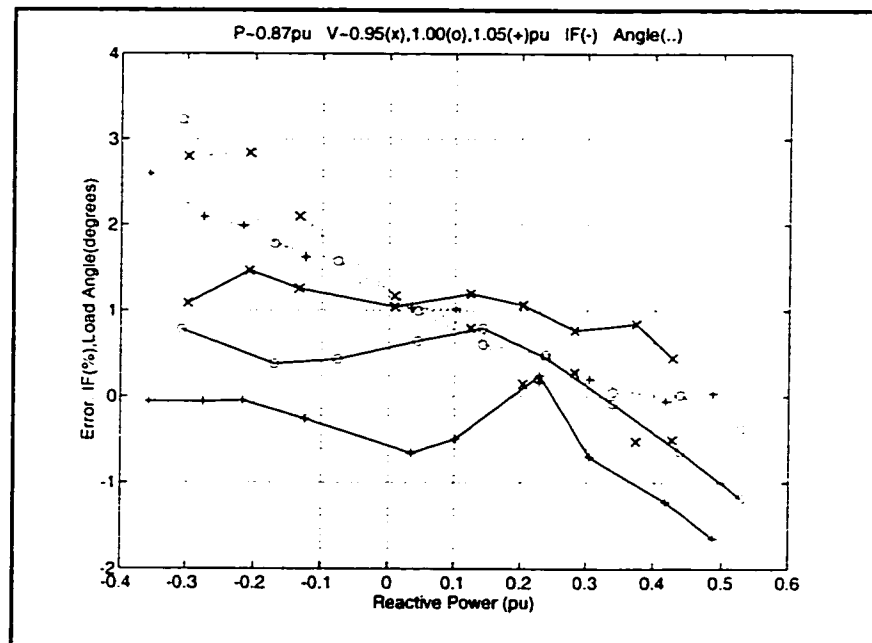


Figure 5-7: Errors for P~0.87 pu Using VGroup1

Table 5-13: Best Performances Using VGroup2

Try	Epoch	Perf	If Error (%)			δ Error (degrees)		
			Mean	StD	Max	Mean	StD	Max
1	35	8.615	0.06	1.19	2.64	0.03	1.33	3.36
2	103	8.420	0.35	1.15	2.30	-0.06	1.32	3.24
3	106	8.906	-0.30	1.11	2.88	-0.07	1.32	3.23
4	129	8.465	0.05	1.16	2.72	-0.24	1.31	2.99
5	46	8.789	0.47	1.26	2.58	-0.36	1.29	2.83

Table 5-14: Best Performance Parameters Using VGroup2

Try	L_{md}	L_{mq}	l_a	A_d	B_d
1	2.1680	1.4664	0.1113	0.0230	5.1763
2	2.1701	1.4628	0.1093	0.0323	4.4900
3	2.1476	1.4624	0.1094	0.0338	4.3660
4	2.1549	1.4427	0.1187	0.0277	4.8331
5	2.1788	1.4384	0.1161	0.0268	4.7269

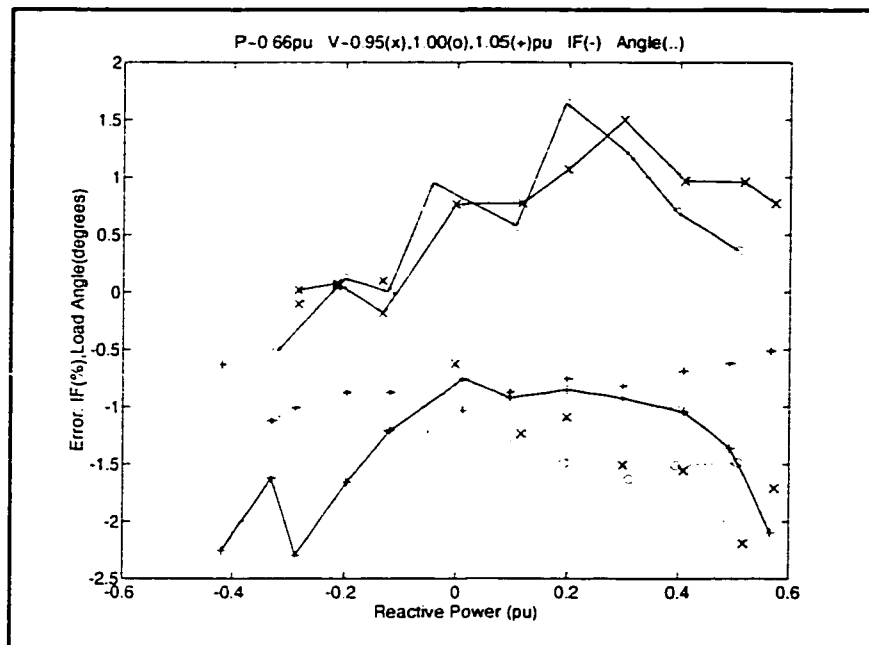


Figure 5-8: Errors for P~0.66 pu Using VGroup2

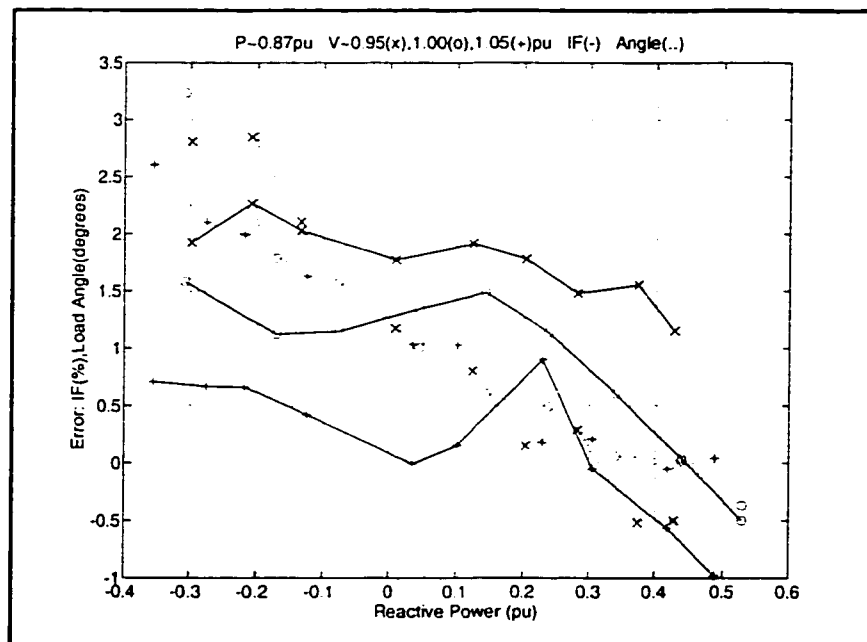


Figure 5-9: Errors for P~0.87 pu Using VGroup2

5.3.3 IfPQ Case

In this case, the training set without the load angle from Table 5-7 and corresponding ANN structure from Table 5-8 are used. The evolution of field current errors through the training process, for try 1, are plotted in Figure 5-10.

Taking into account only the currents to quantify the performances over the VGroup1, it is possible to select the best set of parameters for each try, as shown in Table 5-15 and Table 5-16. In order to check the behaviour of the angles, Table 5-15 also shows the overall performance including the effects of the angles. Generalization can be tested by measuring the performance of the previous sets of parameters over the extended VGroup2 as it is done in Table 5-17. The errors are shown in Figure 5-11 and Figure 5-12.

Using the VGroup2 to make the selection of the best parameters generates the results summarized in Table 5-18 and Table 5-19. The corresponding errors are plotted in Figure 5-13 and Figure 5-14.

The results obtained in Figure 5-11 and Figure 5-12 can be considered as excellent. When compared with the results obtained using an extended validation set in Figure 5-13 and Figure 5-14, the marginal improvement in the field currents is lost in the load angles. What comes as a surprise is that the results are comparable to the ones obtained using the load angle δ as part of the patterns.

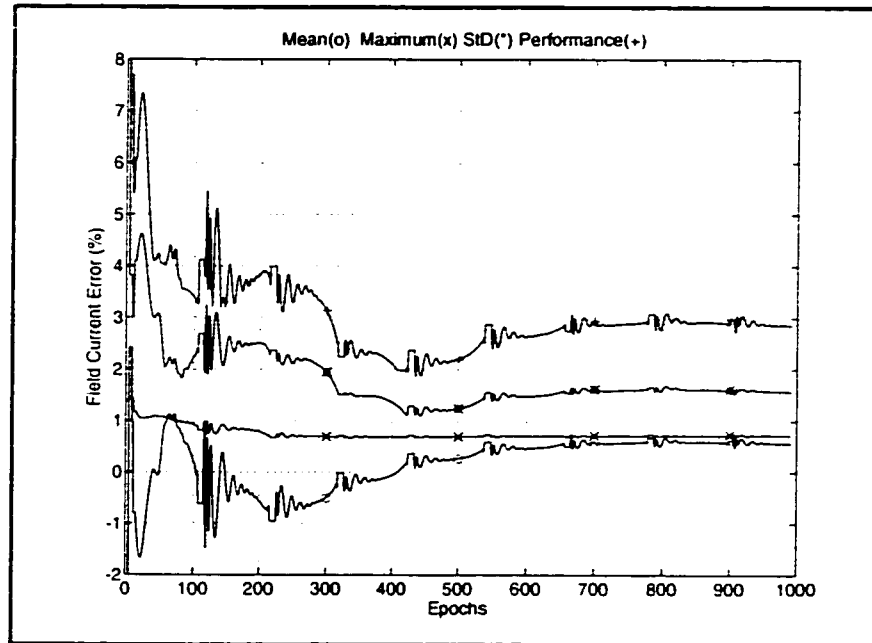


Figure 5-10: Field Current Error for Try 1 Using VGroup1

Table 5-15: Best Performances Using VGroup1									
Try	Epoch	PerfI	If Error (%)			Perf	δ Error (degrees)		
			Mean	StD	Max		Mean	StD	Max
1	434	1.870	0.08	0.67	1.11	6.954	0.05	1.44	3.60
2	45	3.309	0.54	0.91	1.85	11.960	-2.36	1.43	4.86
3	114	3.564	0.08	0.96	2.52	13.227	-2.71	1.47	5.48
4	516	1.960	0.15	0.64	1.17	7.973	0.42	1.48	4.12
5	60	3.559	0.56	0.97	2.03	13.088	-2.67	1.46	5.40

Table 5-16: Best Performance Parameters Using VGroup1

Try	L_{md}	L_{mq}	I_a	A_d	B_d
1	2.1566	1.4749	0.1133	0.0190	5.6605
2	2.1868	1.3345	0.1122	0.0275	4.8657
3	2.1746	1.3129	0.1142	0.0264	4.9194
4	2.1302	1.4931	0.1184	0.0372	4.2290
5	2.1912	1.3164	0.1131	0.0271	4.8656

Table 5-17: Performance Over VGroup2 Using Parameters From VGroup1

Try	Perf VGroup1	Perf VGroup2	If Error (%)			δ Error (degrees)		
			Mean	StD	Max	Mean	StD	Max
1	6.954	9.503	-0.28	1.15	2.91	0.21	1.36	3.60
2	11.960	14.189	0.13	1.43	4.10	-2.26	1.31	4.96
3	13.227	16.261	-0.34	1.47	4.85	-2.62	1.35	5.63
4	7.973	9.952	-0.21	1.03	2.60	0.59	1.41	4.12
5	13.088	15.473	0.14	1.50	4.38	-2.58	1.35	5.54

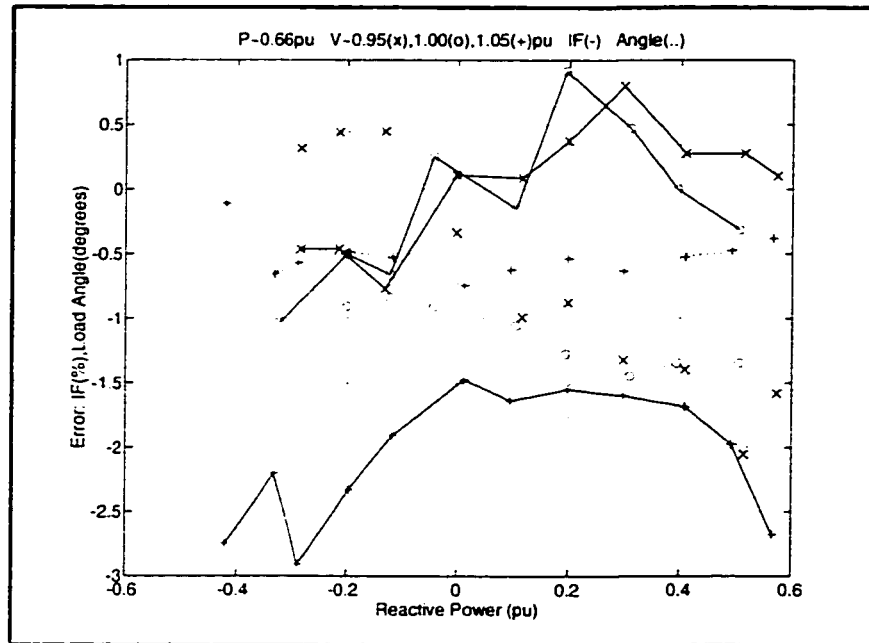


Figure 5-11: Errors for P=0.66 pu Using VGroup1

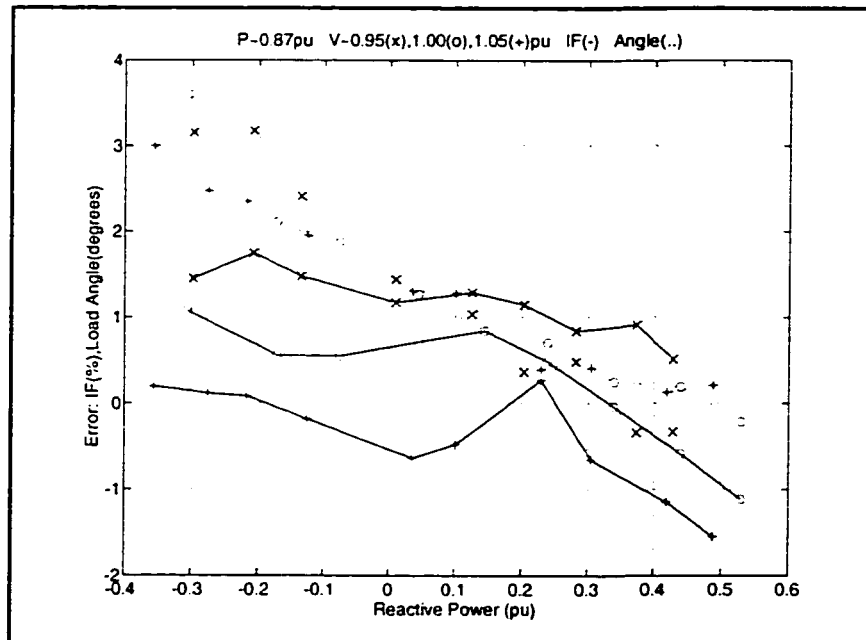


Figure 5-12: Errors for P=0.87 pu Using VGroup1

Table 5-18: Best Performances Using VGroup2

Try	Epoch	PerfI	If Error (%)			Perf	δ Error (degrees)		
			Mean	StD	Max		Mean	StD	Max
1	556	3.868	0.00	1.18	2.68	8.893	0.15	1.35	3.52
2	992	3.899	0.49	1.11	2.30	9.692	0.46	1.39	3.94
3	55	6.028	0.42	1.51	4.09	15.295	-2.51	1.34	5.42
4	430	3.500	0.00	1.06	2.43	9.657	0.60	1.42	4.14
5	670	5.180	1.02	1.13	3.03	12.379	1.02	1.49	4.69

Table 5-19: Best Performance Parameters Using VGroup2

Try	L_{md}	L_{mq}	I_a	A_d	B_d
1	2.1673	1.4731	0.1118	0.0198	5.5597
2	2.1543	1.4892	0.1145	0.0517	3.4285
3	2.2017	1.3198	0.1132	0.0256	4.9970
4	2.1414	1.4949	0.1177	0.0334	4.4451
5	2.1761	1.5286	0.1097	0.0454	3.6998

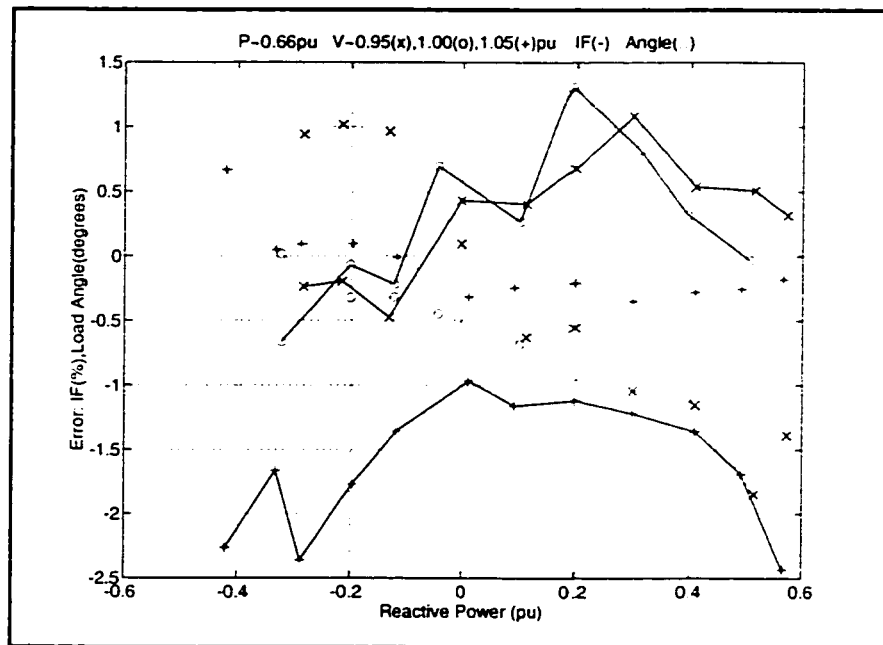


Figure 5-13: Errors for $P=0.66$ pu Using VGroup2

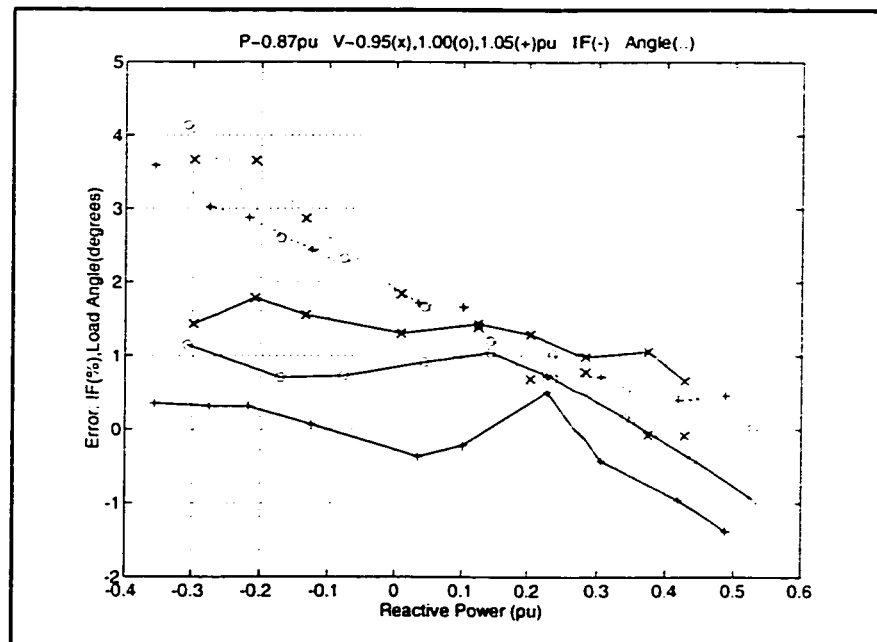


Figure 5-14: Errors for $P=0.87$ pu Using VGroup2

5.4 Case Study: Round Rotor Generator

The Lambton generator extensively studied in the EPRI Report EL-1424 [31] will be used to apply the method to a round rotor SM. The ratings of the generator are:

Table 5-20: Turbogenerator Ratings	
Characteristic	Values
Power:	555 MVA
Voltage:	24.0 KV
Power Factor:	0.9
Speed:	3600 rpm
No. of poles:	2

Appendix E contains details of the measurements obtained from the report. Figure 5-15 displays the points in a PQ graphic.

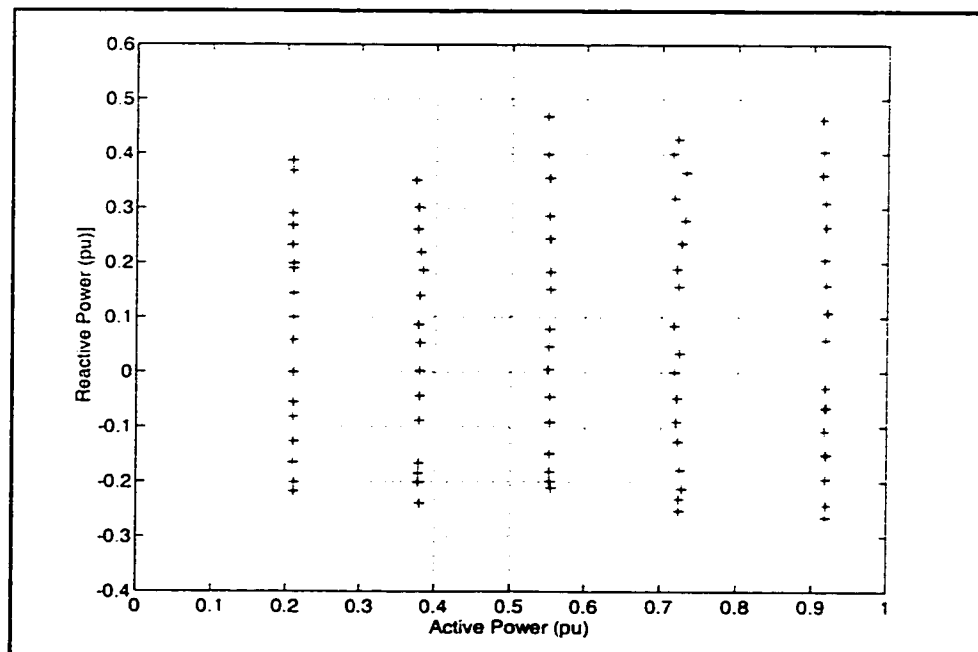


Figure 5-15: Operating Points

5.4.1 General Procedure and Pattern Formation

The procedure is similar to what has already been explained in section 5.3.1 for the salient pole micro-alternator. Table 5-21 shows the points selected from the report [31] to conduct the estimation studies.

Table 5-21: Training and Validation Points		
Groups	PQV Operating Points	
	P(pu)	Point No (refer to Appendix E)
TGroup	~0.72	460 476 490 507 523 532 543 548 568
	~0.91	599 617 700 714 731 736 761 778 801
VGroup1 & VGroup2	~0.72	443 451 468 479 495 515 525 538 545 555 562 566
	~0.91	600 609 623 695 706 721 744 753 763 770 785 807
VGroup2	~0.20	28 45 53 73 87 90 104 118 125 140
	~0.38	170 177 189 191 215 225 233 245 255 259 268 271
	~0.55	305 309 327 344 356 370 374 382 390 411

A population of possible SMs can be generated by imposing random variations within a specified range to the values of a *root set*, as it is specified in Table 5-22.

The set of BCs associated with each SM is based on variations of the original points from the Training Group, as specified in Table 5-23.

Table 5-22: Root Set of Parameters and Ranges

Parameter	Root Value ^a	Range ^b
L_{md}	1.8100	$L_{mdo} \pm 10\%$
L_{mq}	0.0000	$90\text{-}100\% L_{md}$
l_a	0.1600	$l_{ao} \pm 10\%$
S_{1d}^c	0.1400	$S_{1do} \pm 25\%$
S_{2d}	0.5500	$S_{2do} \pm 10\%$
V_{zd}	0.6000	V_{zdo}
V_{od}	0.8000	V_{odo}
S_{1q}	0.0000	$100\text{-}300\% S_{1d}$
S_{2q}	0.0000	$100\text{-}170\% S_{2d}$
V_{zq}	0.4000	V_{zqo}
V_{oq}	0.6000	V_{oqo}
r_a	0.0001	r_{ao}
I_{fnv}^d	1310(A)	I_{fnvo}

- a. Values are in pu unless otherwise specified.
- b. Variables with the final sub-index "o" refer to the root value.
- c. S_{1d} and S_{2d} are the values of the saturation function S_d specified for a voltage V of 1.0 and 1.2 pu respectively.
- d. I_{fnv} is the field current that in absence of saturation would produce a rated open circuit terminal voltage.

Table 5-23: Boundary Conditions and Ranges

TGroup Points	Variable	Range
Point "j" $\Rightarrow \{P_{oj}, Q_{oj}, V_{oj}\}$	P_j	$P_{oj} \pm 0.05$ pu
	Q_j	$Q_{oj} \pm 0.05$ pu
	V_j	V_{jo}

Evaluating the model of the SM for each set of parameters and BCs, and considering that the variables are affected by noise, as specified in Table 5-24, it is possible to form a training set with the characteristics specified in Table 5-25. The ANNs structures for each case are specified in Table 5-26.

Table 5-24: Consideration of Noise	
Variables	Noise
I_f	$\pm 0.5\%$ of I_{fnv}
δ	± 0.5 degrees
P	± 0.0025 pu
Q	± 0.0025 pu

Table 5-25: Training Sets Characteristics		
Attribute	Case	
	$I_f\delta PQ$	$I_f PQ$
No. of SMs	2500	
No. of BCs	18	
Variables per BC	I_f, δ, P, Q	I_f, P, Q
Targets per SM	$L_{md}, L_{mq}, I_a, S_{d1}, S_{d2}, S_{q1}, S_{q2}$	

Table 5-26: ANNs Characteristics		
Attribute	Case	
	$I_f\delta PQ$	$I_f PQ$
No. Inputs	72	54
No. Hidden 1	18	
No. Hidden 2	7	
No. Outputs	7	

5.4.2 If δ PQ Case

The ANN with the structure specified in Table 5-26 is trained with the corresponding training set for this specific case as per Table 5-25.

The errors through the training process for try 4 are plotted in Figure 5-16 and Figure 5-17 for the field current and load angle respectively.

The best performance from each training process measured over the VGroup1 is summarized in Table 5-27 and Table 5-28. Generalization can be tested by measuring the performance of the previous sets of parameters over the extended VGroup2, as is done in Table 5-29. The errors as a function of the active and reactive power are shown in Figure 5-18.

The best performances using VGroup2 can be seen in Table 5-30 and the corresponding parameters are in Table 5-31. The errors are plotted in Figure 5-19.

A closer look at Figure 5-18 shows that the performance of the obtained parameters, using VGroup1, is excellent for the active powers of ~ 0.91 pu, ~ 0.72 pu, and ~ 0.55 pu. When VGroup2 is used, Figure 5-19 clearly shows an overall improvement where the performance for an active power of ~ 0.37 pu can now also be considered as very good. Obviously, this points out more to a defect in the adopted saturation model, as pointed out in section 2.5, than to a problem with the method itself. It seems very difficult to obtain one set of parameters that will fit the model to cover all the capability region with negligible errors.

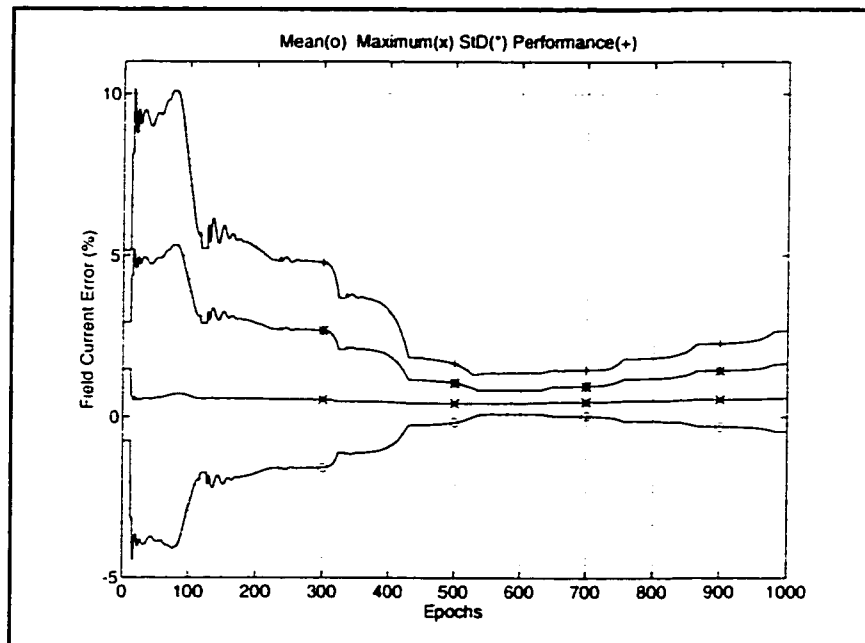


Figure 5-16: Field Current Error for Try 4 Using VGroup1

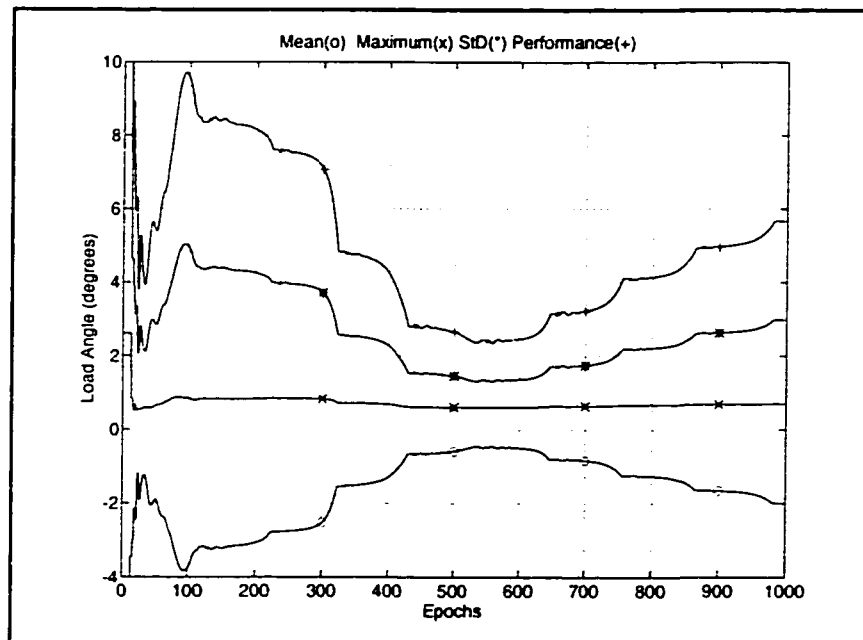


Figure 5-17: Load Angle Error for Try 4 Using VGroup1

Table 5-27: Best Performances Using VGroup1

Try	Epoch	Perf	If Error (%)			δ Error (degrees)		
			Mean	StD	Max	Mean	StD	Max
1	103	4.812	-1.05	0.39	1.75	0.25	0.47	0.90
2	20	4.350	0.67	0.49	1.62	0.00	0.45	1.11
3	91	9.969	-1.02	0.53	2.14	-2.26	0.73	3.29
4	533	3.689	0.04	0.43	0.85	-0.46	0.60	1.31
5	27	6.732	-1.53	0.35	2.17	-0.60	0.69	1.39

Table 5-28: Best Performance Parameters Using VGroup1

Try	L_{md}	L_{mq}	l_a	A_d	B_d	A_q	B_q
1	1.8484	1.8484	0.1609	0.0564	5.8169	1.1154	0.7610
2	1.9191	1.7823	0.1527	0.0557	5.8527	0.2671	2.2844
3	1.8708	1.7340	0.1660	0.0507	6.0734	0.5248	1.6150
4	1.8859	1.7806	0.1706	0.0484	6.1999	1.1726	0.7238
5	1.8534	1.8180	0.1662	0.0392	6.7274	0.1894	3.1841

Table 5-29: Performance Over VGroup2 with Parameters From VGroup1

Try	Perf VGroup1	Perf VGroup2	If Error (%)			δ Error (degrees)		
			Mean	StD	Max	Mean	StD	Max
1	4.812	12.096	0.08	1.98	4.97	-0.58	1.11	3.37
2	4.350	12.955	1.24	1.69	5.21	-0.74	0.94	3.13
3	9.969	17.321	-0.22	2.13	4.85	-2.77	1.39	5.96
4	3.689	13.535	0.54	1.90	4.49	-1.21	1.23	4.17
5	6.732	12.004	-0.83	1.75	4.22	-1.20	0.85	3.15

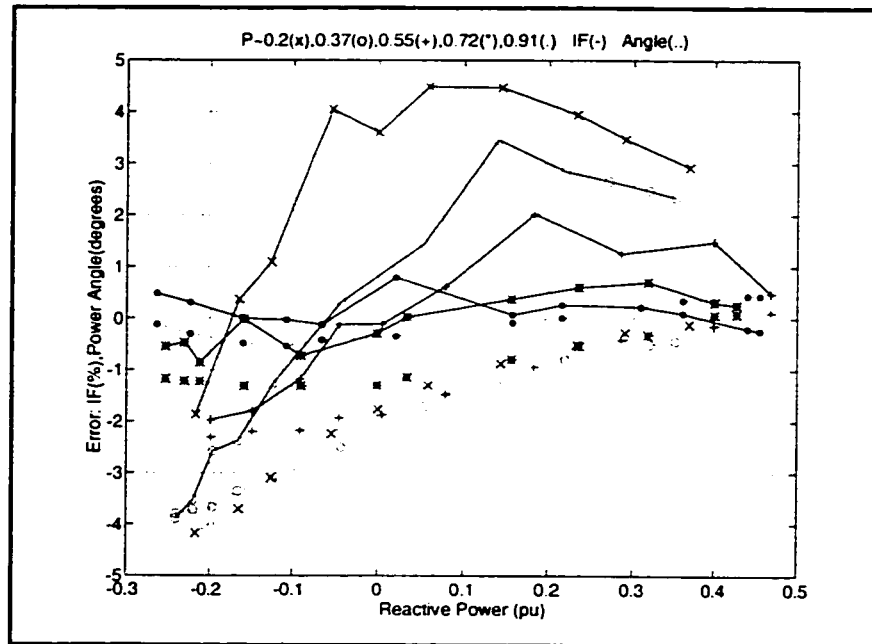
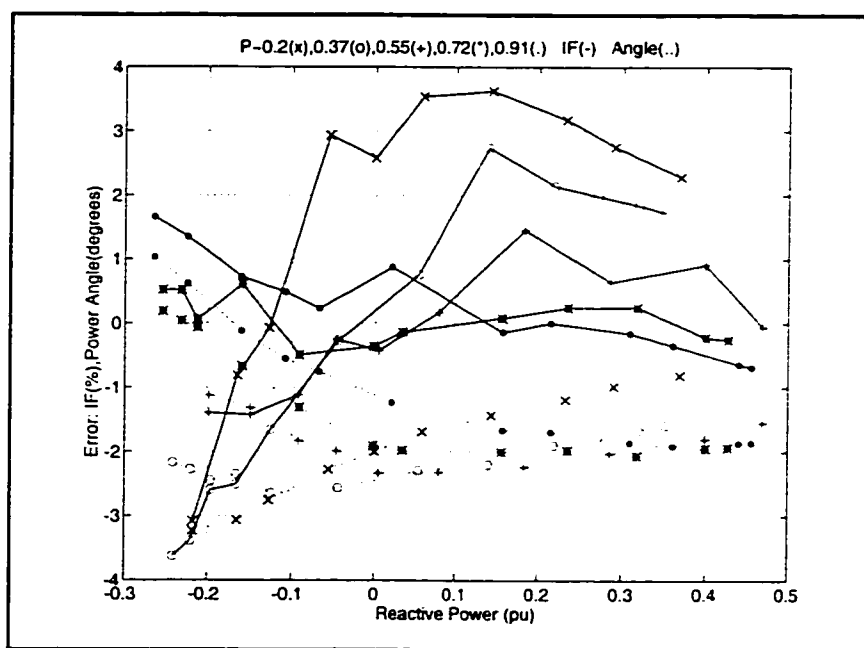


Figure 5-18: Errors Using VGroup1

Table 5-30: Best Performances Using VGroup2								
Try	Epoch	Perf	If Error (%)			δ Error (degrees)		
			Mean	StD	Max	Mean	StD	Max
1	102	11.850	-0.10	2.01	4.93	-0.47	1.10	3.24
2	157	11.311	0.30	1.65	3.63	-1.63	0.87	3.23
3	203	17.200	-0.27	2.17	4.83	-2.76	1.34	5.83
4	558	13.462	0.54	1.90	4.42	-1.21	1.23	4.16
5	27	12.004	-0.83	1.75	4.22	-1.20	0.85	3.15

Table 5-31: Best Performance Parameters Using VGroup2

Try	L_{md}	L_{mq}	I_a	A_d	B_d	A_q	B_q
1	1.8388	1.8388	0.1614	0.0559	5.8362	1.1315	0.7377
2	1.9244	1.8275	0.1614	0.0405	6.5734	0.1300	4.0866
3	1.8592	1.7397	0.1701	0.0508	6.0892	0.4907	1.7270
4	1.8878	1.7782	0.1716	0.0472	6.2661	1.1855	0.7151
5	1.8534	1.8180	0.1662	0.0392	6.7274	0.1894	3.1841

**Figure 5-19: Errors Using VGroup2**

5.4.3 IfPQ Case

Using the specific training set for this case from Table 5-25 the corresponding ANN from Table 5-26 is trained five times for different initializations. The field current errors during the training process for Try 4 are plotted in Figure 5-20.

The best performances and corresponding parameters are summarized in Table 5-32 and Table 5-33. Generalization over the VGroup2 is shown in Table 5-34 and the overall errors are plotted in Figure 5-21.

Using the VGroup2 to select the best set of parameters yields the results shown in Table 5-35 and Table 5-36. Figure 5-22 plots the overall errors with the set obtained for Try 2.

The results shown in Figure 5-21 and Figure 5-22 point to the same conclusion formulated for the case that includes the load angle. Excellent results are obtained for the active powers of $\sim 0.55\text{pu}$, $\sim 0.72\text{pu}$, and $\sim 0.91\text{pu}$. When the extended VGroup2 is used, the results obtained for values of the active power of $\sim 0.37\text{pu}$, and even the ones of $\sim 0.2\text{pu}$, can also be considered very good. But it seems very difficult to attain an appropriate fit of the model to accommodate all ranges.

What should draw the attention again is the fact that the omission of the load angle in the patterns provides comparable results to the case that includes it in the studies.

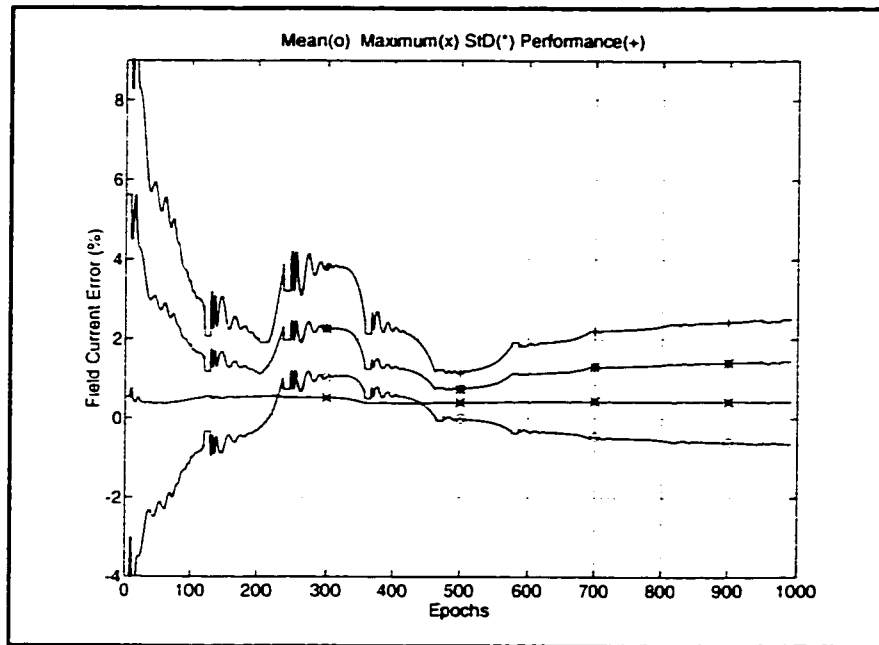


Figure 5-20: Field Current Error for Try 4 Using VGroup1

Table 5-32: Best Performances Using VGroup1									
Try	Epoch	PerfI	If Error (%)			Perf	δ Error (degrees)		
			Mean	StD	Max		Mean	StD	Max
1	10	2.260	-0.49	0.46	1.31	5.131	0.34	0.65	1.88
2	285	1.642	-0.09	0.47	1.07	8.304	-2.64	0.50	3.52
3	224	1.336	-0.12	0.40	0.82	4.108	-0.71	0.55	1.51
4	479	1.131	0.00	0.40	0.73	5.039	-1.31	0.45	2.15
5	74	3.312	-1.08	0.45	1.79	7.337	-1.21	0.78	2.03

Table 5-33: Best Performance Parameters Using VGroup1

Try	L_{md}	L_{mq}	I_a	A_d	B_d	A_q	B_q
1	1.8877	1.7678	0.1611	0.0415	6.5317	0.1726	2.9674
2	1.8972	1.7633	0.1737	0.0469	6.2871	0.2124	3.2732
3	1.8921	1.7950	0.1676	0.0452	6.3331	0.2211	2.8545
4	1.8750	1.7603	0.1702	0.0616	5.5878	0.2658	2.5635
5	1.8851	1.8022	0.1610	0.0392	6.6679	0.1474	3.7601

Table 5-34: Performance Over VGroup2 Using Parameters From VGroup1

Try	Perf VGroup1	Perf VGroup2	If Error (%)			δ Error (degrees)		
			Mean	StD	Max	Mean	StD	Max
1	5.131	8.835	-0.04	1.57	3.53	-0.39	0.89	2.41
2	8.304	16.072	0.34	2.05	4.56	-2.99	0.98	5.15
3	4.108	11.754	0.31	1.74	4.04	-1.33	0.87	3.47
4	5.039	15.443	0.89	1.98	5.47	-1.88	0.97	4.26
5	7.337	12.648	-0.60	1.68	4.25	-1.72	0.84	3.55

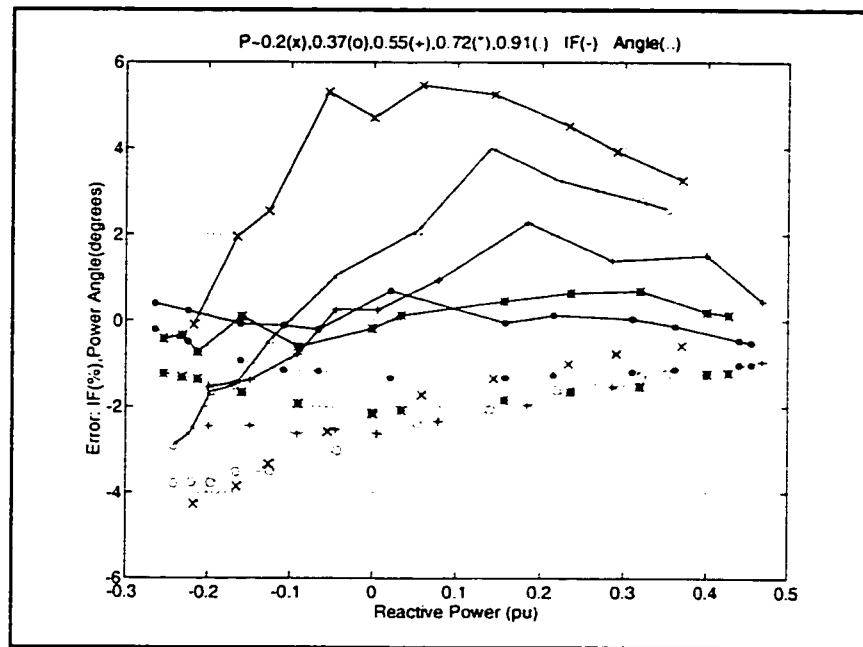
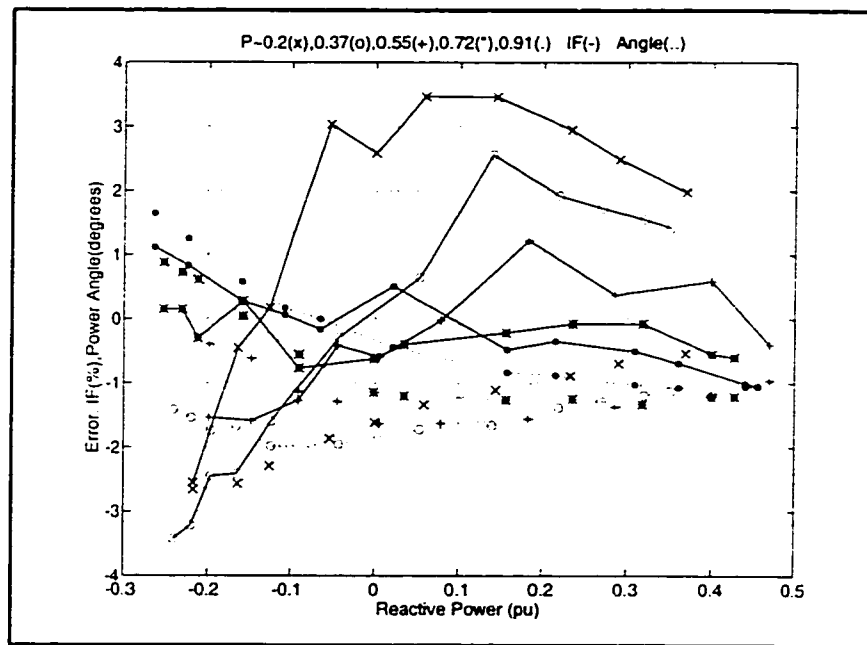


Figure 5-21: Errors Using VGroup1

Table 5-35: Best Performances Using VGroup2									
Try	Epoch	PerfI	If Error (%)			Perf	δ Error (degrees)		
			Mean	StD	Max		Mean	StD	Max
1	10	5.143	-0.04	1.57	3.53	8.835	-0.39	0.89	2.41
2	36	5.137	0.10	1.57	3.47	9.671	-0.99	0.88	2.66
3	18	5.220	-0.53	1.40	3.30	11.283	0.79	1.26	4.01
4	196	5.289	0.03	1.65	3.61	11.278	-1.82	0.91	3.26
5	74	6.540	-0.60	1.68	4.25	12.648	-1.72	0.84	3.55

Table 5-36: Best Performance Parameters Using VGroup2

Try	L_{md}	L_{mq}	I_a	A_d	B_d	A_q	B_q
1	1.8877	1.7678	0.1611	0.0415	6.5317	0.1726	2.9674
2	1.9052	1.8301	0.1614	0.0406	6.5690	0.1410	3.7470
3	1.8640	1.8264	0.1727	0.0330	7.0920	0.0970	4.0592
4	1.9057	1.8197	0.1620	0.0422	6.4764	0.1103	4.4799
5	1.8851	1.8022	0.1610	0.0392	6.6679	0.1474	3.7601

**Figure 5-22: Errors Using VGroup2**

5.5 Results Summary

The proposed method has been successfully applied to the estimation of the parameters responsible for the steady-state behaviour of both a salient pole and a round rotor generator.

The results can be summarized as follows:

- It is possible to estimate a set of parameters using either a restricted or extended set of validation points.
- The obtained parameters can be applied to a wide range of operating conditions.
- It is possible to estimate the parameters omitting the information of the load angle of the patterns. Considering that, in practical terms, the rotor position is the most difficult variable to obtain, this result is a remarkable side effect of the application of the method.

CHAPTER 6

TRANSIENT STATE ANALYSIS

6.1 Introduction

This chapter accounts for the practical application of the proposed method to estimate the parameters of the SM responsible for its transient state behaviour. An experimental study with on-line data from a micro-alternator will validate the method for salient pole machines. Data obtained from a simulation study of a turbo-generator will be used to confirm that the method can also be applied to round rotor machines.

6.2 Boundary Conditions and Pattern Formation

The perturbations that have been used as boundary conditions to measure the transient parameters of a SM can be grouped as *field perturbations* [14] and *system perturbations* [78].

6.2.1 Field Perturbations

Field perturbations consist of a sudden change applied to the voltage reference of the SM, forcing the excitation system to change the field voltage in order to attain the desired output voltage. From a practical point of view this kind of perturbation is very appeal-

ing because it is one of the less intrusive tests that, in general, can actually be performed in a power system, and it is extensively used for control purposes.

From the circuit model of Figure 2-3 and Figure 2-4 it is clear that such a perturbation, initiated in the field winding with a sudden change on v_f , propagates through a restricted circuit path to affect the mutual inductance L_{md} and terminal conditions. The changes generated in the d axis mutual flux linkages as well as the changes induced in the system will propagate to the quadrature axis and so on. It is reasonable and intuitive to expect that the initial perturbation will be limited by the direct axis characteristics.

From expressions (2-6) and (2-7), the armature voltages can be expressed as functions of the flux linkages as:

$$\begin{aligned} v_d(p) &= -\omega\lambda_q(p) - p\lambda_d(p) \\ v_q(p) &= \omega\lambda_d(p) - p\lambda_q(p) \end{aligned} \quad (6-1)$$

where the armature resistance has been neglected. If the expressions for the flux linkages given in equations (2-10) are substituted in (6-1), it is possible to obtain the following expressions for the currents:

$$\begin{aligned} i_d(p) &= \frac{pv_d(p) - \omega v_q(p)}{L_d(p)(p^2 + \omega^2)} + \frac{G(p)}{L_d(p)} v_f(p) \\ i_q(p) &= \frac{\omega v_d(p) + p v_q(p)}{L_q(p)(p^2 + \omega^2)} \end{aligned} \quad (6-2)$$

From the expression for $i_q(p)$ in equations (6-2), it can be observed that the initial perturbation applied to v_f does not have a direct effect on the q axis. Changes in the speed ω and the feedback from the system, through corresponding changes in the armature voltages, are responsible for exciting the quadrature axis dynamics of the SM.

To further understand the propagation of the perturbation, it is important to analyse the term that affects the field voltage v_f in (6-2). It is possible to think of a similar test in

which the SM is attached to an infinite bus where voltages and speed remain constant during the experiment. Under these ideal conditions and from equations (6-2), the changes in the currents will be given by:

$$\Delta i_d(p) = \frac{G(p)}{L_d(p)} \Delta v_f(p) = \frac{L_{md}}{L_d r_{fd}} \frac{(1 + p \frac{l_{2d}}{r_{2d}})}{(1 + p T_d')(1 + p T_d'')} \Delta v_f(p) \quad (6-3)$$

$$\Delta i_q(p) = 0$$

The direct axis response due to a unit-step applied to the field voltage can be expanded as follows:

$$\Delta i_d(p) = K \left(\frac{A}{p} + \frac{B}{1/T_d' + p} + \frac{C}{1/T_d'' + p} \right)$$

$$K = \frac{L_{md}}{L_d r_{fd}} \quad T_{2d} = \frac{r_{2d}}{l_{2d}} \quad (6-4)$$

$$A = 1 \quad ; \quad B = \frac{\frac{T_{2d}}{T_d'} - 1}{1 - \frac{T_d'}{T_d}} \quad ; \quad C = \frac{\frac{T_{2d}}{T_d''} - 1}{1 - \frac{T_d''}{T_d}}$$

Considering that T_{2d} and T_d'' are of the same order of magnitude and that $T_d' \gg T_d''$, it is expected that the absolute values of B and C will tend to be close to 1 and 0 respectively, i.e.:

$$\begin{aligned} |B| &\approx 1 & (B = -1.0055) \\ |C| = |-1 - B| &\approx 0 & (C = 0.0055) \end{aligned} \quad (6-5)$$

where, as an example, the adjusted parameters shown in Table 1-1 have been used to get the numerical values.

Then, the subtransient effects are negligible and the response is fully governed by the direct axis short circuit time constant T_d' . Also, from the expression for K in (6-4), no information concerning the value of the direct axis transient or subtransient reactance can be extracted.

In an actual test, voltages and speed will change as a reaction to the initial perturbation. These variables, that depend on uncontrollable factors like the system dynamics and shaft inertia, are the only ones capable of fully exciting the SM dynamics, as it can be seen in the terms that include the operational inductances $L_d(p)$ and $L_q(p)$ in (6-2). However, this is probably to expect too much from the test because speed changes are slow in nature due to their mechanical origin and a well behaved system will have a tendency to further damp the original perturbation. To expect something else is, most probably, to have to deal with a very serious problem, like stability, SSR, etc., which makes this test impracticable in the first place.

A similar numerical example to that shown in Chapter 1, section 1.2.1, can further illustrate the overall problem. To avoid the SSR effects of the benchmark model [6], the series capacitance of the line has been embedded into the line inductance to produce a single impedance. Also, to allow for a change in the voltage reference, an IEEE type SCR_X (solid state) exciter model provided by the EMTDC simulation package is used [79]. The goal is to check how sensitive are the responses to changes in the subtransient parameters of the SM. The parameters are taken from the adjusted set of Table 1-1, and the subtransient parameters are varied according to Table 6-1. The perturbation consists in a 5% increase in the reference voltage.

After an initial simulation with the original set of parameters is run (case 0), a boundary condition for this perturbation can be defined using the phase and field voltages,

and the rotor speed and angle. Once this boundary condition is fixed, the SM model can be solved for each set of parameters specified for each case.

Table 6-1: Variations in the Transient and Subtransient Parameters				
Cases ^a	L_d'' [pu]	T_{do}'' [s]	L_q'' [pu]	T_{qo}'' [s]
0 ^b	0.217	0.022	0.254	0.074
1	0.175	0.018	=	=
2	0.247	0.018	=	=
3	0.175	=	=	=
4	0.247	=	=	=
5	=	=	0.217	0.020
6	=	=	=	0.020
7	=	=	0.217	=
8	=	=	=	=

- a. Case 0 is just the original data. The symbol '=' means that the original data is used.
- b. The field resistance r_{fd} is obtained using the parameters from case 0 and assuming a mutual inductance $L_{f2d}r=0.049\text{pu}$.

As it is shown in Figure 6-1, cases 1 through 4 induce changes in the direct axis currents. Changes in T_{do}'' (18%) generate insignificant variations and the ones in L_d'' (33%) are also negligible. The cases that affect the quadrature axis currents are presented in Figure 6-2. Here, the responses to changes in the subtransient inductance L_q'' (15%) are insignificant and although the variations can be associated to the changes in T_{qo}'' (73%), their overall importance is also negligible.

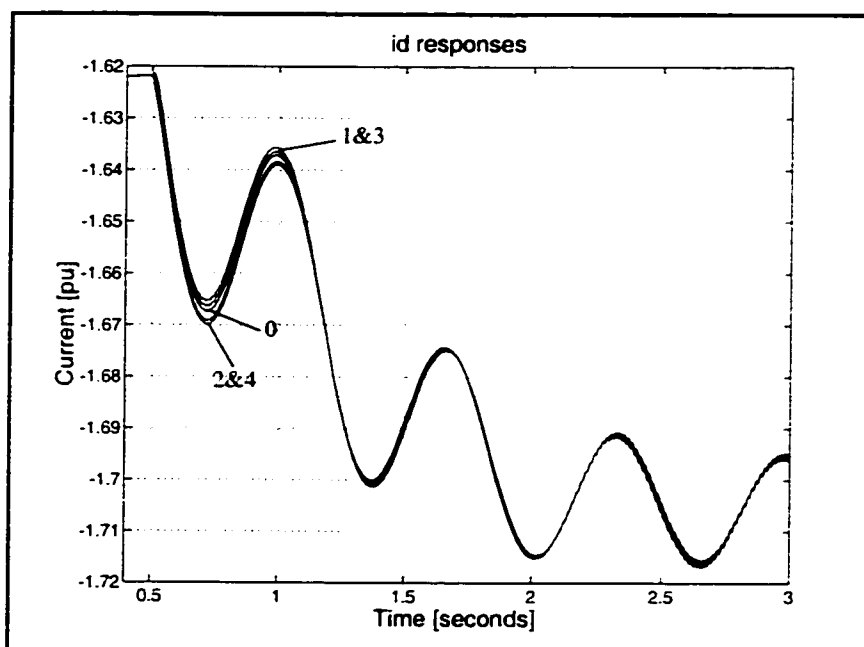


Figure 6-1: Direct Axis Currents

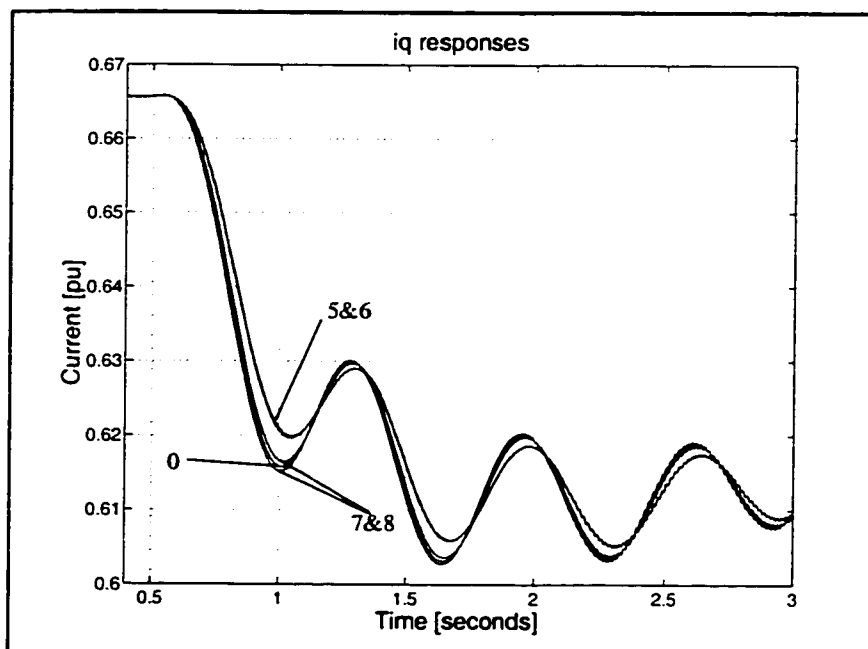


Figure 6-2: Quadrature Axis Currents

It can be concluded that although the subtransient parameters contribute to the overall SM response, their participation is embedded in such a form that it is not possible to detect their actual influence. Moreover, this participation can jeopardize any attempt to extract reliable information of the transient characteristics.

A SM parameter estimation method based on a field perturbation has been reported in a very well known and praised work [14]. The previous discussion presents a very serious objection to the foundation of the method itself and it is a surprise that the authors, and discussers, failed to point out the limitations of the proposed method. The most that can be said of the dynamic parameters obtained with such a method is that they represent the behaviour of that SM for this particular kind of perturbation and the specific system configuration at the moment of the tests.

6.2.2 System Perturbations

System perturbations are sudden changes in the system to which the SM is connected that, eventually, affect the SM. An extreme case is a short circuit that can even be, although unlikely, at the SM terminals.

Using the same equations (6-2) and assuming that during the disturbance the field voltage and speed remain constant, the increments of the currents are given by:

$$\begin{aligned}\Delta i_d(p) &= \frac{p\Delta v_d(p) - \omega\Delta v_q(p)}{L_d(p)(p^2 + \omega^2)} \\ \Delta i_q(p) &= \frac{\omega\Delta v_d(p) + p\Delta v_q(p)}{L_q(p)(p^2 + \omega^2)}\end{aligned}\tag{6-6}$$

These equations are nothing but the very well known starting point for the short-circuit analysis [18] where $v_d(p)$ and $v_q(p)$ are substituted by steps of magnitudes equal to the neg-

ative of the steady-state values. It is clear that a reasonable perturbation will excite the whole dynamics of the SM embedded in the $L_d(p)$ and $L_q(p)$ terms.

6.2.3 Pattern Formation

When a perturbation is defined through its boundary conditions (phase and field voltages, and rotor position and speed) the SM behaviour depends entirely on its electric parameters, i.e., different SMs will react differently to the same boundary conditions, and the information about the parameters is embedded in the SM currents that follow the perturbation. So, the SM pattern is represented by these currents.

Unlike the steady-state case, boundary conditions and responses are defined over the continuous domain. The first natural digital transformation occurs during the measurement phase. In theory, all the measured points could be used to form part of the pattern, which will translate in an unrealistic amount of inputs to the ANN. In practical terms, using points that define the general shape of the waves can be enough. In this sense, more points will be necessary at the very beginning of the perturbation, in order to fully represent the subtransient and transient periods.

6.3 Data Acquisition System

In order to measure the instantaneous signals following transient perturbations, the author of this work has developed a data acquisition software using a Digital Signal Processor (DSP) Board [80,81] which is based on the TMS320C30 DSP [82]. The software has been optimized using both the *Assembler* and *C* programming languages [83,84].

The system is capable of sampling nine analog inputs simultaneously at a frequency of 5 kHz. The general description of the developed software is given in Appendix F, section F.2. The data acquisition software has been extensively used and has also been of crucial importance for the practical developments of other works [85-87].

6.4 Case Study: Salient Pole Micro-Generator

The same micro-generator, for which the steady-state parameters have already been estimated in Chapter 5, will be used to estimate the transient state characteristics. The ratings and manufacturer's parameters of the micro-alternator under consideration are specified in Table D-1 and Table D-2 respectively.

The steady-state parameters estimated in section 5.3, from Try 2 of Table 5-14 (L_{md} , L_{mq} , l_a , A_d and B_d), as well as the defined constants used in the estimation process (V_{zd} and V_{od}), in combination with the measured variables (r_a , r_f and I_{fnv}) are considered as fixed in the following studies. The corresponding values are presented in Table 6-2.

Table 6-2: Steady-State Parameters and Measurements^a			
Parameter	Value	Parameter	Value
L_{md}	2.1701	A_d	0.0323
L_{mq}	1.4628	B_d	4.4900
l_a	0.1093	V_{zd}	0.6
r_a	0.0167180	V_{od}	0.8
r_f	0.0098452	$I_{fnv}[A]$	1.2077

a. Values are in pu unless otherwise specified.

6.4.1 General Procedure and Pattern Formation

Table 6-3 shows the measured boundary conditions presented in section F.3 of Appendix F used to generate the *Training Group* (TGroup) and *Validation Group* (VGroup). Unlike the steady-state case, in transient conditions it is not possible to associate a *Boundary Condition* (BC) to a unique operating point. Rather, each BC is defined by the sequence of samples taken when the perturbation takes place. In this specific case, 15000 samples are recorded during a total sampling period of three seconds, that starts a few milliseconds previous to the insertion of the perturbation.

Table 6-3: Training and Validation Points			
Groups	Perturbations	Sampling Period	Sampling Rate
TGroup	LDIN10	3.0 secs	200 μ secs
VGroup	LDIN67		

The variables measured on each perturbation capable of defining a BC are those that, for a given set of parameters of the SM, allow to solve the differential equations of the SM model. These variables are the phase and field voltages and rotor position and speed. In this sense, the TGroup will be used to generate the training set for the ANN. The pattern of the actual SM under consideration corresponding to each group, will be extracted from measured variables in the respective group.

A population of possible SMs can be generated by imposing random variations to the transient parameters, within a specified and appropriate range [25], as is shown in Table 6-4.

Each SM generated in this way can be evaluated for the BC defined by the TGroup. In this way, each SM will have associated with it a pattern determined by a set of variables

and samples derived from the solution of the differential equations. The axis currents i_d and i_q and the field current i_f will be the only variables used to generate the pattern.

Table 6-4: Transient Parameters Range	
Parameter	Range
L_d'' [pu]	$0.15 \leq L_d'' \leq 0.35$
L_d' [pu]	$0.20 \leq L_d' \leq 0.50$
T_{do}'' [s]	$0.01 \leq T_{do}'' \leq 0.09$
T_{do}' [s]	$0.35 \leq T_{do}' \leq 1.50$
L_q'' [pu]	$0.10 \leq L_q'' \leq 0.45$
T_{qo}'' [s]	$0.01 \leq T_{qo}'' \leq 0.50$

When this is extended over the whole set of generated SMs, a training set for the ANN is obtained, like the one specified in equation (4-3) of Chapter 4. The pattern that

Table 6-5: Training Set Characteristics		
Attribute		Magnitude
No. of SMs		1500
No. of BCs		1
Variables per BC		i_d, i_q, i_f
No. of Samples per Variable	total	30
	$0.0 \leq t < 0.01$ secs	5
	$0.01 \leq t < 0.1$ secs	10
	$0.1 \leq t < 1.0$ secs	10
	$1.0 \leq t < 3.0$ secs	5
Targets per SM		$L_d'', L_d', T_{do}'', T_{do}', L_q'', T_{qo}''$

characterizes the actual SM under consideration has to be formed with the corresponding variables extracted from the TGroup samples from Table 6-3. The target set to train the ANN is given by the parameters of each of the generated SMs, in the form specified in equation (4-4). The training set characteristics are defined in Table 6-5, where the number of samples per variable that form the pattern, as well as their time distribution, can be observed.

To account for the imperfections in the measurement stage, noise is introduced into the training set as a percentage of the rated values of the axis currents (obtained considering the machine ratings specified in Table D-1), and as a percentage of the I_{fnv} magnitude for the field current. The amount of noise considered is specified in Table 6-6.

Table 6-6: Consideration of Noise	
Variables	Noise
i_d	$\pm 1.0\%$ of the rated value
i_q	$\pm 1.0\%$ of the rated value
i_f	$\pm 1.0\%$ of I_{fnv}

The ANN structure is defined in Table 6-7. The learning algorithm used to train the

Table 6-7: ANNs Characteristics	
Attribute	Magnitude
No. Inputs	90
No. Hidden 1	15
No. Hidden 2	6
No. Outputs	6

Table 6-8: Training Parameters			
Parameter	Value	Parameter	Value
η	0.01 ^a	c_i	1.05
α	0.90	c_d	0.70

a. Initial value.

ANNs is the backpropagation method with adaptive learning rate and momentum using the parameters specified in Table 6-8. Five training tries corresponding to different initial sets of weights of the ANN will be shown.

After each epoch of the ANN training process, a presentation of the pattern corresponding to the actual machine will generate a set of parameters. When these parameters are evaluated for the BC of a training group, it is possible to quantify the performance of each set of parameters by comparing the calculated and measured variables. One validation group will be used to confirm the results with a stronger perturbation.

The variables that can be used to measure the errors are the axis and field currents. Given a set of parameters and a BC, the errors are defined as the differences between the *measured pattern (PM)* and the *generated pattern (PG)*. After each epoch of the training process, it is possible to obtain a set of parameters corresponding to that epoch by feeding the ANN with the actual SM pattern *PM*. When this set of parameters are evaluated for the corresponding BC, it is possible to obtain a generated pattern *PG*. Then, the errors after epoch *k* are defined as follows:

$$E_k = [PG_k - PM] 100 [pu \ 100] = \begin{bmatrix} pg_{1,k} - pm_1 \\ \vdots \\ pg_{i,k} - pm_i \\ \vdots \\ pg_{N_i,k} - pm_{N_i} \end{bmatrix} 100 [pu \ 100] \quad (6-7)$$

where pg_i and pm_i are the components of the generated and measured patterns respectively; and N_i is the number of components of the pattern.

The magnitudes of the currents following a perturbation can vary significantly. Considering that errors defined on a percentage basis tend to be significantly higher for magnitudes closer to zero, which can subvert the concept of error itself, this particular definition for the errors has been adopted.

A *performance index* (Perf) can be obtained evaluating the mean value (Mean), standard deviation (StD) and maximum value (Max) of the error, as follows:

$$Perf_k = |Mean(E_k)| + StD(E_k) + Max(|E_k|) \quad (6-8)$$

The performance index is a positive number that sets a simple and direct standard to compare different sets of parameters: the best set of parameters will have its performance index closer to zero (0.0).

6.4.2 Estimation Results

An ANN with the structure specified in Table 6-7 is trained five times for different initializations. During each training process, the performance of each set of parameters is evaluated over the training samples using equations (6-7) and (6-8). The best performances for each training process and corresponding sets of parameters are shown in Table 6-9 and Table 6-10. The total error that considers the errors obtained in all the currents simultaneously is used to evaluate the performance index. Table 6-9 also shows the individual errors for each of the direct, quadrature and field currents. The performances are excellent.

Using the parameters from try 1 and the boundary conditions from the TGroup, it is possible to obtain the currents and compare them with the measured values, as it is done in Figure 6-3. From the errors, shown in Figure 6-4, it is clear that the obtained parameters are capable of reproducing the perturbation used for training purposes.

When the best sets of parameters obtained using the TGroup (Table 6-10) are evaluated over the boundary condition defined by the VGroup, the performances specified in Table 6-11 are obtained. When compared with the performances of Table 6-9, a fairly good correlation can be observed i.e., the best sets of parameters tend to perform better in both perturbations.

Again, using the set of parameters obtained in try 1 and now the boundary conditions from the VGroup, it is possible to solve for the currents and compare them with the measured values, as is done in Figure 6-5 and Figure 6-6. The curves are reproduced remarkably well. The errors through time in Figure 6-6 show their peaks at the very inception of the perturbation, when the subtransient characteristics are crucial. Although they are bigger than what was obtained for the TGroup case, their peaks are below 0.06 pu which is still excellent, considering the magnitude of the perturbation.

Another important aspect that can be noted in Figure 6-6 is that the estimated and measured axis currents are shifted. The source of this problem is in the steady-state param-

eters that are being used. As it was shown in Figure 5-8 and Figure 5-9, the chosen steady-state parameters have a very good response for a $\{P,Q,V\}$ state of $\{-0.87,-0.4,1.0\}$ which corresponds to the initial conditions of the current TGroup. But this is not the case for an initial condition given by a $\{P,Q,V\}$ state of $\{-0.66,-0.0,1.0\}$ that matches the current VGroup. Indeed, if the initial bias is removed from both currents, the performance improves considerably for this particular case. But this is not a practice that can be generalized because the bias strictly depends on the steady-state parameters being used, and the opposite could be true as well.

Table 6-9: Best Performances

Try	Epoch	Perf	Total Error			i_d Error			i_q Error			i_f Error		
			Mean	StD	Max	Mean	StD	Max	Mean	StD	Max	Mean	StD	Max
1	1000	1.342	-0.02	0.31	1.01	0.15	0.35	1.01	-0.04	0.21	0.66	-0.18	0.27	0.69
2	804	2.423	-0.14	0.61	1.68	0.08	0.52	1.30	-0.07	0.54	1.67	-0.42	0.65	1.68
3	66	4.085	-0.39	0.87	2.82	-0.36	0.72	1.56	-0.04	0.37	1.13	-0.79	1.17	2.82
4	135	2.140	0.11	0.45	1.58	0.08	0.42	1.07	0.12	0.35	1.11	0.13	0.56	1.58
5	1000	2.234	-0.30	0.52	1.42	-0.48	0.55	1.32	-0.04	0.30	0.96	-0.36	0.57	1.42

Table 6-10: Best Performance Parameters

Try	L_d'' [pu]	L_d' [pu]	T_{do}'' [s]	T_{do}' [s]	L_q'' [pu]	T_{qo}'' [s]
1	0.2203	0.2585	0.0220	0.8128	0.2247	0.0838
2	0.2274	0.2615	0.0202	0.8616	0.2717	0.0968
3	0.2163	0.2927	0.0358	0.9780	0.2452	0.0908
4	0.2227	0.2233	0.0266	0.8231	0.2197	0.1076
5	0.1933	0.2305	0.0214	0.9008	0.2350	0.0864

Table 6-11: Performances Over VGroup

Try	Perf	Total Error			i_d Error			i_q Error			i_f Error		
		Mean	StD	Max	Mean	StD	Max	Mean	StD	Max	Mean	StD	Max
1	9.053	0.76	2.03	6.26	1.45	1.70	6.26	1.85	1.56	3.99	-1.01	1.52	4.23
2	14.718	0.23	3.68	10.81	1.24	2.42	7.67	1.54	4.07	10.81	-2.09	3.27	10.11
3	23.423	-0.88	4.79	17.76	-0.51	2.98	5.46	1.80	2.74	6.66	-3.91	6.07	17.76
4	13.149	1.50	2.59	9.06	0.93	1.99	6.34	3.08	2.45	9.06	0.49	2.58	7.89
5	12.307	-0.42	2.93	8.96	-1.39	2.53	5.15	1.81	2.17	5.07	-1.68	2.74	8.96

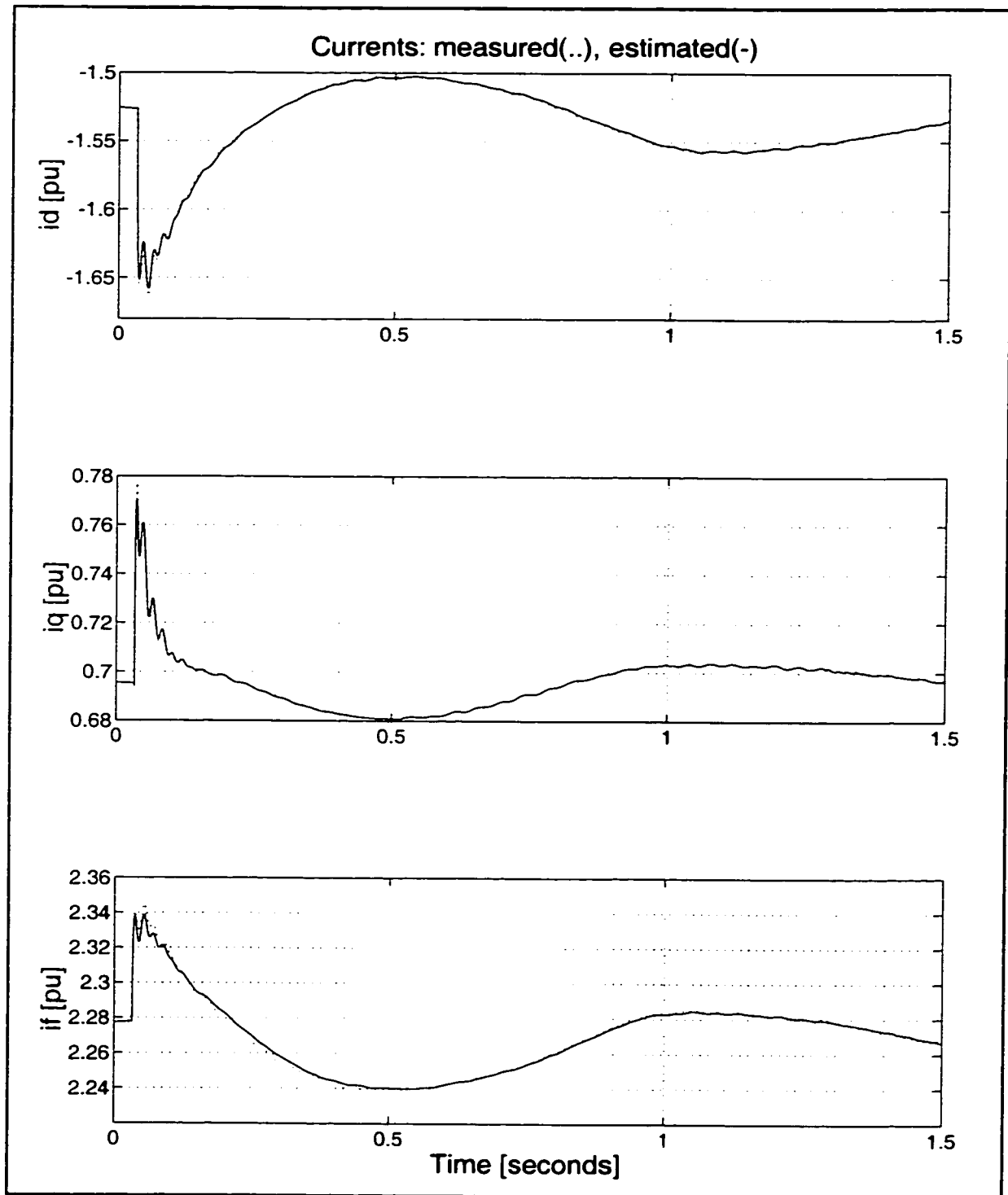


Figure 6-3: Estimated and Measured Currents Using the TGroup

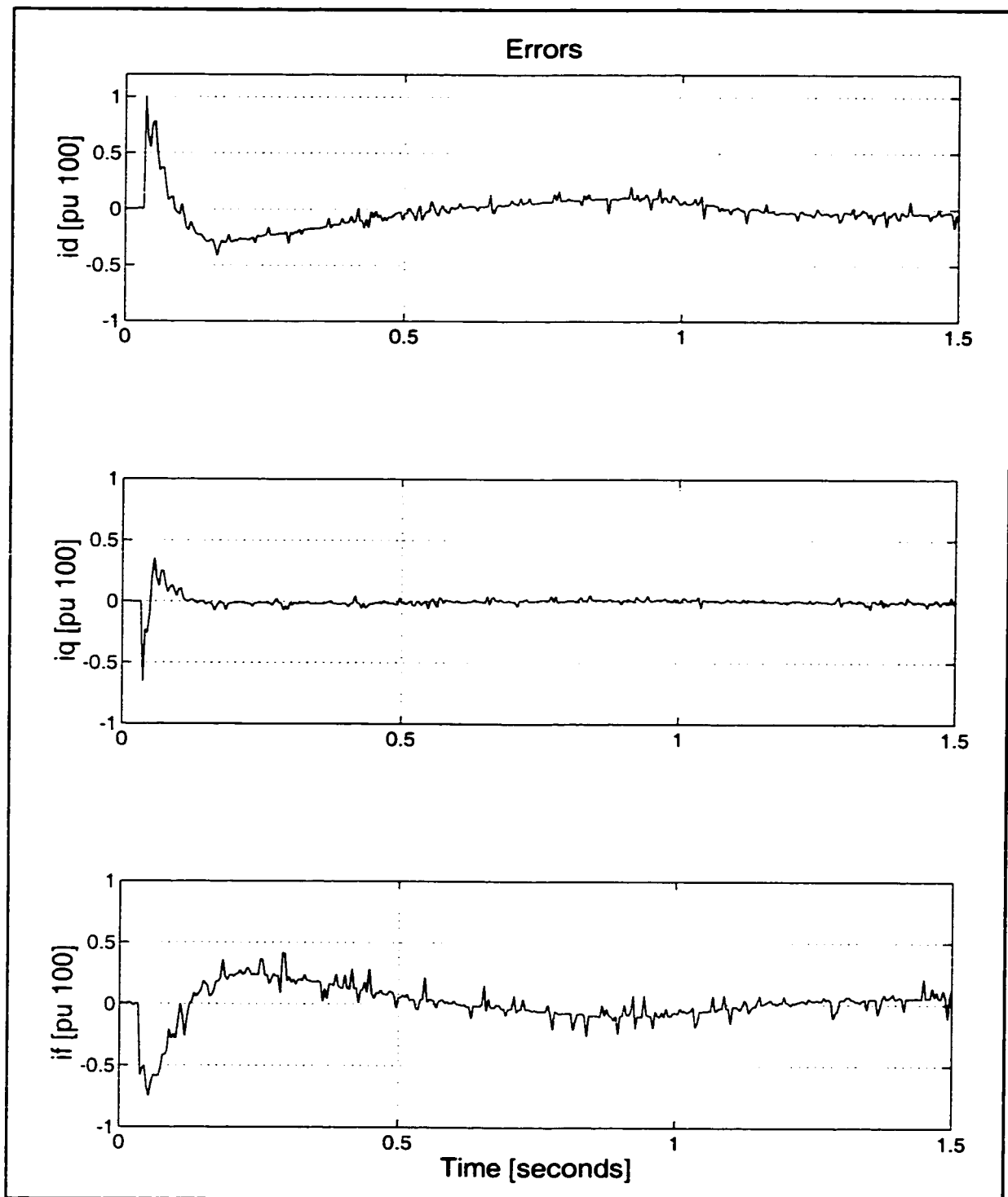


Figure 6-4: Errors in the Currents Using the TGroup

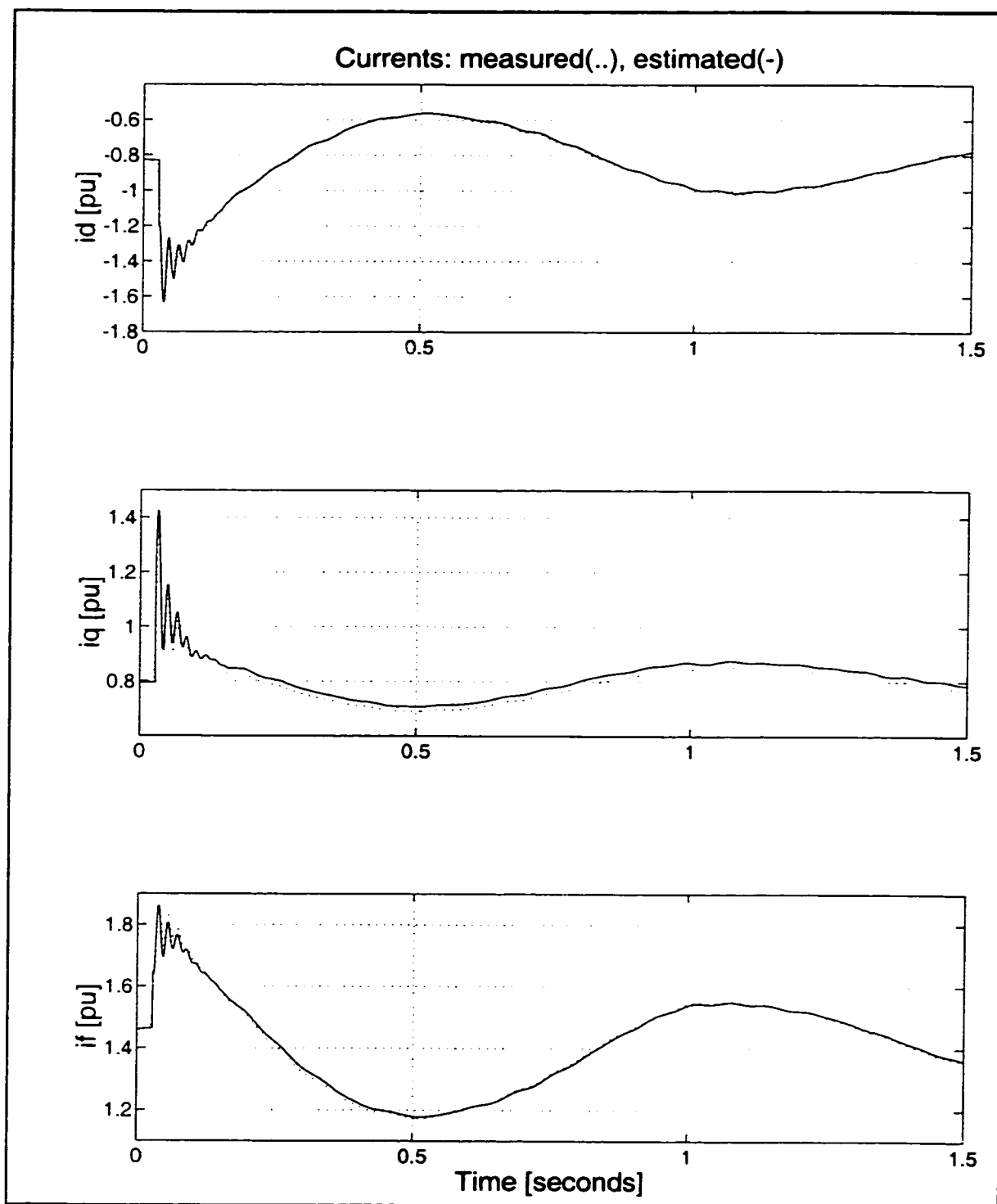


Figure 6-5: Estimated and Measured Currents Using the VGroup

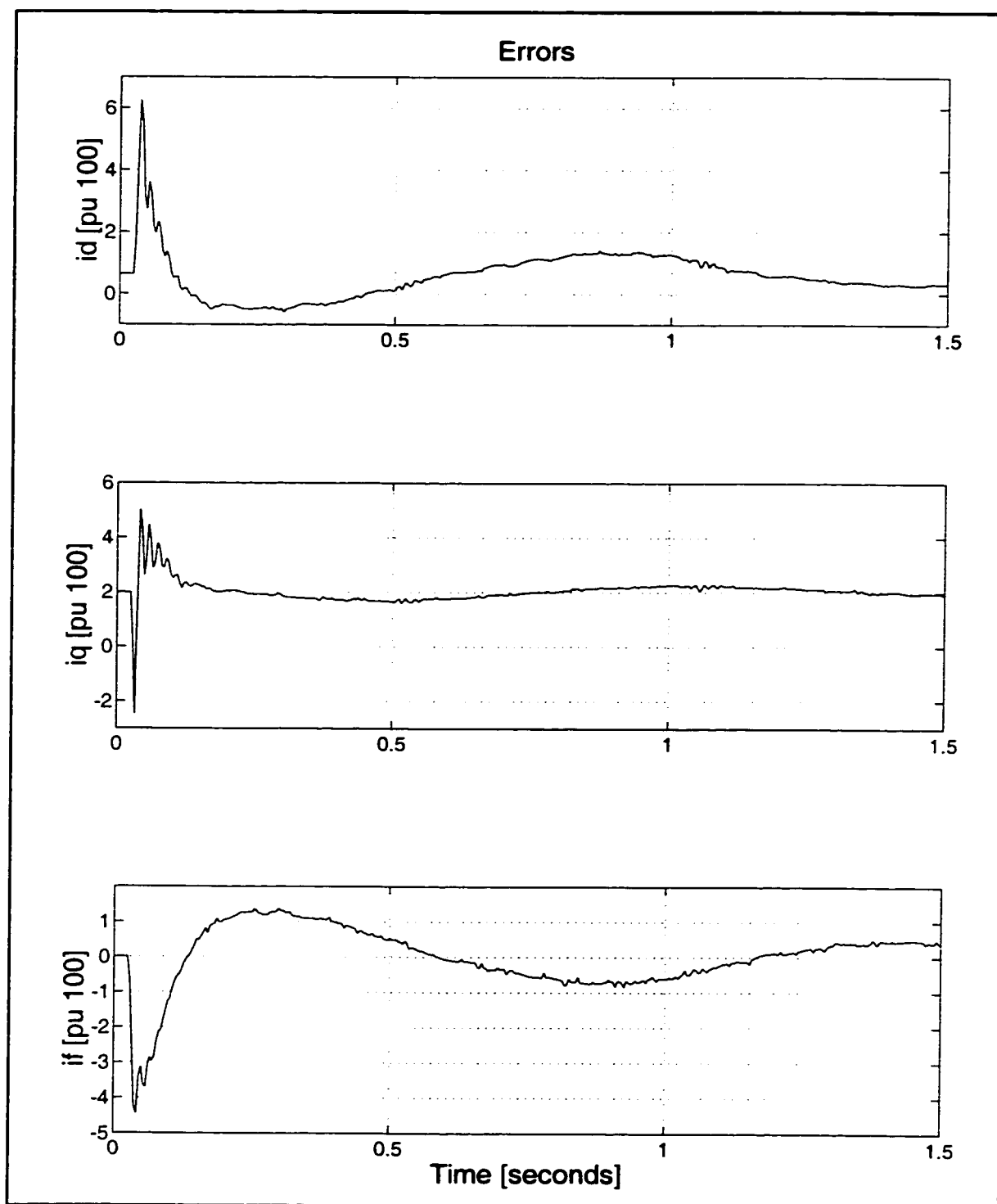


Figure 6-6: Errors in the Currents Using the VGroup

6.5 Simulation Study: Round Rotor Generator

A numerical example based on the SSR benchmark model [6] will be used to perform the simulation studies. The original model has been modified to avoid any SSR effects: the series capacitance of the line has been embedded into the line inductance to produce a single impedance. Also, an IEEE type SCRX (solid state) exciter model provided by the EMTDC simulation package is used [79]. The purpose is to be able to simulate the sudden insertion of loads, as is shown in the schematic of Figure 6-7: once the SM has reached its steady-state, the switch “Brk” is closed and simulated measurements corresponding to the *actual* SM can be extracted.

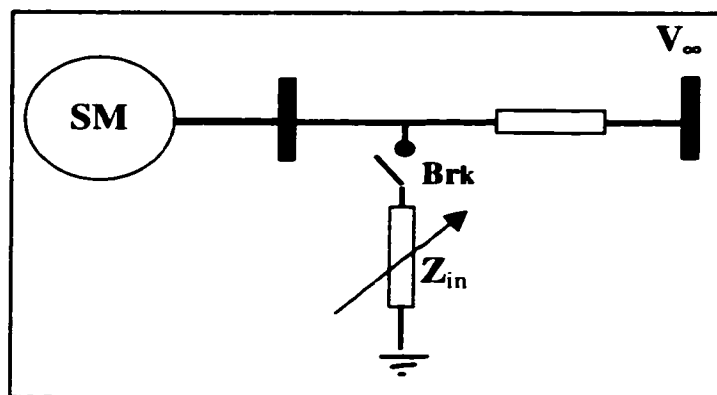


Figure 6-7: Simulation Circuit Schematic

The generator ratings are those of the SSR benchmark model: 892.4MVA, 26kV, and 3600 rpm. The manufacturer’s parameters as well as the adjusted numerical values are those given in Table 1-1. The *actual* parameters of the SM are based on the adjusted values as follows:

- the steady-state parameters (L_{md} , L_{mq} , l_a) and measured constants (r_a , r_f , I_{fnv}) are assumed to be known, according to Table 6-12;

- the *unknown* transient parameters are given in Table 6-13.

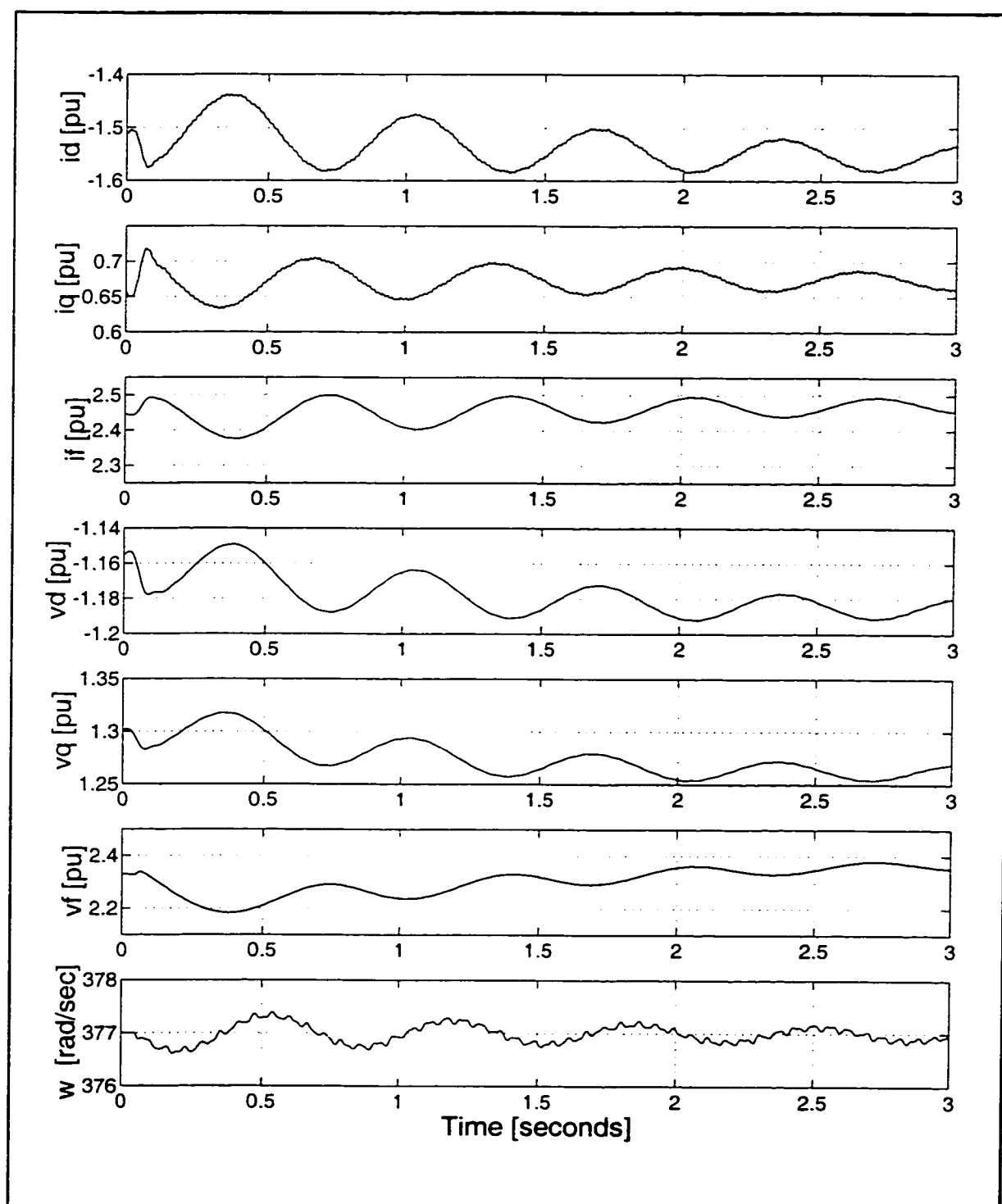
Table 6-12: Steady-State Parameters and Measurements^a			
Parameter	Value	Parameter	Value
L_{md}	1.6500	r_a	0.00
L_{mq}	1.6000	r_f^b	0.000632257
I_a	0.1600	$I_{fiv}[A]$	1310

- a. Values are in pu unless otherwise specified.
b. The field resistance is based on the assumption that the actual SM has a mutual inductance L_{I2d} of 0.027 pu.

Table 6-13: Transient State Parameters of the Actual SM^a			
Parameter	Value	Parameter	Value
L_d''	0.217	L_q''	0.254
L_d'	0.300	L_q'	0.610
T_{do}''	0.022	T_{qo}''	0.074
T_{do}'	7.800	T_{qo}'	0.900

- a. Inductances are in pu and time constants in seconds.

Using these parameters and the EMTDC simulation software [79], the following transient study is carried out: a resistive impedance, equivalent in power to a 10% of the machine rating, is suddenly inserted at the machine terminals. The obtained variables for this case, called LDIN10, are displayed in Figure 6-8.

**Figure 6-8: LDIN10 Response**

6.5.1 General Procedure and Pattern Formation

The procedure is basically the same already described for the salient pole micro-alternator. The 10% load insertion, presented in the previous section as LDIN10, is used to create the training group TGroup. The reason for not having a validation group is going to be evident in the next section, when the actual estimation results are shown.

Table 6-14: Training Group			
Groups	Perturbations	Sampling Period	Sampling Rate
TGroup	LDIN10	3.0 secs	200 μ secs

A population of possible SMs can be generated by imposing random variations to the transient parameters within a predetermined and appropriate range [25], as it is specified in Table 6-15.

Table 6-15: Transient Parameters Range	
Parameter	Range
L_d'' [pu]	$0.12 \leq L_d'' \leq 0.25$
L_d' [pu]	$0.15 \leq L_d' \leq 0.40$
T_{do}'' [s]	$0.01 \leq T_{do}'' \leq 0.40$
T_{do}' [s]	$3.00 \leq T_{do}' \leq 10.0$
L_q'' [pu]	$0.12 \leq L_q'' \leq 0.30$
L_q' [pu]	$0.30 \leq L_q' \leq 1.00$
T_{qo}'' [s]	$0.02 \leq T_{qo}'' \leq 0.10$
T_{qo}' [s]	$0.50 \leq T_{qo}' \leq 2.00$

Table 6-16: Training Set Characteristics		
Attribute		Magnitude
No. of SMs		1500
No. of BCs		1
Variables per BC		i_d, i_q, i_f
No. of Samples per Variable	total	30
	$0.0 \leq t < 0.01$ secs	5
	$0.01 \leq t < 0.1$ secs	10
	$0.1 \leq t < 1.0$ secs	10
	$1.0 \leq t < 3.0$ secs	5
Targets per SM		$L_d'', L_d', T_{do}'', T_{do}'$ $L_q'', L_q', T_{qo}'', T_{qo}'$

When the model of the SM is evaluated for each set of parameters and BC, it is possible to form a training set with the characteristics specified in Table 6-16. Once this is done, noise can be added to the training set, as specified in Table 6-17.

Table 6-17: Consideration of Noise	
Variables	Noise
i_d	$\pm 1.0\%$ of the rated value
i_q	$\pm 1.0\%$ of the rated value
i_f	$\pm 1.0\%$ of I_{fnv}

Finally, the ANN to be trained by the previous training set has the structure defined in Table 6-18.

Table 6-18: ANNs Characteristics	
Attribute	Magnitude
No. Inputs	90
No. Hidden 1	15
No. Hidden 2	8
No. Outputs	8

6.5.2 Estimation Results

An ANN with the structure specified in Table 6-18 is trained five times for different weight initializations. The best performances from each training process measured over the training group TGroup for each try are given in Table 6-19 and the corresponding parameters in Table 6-20. Comparing the performances, the best set of parameters is obtained in try 4. It can also be observed how close these parameters are to those of the *actual SM* showed in Table 6-13. This confirms the accuracy of the results and makes it unnecessary to have a validation group.

Using the parameters from try 4 and the boundary conditions from the TGroup it is possible to compare the estimated and *measured* currents. The errors through the perturbation for each current are plotted in Figure 6-9. As it is expected for such a close match in the parameters, the errors are more significant at the inception of the perturbation but their overall importance is negligible.

Table 6-19: Best Performances

Try	Epoch	Perf	Total Error			i_d Error			i_q Error			i_f Error		
			Mean	StD	Max	Mean	StD	Max	Mean	StD	Max	Mean	StD	Max
1	759	1.178	0.01	0.37	0.79	-0.10	0.42	0.74	0.02	0.09	0.27	0.11	0.46	0.79
2	983	1.129	0.02	0.26	0.85	-0.01	0.12	0.22	0.03	0.40	0.85	0.05	0.16	0.29
3	9	0.854	-0.05	0.17	0.63	-0.09	0.14	0.34	0.00	0.08	0.20	-0.06	0.24	0.63
4	8	0.366	0.00	0.11	0.25	0.02	0.12	0.19	0.01	0.09	0.25	-0.04	0.12	0.22
5	293	1.263	-0.02	0.30	0.94	-0.13	0.29	0.56	0.05	0.08	0.21	0.02	0.42	0.94

Table 6-20: Best Performance Parameters

Try	L_d'' [pu]	L_d' [pu]	T_{do}'' [s]	T_{do}' [s]	L_q'' [pu]	L_q' [pu]	T_{qo}'' [s]	T_{qo}' [s]
1	0.2006	0.3320	0.0248	7.9832	0.2762	0.6787	0.0906	1.0196
2	0.2201	0.3095	0.0221	7.7838	0.2579	0.5592	0.0979	0.9677
3	0.2484	0.3054	0.0240	8.0525	0.2671	0.6280	0.0751	0.9057
4	0.2247	0.2921	0.0236	7.7890	0.2422	0.6023	0.0768	0.9184
5	0.2304	0.3206	0.0245	8.0938	0.2559	0.6756	0.0984	1.0775

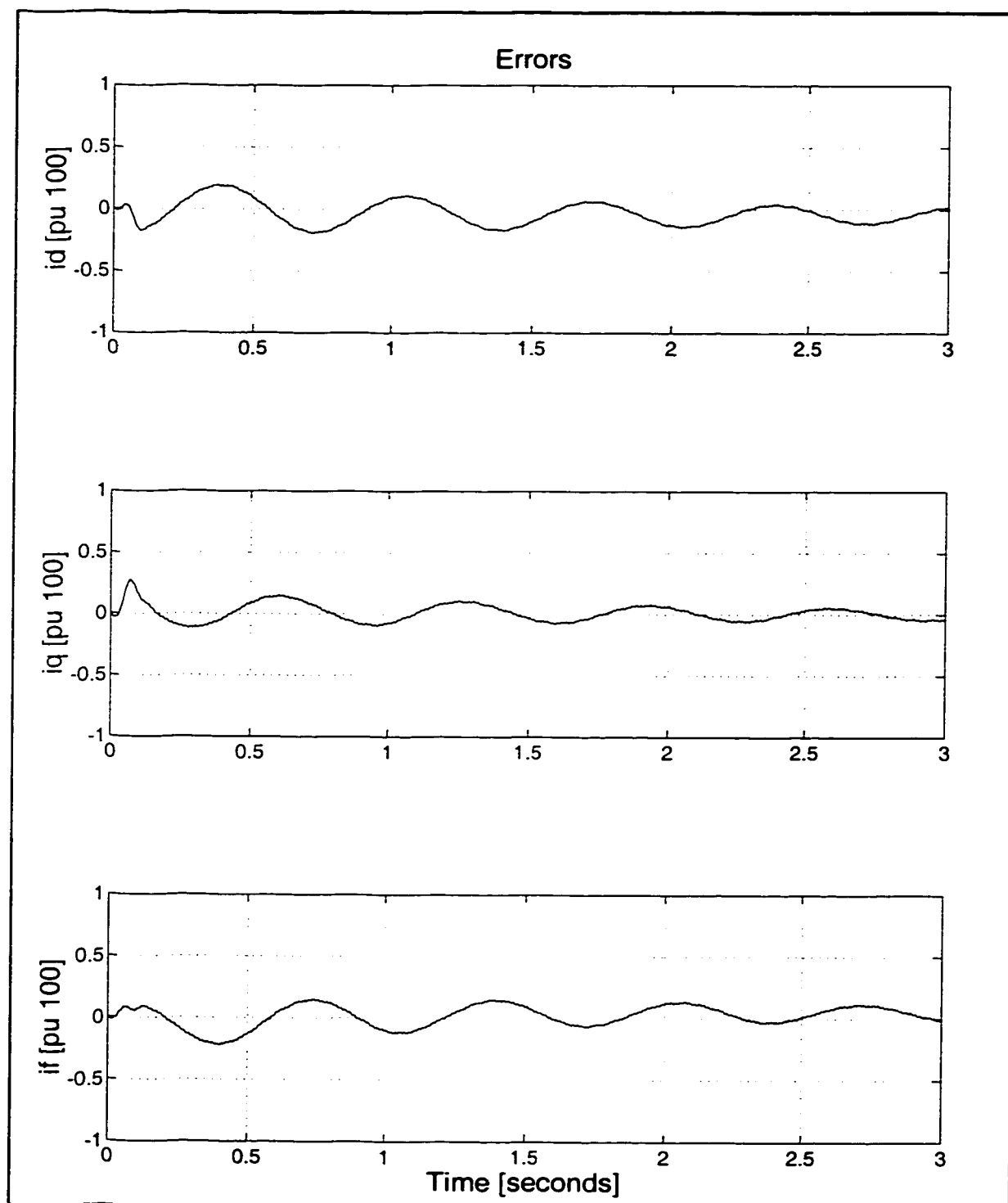


Figure 6-9: Time Varying Errors for Set 4

6.6 Results Summary

The proposed method has been successfully applied to the estimation of the parameters that affect the transient behaviour of a salient pole synchronous generator. A simulation study has also shown that it is possible to apply the same method to a round rotor SM.

The main points to note are:

- It is possible to obtain the parameters using a small system perturbation. A 10% of load insertion has proven to be enough in the experimental and simulation studies.
- Only one perturbation seems to be enough to perform the estimation.
- The performance of the obtained transient parameters is affected by the accuracy of the steady-state parameters being used.

CHAPTER 7

CONCLUSIONS

7.1 Introduction

Presented in this chapter are the conclusions of this dissertation. Also, possible ways to further expand this work are outlined.

7.2 Conclusions

Economic factors are constantly pushing the power systems to be operated at optimal capacity. For this to be possible, sophisticated models and accurate parameters of the electric components of the systems are required. Having reliable parameters for these models is as important as the refined models themselves. Many methods for SMs parameters estimation have been developed during the years. Among them, the stand still frequency response test remains the state of the art in parameter estimation because it has been fully tested by many research groups on a variety of SMs, in size and design, which has provided the test with un-disputable consensus about its reliability and performance.

This work has presented an original and alternative approach that can be used to deal with the parameter estimation problem. The basic idea has been to introduce the reader to the problems associated with parameter estimation and walk through some of the several approaches that can be used for parameter estimation. There is agreement that an on-line based method that could perform the task of parameter estimation in a reasonable and reli-

able way would be the perfect solution to the problem. So far, very few attempts have followed this path, though.

The first step of this work has been to define a SM model establishing the linear parameters and saturation factors. A detailed analysis on how to convert the manufacturer's parameters into circuit parameters has been developed in a deductive way and has been extended to consider these transformations when the field resistance is known.

The second step has been to present the tool to solve the problem. ANNs have been applied to many disciplines and areas of Power System Analysis and this is the first time that ANN have been used for parameter estimation purposes. The goal of the presentation has been to emphasize their capability as a powerful tool for pattern recognition.

Finally, an original method for SM parameter estimation has been presented. The solution has been devised similar to that of solving a pattern recognition problem. This is an entirely new concept in the field.

The practical implementation of the method has shown its viability as a powerful method to estimate all the parameters involved in the SM model, including saturation. Taking into account the nature of the method (on-line based) this is an unavoidable feature, but considering that all the standard methods restrict their estimation to the linear characteristics of the model, this is by itself an important achievement.

The main difficulty encountered in the application of the method to obtain the steady-state characteristics of the SM has been to deal with saturation. The method has shown that it can overcome the problem. Furthermore, it has been shown that information from only a few points is enough to obtain parameters that define, with an acceptable margin of error, an accurate behaviour in a far reaching area within the capability region of the SM.

A surprising side effect of the application of the method has been to be able to obtain very good results without using the rotor position information through the load angle

variable. It is probably premature though, to assert that the method offers this capability as a feature, and further experimental work is required, but the sole results of this work are extremely promising.

The method has also been applied to estimate the SM dynamic parameters of a salient pole SM and simulation studies have shown that it is possible to obtain the parameters of a round rotor generator. The goal has been to show that the estimation can be carried out using the information from a small system disturbance capable of exciting all the dynamic parameters of the SM. In the case tested, a 10% load insertion at the machine terminals seems to be enough for this purpose. This is a crucial factor that highlights the feasibility of the method itself in view of the fact that for stability reasons, power systems have to be able to cope with small disturbances on a daily basis and it is expected that the same results can be obtained through other perturbations as well.

The results obtained in both the steady-state and transient state analysis are very encouraging. Among the main features of the method are:

- **Accurate**

The experimental results have shown that the parameters obtained with this method are very reliable and are suitable for the model used to predict the behaviour of the SM in a wider set of operating conditions than those used for the estimation purpose.

- **Feasible**

The requirements of the method are to obtain steady-state information of the behaviour of the SMs determined by a series of boundary conditions that expand, as much as possible, throughout the saturation characteristics. In transient state, a system disturbance capable of exciting the dynamic behaviour of the SM seems to be enough to extract the information required. These are very loose operating requirements, when compared with other tests, and are not that far away from the normal operation of the

SM. This is arguably true for any dynamic disturbance, but having shown that any test based on a field perturbation is conceptually wrong, this is the least intrusive requirement that can be formulated.

- **Flexible**

One aspect that highlights the flexibility of the method is related to the loose requirements of the method. Indeed, the boundary conditions can be imposed on the method by operating restrictions and the method still be capable of estimating the parameters. Another side to consider is that there are no restrictions on the model of the SM. Eventually, other saturation models can be easily considered.

- **Inexpensive**

Economic factors push the electric utilities to perform tests to obtain more accurate parameters of the SMs. Because the tests are expensive to perform, economic factors are also a reason why tests are usually avoided. The proposed method is very inexpensive to apply for two reasons. There is no specialized equipment involved during the tests other than that required to record all the measurable variables of the SM, and the measurements can take place during normal operating conditions.

The most important limitations of the method are those that any on-line approach has to overcome.

- **Rotor Position**

The rotor position is not a variable that is usually available. Indeed, it can even be a challenge to have access to a suitable portion of the rotor to implement a mechanism that grabs information about it. This, added to the special requirements to measure the rotor position, makes this variable the biggest challenge in the measurement stage. Although it has been shown that excellent results can be obtained for steady-state parameters without

the usage of the rotor position, its availability is crucial to obtain the dynamic parameters.

- **System Perturbations**

To obtain the transient parameters of the SM, the method requires to extract information derived from the incidence that a small system perturbation has on the SM under consideration. There are no limitations in this sense, as long as the disturbance is strong enough to excite all the dynamic characteristics of the SM. Despite the fact that small disturbances are not an unlikely characteristic in the operation of an electric power system, the possibility of having an electric utility performing one for the sole purpose of measuring the parameters of a SM can prove to be the most challenging requirement of the method.

The proposed method has evolved from its early theoretical stage [88] to the current phase, in which theory and practice have converged to produce a well-founded and realistic approach to the parameter estimation problem using on-line data.

It is expected that this thesis will help to provide an alternative and new path in this area, serving as an initial and fundamental contribution that will inspire further developments in the field.

7.3 Future Work

- **Further Experimental Work**

This study has presented a new method for parameter estimation and it has shown its feasibility through a successful practical implementation. Far from over, this work has to be considered as a very important first step. In this sense, further experimental studies that confirm these results on a vari-

ety of SMs, in size and design, will contribute towards the consolidation of the method as a viable and reliable alternative for parameter estimation.

- **Alternative Implementations**

It is not difficult to think of different alternatives in the practical implementation of the method. This work has explored the application through two natural stages: steady-state and transient state. This is not imposed by the method itself, but has been adopted here for convenience. Since all the steady-state characteristics are contained in the dynamic response an interesting extension, that future work will have to deal with, is to perform both stages at once through an integrated approach. Recurrent ANNs can be specially useful for this extension.

- **SM Models**

Although the approach of this work has been to define a SM model of the SM and estimate its parameters, this is not a restriction of the method. Indeed, the method is very flexible and other models of the SM that consider, for example, the sub-subtransient characteristics of the SM, can easily be implemented. Other saturation models can also be incorporated in the estimation process. All these possible variations are an interesting open field that future work has to explore.

REFERENCES

- [1] IEEE Standard 115-1995 IEEE Guide: Test Procedures for Synchronous Machines, Part I--Acceptance and Performance Testing, Part II--Test Procedures and Parameter Determination for Dynamic Analysis.
- [2] Dandeno, P.L., Kundur, P., "Stability Performance of 555 MVA turboalternators - Digital Comparisons with System Operating Tests", IEEE Trans. on Power Apparatus and Systems, Vol. PAS-93, No. 3, May/June 1974, pp. 767-776.
- [3] Butler, J.W., Concordia, C., "Analysis of Series Capacitor application Problems". AIEE Tran., 1937.
- [4] Bowler C.E.J., Ewart, D.N., Concordia, C., "Self Excited Torsional Frequency Oscillations with Series Capacitors". IEEE Trans. on Power Apparatus and Systems. Vol. PAS-92, No.5, November/December 1973, pp. 1688-1695.
- [5] Ballance, J.W., Goldberg, S., Subsynchronous Resonance in Series Compensated Transmission Lines". IEEE Trans. on Power Apparatus and Systems, Vol. PAS-92. No.5, November/December 1973, pp. 1649-1658.
- [6] IEEE Subsynchronous Resonance Task Force of the Dynamic System Performance Working Group, Power System Engineering Committee, "First Benchmark Model for Computer Simulation of Subsynchronous Resonance", IEEE Trans. on Power Apparatus and Systems, PAS-96, No. 5, September/October 1977, pp. 1565-1572.
- [7] IEEE Committee Report, "Current Usage and Suggested practices in Power System Stability Simulations for Synchronous Machines", IEEE Transactions on Energy Conversion, Vol. EC-1, No. 1, March 1986, pp. 77-93.

- [8] Dandeno, P.L., Hauth, R.L., Schulz, R.P., "Effects of Synchronous Machine Modeling in Large Scale System Studies", IEEE Trans. on Power Apparatus and Systems, Vol. PAS-92, No. 2, March/April 1973, pp. 574-582.
- [9] Minnich, S.H., Schulz, R.P., Baker, D.H., Farmer, R.G., Sharma, D.K., Fish, J.H., "Saturation Functions For Synchronous Generators From Finite Elements", IEEE Trans. on Energy Conversion, Vol. EC-2, No. 4, Dec. 1987, pp. 680-692.
- [10] Schulz, R.P., Goering, C.J., Farmer, R.G., Bennett, S.M., Selin, D.A., "Benefit Assessment of Finite-Element Based Generator Saturation Model", IEEE Transactions on Power Systems, Vol. PWRS-2, No. 4, November 1987, pp. 1027-1033.
- [11] Dougherty, J.W., Minnich, S.M., "Operational Inductances of Turbine Generators; Test Data Versus Finite-Element Calculations", IEEE Trans. on Power Apparatus and Systems, Vol. PAS-102, No. 10, October 1983, pp. 3393-3404.
- [12] Dougherty, J.W., Minnich, S.M., "Finite Element Modelling of Large Turbine Generators: Calculations versus Load Test Data", IEEE Trans. on Power Apparatus and Systems, Vol. PAS-100, No. 8, August 1981, pp. 3921-3929.
- [13] Tahan, S.A., Kamwa, I., "A Two-factor Saturation Model for Synchronous Machines with Multiple Rotor Circuits", IEEE Trans. on Energy Conversion, Vol. EC-10, No. 4, December 1995, pp. 609-616.
- [14] Tsai, H., Keyhani, A., Demcko, J., Farmer, R.G., "On-Line Synchronous Machine Parameter Estimation from Small Disturbance Operating Data", IEEE Trans. on Energy Conversion, Vol. EC-10, No. 1, March 1995, pp. 25-36.
- [15] Tumageanian, A., Keyhani, A., "Identification of Synchronous Machine Linear Parameters from Standstill Step Voltage Input Data", IEEE Trans. on Energy Conversion, Vol. EC-10, No. 2, June 1995, pp. 232-240.
- [16] Kilgore, L.A., "Calculations of Synchronous Machine Constants", AIEE Trans. Vol. 50, December 1931, pp. 1201-1214.

- [17] Wright, S.H., "Determination of Synchronous Machine Constants by Test", AIEE Trans. Vol. 50, December 1931, pp. 1331-1351.
- [18] Adkins, B., Harley, R.G., "The General Theory of Alternating Current Machines". Chapman and Hall, London, 1975.
- [19] IEEE Std. 1110-1991, "IEEE Guide for Synchronous Generator Modeling Practices in Stability Analyses".
- [20] Shackshaft, G., Poray, A.T., "Implementation of New Approach to Determination of Synchronous Machine Parameteres from Tests", Proc. IEE, Vol. 124, No. 12, December 1977, pp. 1170-1178.
- [21] Shackshaft, G., "New Approach to the Determination of Synchronous Machine Parameteres from Tests", Proc. IEE, Vol. 121, No. 11, November 1974, pp. 1385-1392.
- [22] Takeda, Y., Adkins, B., "Determination of Synchronous Machine Parameteres Allowing for Unequal Mutual Inductances", Proc. IEE, Vol. 121, No. 12, December 1974, pp. 1501-1504.
- [23] deMello, F.P., Hannett, L.N., "Validation of Synchronous Machine Models and Determination of Model parameteres from Tests", IEEE Trans. on Power Apparatus and Systems, Vol. PAS-100, No. 2, February 1981, pp. 662-672.
- [24] deMello, F.P., Ribeiro, J.R., "Derivation of Synchronous Machine Parameters from Tests", IEEE Trans. on Power Apparatus and Systems, Vol. PAS-96, July/August 1977, pp. 1211-1218.
- [25] Kundur, P., "Power System Stability and Control". McGraw-Hill Inc., 1994.
- [26] Atarod, V., Dandeno, P.L., Iravani, M.R., "Impact of Synchronous Machine Constants and Models on the Analysis of Torsional Dynamics", IEEE Transactions on Power Systems, Vol. PWRS-7, No. 4, November 1992, pp. 1456-1463.

- [27] Kirtley, J.L., "On Turbine-Generator Equivalent Circuits". IEEE Trans. on Power System, Vol. PWRS-9, No. 1, February 1994, pp. 262-271.
- [28] Dandeno P.L., Kundur, P., Poray, A.T, Coultres, M.E., "Validation of Turbogenerator Stability Models by Comparison with Power System Tests", IEEE Trans. on Power Apparatus and Systems, Vol. PAS-100, No. 4, April 1981, pp. 1637-1645.
- [29] Coultres, M.E., Watson, W., "Synchronous Machine Models by Standstill Frequency Response Tests", IEEE Trans. on Power Apparatus and Systems, Vol. PAS-100, No. 4, April 1981, pp. 1480-1489.
- [30] Dandeno, P.L., Poray, A.T., "Development of Detailed Turbogenerator Equivalent Circuits from Standstill Frequency Response Measurements", IEEE Trans. on Power Apparatus and Systems, Vol. PAS-100, No. 4, April 1981, pp. 1646-1655.
- [31] EPRI Report EL-1424, "Determination of Synchronous Machine Stability Constants", Vol.2, prepared by Ontario Hydro, December 1980.
- [32] IEEE Standard 115A-1984, "IEEE Trial Use Standard Procedures for Obtaining Synchronous Machine Parameters by Standstill Frequency Response Testing.
- [33] Dandeno P.L., Kundur, P., Poray, A.T., Zein El-Din, H.M., "Adaptation and Validation of Turbogenerator Models Parameters though On-Line Frequency Response Measurements", IEEE Trans. on Power Apparatus and Systems, Vol. PAS-100, No. 4, April 1981, pp. 1656-1664.
- [34] Canay, I.M., "Determination of Model Parameters of Machines From The Reactance Operators $X_d(p)$, $X_q(p)$ ", IEEE Trans. on Energy Conversion, Vol. EC-8, No. 2, June 1993, pp.272-279.
- [35] Canay, I.M., "Modeling of Alternating-Current Machines Having Multiple Rotor Circuits", IEEE Trans.on Energy Conversion, Vol. EC-8, No. 2, June 1993, pp.280-296.

- [36] Schulz, R.P., Jones, W.D., Ewart, D.N., "Dynamic Models of Turbine Generators Derived From Solid Rotor Equivalent Circuits", IEEE Trans. on Power Apparatus and Systems, Vol. PAS-92, No. 3, May/June 1973, p. 926-933.
- [37] EPRI Report EL- 3359, "Improvement in Accuracy of Prediction of Electrical Machine Constants and Generator Models for Subsynchronous Resonance Conditions. Volume 2: Application of Two-Dimensional Finite-Element Techniques for Synchronous Machine Modeling", prepared by General Electric Company. April 1984.
- [38] Balda, J.C., Hadingham, M.F., Fairbairn, R.E., Harley, Eitelberg, E., "Measurement of Synchronous Machine Parameters by a Modified Frequency Response Method - Part I: Theory", IEEE Trans. on Energy Conversion, Vol. EC-2, No.4, December 1987, pp. 646-651.
- [39] Balda, J.C., Hadingham, M.F., Fairbairn, R.E., Harley, Eitelberg, E., "Measurement of Synchronous Machine Parameters by a Modified Frequency Response Method - Part II: Measured Results", IEEE Trans. on Energy Conversion, Vol. EC-2, No.4, December 1987, pp. 652-657.
- [40] Bissig, H., Reichert, K., Kulig, T.S., "Modelling and identification of Synchronous Machines, a New Approach with an Extended Frequency Range", IEEE Trans. on Energy Conversion, Vol. EC-8, No.2, June 1993, pp. 263-261.
- [41] Boje, E.S., Balda, J.C., Harley, R.G., Beck, R.C., "Time-Domain Identification of Synchronous machine Parameters From Simple Standstill Tests", IEEE Trans. on Energy Conversion, Vol. EC-5, No.1, March 1990, pp. 164-175.
- [42] de Mello, F.P., Hannett, L.N., "Determination of Synchronous machine Electrical Characteristics by Test", IEEE Trans. on Power Apparatus and Systems, Vol. PAS-102, No. 12, December 1983, pp. 3810-3815.
- [43] El-Serafi, A.M., Wu, J., "Determination of the Parameters Representing the Cross-Magnetizing Effect in Saturated Synchronous Machines", IEEE Trans. on Energy Conversion, Vol. EC-8, No. 3, September 1993, pp. 333-342.

- [44] Huang, C.T., Chen, Y.T., Chang, C.L., Huang, C.Y., Chiang, H.D., Wang, J.C., "On-line Measurement-based Model Parameter Estimation for Synchronous Generators: Model Development & Identification Schemes". *IEEE Trans. on Energy Conversion*, Vol. EC-9, No. 2, June 1994, pp. 330-336.
- [45] Wang, J.C., Chiang, H.D., Huang, C.T., Chen, Y.T., Chang, C.L., Chiou, C.Y., "On-line Measurement-based Model Parameter Estimation for Synchronous Generators: Solution Algorithm and Numerical Studies", *IEEE Trans. on Energy Conversion*, Vol. EC-9, No. 2, June 1994, pp. 337-343.
- [46] Keyhani, A., Hao, S., Schulz, R., "Maximum Likelihood Estimation of Generator Stability Constants Using SSFR Test Data", *IEEE Trans. on Energy Conversion*, Vol. EC-6, No. 1, March 1991, pp. 140-154.
- [47] Namba, M., Nishiwaki, T., Yokikawa, S., Ohtsuka, K., Ueki, Y., "Identification of Parameters for Power System Stability Analysis Using Kalman Filter", *IEEE Trans. on Power Apparatus and Systems*, Vol. PAS-100, No. 7, July 1981, pp. 3304-3311.
- [48] Anderson, P.M., Fouad, A.A., "Power System Control and Stability". *IEEE Press*. Revised printing, 1994.
- [49] Gibbs, W.J., "Electric Machine Analysis Using Matrices". *Pitman & Sons Ltd.*, London, 1962.
- [50] Kimbark, E.W., "Power System Stability, Vol. III, Synchronous Machines". *John Wiley & Sons, Inc.*, New York, 1956.
- [51] Concordia, C., "Synchronous Machines - Theory and Performance". *John Wiley & Sons, Inc.*, New York, 1951.
- [52] Jones, C.V., "The Unified Theory of Electrical Machines". *Butterworths & Co. (Publishers) Ltd.*, 1967.
- [53] Park, R.H., "Two Reaction Theory of Synchronous Machines - Part I", *AIEE Trans.* No. 48, July 1929, pp. 716-730.

- [54] Park, R.H., "Two Reaction Theory of Synchronous Machines - II", AIEE Trans. No. 52, June 1933, pp. 352-355.
- [55] Canay, I.M., "Causes of Discrepancies on Calculations of Rotor Quantities and Exact Equivalent Diagrams of the Synchronous Machine", IEEE Trans. on Power Apparatus and Systems, Vol. PAS-88, No. 7, July 1969, pp. 1114-1120.
- [56] Shackshaft, G., "Model of Generator Saturation for Use in Power System Studies", Proc. IEE, Vol. 126, No. 8, August 1979, pp. 759-763.
- [57] Harley, R.G., Limebeer, D.J.N., Chirricozzi, E., "Comparative Study of Saturation Methods in Synchronous Machine Models", Proc. IEE, Vol. 127, Pt. B. No. 1, Jan. 1980, pp. 1-7.
- [58] Walker, J.H., "Operating Characteristics of Salient-Pole Machines", Proc. IEE, Vol. 100, Part II, 1953, pp. 13-24.
- [59] Szwander, W., "Fundamental Electrical Characteristics of Synchronous Turbo-Generators", Jour. IEE, Vol. 91, Part II, 1944, pp. 185-194.
- [60] Kahaner, D., Moler, C., Nash, S., "Numerical Methods and Software". Prentice-Hall Inc., 1989.
- [61] Dommel, H.W., "Digital Computer Solution of Electromagnetic Transients in Single and Multiphase Networks", IEEE Trans. on Power Apparatus and Systems, Vol. PAS-88, No. 4, April 1969, pp. 388-399.
- [62] Woodford, D.A., Gole, A.M., Menzies, R.W., "Digital Simulation of DC Links and AC Machines", IEEE Trans. on Power Apparatus and Systems, Vol. PAS-103, No. 6, June 1983, pp. 1616-1623.
- [63] Haykin, S., "Neural Networks". Macmillan, 1994.
- [64] Hertz, J., Krogh, A., Palmer, R.G., "Introduction to the Theory of Neural Computation". Addison-Wesley, 1991.

- [65] Masters, M., "Practical Neural Network Recipes in C++". Academic Press Inc., 1993.
- [66] Hecht-Nielsen, R., "Neurocomputing". Addison-Wesley, 1990.
- [67] Werbos, P.J., "Beyond regression: New Tools for Prediction and Analysis in the Behavioral Sciences". Ph.D. Thesis, Harvard University, 1974.
- [68] Press, W.H., Teukolky, S.A., Vetterling, W.T., Flannery, B.P., "Numerical Recipes in C". Second Edition, Cambridge University Press, 1992.
- [69] Johansson, E.M., Dowla, F.U., Goodman, D.M., "Backpropagation Learning for Multi-Layer Feed-Forward Neural Networks Using the Conjugate Gradient method", Report UCRL-JC 104850, Lawrence Livermore National Laboratory, 1990..
- [70] Dennis, J.E., Schnabel, R.B., "Numerical Methods for Unconstrained Optimization and Nonlinear Equations". Prentice-Hall Inc., 1983.
- [71] Hagan, M.T., Menhaj, M.B., "Training Feedforward Networks with the Marquardt Algorithm", IEEE Trans. on Neural Networks, Vol. 5, No. 6, November 1994, pp.989-993.
- [72] Box, G.E.P., Jenkins, G.M., "Time Series Analysis, Forecasting and Control". Holden Day, Revised Ed., 1976.
- [73] Gaupe, D., "Identification of Systems". Van Nostrand Reinhold Company, 1972.
- [74] Fu, K.S. (ed.), "Application of Pattern Recognition". CRC Press, Inc., 1982.
- [75] Meisel, W.S., "Computer-Oriented Approaches to Pattern Recognition". Academic Press, 1972.
- [76] Bishop, C.M., "Neural Networks for Pattern Recognition". Oxford University Press, 1995.
- [77] Widrow, B., Winter, R.G., Baxter R.A., "Layered neural Nets for Pattern Recognition", IEEE Trans. on Acoustics, Speech, and Signal Processing, Vol. 36, No. 7, July 1988, pp. 1109-1118.

- [78] Fairbairn, R.E., Harley, R.G., "On-Line Measurement of Synchronous Machine Parameters", IEEE Trans. on Industry Applications, Vol. 28, No. 3, May/June 1992, pp. 639-645.
- [79] EMTDC User Manual. Manitoba HVDC Research Centre. 1988.
- [80] Spectrum Signal Processor Inc., "TMS320C30 System Board User's Manual". Issue 1.0 May, 1990.
- [81] Spectrum Signal Processor Inc., "TMS320C30 System Board Technical Reference Manual". Issue 1.0 May, 1990.
- [82] Texas Instruments Incorporated, "TMS320C30x User's Guide". 2558539-9721 revision E, June 1991.
- [83] Texas Instruments Incorporated, "TMS320 Floating-Point DSP Assembly Language Tools User's Guide". 2576328-9761, revision B, February, 1995.
- [84] Texas Instruments Incorporated, "TMS320 Floating-Point DSP Optimizing C Compiler User's Guide". 2576391-9761, revision B, February, 1995.
- [85] Funk, A.T., "Distance Protection Based on an Adaptive Window Length Filtering Algorithm". Ph.D. Dissertation, The University of Calgary, 1998.
- [86] Megahed, A.I., "Neural Network Based Digital Differential Relay for Synchronous Generators". Ph.D. Dissertation, The University of Calgary, 1998.
- [87] Sanaye-Pasand, M., "Transmission Line Directional Protection Using Neural Networks and Filtering Algorithms". Ph.D. Dissertation, The University of Calgary, 1998.
- [88] Calvo, M., Malik, O.P., "Estimation of Synchronous Machine Steady State Parameters Using Artificial Neural Networks". Proceedings, COPIMERA '95 (XV Pan-American Congress of Mechanical, Electrical and Allied Engineering). Paname, October 2-6, 1995, Paper #4, Canadian Contribution, 8 pages.

- [89] Umans, S.D., Mallick, S.A., Wilson, G.L., "Modelling of Solid Rotor Turbogenerators. Part I: Theory and Techniques", *IEEE Trans. on Power Apparatus and Systems*, Vol. PAS-97, No. 1, January/February 1978, pp. 269-277.
- [90] Umans, S.D., Mallick, S.A., Wilson, G.L., "Modelling of Solid Rotor Turbogenerators. Part II: Example of Model Derivation and Use in Digital Simulation", *IEEE Trans. on Power Apparatus and Systems*, Vol. PAS-97, No. 1, January/February 1978, pp. 278-291.
- [91] Kamwa, I., Viarouge, P., Dickinson, E.J., "Identification of Generalised Models of Synchronous Machines From Time-Domain Tests", *Proc. IEE*, Vol. 138, Pt. C. No. 6, Nov. 1991, pp. 485-498.
- [92] Harris, M.R., Lawrenson, P.J., Stephenson, J.M., "Per Unit Systems with Special Reference to Electrical Machines". IEE Monograph, Cambridge Univ. Press, London, 1970.
- [93] Pahalawaththa, N.C., Hancock, G.C., Hope, G.S., Malik, O.P., "Linear Fast Measurement of Speed Deviation for On-Line Control of a Generating Unit Physical Model", *Measurement*, Vol. 10, No. 4, Oct-Dec 1992.

APPENDIX A

STANDARD CHARACTERISTICS AND CIRCUIT PARAMETERS

A.1 Introduction

This appendix accounts for a detailed development of an accurate equivalence between the standard characteristics and the circuit parameters. The developments are complemented with the presentation of the corresponding relationships that are part of the classical theory of synchronous machines.

A.2 Exact Equivalence

Until recently there was no exact equivalence between circuit parameters and standard characteristics. Even the best available algorithms [31,89-90], when compared [91], can give up to 2000% of discrepancy for the field winding reactance when referring to the same SM. Recently [35], a widely respected solution to this problem has been provided. Because the original reference lacks of any deductive approach¹ and the practical importance of the results, this section develops the exact equivalence for the specific case of two rotor circuits.

1. Which forced some of the discussers of the original paper to provide further numerical examples to confirm the results.

A.2.1 Operational Equations of the SM

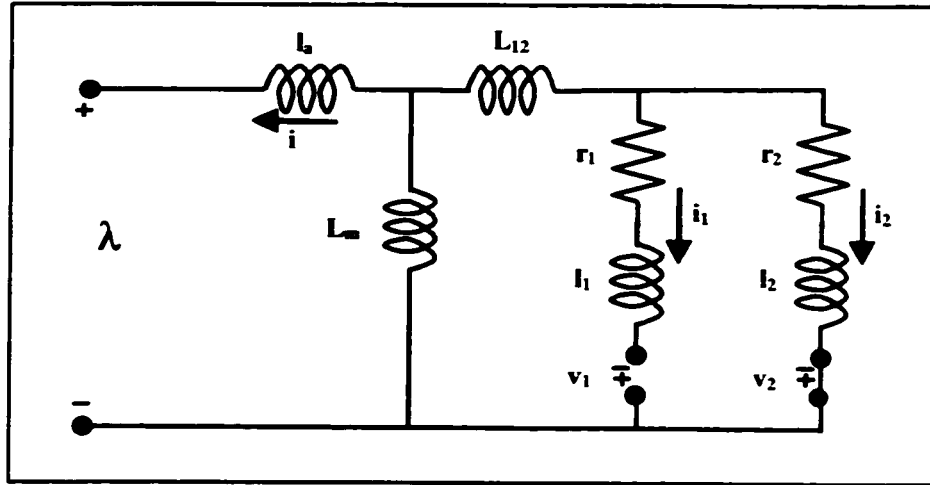


Figure A-1: Generic Equivalent Circuit

Given the equivalent circuit of Figure A-1 the following equations for the voltages and flux linkage are valid:

$$\begin{bmatrix} v_1 \\ v_2 \\ \lambda \end{bmatrix} = - \begin{bmatrix} r_1 + (l_1 + L_{12} + L_m)p & (L_{12} + L_m)p & L_m p \\ (L_{12} + L_m)p & r_2 + (l_2 + L_{12} + L_m)p & L_m p \\ L_m & L_m & l_a + L_m \end{bmatrix} \begin{bmatrix} i_1 \\ i_2 \\ i \end{bmatrix} \quad (\text{A-1})$$

Considering that

$$\begin{aligned} L &= l_a + L_m \\ X_{1\sigma} &= l_1 + L_{12} \\ X_{2\sigma} &= l_2 + L_{12} \end{aligned} \quad (\text{A-2})$$

and using the following *open circuit* definitions

$$\begin{aligned} T_{o1} &= (L_m + L_{12} + l_1)/r_1 = (L_m + X_{1\sigma})/r_1 \\ T_{o2} &= (L_m + L_{12} + l_2)/r_2 = (L_m + X_{2\sigma})/r_2 \\ X_{120} &= L_{12} + L_m \end{aligned} \quad (\text{A-3})$$

equations (A-1) can be rewritten as:

$$\begin{bmatrix} v_1 \\ v_2 \\ \lambda \end{bmatrix} = - \left[\begin{array}{cc|c} r_1(1+T_{o1}p) & -X_{120}p & L_m p \\ X_{120}p & r_2(1+T_{o2}p) & L_m p \\ \hline L_m & L_m & L \end{array} \right] \begin{bmatrix} i_1 \\ i_2 \\ i \end{bmatrix} \quad (\text{A-4})$$

Defining the *coupling matrix* CM as being formed by the terms within the dashed box in (A-4), its inverse is given by:

$$[CM]^{-1} = \begin{bmatrix} r_1(1+T_{o1}p) & X_{120}p \\ X_{120}p & r_2(1+T_{o2}p) \end{bmatrix}^{-1} = \frac{1}{r_1 r_2} \begin{bmatrix} r_2(1+T_{o2}p) & -X_{120}p \\ -X_{120}p & r_1(1+T_{o1}p) \end{bmatrix} \quad (\text{A-5})$$

$$= \frac{1}{1 + (T_{o1} + T_{o2})p + T_{o1}T_{o2}} \frac{1}{k_{120}p^2}$$

where the factor k_{120} is given by

$$k_{120} = \frac{\begin{vmatrix} r_1 T_{o1} & X_{120} \\ X_{120} & r_2 T_{o2} \end{vmatrix}}{r_1 T_{o1} r_2 T_{o2}} = 1 - \frac{X_{120}^2}{r_1 T_{o1} r_2 T_{o2}} \quad (\text{A-6})$$

From equations (A-4), the currents are given by

$$\begin{bmatrix} i_1 \\ i_2 \end{bmatrix} = -[CM]^{-1} \begin{bmatrix} 1 \\ 1 \end{bmatrix} L_m p i - [CM]^{-1} \begin{bmatrix} v_1 \\ 0 \end{bmatrix} \quad (\text{A-7})$$

Then, the flux linkage of (A-4)) can be equated as:

$$\lambda = -L \frac{1 + \left(T_{o1} + T_{o2} - \frac{L_m^2}{L} \left[\frac{1}{r_1} + \frac{1}{r_2} \right] \right) p + \left(\frac{L_m^2}{L} \left[\frac{2X_{12O}}{r_1 r_2} - \frac{T_{o1}}{r_2} - \frac{T_{o2}}{r_1} \right] + T_{o1} T_{o2} k_{12O} \right) p^2}{1 + (T_{o1} + T_{o2})p + T_{o1} T_{o2} k_{12O} p^2} i$$

$$+ \frac{\frac{L_m}{r_1} \left(1 + \frac{l_2}{r_2} p \right)}{1 + (T_{o1} + T_{o2})p + T_{o1} T_{o2} k_{12O} p^2} v_1 \quad (\text{A-8})$$

With the following *short circuit* definitions

$$X_\delta = \frac{l_a L_m}{L}$$

$$T_1 = \left(\frac{l_a L_m}{L} + L_{12} + l_1 \right) / r_1 = (X_\delta + X_{1\sigma}) / r_1$$

$$T_2 = \left(\frac{l_a L_m}{L} + L_{12} + l_2 \right) / r_2 = (X_\delta + X_{2\sigma}) / r_2$$

$$X_{12S} = L_{12} + X_\delta \quad (\text{A-9})$$

a factor similar to (A-6) can be defined as:

$$k_{12S} = \frac{\begin{vmatrix} r_1 T_1 & X_{12S} \\ X_{12S} & r_2 T_2 \end{vmatrix}}{r_1 T_1 r_2 T_2} = 1 - \frac{X_{12S}^2}{r_1 T_1 r_2 T_2} \quad (\text{A-10})$$

With these definitions, the expression for the flux linkages (A-8) can be compacted to the more familiar form [18] of the operational equation of the SM:

$$\lambda = -L \frac{1 + (T_1 + T_2)p + T_1 T_2 k_{12S} p^2}{1 + (T_{o1} + T_{o2})p + T_{o1} T_{o2} k_{12O} p^2} i + \frac{\frac{L_m}{r_1} \left(1 + \frac{l_2}{r_2} p \right)}{1 + (T_{o1} + T_{o2})p + T_{o1} T_{o2} k_{12O} p^2} v_1 \quad (\text{A-11})$$

$$= -L(p)i + G(p)v_1$$

The circuit shown in Figure A-1 is usually the one used for the d axis. The equivalent circuit for the quadrature axis is a simplified version of this one, without the mutual inductance L_{12} and without the field source v_f . With these simplifications, a corresponding operational equation can easily be obtained for the q axis as:

$$\begin{aligned}\lambda &= -L \frac{1 + (T_1 + T_2)p + T_1 T_2 k_{12s} p^2}{1 + (T_{o1} + T_{o2})p + T_{o1} T_{o2} k_{12o} p^2} i \\ &= -L(p) i\end{aligned}\tag{A-12}$$

A.2.2 Transient and Subtransient Parameters

The operational inductance $L(p)$ from (A-11) can be expressed as a function of the *open-circuit* and *short-circuit* polynomials, $P_o(p)$ and $P(p)$ respectively:

$$\begin{aligned}L(p) &= L \frac{1 + (T_1 + T_2)p + T_1 T_2 k_{12s} p^2}{1 + (T_{o1} + T_{o2})p + T_{o1} T_{o2} k_{12o} p^2} \\ &= L \frac{P(s)}{P_o(p)} = L \frac{1 + Ap + Bp^2}{1 + A_o p + B_o p^2} = L \frac{(1 + T' p)(1 + T'' p)}{(1 + T_o' p)(1 + T_o'' p)}\end{aligned}\tag{A-13}$$

From the *short circuit* polynomial $P(p)$, the *transient* and *subtransient short circuit time constants* can be obtained as:

$$T' = \frac{A + \sqrt{A^2 - 4B}}{2} \quad ; \quad T'' = \frac{A - \sqrt{A^2 - 4B}}{2}\tag{A-14}$$

Similar expressions can be obtained for the *transient* and *subtransient open circuit time constants* using $P_o(p)$.

It is very common in the literature to find an expression for the inverse of the operational inductance $L(p)$, as a function of the short circuit time constants:

$$\frac{1}{L(p)} \frac{1}{p} = \frac{1}{L} \frac{(1 + T_o' p)(1 + T_o'' p)}{(1 + T' p)(1 + T'' p)} \frac{1}{p} = \frac{A}{p} + \frac{BT'}{(1 + T' p)} + \frac{BT''}{(1 + T'' p)} \quad (\text{A-15})$$

which can be expressed as

$$\frac{1}{L(p)} = \frac{1}{L} + \left(\frac{1}{L} - \frac{1}{L'} \right) \frac{T' p}{(1 + T' p)} + \left(\frac{1}{L'} - \frac{1}{L''} \right) \frac{T'' p}{(1 + T'' p)} \quad (\text{A-16})$$

using the following definitions for the *transient* and *subtransient inductances*

$$L' = \frac{L}{1 + \frac{(T' - T_o')(T'' - T_o'')}{(T' - T'')T'}} ; \quad L'' = \frac{L}{\frac{L}{L'} + \frac{(T'' - T_o'')(T' - T_o')}{(T'' - T')T'}} = L \frac{T' T''}{T_o' T_o''} \quad (\text{A-17})$$

A.2.3 Circuit Parameters

Given the circuit of Figure A-2(a), the external admittance as seen from the terminals is:

$$\frac{1}{L_i(p)} = \frac{1}{L_{mi}} + \frac{\frac{1}{r_{1i}} p}{(1 + \frac{l_{1i}}{r_{1i}} p)} + \frac{\frac{1}{r_{2i}} p}{(1 + \frac{l_{2i}}{r_{2i}} p)} \quad (\text{A-18})$$

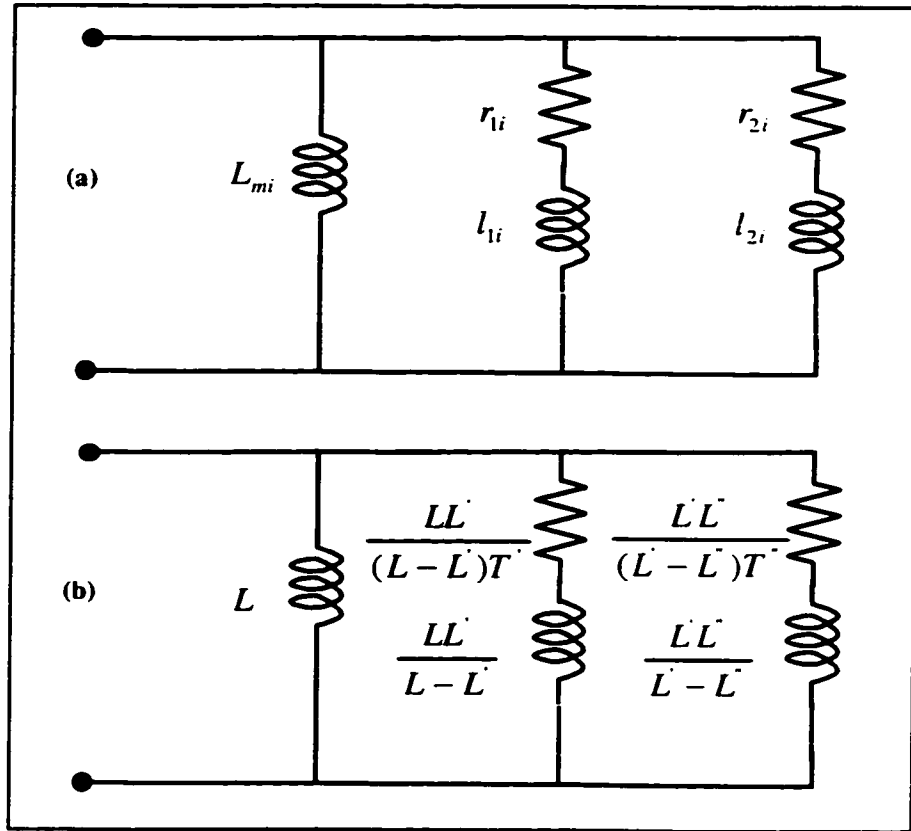


Figure A-2: Equivalent Circuit with Embedded Leakage Reactance

By comparison, it is clear that expression (A-16) is the admittance of a circuit similar to the one shown in Figure A-2(a), but with the parameters as defined in circuit (b) of the same figure.

This circuit has embedded the *leakage* inductance of the armature l_a . The operational inductance of the equivalent circuit without this reactance is given by:

$$\begin{aligned}
 L_e(p) &= L(p) - l_a = L \frac{P(s)}{P_o(p)} - l_a = L \frac{1 + Ap + Bp^2}{1 + A_o p + B_o p^2} - l_a \\
 &= (L - l_a) \frac{1 + \frac{LA - l_a A_o}{L - l_a} p + \frac{LA - l_a A_o}{L - l_a} p^2}{1 + A_o p + B_o p^2} = L_m \frac{P_e(s)}{P_o(p)}
 \end{aligned} \tag{A-19}$$

With the leakage reactance removed, as expected, the same *open circuit* polynomial is valid. The coefficients of the *short circuit* polynomial are redefined as follows:

$$\begin{aligned}
 A_e &= \frac{LA - l_a A_o}{L - l_a} = \frac{1}{L - l_a} [L(T' + T'') - l_a(T_o' + T_o'')] \\
 B_e &= \frac{LB - l_a B_o}{L - l_a} = \frac{1}{L - l_a} [LT'T'' - l_a T_o' T_o''] = \frac{L' - l_a}{L - l_a} T_o' T_o''
 \end{aligned} \tag{A-20}$$

With this polynomial, the *transient* and *subtransient* short circuit time constants, T'_e and T''_e , can be obtained with expressions of the form of (A-14). Then, expressions similar to (A-17) can be used to obtain the *transient* and *subtransient* inductances, L'_e and L''_e , respectively.

With the information gathered so far, a circuit similar to the one shown in Figure A-2(b) can be formed for the equivalent circuit without the stator leakage reactance. If the leakage component is added, the circuit shown in Figure A-3 can be obtained.

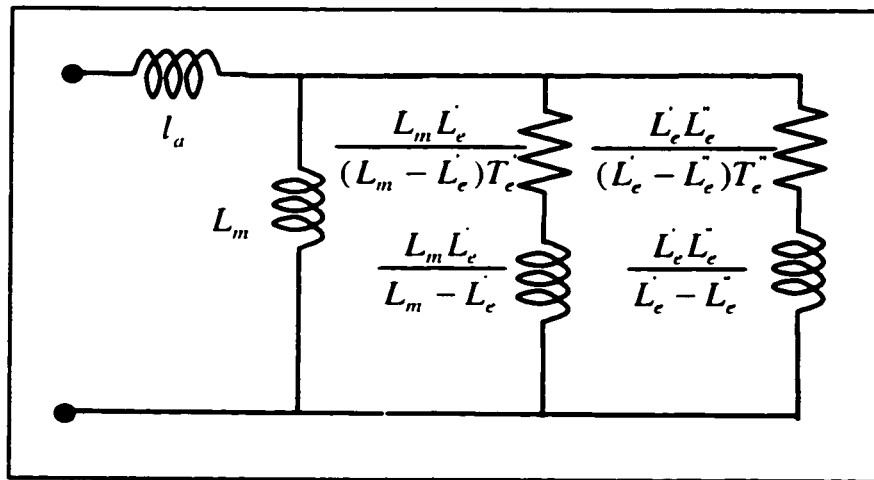


Figure A-3: Equivalent Circuit without the Mutual Inductance L_{12} .

This circuit has the same *open circuit* and *short circuit* time constants as the one shown in Figure A-1 meaning that, from a stator point of view, both circuits have the same behaviour. The same is not true for the field winding [55] where, in general, the field current of both circuits is different for any given perturbation.

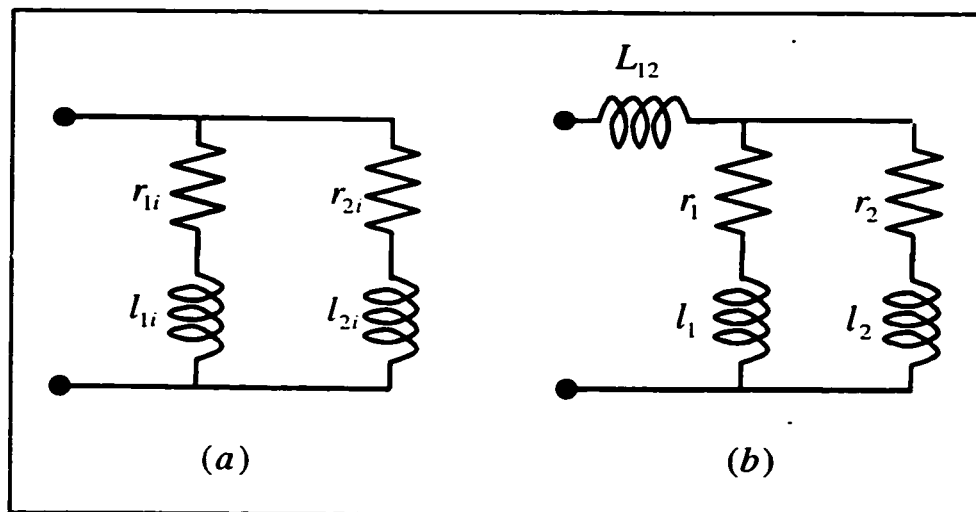


Figure A-4: Equivalent Circuits with Embedded and External Inductance L_{12}

A.2.3.1 Circuit Parameters Using The Short Circuit Current

It has been proposed in [34,35] to use the field current following a short circuit test to obtain the mutual inductance L_{12} that will turn the circuit shown in Figure A-3 into the one of Figure A-1.

In order to accomplish this, circuit (a) has to turn into (b) in Figure A-4, keeping the same external impedance. Because circuit (a) has the mutual inductance L_{12} embedded, the following relationship can be written for the impedance of the two parallel branches of circuit (b):

$$\begin{aligned}
 Z_{12}(p) &= Z_i(p) - L_{12}s \\
 &= \frac{1 + \left(\frac{l_{1i} - L_{12}}{r_{1i}} + \frac{l_{2i} - L_{12}}{r_{2i}} \right) p + \left(\frac{l_{1i}l_{2i} - L_{12}(l_{1i} + l_{2i})}{r_{1i}r_{2i}} \right) p^2}{\frac{r_{1i} + r_{2i}}{r_{1i}r_{2i}} + \frac{l_{1i} + l_{2i}}{r_{1i}r_{2i}} p} \quad (\text{A-21}) \\
 &= \frac{P_{12}(p)}{P_{12o}(p)} = \frac{1 + A_{12}p + B_{12}p^2}{P_{12o}(p)} = \frac{(1 + T_1p)(1 + T_2p)}{P_{12o}(p)}
 \end{aligned}$$

where T_1 and T_2 are the *short circuit* time constants, i.e.: the time constants of each of the parallel branches of circuit (b) in Figure A-4:

$$T_1 = \frac{l_1}{r_1} = \frac{A_{12} + \sqrt{A_{12}^2 - 4B_{12}}}{2} \quad ; \quad T_2 = \frac{l_2}{r_2} = \frac{A_{12} - \sqrt{A_{12}^2 - 4B_{12}}}{2} \quad (\text{A-22})$$

The open circuit polynomials of both circuits of Figure A-4 should be the same. This is equivalent to saying that the denominators of $Z(p)$ and $Z_{12}(p)$ are the same, from where the following relationships can be obtained:

$$\frac{r_1 + r_2}{r_1 r_2} = \frac{r_{1i} + r_{2i}}{r_{1i} r_{2i}}$$

(A-23)

$$\frac{l_1 + l_2}{r_1 r_2} = \frac{l_{1i} + l_{2i}}{r_{1i} r_{2i}}$$

Equations (A-22) and (A-23) can be combined to obtain the following expressions for the resistances:

$$r_1 = \frac{r_{1i} r_{2i} (T_1 - T_2)}{(r_{1i} + r_{2i}) T_1 - l_{1i} - l_{2i}}$$

(A-24)

$$r_2 = \frac{-r_{1i} r_{2i} (T_1 - T_2)}{(r_{1i} + r_{2i}) T_2 - l_{1i} - l_{2i}}$$

Then, knowing the parameters of circuit (a) of Figure A-4 and the current i_I for a predetermined perturbation (say, as it was mentioned before, the current following a short circuit test), a search over a suitable range of L_{I2} is done in order to obtain the final set of values $\{L_{I2}, r_I, r_2, l_I, l_2\}$ that will provide the actual current i_I .

A.2.3.2 Circuit Parameters Using The Field Resistance

There is another procedure that the author of this work has developed to turn the circuit shown in Figure A-3 into the one of Figure A-1. Instead of using a short circuit test, an alternative and accurate approach to obtain the mutual inductance L_{I2} is to use a measured value of the field resistance r_I .

The impedances of both circuits shown in Figure A-4 should be the same. This is equivalent to saying that the open circuit polynomials and short circuit polynomials of both circuits are the same. From this equality, it is possible to obtain the following equations:

$$\begin{aligned}
 k_1 &= \frac{r_{1i} + r_{2i}}{r_{1i} r_{2i}} = \frac{r_1 + r_2}{r_1 r_2} \\
 k_2 &= \frac{l_{1i} + l_{2i}}{r_{1i} r_{2i}} = \frac{l_1 + l_2}{r_1 r_2} \\
 k_3 &= \frac{l_{1i}}{r_{1i}} + \frac{l_{2i}}{r_{2i}} = \frac{l_1}{r_1} + \frac{l_2}{r_2} + L_{12} \left(\frac{1}{r_1} + \frac{1}{r_2} \right) \\
 k_4 &= \frac{l_{1i} l_{2i}}{r_{1i} r_{2i}} = \frac{l_1 l_2 + L_{12} (l_1 + l_2)}{r_1 r_2}
 \end{aligned} \tag{A-25}$$

where the constants k_1 through k_4 have been defined considering that the terms in 'i' are known.

From the first relationship of (A-25) it is possible to obtain r_2 as:

$$r_2 = \frac{r_1}{k_1 r_1 - 1} \tag{A-26}$$

Solving for l_1 , the following quadratic relationship is found:

$$\begin{aligned}
 a &= -1/r_1 r_2 \quad ; \quad b = k_2 \left(1 + \frac{r_1 - r_2}{k_1 r_1 r_2} \right) \quad ; \quad c = -k_4 + \frac{k_2}{k_1} (r_1 k_2 + k_3) \\
 l_1 &= \frac{-b - \sqrt{b^2 - 4ac}}{2a}
 \end{aligned} \tag{A-27}$$

where only the positive value is considered. Then, it is straightforward to obtain l_2 and L_{12} with the following relationships:

$$l_2 = k_2 r_1 r_2 - l_1$$

$$L_{12} = \left(k_3 + l_1 \frac{r_1 - r_2}{k_1 r_1 r_2} - k_2 r_1 \right) \frac{1}{k_1} \quad (\text{A-28})$$

A.2.4 Relationships Between Time Constants

Of the six parameters that affect the dynamic behaviour of the synchronous machine on each axis, and according to the definitions adopted in equations (A-17), only four are independent. This means that given either the open circuit or the short circuit time constants, the other subset of time constants can be obtained as a function of the given one.

A.2.4.1 Obtaining the Open Circuit Time Constants

Given T' , T'' , L' and L'' , equation (A-16) can be used to obtain the *open circuit* polynomial as a function of the reactances and *short circuit* time constants:

$$P_o(p) = 1 + \left(\frac{L}{L'} T' + \left(1 + \frac{L}{L'} - \frac{L}{L'} \right) T'' \right) p + \frac{L T' T''}{L} p^2 = 1 + A_o p + B_o p^2 \quad (\text{A-29})$$

from where the *open circuit* time constants T'_o and T''_o can be obtained using expressions similar to (A-14).

A.2.4.2 Obtaining the Short Circuit Time Constants

In this case, T'_o , T''_o , L' and L'' are known. From equation (A-29), it follows that

$$A_o = \frac{L}{L'} T' + \left(1 + \frac{L}{L'} - \frac{L}{L''}\right) T'' = T'_o + T''_o \quad (\text{A-30})$$

$$B_o = \frac{L T' T''}{L'} = T'_o T''_o$$

where it can be noticed that the expression for B_o is nothing but the relationship given by definition (A-17). Then, T'' can be substituted to obtain the following polynomial in T' :

$$P(T') = T'^2 - (T'_o + T''_o) \frac{L}{L'} T' + \frac{T'_o T''_o}{L} \left(\frac{L' L''}{L} + L' - L'' \right) = a T'^2 + b T' + c \quad (\text{A-31})$$

Of the two possible values for T' the larger one will give the right result when substituted in the relationship for B_o to obtain T'' , i.e. $T' > T''$.

A.3 Classical Approach

The classical approach to define the equivalence between circuit parameters and standard characteristics is based on approximations founded on physical assumptions. There is agreement though, that these approximations can account for serious discrepancies between the calculated parameters and what is derived from test measurements [35,21].

A.3.1 Standard Characteristics

Given a generic equivalent circuit like the one showed in Figure A-1, it is easy to derive the corresponding transient and subtransient time constants and reactances, as it is shown in equations (A-32), based on the assumptions that $r_1=0$ during the subtransient period and that $r_2=\infty$ during the transient period [19].

$$L = L_m + l_a$$

$$L' = l_a + \frac{1}{\frac{1}{L_m} + \frac{1}{l_1 + L_{12}}} \quad ; \quad L'' = l_a + \frac{1}{\frac{1}{L_m} + \frac{1}{L_{12} + \frac{1}{\frac{1}{l_1} + \frac{1}{l_2}}}}$$

$$T_o' = \frac{L_m + L_{12} + l_1}{r_1} \quad ; \quad T' = \frac{1}{r_1} \left(l_1 + L_{12} + \frac{1}{\frac{1}{l_a} + \frac{1}{L_m}} \right) \quad (\text{A-32})$$

$$T_o'' = \frac{1}{r_2} \left(l_2 + \frac{1}{\frac{1}{L_{12} + L_m} + \frac{1}{l_1}} \right) \quad ; \quad T'' = \frac{1}{r_2} \left(l_2 + \frac{1}{\frac{1}{l_1} + \frac{1}{L_{12} + \frac{1}{\left(\frac{1}{l_a} + \frac{1}{L_m} \right)}}} \right)$$

These formulas are valid for a generic circuit form that, in general, will correspond to the d axis model. The q axis is modelled without the mutual inductance L_{12} , in which case, this value should be zeroed when performing the calculations.

A.3.2 Circuit Parameters

Using the relationships of (A-32), it can easily be verified by substitution that the following relationships are valid:

$$\dot{L} = L \frac{T'}{T_o'} \quad \dot{L} = L' \frac{T'}{T_o'} \quad (\text{A-33})$$

which were obtained in equations (2-12) and (2-13).

This reduces the amount of independent variables to four, meaning that only four circuit parameters can be determined. Then, knowing the standard characteristics, there is enough information to determine the parameters of a circuit like the one of Figure A-1 without the mutual inductance L_{12} . Zeroing L_{12} in the relationships given by (A-32) the following equations can be derived:

$$\begin{aligned} l_1 &= \frac{1}{\frac{1}{\dot{L} - l_a} + \frac{1}{L_m}} \\ r_1 &= \frac{l_1 + L_m}{T_o'} = \left(l_1 + \frac{1}{l_a + L_m} \right) \frac{1}{T'} \\ l_2 &= \frac{1}{\frac{1}{\dot{L} - l_a} - \frac{1}{L_m} - \frac{1}{l_1}} \\ r_2 &= \left(l_2 + \frac{1}{\frac{1/l_1 + 1/L_m}} \right) \frac{1}{T_o'} = \left(l_2 + \frac{1}{\frac{1/l_1 + 1/L_m + 1/l_a}} \right) \frac{1}{T'} \end{aligned} \quad (\text{A-34})$$

APPENDIX B

CONSISTENCY CHECK OF THE STANDARD CHARACTERISTICS

B.1 Introduction

The standard characteristics of a synchronous generator are specified according to a well defined model of the machine. For these characteristics to be valid they must comply, at least to a certain degree, with the inherent relationships of the mathematical model. Considering this, a consistency check can be performed on the parameters of the model against the equations derived from the model.

The goal here is to use the relationships derived in Appendix A to perform a consistency check on the data offered by the manufacturer.

B.2 Data and Calculations

Tables B-1 to B-4 show different sets of typical parameters of SMs obtained from manufacturers [48] for *Fossil Steam Units (F)* and *Cross-Compound Fossil Steam Units (CF)*. The notation for the parameters and calculations followed on these table are:

- Data provided by the manufacturer:
 - (a) X, l_a - reactances in pu.
 - (b) T - time constants in seconds.

- Parameters derived from the manufacturer's data:
 - (a) r - circuit resistances in pu.
 - (b) x - circuit reactances in pu.
 - (c) T - time constants in seconds.
- Indices "tt" and "t" mean sub-transient and transient respectively;
- Indices "E" (exact) and "C" (classical) refer to the method used to calculate those parameters according to Appendix A.
- Indices "sc" (short circuit) and "oc" (open circuit) following the kind of method to perform the calculations ("E" or "C") mean that the "sc" or "oc" time constants given by the manufacturer were used to perform all the calculations using the specified method.
- Comparison "xx vs yy" are evaluated as: $(xx-yy)/yy*100$.
- "~"/"err". Whenever it is not possible to perform the calculations because there is insufficient data, or previous errors in the calculations, it is noted with "~". When the method applied generates errors or inconsistencies, this is noted with "err".

Following the previous notation it is possible to distinguish the following blocks in Tables B-1 to B-4:

- (a) *Manufacturer's data* - The first eight parameters is the data provided by the manufacturer.
- (b) *Exact calculations* - Using the exact method, the open circuit time constants and circuit parameters are calculated as a function of the short circuit

time constants. The short circuit time constants and circuit parameters can also be obtained using the open circuit time constants.

- (c) *Classical approximations* - The open circuit time constants and circuit resistances are obtained as a function of the short circuit time constants. In a similar way, the short circuit time constants and circuit resistances are calculated as a function of the open circuit time constants. The circuit reactances are obtained as a function of the transient and subtransient reactances.
- (d) *Calculations versus manufacturer's data* - The calculated time constants using both approaches are compared to the original data. These amounts, together with the fact of being able (or not) to obtain the circuit parameters, checks the consistency of the data.
- (e) *Circuit parameters comparison using either set of time constants* - The calculated parameters using one set of time constants (either open circuit or short circuit) are compared with the ones obtained using the other set of time constants for the same method. This checks how much the models will diverge working with either set of time constants.
- (f) *Exact versus classical* - The circuit parameters obtained with the Classical approach are compared with the ones using the Exact method. This tells how much the model will diverge working with either method.

Table B-1: Machine Data and Calculations - (a)

Variables	F1		F4		F5		F6		F7	
	d	q	d	q	d	q	d	q	d	q
Xtt	0.1200	0.1200	0.1300	0.1300	0.1450	0.1450	0.1340	0.1340	0.2160	0.2160
Xt	0.2320	0.7150	0.1850	0.3600	0.2200	0.3800	0.1740	0.2500	0.2990	0.9760
X	1.2500	1.2200	1.0500	0.9800	1.1800	1.0500	1.2200	1.1600	1.5370	1.5200
la	0.1340	0.1340	0.0700	0.0700	0.0750	0.0750	0.0780	0.0780	0.1330	0.1330
Ttt	0.0350	0.0350	-	-	-	-	0.0230	0.0230	0.0350	0.0072
Tt	0.8820	-	-	-	-	-	1.2800	0.6400	-	-
Tott	0.0590	0.2100	0.0380	0.0990	0.0420	0.0920	0.0330	0.0700	0.0484	0.2180
Tot	4.7500	1.5000	6.1000	0.3000	5.9000	0.3000	8.9700	0.5000	4.3000	1.5000
TottEsc	0.0657	-	-	-	-	-	0.0297	0.0419	-	-
TotEsc	4.8975	-	-	-	-	-	9.0161	3.0431	-	-
r1Esc	err	-	-	-	-	-	0.0004	0.0012	-	-
x1Esc	err	-	-	-	-	-	0.1064	0.2128	-	-
r2Esc	err	-	-	-	-	-	0.0201	0.0156	-	-
x2Esc	err	-	-	-	-	-	0.1318	0.0817	-	-
TttEoc	0.0314	0.0396	0.0269	err	0.0280	err	0.0255	err	0.0354	0.0525
TtEoc	0.8574	0.7827	1.0653	err	1.0881	err	1.2728	err	0.8254	0.8846
r1Eoc	err	err	0.0005	-	0.0006	-	0.0004	-	0.0010	0.0073
x1Eoc	err	err	0.1330	-	0.1703	-	0.1066	-	0.1972	2.3118
r2Eoc	err	err	0.0164	-	0.0173	-	0.0181	-	0.0174	0.0104
x2Eoc	err	err	0.1231	-	0.1332	-	0.1315	-	0.1596	0.0918
x1C	err	err	0.1303	0.4256	0.1669	0.4438	0.1048	0.2045	0.1883	2.1493
x2C	err	err	0.1255	0.0757	0.1353	0.0909	0.1344	0.0830	0.1660	0.0921
TottCsc	0.0677	0.2085	-	-	-	-	0.0299	0.0429	0.0484	0.0325
TotCsc	4.7522	-	-	-	-	-	8.9747	2.9696	-	-
r1Csc	err	err	-	-	-	-	0.0004	0.0011	-	-
r2Csc	err	err	-	-	-	-	0.0205	0.0158	0.0182	0.0762
TttCoc	0.0305	0.0352	0.0267	0.0358	0.0277	0.0351	0.0254	0.0375	0.0350	0.0482
TtCoc	0.8816	0.8791	1.0748	0.1102	1.1000	0.1086	1.2793	0.1078	0.8365	0.9632
r1Coc	err	err	0.0005	0.0118	0.0006	0.0125	0.0004	0.0068	0.0010	0.0063
r2Coc	err	err	0.0168	0.0098	0.0177	0.0114	0.0185	0.0097	0.0182	0.0114
TttEoc vs Ttt	-10.35	13.10	-	-	-	-	11.06	-	1.24	629.61
TtEoc vs Tt	-2.78	-	-	-	-	-	-0.57	-	-	-
TottEsc vs Tott	11.29	-	-	-	-	-	-9.91	-40.18	-	-
TotEsc vs Tot	3.11	-	-	-	-	-	0.51	508.62	-	-
TttCoc vs Ttt	-12.81	0.70	-	-	-	-	10.49	63.13	-0.10	570.08
TtCoc vs Tt	-0.05	-	-	-	-	-	-0.05	-83.16	-	-
TottCsc vs Tott	14.69	-0.69	-	-	-	-	-9.50	-38.70	0.10	-85.08
TotCsc vs Tot	0.05	-	-	-	-	-	0.05	493.92	-	-
r1Eoc vs r1Esc	-	-	-	-	-	-	0.72	-	-	-

Table B-1: (Continued) Machine Data and Calculations - (a)

Variables	F1		F4		F5		F6		F7	
	d	q	d	q	d	q	d	q	d	q
x1Eoc vs x1Esc	-	-	-	-	-	-	0.18	-	-	-
r2Eoc vs r2Esc	-	-	-	-	-	-	-10.13	-	-	-
x2Eoc vs x2Esc	-	-	-	-	-	-	-0.23	-	-	-
r1Coc vs r1Csc	-	-	-	-	-	-	0.05	493.92	-	-
r2Coc vs r2Csc	-	-	-	-	-	-	-9.50	-38.70	0.10	-85.08
TttCsc vs TttEsc	-2.74	-10.97	-0.88	-	-1.08	-	-0.51	-	-1.33	-8.16
TtCsc vs TtEsc	2.82	12.32	0.89	-	1.09	-	0.52	-	1.34	8.88
TottCsc vs TottEsc	3.06	-	-	-	-	-	0.46	2.48	-	-
TotCsc vs TotEsc	-2.97	-	-	-	-	-	-0.46	-2.42	-	-
r1Csc vs r1Esc	-	-	-	-	-	-	-1.20	-3.40	-	-
x1C vs x1Esc	-	-	-	-	-	-	-1.51	-3.90	-	-
r2Csc vs r2Esc	-	-	-	-	-	-	1.62	1.06	-	-
x2C vs x2Esc	-	-	-	-	-	-	1.94	1.58	-	-
r1Coc vs r1Eoc	-	-	-2.54	-	-2.77	-	-1.86	-	-4.94	-14.45
x1C vs x1Eoc	-	-	-2.00	-	-2.00	-	-1.69	-	-4.52	-7.03
r2Coc vs r2Eoc	-	-	2.49	-	2.43	-	2.34	-	4.45	9.00
x2C vs x2Eoc	-	-	1.93	-	1.62	-	2.17	-	3.99	0.30

Table B-2: Machine Data and Calculations - (b)

Variables	F8		F9		F10		F13		F14	
	d	q	d	q	d	q	d	q	d	q
Xtt	0.1850	0.1850	0.1710	0.1710	0.2490	0.2480	0.2600	0.2550	0.2284	0.2239
Xt	0.2450	0.3800	0.2320	0.3800	0.3240	0.9180	0.3240	1.0510	0.2738	1.0104
X	1.7000	1.6400	1.6510	1.5900	1.5690	1.5480	1.7980	1.7780	1.7668	1.7469
la	0.1100	0.1100	0.1020	0.1020	0.2040	0.2040	0.1930	0.1930	0.1834	0.1834
Ttt	-	-	0.0230	0.0230	0.3500	-	0.0350	0.0350	-	-
Tt	-	-	0.8290	0.4150	0.9500	-	0.1590	0.5810	-	-
Tott	0.0330	0.0760	0.0330	0.0780	0.0437	0.1410	0.0420	0.0420	0.0420	0.1580
Tot	5.9000	0.5400	5.9000	0.5350	5.1400	1.5000	5.2100	1.5000	5.4320	1.5000
TottEsc	-	-	0.0309	0.0485	0.4152	-	0.0417	0.1325	-	-
TotEsc	-	-	5.9499	1.8285	5.0457	-	0.9235	1.0702	-	-
r1Esc	-	-	0.0008	0.0030	0.0025	-	0.0078	0.0102	-	-
x1Esc	-	-	0.1458	0.3656	0.5217	-	0.2412	2.0595	-	-
r2Esc	-	-	0.0230	0.0190	0.0011	-	0.0133	0.0170	-	-
x2Esc	-	-	0.1431	0.0902	0.0511	-	0.0985	0.0666	-	-
TttEoc	0.0251	err	0.0245	err	0.0338	0.0403	0.0340	0.0103	0.0353	0.0378
TtEoc	0.8433	err	0.8215	err	1.0533	0.8403	0.9319	0.8731	0.8358	0.8045
r1Eoc	0.0008	-	0.0008	-	0.0008	0.0058	0.0009	0.0063	0.0009	0.0068
x1Eoc	0.1517	-	0.1461	-	0.1426	1.6586	0.1518	1.9052	0.1060	1.9062
r2Eoc	0.0236	-	0.0216	-	0.0113	0.0135	0.0162	0.0575	0.0107	0.0136
x2Eoc	0.1636	-	0.1428	-	0.0691	0.0468	0.1296	0.0668	0.0823	0.0425
x1C	0.1475	0.3279	0.1419	0.3419	0.1316	1.5232	0.1426	1.8706	0.0959	1.7556
x2C	0.1687	0.1038	0.1470	0.0918	0.0720	0.0469	0.1371	0.0668	0.0896	0.0426
TottCsc	-	-	0.0312	0.0511	0.4554	-	0.0436	0.1443	-	-
TotCsc	-	-	5.8995	1.7364	4.6005	-	0.8824	0.9829	-	-
r1Csc	-	-	0.0008	0.0028	0.0009	-	0.0053	0.0093	-	-
r2Csc	-	-	0.0236	0.0192	0.0011	-	0.0163	0.0170	-	-
TttCoc	0.0249	0.0370	0.0243	0.0351	0.0336	0.0381	0.0337	0.0102	0.0350	0.0350
TtCoc	0.8503	0.1251	0.8291	0.1279	1.0614	0.8895	0.9388	0.8867	0.8418	0.8676
r1Coc	0.0008	0.0091	0.0008	0.0091	0.0008	0.0051	0.0009	0.0061	0.0008	0.0059
r2Coc	0.0244	0.0130	0.0223	0.0126	0.0117	0.0143	0.0169	0.0584	0.0114	0.0146
TttEoc vs Ttt	-	-	6.73	-	-90.33	-	-2.99	-70.43	-	-
TtEoc vs Tt	-	-	-0.90	-	10.87	-	486.12	50.27	-	-
TottEsc vs Tott	-	-	-6.24	-37.77	850.19	-	-0.78	215.43	-	-
TotEsc vs Tot	-	-	0.85	241.78	-1.83	-	-82.27	-28.65	-	-
TttCoc vs Ttt	-	-	5.75	52.61	-90.40	-	-3.70	-70.88	-	-
TtCoc vs Tt	-	-	0.01	-69.19	11.73	-	490.47	52.61	-	-
TottCsc vs Tott	-	-	-5.44	-34.47	942.15	-	3.85	243.46	-	-
TotCsc vs Tot	-	-	-0.01	224.57	-10.50	-	-83.06	-34.47	-	-
r1Eoc vs r1Esc	-	-	1.09	-	-67.02	-	-88.04	-38.24	-	-

Table B-2: (Continued) Machine Data and Calculations - (b)

Variables	F8		F9		F10		F13		F14	
	d	q	d	q	d	q	d	q	d	q
x1Eoc vs x1Esc	-	-	0.22	-	-72.66	-	-37.06	-7.49	-	-
r2Eoc vs r2Esc	-	-	-6.46	-	945.37	-	21.81	238.01	-	-
x2Eoc vs x2Esc	-	-	-0.21	-	35.18	-	31.64	0.26	-	-
r1Coc vs r1Csc	-	-	-0.01	224.57	-10.50	-	-83.06	-34.47	-	-
r2Coc vs r2Csc	-	-	-5.44	-34.47	942.15	-	3.85	243.46	-	-
TttCsc vs TttEsc	-0.82	-	-0.91	-	-0.77	-5.53	-0.74	-1.53	-0.71	-7.27
TtCsc vs TtEsc	0.83	-	0.92	-	0.77	5.86	0.74	1.56	0.71	7.84
TottCsc vs TottEsc	-	-	0.86	5.30	9.68	-	4.66	8.89	-	-
TotCsc vs TotEsc	-	-	-0.85	-5.04	-8.82	-	-4.45	-8.16	-	-
r1Csc vs r1Esc	-	-	-2.15	-5.81	-65.50	-	-33.00	-8.81	-	-
x1C vs x1Esc	-	-	-2.68	-6.49	-74.78	-	-40.85	-9.17	-	-
r2Csc vs r2Esc	-	-	2.22	1.01	3.01	-	22.96	-0.07	-	-
x2C vs x2Esc	-	-	2.77	1.74	40.92	-	39.28	0.33	-	-
r1Coc vs r1Eoc	-3.01	-	-3.21	-	-6.36	-12.87	-5.16	-3.25	-7.40	-14.30
x1C vs x1Eoc	-2.76	-	-2.89	-	-7.76	-8.17	-6.03	-1.82	-9.56	-7.90
r2Coc vs r2Eoc	3.43	-	3.34	-	2.69	5.66	4.82	1.55	6.39	7.68
x2C vs x2Eoc	3.16	-	2.99	-	4.25	0.25	5.80	0.06	8.94	0.19

Table B-3: Machine Data and Calculations - (c)

Variables	F15		F18		F19		CFIH		CFIL	
	d	q	d	q	d	q	d	q	d	q
Xtt	0.2050	0.2050	0.2150	0.2150	0.3390	0.3320	0.1710	0.1710	0.2500	0.2500
Xt	0.2650	0.4600	0.2800	0.4900	0.4130	1.2850	0.2320	0.3200	0.3690	0.5650
X	1.6700	1.6000	2.1100	2.0200	2.1830	2.1570	1.6800	1.6100	1.6600	1.5900
la	0.1500	0.1500	0.1550	0.1550	0.2460	0.2460	0.0950	0.0950	0.1400	0.1400
Ttt	0.0230	-	0.0225	0.0225	-	-	0.0230	0.0230	0.0230	0.0230
Tt	1.0700	-	-	-	-	-	0.8150	0.4100	1.1300	0.5700
Tott	0.0320	0.0600	0.0320	0.0620	0.0410	0.1440	0.0340	0.0800	0.0370	0.0700
Tot	3.7000	0.4700	4.2000	0.5650	5.6900	1.5000	5.8900	0.6000	5.1000	0.3260
TottEsc	0.0296	-	-	-	-	-	0.0309	0.0414	0.0337	0.0503
TotEsc	6.7789	-	-	-	-	-	5.9532	2.1453	5.1220	1.6583
r1Esc	0.0007	-	-	-	-	-	0.0008	0.0024	0.0009	0.0035
x1Esc	0.1289	-	-	-	-	-	0.1535	0.2802	0.2745	0.6271
r2Esc	0.0193	-	-	-	-	-	0.0256	0.0206	0.0341	0.0291
x2Esc	0.1024	-	-	-	-	-	0.1663	0.1120	0.2088	0.1469
TttEoc	0.0250	0.0390	0.0249	0.0431	0.0338	0.0395	0.0253	err	0.0253	err
TtEoc	0.5809	0.0927	0.5508	0.0865	1.0705	0.8426	0.8056	err	1.1242	err
r1Eoc	0.0013	0.0371	0.0014	0.0534	0.0010	0.0084	0.0008	-	0.0010	-
x1Eoc	0.1340	1.0693	0.1440	1.4642	0.1916	2.4470	0.1539	-	0.2750	-
r2Eoc	0.0174	0.0115	0.0189	0.0111	0.0233	0.0197	0.0232	-	0.0310	-
x2Eoc	0.0994	0.0604	0.1086	0.0647	0.1993	0.0935	0.1658	-	0.2085	-
x1C	0.1244	0.3943	0.1335	0.4083	0.1828	2.2770	0.1500	0.2642	0.2696	0.6012
x2C	0.1054	0.0669	0.1154	0.0731	0.2099	0.0938	0.1707	0.1148	0.2117	0.1484
TottCsc	0.0297	-	0.0293	0.0513	-	-	0.0312	0.0430	0.0339	0.0520
TotCsc	6.7430	-	-	-	-	-	5.9017	2.0628	5.0835	1.6041
r1Csc	0.0006	-	-	-	-	-	0.0008	0.0023	0.0009	0.0034
r2Csc	0.0197	-	0.0218	0.0211	-	-	0.0262	0.0209	0.0344	0.0293
TttCoc	0.0248	0.0267	0.0246	0.0272	0.0337	0.0372	0.0251	0.0428	0.0251	0.0310
TtCoc	0.5871	0.1351	0.5573	0.1371	1.0765	0.8936	0.8134	0.1193	1.1337	0.1158
r1Coc	0.0012	0.0104	0.0013	0.0107	0.0010	0.0074	0.0008	0.0079	0.0009	0.0167
r2Coc	0.0183	0.0167	0.0199	0.0175	0.0244	0.0209	0.0240	0.0113	0.0316	0.0217
TttEoc vs Ttt	8.78	-	10.51	91.51	-	-	10.02	-	9.90	-
TtEoc vs Tt	-45.71	-	-	-	-	-	-1.16	-	-0.51	-
TottEsc vs Tott	-7.58	-	-	-	-	-	-9.02	-48.27	-8.94	-28.17
TotEsc vs Tot	83.21	-	-	-	-	-	1.07	257.54	0.43	408.70
TttCoc vs Ttt	7.63	-	9.21	20.91	-	-	8.96	85.87	8.99	34.67
TtCoc vs Tt	-45.13	-	-	-	-	-	-0.20	-70.91	0.33	-79.68
TottCsc vs Tott	-7.09	-	-8.43	-17.29	-	-	-8.22	-46.20	-8.25	-25.74
TotCsc vs Tot	82.24	-	-	-	-	-	0.20	243.80	-0.32	392.05
r1Eoc vs r1Esc	89.55	-	-	-	-	-	1.40	-	0.68	-

Table B-3: (Continued) Machine Data and Calculations - (c)

Variables	F15		F18		F19		CFIH		CFIL	
	d	q	d	q	d	q	d	q	d	q
x1Eoc vs x1Esc	3.91	-	-	-	-	-	0.28	-	0.19	-
r2Eoc vs r2Esc	-9.87	-	-	-	-	-	-9.33	-	-9.12	-
x2Eoc vs x2Esc	-2.90	-	-	-	-	-	-0.30	-	-0.15	-
r1Coc vs r1Csc	82.24	-	-	-	-	-	0.20	243.80	-0.32	392.05
r2Coc vs r2Csc	-7.09	-	-8.43	-17.29	-	-	-8.22	-46.20	-8.25	-25.74
TttCsc vs TttEsc	-1.06	-31.43	-1.18	-36.87	-0.56	-5.70	-0.96	-	-0.83	-
TtCsc vs TtEsc	1.07	45.83	1.19	58.40	0.56	6.05	0.97	-	0.84	-
TottCsc vs TottEsc	0.53	-	-	-	-	-	0.87	4.00	0.76	3.38
TotCsc vs TotEsc	-0.53	-	-	-	-	-	-0.86	-3.84	-0.75	-3.27
r1Csc vs r1Esc	-2.61	-	-	-	-	-	-1.88	-5.02	-1.50	-3.78
x1C vs x1Esc	-3.50	-	-	-	-	-	-2.30	-5.71	-1.78	-4.13
r2Csc vs r2Esc	2.02	-	-	-	-	-	2.18	1.73	1.11	0.65
x2C vs x2Esc	2.97	-	-	-	-	-	2.62	2.48	1.40	1.02
r1Coc vs r1Eoc	-6.36	-71.94	-6.61	-80.00	-3.95	-11.98	-3.04	-	-2.47	-
x1C vs x1Eoc	-7.13	-63.13	-7.29	-72.11	-4.63	-6.95	-2.57	-	-1.97	-
r2Coc vs r2Eoc	5.17	45.50	5.53	57.41	4.57	6.02	3.43	-	2.07	-
x2C vs x2Eoc	6.04	10.70	6.30	12.91	5.31	0.29	2.92	-	1.55	-

Table B-4: Machine Data and Calculations - (d)

Variables	CF2H		CF3H		CF3L		CF5H		CF5L	
	d	q	d	q	d	q	d	q	d	q
Xtt	0.2250	0.2240	0.2310	0.2290	0.2520	0.2480	0.2200	0.2200	0.2050	0.2050
Xt	0.3150	0.9580	0.3110	0.9790	0.3800	0.9550	0.2850	0.4900	0.2850	0.4850
X	1.6700	1.6400	1.6750	1.6480	1.5810	1.5310	1.8000	1.7200	1.7500	1.5800
la	0.1860	0.1860	0.3040	0.3040	0.2910	0.2910	0.1600	0.1600	0.1550	0.1550
Ttt	-	-	0.0230	0.0230	0.0230	0.0230	0.0230	0.0230	0.0230	0.0230
Tt	0.8200	-	1.0000	0.5000	1.2920	0.6500	0.5860	0.2930	1.3600	0.6800
Tott	0.0430	0.1500	0.0470	0.1500	0.0530	0.1350	0.0320	0.0600	0.0350	0.0700
Tot	5.0000	1.5000	5.4000	1.5000	5.3900	1.5000	3.7000	0.4800	8.4000	0.4600
TottEsc	-	-	0.0308	0.0920	0.0344	0.0851	0.0295	0.0478	0.0318	0.0527
TotEsc	-	-	5.4210	0.8995	5.4126	1.0851	3.7375	1.1028	8.3972	2.2879
r1Esc	-	-	err	err	err	err	0.0013	0.0057	0.0006	0.0023
x1Esc	-	-	err	err	err	err	0.1445	0.4787	0.1462	0.4556
r2Esc	-	-	err	err	err	err	0.0206	0.0208	0.0173	0.0189
x2Esc	-	-	err	err	err	err	0.1094	0.0718	0.0798	0.0585
TttEoc	0.0310	0.0375	0.0353	0.0374	0.0355	0.0368	0.0250	0.0386	0.0253	err
TtEoc	0.9329	0.8190	0.9926	0.8354	1.2817	0.8921	0.5796	0.0955	1.3597	err
r1Eoc	0.0009	0.0063	err	err	err	err	0.0014	0.0361	0.0006	-
x1Eoc	0.1540	1.7862	err	err	err	err	0.1455	1.0658	0.1467	-
r2Eoc	0.0112	0.0134	err	err	err	err	0.0189	0.0124	0.0157	-
x2Eoc	0.0541	0.0399	err	err	err	err	0.1089	0.0663	0.0797	-
x1C	0.1413	1.6459	err	err	err	err	0.1353	0.4185	0.1415	0.4295
x2C	0.0559	0.0400	err	err	err	err	0.1154	0.0733	0.0812	0.0589
TottCsc	-	-	0.0310	0.0983	0.0347	0.0886	0.0298	0.0512	0.0320	0.0544
TotCsc	4.3473	-	5.3859	0.8417	5.3754	1.0420	3.7011	1.0285	8.3509	2.2153
r1Csc	0.0010	-	err	err	err	err	0.0013	0.0051	0.0006	0.0022
r2Csc	-	-	err	err	err	err	0.0214	0.0209	0.0175	0.0190
TttCoc	0.0307	0.0351	0.0349	0.0351	0.0351	0.0351	0.0247	0.0269	0.0252	0.0296
TtCoc	0.9431	0.8762	1.0026	0.8911	1.2955	0.9357	0.5858	0.1367	1.3680	0.1412
r1Coc	0.0009	0.0055	err	err	err	err	0.0013	0.0109	0.0005	0.0107
r2Coc	0.0114	0.0144	err	err	err	err	0.0199	0.0178	0.0160	0.0147
TttEoc vs Ttt	-	-	53.32	62.72	54.47	59.86	8.56	67.67	10.13	-
TtEoc vs Tt	13.77	-	-0.74	67.08	-0.80	37.25	-1.10	-67.40	-0.02	-
TottEsc vs Tott	-	-	-34.54	-38.66	-35.01	-37.00	-7.80	-20.37	-9.14	-24.73
TotEsc vs Tot	-	-	0.39	-40.04	0.42	-27.66	1.01	129.75	-0.03	397.37
TttCoc vs Ttt	-	-	51.78	52.55	52.81	52.42	7.40	17.13	9.46	28.64
TtCoc vs Tt	15.01	-	0.26	78.22	0.27	43.95	-0.03	-53.33	0.59	-79.23
TottCsc vs Tott	-	-	-34.12	-34.45	-34.56	-34.39	-6.89	-14.62	-8.64	-22.26
TotCsc vs Tot	-13.05	-	-0.26	-43.89	-0.27	-30.53	0.03	114.27	-0.58	381.58
r1Eoc vs r1Esc	-	-	-	-	-	-	1.63	529.06	0.28	-

Table B-4: (Continued) Machine Data and Calculations - (d)

Variables	CF2H		CF3H		CF3L		CF5H		CF5L	
	d	q	d	q	d	q	d	q	d	q
x1Eoc vs x1Esc	-	-	-	-	-	-	0.69	122.66	0.34	-
r2Eoc vs r2Esc	-	-	-	-	-	-	-8.20	-40.19	-9.29	-
x2Eoc vs x2Esc	-	-	-	-	-	-	-0.52	-7.63	-0.18	-
r1Coc vs r1Csc	-13.05	-	-	-	-	-	0.03	114.27	-0.58	381.58
r2Coc vs r2Csc	-	-	-	-	-	-	-6.89	-14.62	-8.64	-22.26
TtCsc vs TtEsc	-1.08	-6.53	-1.00	-6.25	-1.07	-4.65	-1.07	-30.15	-0.61	-
TtCsc vs TtEsc	1.09	6.99	1.01	6.67	1.08	4.88	1.08	43.15	0.61	-
TottCsc vs TottEsc	-	-	0.65	6.87	0.69	4.13	0.98	7.22	0.55	3.28
TotCsc vs TotEsc	-	-	-0.65	-6.43	-0.69	-3.97	-0.97	-6.74	-0.55	-3.18
r1Csc vs r1Esc	-	-	-	-	-	-	-4.79	-11.08	-2.39	-5.05
x1C vs x1Esc	-	-	-	-	-	-	-6.36	-12.56	-3.17	-5.73
r2Csc vs r2Esc	-	-	-	-	-	-	3.68	0.50	1.01	0.07
x2C vs x2Esc	-	-	-	-	-	-	5.43	2.20	1.82	0.79
r1Coc vs r1Eoc	-7.17	-13.56	-	-	-	-	-6.29	-69.71	-3.23	-
x1C vs x1Eoc	-8.28	-7.86	-	-	-	-	-7.00	-60.73	-3.49	-
r2Coc vs r2Eoc	2.04	6.80	-	-	-	-	5.17	43.46	1.73	-
x2C vs x2Eoc	3.28	0.19	-	-	-	-	5.97	10.64	2.00	-

B.3 Consistency Check

All the information necessary to compare the data is in the previous tables. However, in order to be able to analyse and measure the overwhelming amount of numbers presented, these tables have been summarized in Table B-5 where the following notation has been added:

- "cp", and "tc" are used to refer to the circuit parameters and time constants respectively;
- "y" and "n" denote success and failure (comparisons succeed if they are within a 10% range).

- The logic to define a subset of parameters as being "OK" is set by the following rules:
 - (a) If it is not possible to calculate (or the errors are not within the margin of error of) the time constants with both the exact method and the classical method, then the data is *not OK* (n).
 - (b) If it is not possible to obtain the circuit parameters using the exact method and there are also problems applying the classical method, then the data is *not OK* (n).
 - (c) same as previous but being able to obtain the circuit parameters applying the Classical method, the data is considered *partially OK* (p).
 - (d) if none of the above apply, then the data is *OK* (y).

Also, because the direct and quadrature axis parameters can be analysed separately, the study is carried out considering each subset of data corresponding to the d and q axis individually.

This information can be further compacted as it has been done in Table B-6. Here the data has been summarized adding all the results obtained from Table B-5 and displayed on a per axis and overall basis. It can be seen that, according to this criteria, only 45% of the subsets can be considered fully consistent. When this analysis is done considering to which axis each individual subset belongs, 55% and 35% of the d and q axis subsets are consistent.

Table B-7 has been obtained repeating the previous steps, increasing the margin of an acceptable error to 100%. In this case the overall picture is that only 55% of the data can be considered consistent. (75% and 35.0% for the d and q axis respectively).

Table B-6:Consistency Check Summary with 10% Margin of Error

variables	d			q			all		
	y	p	n	y	p	n	y	p	n
tcEsc	12(100.0)	0(0.0)	0(0.0)	9(100.0)	0(0.0)	0(0.0)	21(100.0)	0(0.0)	0(0.0)
vs data	6(50.0)	0(0.0)	6(50.0)	0(0.0)	0(0.0)	9(100.0)	6(28.6)	0(0.0)	15(71.4)
cpEsc	9(75.0)	0(0.0)	3(25.0)	7(77.8)	0(0.0)	2(22.2)	16(76.2)	0(0.0)	5(23.8)
tcEoc	20(100.0)	0(0.0)	0(0.0)	12(60.0)	0(0.0)	8(40.0)	32(80.0)	0(0.0)	8(20.0)
vs data	3(25.0)	0(0.0)	9(75.0)	0(0.0)	0(0.0)	4(100.0)	3(18.8)	0(0.0)	13(81.3)
cpEoc	17(85.0)	0(0.0)	3(15.0)	9(75.0)	0(0.0)	3(25.0)	26(81.3)	0(0.0)	6(18.8)
tcCsc	12(100.0)	0(0.0)	0(0.0)	9(100.0)	0(0.0)	0(0.0)	21(100.0)	0(0.0)	0(0.0)
vs data	6(50.0)	0(0.0)	6(50.0)	0(0.0)	0(0.0)	9(100.0)	6(28.6)	0(0.0)	15(71.4)
rCsc	9(75.0)	0(0.0)	3(25.0)	7(70.0)	0(0.0)	3(30.0)	16(72.7)	0(0.0)	6(27.3)
tcCoc	20(100.0)	0(0.0)	0(0.0)	20(100.0)	0(0.0)	0(0.0)	40(100.0)	0(0.0)	0(0.0)
vs data	5(41.7)	0(0.0)	7(58.3)	0(0.0)	0(0.0)	9(100.0)	5(23.8)	0(0.0)	16(76.2)
rCoc	17(85.0)	0(0.0)	3(15.0)	17(85.0)	0(0.0)	3(15.0)	34(85.0)	0(0.0)	6(15.0)
xC	17(85.0)	0(0.0)	3(15.0)	17(85.0)	0(0.0)	3(15.0)	34(85.0)	0(0.0)	6(15.0)
data is Ok	11(55.0)	2(10.0)	7(35.0)	7(35.0)	3(15.0)	10(50.0)	18(45.0)	5(12.5)	17(42.5)

Table B-7:Consistency Check Summary with 100% Margin of Error

variables	d			q			all		
	y	p	n	y	p	n	y	p	n
tcEsc	12(100.0)	0(0.0)	0(0.0)	9(100.0)	0(0.0)	0(0.0)	21(100.0)	0(0.0)	0(0.0)
vs data	11(91.7)	0(0.0)	1(8.3)	2(22.2)	0(0.0)	7(77.8)	13(61.9)	0(0.0)	8(38.1)
cpEsc	9(75.0)	0(0.0)	3(25.0)	7(77.8)	0(0.0)	2(22.2)	16(76.2)	0(0.0)	5(23.8)
tcEoc	20(100.0)	0(0.0)	0(0.0)	12(60.0)	0(0.0)	8(40.0)	32(80.0)	0(0.0)	8(20.0)
vs data	11(91.7)	0(0.0)	1(8.3)	4(100.0)	0(0.0)	0(0.0)	15(93.8)	0(0.0)	1(6.3)
cpEoc	17(85.0)	0(0.0)	3(15.0)	9(75.0)	0(0.0)	3(25.0)	26(81.3)	0(0.0)	6(18.8)
tcCsc	12(100.0)	0(0.0)	0(0.0)	9(100.0)	0(0.0)	0(0.0)	21(100.0)	0(0.0)	0(0.0)
vs data	11(91.7)	0(0.0)	1(8.3)	2(22.2)	0(0.0)	7(77.8)	13(61.9)	0(0.0)	8(38.1)
rCsc	9(75.0)	0(0.0)	3(25.0)	7(70.0)	0(0.0)	3(30.0)	16(72.7)	0(0.0)	6(27.3)
tcCoc	20(100.0)	0(0.0)	0(0.0)	20(100.0)	0(0.0)	0(0.0)	40(100.0)	0(0.0)	0(0.0)
vs data	11(91.7)	0(0.0)	1(8.3)	9(100.0)	0(0.0)	0(0.0)	20(95.2)	0(0.0)	1(4.8)
rCoc	17(85.0)	0(0.0)	3(15.0)	17(85.0)	0(0.0)	3(15.0)	34(85.0)	0(0.0)	6(15.0)
xC	17(85.0)	0(0.0)	3(15.0)	17(85.0)	0(0.0)	3(15.0)	34(85.0)	0(0.0)	6(15.0)
data is Ok	15(75.0)	0(0.0)	5(25.0)	7(35.0)	3(15.0)	10(50.0)	22(55.0)	3(7.5)	15(37.5)

B.4 Discussion

It can be concluded that the accuracy of the data presented here, from a consistency point of view, is extremely questionable. While this assertion is valid for both axes, the d axis shows a better performance than the q axis, where the lack of reliable data is evident. Although there is not enough data available to generalize and make this exercise conclusive, the obtained results are impressive for the following reasons:

- It has been the intention to avoid any bias against the data offered by the manufacturer. This has been accomplished by setting rules that give a strong weight to the classic approach, and avoiding the use of the comparisons between methods and the ones obtained working with either set of time constants, when discriminating between good and bad data.
- When only the open circuit or short circuit time constants are available, time comparisons are considered OK by definition, and this is the case for 13 subsets (32.5%)
- The nature of the checking itself, i.e., the data is only analysed against the mathematical model that it is supposed to represent. At no time is it being discussed here if the data corresponds to the physical model of the actual machine.

APPENDIX C

PER UNIT SYSTEM

C.1 Introduction

There is no standard per unit system for synchronous machines. This has made the topic controversial and some times confusing. The most comprehensive treatment of different per unit systems has been done in [92]. The system adopted here follows that presented in [48].

C.2 Adopted Per Unit System

The following table shows how the base quantities are chosen once the machine power and voltage ratings are given ($S_{3\phi}$, V_{LL}), and the direct axis mutual inductance (L_{md}) and the field current that in absence of saturation generates a rated open circuit armature voltage (I_{FNV}) are known.

Table C-1: Base Values	
Variable	Value
S_B	$S_{3\phi}/3$
V_B	$V_{LL}/\sqrt{3}$

Table C-1: (Continued) Base Values	
Variable	Value
I_B	S_B/V_B
ω_B	$2 \pi f$
R_B	V_B/I_B
L_B	R_B/ω_B
S_{FB}	S_B
I_{FB}	$I_{FNV} L_{md(pu)} / \sqrt{3}$
V_{FB}	S_{FB}/I_{FB}
R_{FB}	V_{FB}/I_{FB}
L_{FB}	R_{FB}/ω_B

C.3 Normalized Field Magnitudes

One of the problems of per unit systems is that rated values are not necessarily reflected as 1.0 pu values. This is particularly true for the field magnitudes.

The magnitude of the field current I_{FNV} can be referred to as a normalized field current of 1.0 [79]. Appendix 7A of reference [19] refers to this particular transformation as *reciprocal system*. This amount, in Amps, has been referred to as I_{FNV} in Table C-1, from where it is easily obtained its per unit value as $\sqrt{3}/L_{md(pu)}$. A similar relationship can be obtained for the field voltage.

Because the transformation of one variable into its per unit counterpart is usually referred as normalization of the variable, care must be taken in order to avoid any confusion.

APPENDIX D

STEADY-STATE MEASUREMENTS

D.1 Introduction

This section has the experimental data obtained from steady-state measurements carried out on a micro-alternator in the Power Lab of the Department of Electrical and Computer Engineering of the University of Calgary.

D.2 Micro Alternator Characteristics

The micro-alternator under consideration has the following rated characteristics:

Table D-1: Micro-Alternator Ratings	
Characteristics	Values
Power:	3.0 KVA
Voltage:	220 V
Power Factor:	0.8
Speed:	1800 rpm
No. of poles:	4

and the following set of parameters have been offered by the manufacturer

Table D-2: Manufacturer's Data		
Parameter	d-axis ^a	q-axis
l_a	0.128	0.128
L_m	2.042	2.042
L'	0.375	0.375
L''	0.233	~
T_o'	0.756 secs	~
T_o''	0.076 secs	0.395 secs
T'	0.131 secs	
T''	0.047 secs	0.054 secs
R_a	0.0047	

a. Values are in pu unless specified

D.3 Operating Points

Figure D-1 shows a schematic of the general setup used to obtain the steady-state data. This configuration permits to control

- the active power delivered by the SM: varying the excitation of the Prime Mover (M);
- the reactive power delivered by the SM: varying the field current of the SM;

- the terminal voltage of the SM: varying the turns-ratio of the auto-transformer.

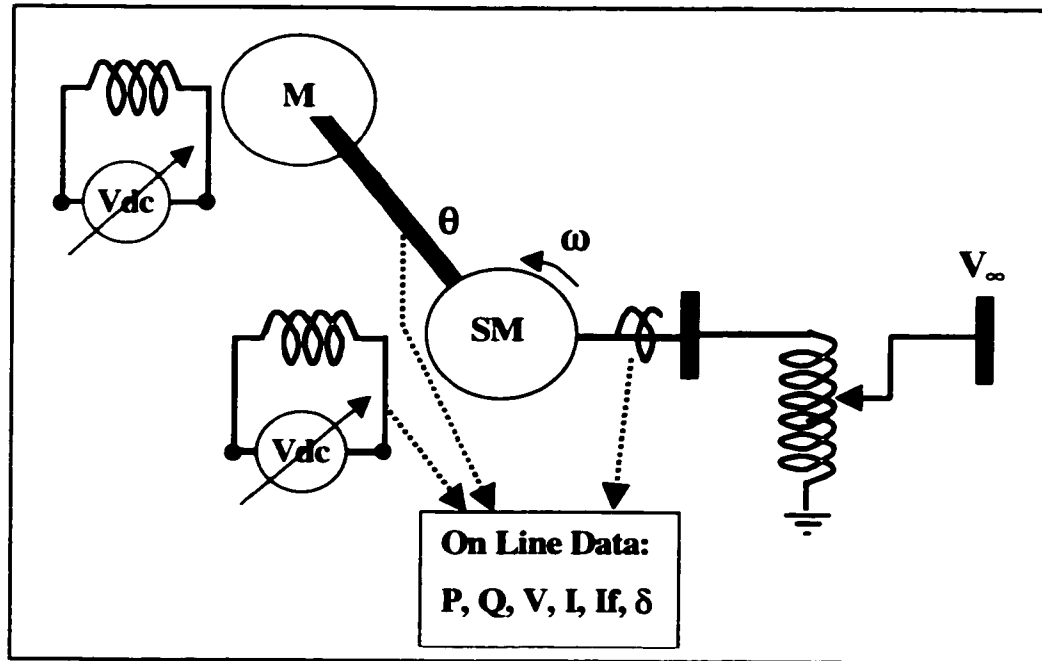


Figure D-1: Setup for the Steady-State Measurements

Table D-3 contains the measurements taken for two values of active power P ($\sim 0.87, \sim 0.66$) and three values of terminal voltage V ($\sim 0.95, \sim 1.00, \sim 1.05$) over the range of the reactive power Q within the capability limits. The readings reflect the active and reactive power, terminal voltage, armature current, field current, and load angle. To check the validity of the data, the last column of the table presents the comparison between the measured armature current and the calculated value as a function of the PQV values. The load angle is available from the control panel [93], and the other variables were measured with portable instruments.

Table D-3: Steady-State Operating Points

No	P(pu)	Q(pu)	V(pu)	I _a (pu)	I _F (A)	δ(deg)	I _{err} (%)
1	0.8440	0.4550	0.9459	1.0187	3.500	39.70	0.50
2	0.8467	0.4272	0.9459	1.0098	3.450	40.45	0.72
3	0.8493	0.3995	0.9459	1.0009	3.390	41.25	0.87
4	0.8560	0.3741	0.9441	0.9907	3.350	42.40	0.12
5	0.8587	0.3464	0.9455	0.9844	3.300	42.85	0.52
6	0.8627	0.3164	0.9455	0.9755	3.245	43.95	0.37
7	0.8667	0.2817	0.9455	0.9679	3.195	44.85	0.41
8	0.8600	0.2702	0.9482	0.9577	3.160	44.85	0.74
9	0.8640	0.2402	0.9500	0.9488	3.100	45.95	0.51
10	0.8693	0.2032	0.9464	0.9463	3.050	47.80	0.31
11	0.8760	0.1732	0.9445	0.9437	3.000	48.65	-0.17
12	0.8773	0.1432	0.9455	0.9425	2.950	50.00	0.24
13	0.8693	0.1247	0.9509	0.9272	2.910	49.95	0.40
14	0.8720	0.0878	0.9509	0.9260	2.860	51.00	0.47
15	0.8693	0.0508	0.9527	0.9234	2.800	52.55	1.03
16	0.8720	0.0092	0.9532	0.9234	2.750	54.45	0.93
17	0.8760	-0.0346	0.9518	0.9260	2.700	56.00	0.53
18	0.8773	-0.0831	0.9509	0.9310	2.650	58.45	0.46
19	0.8773	-0.1339	0.9509	0.9425	2.600	60.75	0.98
20	0.8800	-0.2078	0.9514	0.9552	2.540	64.00	0.50
21	0.8787	-0.2979	0.9486	0.9844	2.500	69.35	0.65
22	0.8760	-0.3764	0.9486	1.0187	2.460	73.85	1.35
23	0.8733	0.5566	1.0023	1.0479	3.740	36.35	1.42
24	0.8760	0.5289	1.0023	1.0314	3.700	36.85	1.02
25	0.8760	0.5011	1.0000	1.0161	3.620	37.65	0.69
26	0.8787	0.4965	0.9991	1.0136	3.600	37.85	0.34
27	0.8787	0.4688	1.0000	1.0034	3.550	38.50	0.76
28	0.8800	0.4388	1.0014	0.9933	3.500	38.85	1.15
29	0.8827	0.4111	1.0018	0.9793	3.430	39.95	0.76
30	0.8853	0.3880	1.0005	0.9755	3.400	40.30	0.96
31	0.8853	0.3649	1.0014	0.9628	3.350	40.75	0.68
32	0.8867	0.3395	0.9991	0.9602	3.300	41.85	1.05
33	0.8893	0.3164	0.9977	0.9526	3.250	42.65	0.69
34	0.8880	0.2910	0.9991	0.9425	3.200	43.30	0.77
35	0.8880	0.2633	1.0005	0.9336	3.150	43.95	0.84
36	0.8893	0.2379	1.0005	0.9298	3.100	44.60	1.04

Table D-3: (Continued) Steady-State Operating Points

No	P(pu)	Q(pu)	V(pu)	I _a (pu)	I _F (A)	δ(deg)	I _{err} (%)
37	0.8880	0.2125	1.0000	0.9234	3.050	45.55	1.13
38	0.8933	0.1709	0.9991	0.9171	2.990	47.15	0.74
39	0.8960	0.1432	0.9964	0.9145	2.950	48.15	0.42
40	0.8933	0.1155	0.9968	0.9082	2.900	48.95	0.50
41	0.8920	0.0808	0.9982	0.9044	2.850	49.95	0.79
42	0.8947	0.0439	0.9973	0.9044	2.800	51.50	0.69
43	0.8947	0.0069	0.9968	0.9031	2.750	52.80	0.62
44	0.8973	-0.0393	0.9977	0.9082	2.700	54.70	0.88
45	0.8947	-0.0762	0.9977	0.9094	2.650	56.10	1.05
46	0.8973	-0.1224	0.9977	0.9145	2.595	58.30	0.75
47	0.8933	-0.1709	0.9973	0.9171	2.550	60.45	0.55
48	0.8973	-0.2286	0.9955	0.9298	2.500	63.15	-0.05
49	0.8947	-0.3072	0.9945	0.9526	2.450	66.50	0.16
50	0.8973	-0.4319	0.9941	1.0060	2.400	74.05	0.42
51	0.8933	0.5265	1.0500	0.9895	3.700	35.70	0.19
52	0.8933	0.5081	1.0500	0.9806	3.650	36.20	0.18
53	0.8947	0.4873	1.0500	0.9691	3.610	36.55	-0.11
54	0.8960	0.4665	1.0509	0.9602	3.550	37.35	-0.10
55	0.8920	0.4503	1.0555	0.9425	3.505	37.30	-0.45
56	0.8920	0.4180	1.0555	0.9336	3.445	38.05	0.03
57	0.8960	0.3972	1.0555	0.9272	3.400	38.45	-0.15
58	0.8960	0.3741	1.0555	0.9158	3.350	39.15	-0.45
59	0.8947	0.3487	1.0545	0.9107	3.295	39.80	0.02
60	0.8907	0.3187	1.0555	0.9018	3.240	40.35	0.62
61	0.8907	0.3048	1.0577	0.8929	3.205	40.65	0.33
62	0.8893	0.2794	1.0577	0.8828	3.150	41.35	0.16
63	0.8907	0.2587	1.0482	0.8840	3.100	42.55	-0.09
64	0.8920	0.2286	1.0455	0.8790	3.050	43.45	-0.21
65	0.8920	0.1824	1.0505	0.8751	3.000	44.20	0.97
66	0.8920	0.1501	1.0500	0.8701	2.950	45.10	1.00
67	0.8960	0.1293	1.0527	0.8624	2.900	45.75	0.29
68	0.8907	0.1016	1.0536	0.8574	2.850	46.40	0.77
69	0.8893	0.0670	1.0536	0.8548	2.800	47.80	0.99
70	0.8893	0.0346	1.0527	0.8536	2.750	48.85	0.96
71	0.8933	-0.0046	1.0509	0.8536	2.700	50.45	0.41
72	0.8933	-0.0370	1.0495	0.8612	2.650	51.75	1.09
73	0.8920	-0.0808	1.0495	0.8637	2.600	53.40	1.21
74	0.8960	-0.1247	1.0486	0.8663	2.550	55.30	0.41

Table D-3: (Continued) Steady-State Operating Points

No	P(pu)	Q(pu)	V(pu)	I _a (pu)	I _F (A)	δ(deg)	I _{err} (%)
75	0.8960	-0.1663	1.0482	0.8739	2.500	56.75	0.51
76	0.8960	-0.2171	1.0486	0.8828	2.450	59.30	0.41
77	0.8947	-0.2748	1.0477	0.8942	2.400	62.15	0.10
78	0.8933	-0.3556	1.0473	0.9196	2.345	66.00	0.16
79	0.8960	-0.4573	1.0459	0.9552	2.300	71.80	-0.69
80	0.6640	0.5727	0.9500	0.9209	3.455	31.40	-0.23
81	0.6613	0.5543	0.9514	0.9120	3.405	31.75	0.55
82	0.6627	0.5381	0.9505	0.8967	3.350	32.25	-0.15
83	0.6627	0.5150	0.9514	0.8853	3.305	33.10	0.36
84	0.6613	0.4942	0.9545	0.8663	3.250	32.80	0.16
85	0.6613	0.4711	0.9545	0.8574	3.200	33.40	0.79
86	0.6613	0.4388	0.9505	0.8447	3.145	34.15	1.15
87	0.6600	0.4180	0.9505	0.8282	3.090	34.60	0.75
88	0.6627	0.4088	0.9509	0.8256	3.055	35.15	0.83
89	0.6613	0.3880	0.9514	0.8154	3.000	35.80	1.18
90	0.6627	0.3626	0.9500	0.8040	2.950	36.35	1.12
91	0.6627	0.3349	0.9514	0.7900	2.900	37.05	1.23
92	0.6667	0.3141	0.9523	0.7773	2.840	37.75	0.45
93	0.6640	0.3002	0.9505	0.7723	2.800	38.35	0.73
94	0.6653	0.2702	0.9505	0.7621	2.750	39.15	0.87
95	0.6667	0.2494	0.9505	0.7519	2.710	39.85	0.41
96	0.6680	0.2240	0.9505	0.7469	2.650	40.60	0.75
97	0.6667	0.1986	0.9495	0.7392	2.605	41.55	0.91
98	0.6680	0.1732	0.9509	0.7392	2.550	42.60	1.86
99	0.6667	0.1478	0.9514	0.7253	2.500	43.65	1.05
100	0.6667	0.1155	0.9505	0.7215	2.450	44.90	1.35
101	0.6667	0.0878	0.9514	0.7151	2.400	45.75	1.18
102	0.6680	0.0577	0.9518	0.7113	2.350	47.00	0.97
103	0.6693	0.0323	0.9514	0.7100	2.305	48.40	0.80
104	0.6707	-0.0023	0.9505	0.7088	2.255	49.80	0.44
105	0.6693	-0.0416	0.9495	0.7113	2.200	51.85	0.71
106	0.6693	-0.0785	0.9500	0.7176	2.150	53.55	1.16
107	0.6707	-0.1316	0.9482	0.7240	2.095	56.25	0.44
108	0.6693	-0.1709	0.9482	0.7342	2.045	58.65	0.77
109	0.6707	-0.2148	0.9491	0.7456	2.000	61.45	0.49
110	0.6680	-0.2841	0.9491	0.7685	1.940	66.30	0.47
111	0.6693	-0.3649	0.9491	0.8040	1.900	72.30	0.10
112	0.6547	0.6028	1.0027	0.8866	3.500	28.75	-0.10

Table D-3: (Continued) Steady-State Operating Points

No	P(pu)	Q(pu)	V(pu)	I _a (pu)	I _F (A)	δ(deg)	I _{err} (%)
113	0.6573	0.5843	1.0027	0.8701	3.440	29.30	-0.80
114	0.6573	0.5658	0.9991	0.8574	3.400	29.75	-1.24
115	0.6573	0.5381	1.0005	0.8485	3.340	30.25	-0.07
116	0.6560	0.5219	1.0018	0.8370	3.300	30.55	0.03
117	0.6573	0.5058	1.0023	0.8243	3.250	31.00	-0.38
118	0.6573	0.4873	1.0018	0.8154	3.200	31.40	-0.16
119	0.6587	0.4665	1.0018	0.8027	3.160	31.80	-0.36
120	0.6573	0.4457	1.0023	0.7900	3.100	32.45	-0.30
121	0.6600	0.4180	1.0014	0.7812	3.050	33.00	0.13
122	0.6600	0.3949	1.0014	0.7697	2.990	33.75	0.21
123	0.6600	0.3811	1.0018	0.7621	2.955	34.10	0.18
124	0.6627	0.3533	0.9986	0.7507	2.900	34.95	-0.18
125	0.6627	0.3302	0.9986	0.7405	2.850	35.65	-0.12
126	0.6627	0.3118	0.9973	0.7329	2.800	36.35	-0.20
127	0.6627	0.2841	0.9991	0.7227	2.750	36.95	0.15
128	0.6653	0.2610	1.0005	0.7138	2.700	37.55	-0.07
129	0.6667	0.2402	1.0000	0.6999	2.650	38.40	-1.23
130	0.6667	0.2171	1.0005	0.6961	2.600	39.10	-0.68
131	0.6667	0.1940	1.0009	0.6884	2.550	39.90	-0.76
132	0.6667	0.1663	1.0009	0.6846	2.500	40.55	-0.27
133	0.6653	0.1455	1.0000	0.6795	2.455	41.70	-0.22
134	0.6653	0.1039	1.0009	0.6745	2.400	42.90	0.25
135	0.6653	0.0808	1.0000	0.6707	2.355	43.95	0.06
136	0.6693	0.0416	1.0000	0.6694	2.300	45.15	-0.19
137	0.6693	0.0231	1.0000	0.6681	2.255	46.40	-0.24
138	0.6680	-0.0162	1.0014	0.6681	2.200	48.00	0.12
139	0.6707	-0.0439	1.0009	0.6694	2.150	49.40	-0.31
140	0.6680	-0.0808	1.0000	0.6732	2.095	51.40	0.05
141	0.6680	-0.1224	1.0000	0.6757	2.050	53.30	-0.50
142	0.6667	-0.1617	1.0000	0.6859	2.000	55.45	-0.01
143	0.6680	-0.2009	1.0009	0.6961	1.950	57.80	-0.13
144	0.6667	-0.2633	1.0009	0.7113	1.900	61.45	-0.67
145	0.6667	-0.3233	1.0000	0.7392	1.850	65.60	-0.23
146	0.6653	-0.4365	0.9982	0.7951	1.800	73.95	-0.26
147	0.6520	0.5889	1.0536	0.8358	3.505	26.95	0.23
148	0.6520	0.5658	1.0541	0.8193	3.440	27.30	0.04
149	0.6520	0.5519	1.0536	0.8129	3.400	27.70	0.26
150	0.6547	0.5335	1.0505	0.8027	3.345	28.25	-0.15

Table D-3: (Continued) Steady-State Operating Points

No	P(pu)	Q(pu)	V(pu)	I _a (pu)	I _F (A)	δ(deg)	I _{err} (%)
151	0.6547	0.5104	1.0495	0.7939	3.300	28.70	0.37
152	0.6573	0.4919	1.0514	0.7812	3.250	29.10	0.03
153	0.6547	0.4688	1.0532	0.7685	3.200	29.40	0.51
154	0.6560	0.4480	1.0532	0.7596	3.155	29.85	0.70
155	0.6560	0.4295	1.0527	0.7494	3.110	30.40	0.61
156	0.6573	0.4088	1.0532	0.7367	3.050	30.90	0.23
157	0.6560	0.3880	1.0541	0.7253	3.005	31.40	0.31
158	0.6573	0.3626	1.0536	0.7151	2.950	32.05	0.37
159	0.6573	0.3395	1.0536	0.7062	2.900	32.60	0.58
160	0.6573	0.3164	1.0527	0.6961	2.850	33.25	0.44
161	0.6587	0.3002	1.0541	0.6922	2.810	33.70	0.80
162	0.6600	0.2794	1.0532	0.6795	2.760	34.40	-0.14
163	0.6613	0.2494	1.0536	0.6719	2.700	35.20	0.16
164	0.6600	0.2194	1.0545	0.6630	2.645	36.05	0.53
165	0.6613	0.1986	1.0541	0.6579	2.600	36.60	0.44
166	0.6613	0.1755	1.0532	0.6503	2.550	37.50	0.10
167	0.6627	0.1547	1.0536	0.6465	2.505	38.15	0.10
168	0.6613	0.1201	1.0545	0.6389	2.445	39.25	0.24
169	0.6627	0.0947	1.0545	0.6364	2.400	40.15	0.25
170	0.6653	0.0716	1.0541	0.6351	2.350	41.10	0.04
171	0.6667	0.0370	1.0545	0.6338	2.300	42.45	0.10
172	0.6653	0.0115	1.0532	0.6325	2.250	43.60	0.11
173	0.6653	-0.0208	1.0523	0.6338	2.200	44.65	0.19
174	0.6653	-0.0577	1.0523	0.6351	2.145	46.20	0.07
175	0.6627	-0.0854	1.0514	0.6376	2.100	47.85	0.33
176	0.6653	-0.1178	1.0536	0.6414	2.050	49.10	0.02
177	0.6667	-0.1524	1.0532	0.6452	2.000	50.85	-0.63
178	0.6653	-0.1963	1.0545	0.6567	1.950	53.05	-0.17
179	0.6640	-0.2402	1.0541	0.6694	1.900	55.50	-0.07
180	0.6627	-0.2887	1.0541	0.6884	1.850	58.45	0.40
181	0.6640	-0.3326	1.0545	0.7049	1.800	61.35	0.10
182	0.6613	-0.4203	1.0545	0.7469	1.745	66.80	0.51
183	0.6587	-0.5543	1.0500	0.8193	1.700	76.90	-0.07

D.4 Open Circuit Characteristic

With the SM operating at rated speed and disconnected from the network, the following open circuit magnitudes for the field current and corresponding terminal voltage were obtained:

Table D-4: Open Circuit Measurements					
No	$I_F(A)$	$V_{ab}(V)$	No	$I_F(A)$	$V_{ab}(V)$
1	0.205	36	44	2.600	324
2	0.300	52	45	2.550	322
3	0.420	75	46	2.500	320
4	0.490	88	47	2.440	317
5	0.550	100	48	2.400	315
6	0.610	112	49	2.350	313
7	0.680	123	50	2.300	310
8	0.700	128	51	2.250	307
9	0.740	134	52	2.190	305
10	0.800	143	53	2.130	300
11	0.860	156	54	2.050	296
12	0.900	162	55	1.980	292
13	0.940	168	56	1.940	288
14	0.980	176	57	1.880	284
15	1.040	186	58	1.850	282
16	1.095	194	59	1.800	278
17	1.120	197	60	1.750	274
18	1.150	202	61	1.700	270
19	1.200	210	62	1.650	265
20	1.260	218	63	1.600	260
21	1.300	223	64	1.550	256
22	1.340	228	65	1.500	250
23	1.390	236	66	1.430	244
24	1.450	242	67	1.400	238
25	1.480	245	68	1.360	232
26	1.540	251	69	1.290	224
27	1.580	255	70	1.220	215
28	1.640	260	71	1.160	205

Table D-4: (Continued) Open Circuit Measurements					
No	$I_F(A)$	$V_{ab}(V)$	No	$I_F(A)$	$V_{ab}(V)$
29	1.690	266	72	1.100	196
30	1.740	270	73	1.040	188
31	1.820	279	74	1.000	181
32	1.900	283	75	0.930	169
33	2.000	290	76	0.870	160
34	2.100	298	77	0.800	149
35	2.150	300	78	0.750	138
36	2.210	304	79	0.700	130
37	2.250	305	80	0.630	118
38	2.310	309	81	0.570	107
39	2.400	315	82	0.500	94
40	2.500	319	83	0.440	81
41	2.550	322	84	0.350	65
42	2.600	324	85	0.300	56
43	2.650	326	86	0.230	43
			87	0.160	30

From the open circuit characteristic the field current that in absence of saturation would produce a rated open circuit terminal voltage I_{fnv} , can be extracted as being 1.2077 Amps.

D.5 Armature and Field Resistances

After being operated under rated load, the armature and field resistance were measured, obtaining the values shown in Table D-5.

Table D-5: Armature and Field Resistances	
r_a	0.2694 ohms
r_f	4.3000 ohms

APPENDIX E

TURBO-GENERATOR STEADY-STATE DATA

E.1 Introduction

This section has the experimental data obtained by Ontario Hydro for the Lambton generator [31] that has been used during the course of this work.

E.2 Turbo-Alternator Characteristics

The cylindrical rotor machine under consideration has the following rated characteristics:

Table E-1: Turbo-Alternator Ratings	
Characteristics	Values
Power:	555 MVA
Voltage:	24.0 KV
Power Factor:	0.9
Speed:	3600 rpm
No. of poles:	2

The parameters offered by the manufacturer are summarized in Table E-2.

Table E-2: Manufacturer's Data		
Parameter	d-axis ^a	q-axis
l_a	0.160	0.160
L_m	1.810	1.707
L'	0.270	0.473
L''	0.215	0.213
T_o'	0.430 secs	0.560 secs
T_o''	0.031 secs	0.061 secs

a. Parameter values in pu unless specified

E.3 Operating Points

Next table summarize the measurements taken for five values of active power "P" (~0.2,~0.38,~0.55,~0.72,~0.91). The readings reflect the active and reactive power, terminal voltage, armature current, field current, and load angle. Also, the last column presents the comparison between the measured armature current and the calculated value.

Table E-3: Steady-State Operating Points							
No	P(pu)	Q(pu)	V(pu)	I_a (pu)	I_F (A)	δ (deg)	Ierr(%)
28	0.2075	0.3686	1.0400	0.4130	2684	9.8	1.54
45	0.2072	0.2903	1.0417	0.3494	2452	10.6	2.05
53	0.2074	0.2329	1.0367	0.3068	2268	11.5	1.98
73	0.2090	0.1440	1.0221	0.2537	1978	13.3	2.15
87	0.2084	0.0589	1.0088	0.2192	1716	15.3	2.11

Table E-3: (Continued) Steady-State Operating Points

No	P(pu)	Q(pu)	V(pu)	I _a (pu)	I _F (A)	δ(deg)	I _{err} (%)
90	0.2092	0.0000	0.9992	0.2147	1551	17.2	2.59
104	0.2092	-0.0547	0.9908	0.2237	1381	19.2	2.53
118	0.2093	-0.1264	0.9792	0.2537	1204	22.6	1.57
125	0.2090	-0.1647	0.9721	0.2783	1096	24.9	1.69
140	0.2101	-0.2173	0.9725	0.3135	986	27.6	0.89
170	0.3740	0.3512	1.0354	0.5043	2758	17.9	1.78
177	0.3762	0.3199	1.0363	0.4856	2672	18.5	1.91
189	0.3787	0.2704	1.0367	0.4564	2536	19.5	1.69
191	0.3807	0.2192	1.0321	0.4332	2387	20.8	1.78
215	0.3798	0.1399	1.0196	0.4033	2140	23.3	1.60
225	0.3802	0.0536	1.0046	0.3898	1933	26.5	2.00
233	0.3798	-0.0434	0.9883	0.3936	1686	31.2	1.76
245	0.3805	-0.1246	0.9758	0.4168	1505	36.1	1.58
255	0.3791	-0.1661	0.9667	0.4347	1415	39.0	1.53
259	0.3791	-0.1964	0.9667	0.4482	1354	41.0	1.48
268	0.3803	-0.2203	0.9654	0.4617	1320	42.7	1.40
271	0.3800	-0.2414	0.9654	0.4729	1283	44.1	1.42
305	0.5481	0.4684	1.0413	0.7048	3332	22.4	1.80
309	0.5485	0.3991	1.0421	0.6600	3113	23.8	1.39
327	0.5508	0.2858	1.0400	0.6083	2821	26.4	1.95
344	0.5524	0.1832	1.0242	0.5769	2520	30.0	1.52
356	0.5517	0.0787	1.0075	0.5634	2282	34.3	1.86
370	0.5503	0.0052	0.9967	0.5627	2119	37.8	1.91
374	0.5526	-0.0452	0.9858	0.5709	2008	40.7	1.51
382	0.5526	-0.0914	0.9767	0.5821	1931	43.7	1.51
390	0.5521	-0.1487	0.9671	0.6008	1832	47.4	1.63
411	0.5526	-0.1987	0.9671	0.6166	1753	50.4	1.54
443	0.7214	0.4264	1.0421	0.8141	3458	29.3	1.23
451	0.7150	0.4000	1.0429	0.7946	3380	29.6	1.16
460	0.7324	0.3654	1.0363	0.7984	3297	31.3	1.08
468	0.7173	0.3182	1.0292	0.7722	3148	32.4	1.27
476	0.7317	0.2774	1.0233	0.7729	3065	34.3	1.08
479	0.7270	0.2356	1.0167	0.7610	2959	35.6	1.23
490	0.7209	0.1886	1.0108	0.7445	2836	37.3	0.99
495	0.7236	0.1564	1.0108	0.7415	2777	38.3	1.25
507	0.7175	0.0848	1.0117	0.7228	2617	40.6	1.21
515	0.7247	0.0344	1.0054	0.7303	2532	43.1	1.21
523	0.7186	0.0002	1.0008	0.7258	2459	44.5	1.09

Table E-3: (Continued) Steady-State Operating Points

No	P(pu)	Q(pu)	V(pu)	I _a (pu)	I _F (A)	δ(deg)	I _{err} (%)
525	0.7203	-0.0014	1.0000	0.7287	2460	44.8	1.17
532	0.7216	-0.0475	0.9921	0.7385	2356	47.4	1.31
538	0.7205	-0.0905	0.9875	0.7430	2312	49.5	1.03
543	0.7231	-0.1267	0.9808	0.7580	2265	51.9	1.28
545	0.7344	-0.1589	0.9738	0.7834	2231	54.5	1.52
548	0.7259	-0.1787	0.9721	0.7782	2199	55.4	1.18
555	0.7286	-0.2126	0.9650	0.7969	2172	57.9	1.31
562	0.7247	-0.2313	0.9654	0.7976	2131	58.8	1.23
566	0.7229	-0.2540	0.9658	0.8031	2109	60.0	1.23
568	0.7247	-0.2527	0.9658	0.8029	2118	59.9	1.04
599	0.9122	0.4624	1.0400	0.9937	3867	34.3	1.04
600	0.9101	0.4549	1.0400	0.9884	3847	34.4	1.04
609	0.9137	0.4396	1.0408	0.9839	3815	34.8	1.01
617	0.9137	0.4037	1.0413	0.9690	3735	35.7	1.01
623	0.9122	0.3607	1.0417	0.9510	3615	36.6	0.99
695	0.9166	0.3096	1.0350	0.9435	3497	38.4	0.94
700	0.9167	0.2651	1.0292	0.9368	3396	40.0	1.03
706	0.9155	0.2155	1.0229	0.9293	3286	41.7	1.08
714	0.9157	0.2059	1.0233	0.9263	3266	42.0	1.00
721	0.9193	0.1577	1.0217	0.9226	3183	43.7	1.06
731	0.9200	0.1089	1.0154	0.9211	3086	45.7	0.96
736	0.9175	0.0589	1.0125	0.9181	2994	47.6	1.11
744	0.9175	0.0211	1.0054	0.9211	2911	49.5	0.91
753	0.9175	-0.0662	0.9938	0.9361	2808	53.8	1.13
761	0.9169	-0.0661	0.9938	0.9361	2802	53.8	1.19
763	0.9166	-0.1078	0.9867	0.9465	2752	56.2	1.20
770	0.9135	-0.1602	0.9796	0.9578	2686	59.0	1.16
778	0.9185	-0.1516	0.9800	0.9607	2711	58.6	1.14
785	0.9184	-0.2245	0.9675	0.9877	2641	63.1	1.08
801	0.9175	-0.2648	0.9650	1.0004	2606	65.3	1.10
807	0.9229	-0.2646	0.9654	1.0064	2618	65.3	1.20

E.4 Open Circuit Characteristic

Data for the open circuit characteristics is not provided in the original reference [31]. What is available is the field current that in the absence of saturation would produce a rated open circuit terminal voltage I_{fnv} as being 1310 Amps.

APPENDIX F

TRANSIENT STATE MEASUREMENTS

F.1 Introduction

This section introduces the data acquisition system developed to be able to measure on-line instantaneous voltages, currents and rotor position of a SM. It also presents the general set up and experiments carried out to obtain the transient state measurements of a micro-alternator in the Power Lab of the Department of Electrical and Computer Engineering of the University of Calgary.

F.2 Data Acquisition System

A Data Acquisition System (DAS) has been developed in order to be able to measure on-line instantaneous voltages, currents and the rotor position of a SM. The author of this work has been responsible for all the software developments and Mr. Garwin Hancock has been in charge of the hardware implementation¹.

The DAS is based on a Digital Signal Processor (DSP) Board [80,81] that uses the TMS320C30 DSP [82]. The TMS320C30 processor is a very high speed floating-point device with an instruction set tailored to the real-time manipulation of sampled data.

1. Proper documentation of the hardware implementation is available in the Power Lab of the University of Calgary.

Figure F-1 shows the main components of the DAS. The general functional design can be better analysed in two steps.

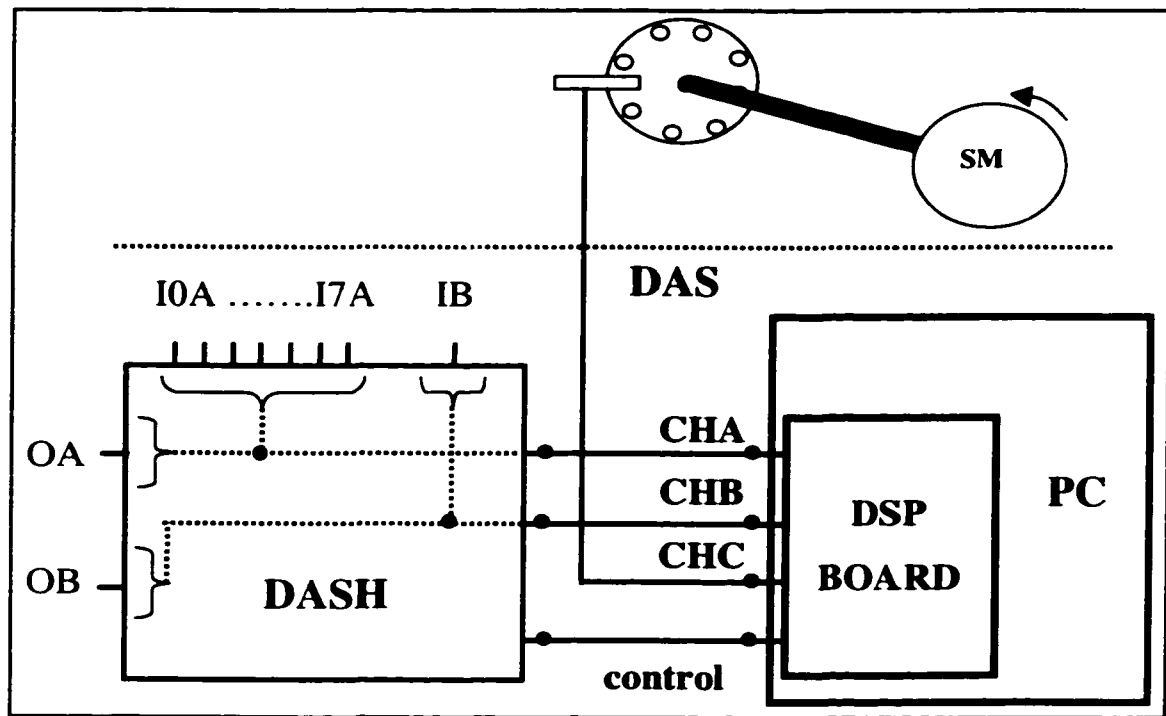


Figure F-1: DAS Schematic Diagram

F.2.1 General Inputs/Outputs: CHA & CHB

In its more generic form, the DAS is capable of handling nine analog inputs and two analog outputs. As it can be observed in the hardware component of the DAS (DASH), the actual inputs and outputs are transmitted through two channels: CHA and CHB.

The DSP Board controls when the signals are sampled with a sample and hold mechanism. This allows the DSP to sample all the inputs simultaneously, read them afterwards, and end the cycle with the transmission of the outputs to the DASH.

The internal software design, which is generally hidden from the user, has been optimized using both the *assembler* and *C* programming languages [83,84]. In any case, the DASH response is the limiting factor when considering speed. With all the inputs and outputs, the maximum sampling rate that the DAS is able to handle is 5000 Hz (a period of 200 μ secs). This limit can be further increased if only a few inputs are considered for CHA.

This general purpose portion of the DAS, with more details concerning its specific usage, has been summarized in a User's Guide (see Figure F-2) and several specific examples, which have been made available to other users [85-87].

F.2.2 External Interrupt Input Signal: CHC

The TMS320C3x DSPs support multiple internal and external interrupts that can be used for a variety of applications. For this specific application, internal interrupts have been used to control the periodic sampling rate and an external interrupt, activated by the input CHC in Figure F-1, to measure the rotor position of the SM.

As the schematic of Figure F-1 shows, a 30 hole disk attached to the rotor of the SM is the primary source of the signals. When the light spectrum of an infrared light emitting diode is detected by an infrared photo transistor on the other side of the disk, a signal is generated. These signals generate interrupts in the DSP board, which in software terms translates in a sudden execution of a predetermined software function. This function keeps track of the time when each specific hole is detected.

These interrupts are not in synchronism with the sampling frequency of the general inputs. In order to solve this and have a complete picture of the SM that includes the rotor position for each sample, the DSP Board buffers the samples and whenever the rotor information is obtained, it is distributed among the samples using an average displacement be-

```

/*****
/* DAS: USER'S GUIDE_DSP.C */
/*
/* MARIANO CALVO & GARWIN HANCOCK */
/* Department of Electrical & Comp. Engineering - The University of Calgary*/
/*
/* Last updated: */
/* 97/05/15 created */
/* 05/16 modified */
*****/

```

Technical DATA

Analog Inputs: 1-9

- DSP analog channel CHB (standard un-buffered)
- DSP analog channel CHA plus external hardware Channels 0 - 7

Outputs: 1-2

- DSP analog outputs CHA and CHB (standard un-buffered)

Gains:

channel	Gain Position	Gains	Max. Ext. Input(Volts)
CHB		(DSP standard) 1.00	+/- 3.00
CHA(0-8)	1	0.25	+/- 12.00
	2	0.50	+/- 6.00
	5	5.00	+/- 0.60
	10	10.00	+/- 0.30
	20	20.00	+/- 0.15

DAS Software related files

DAS.H

DAS.C (DAS.OBJ)

"DAS.H" has all the prototypes of the functions and global variables considered "a must" to run the DAS. "DAS.C" contains the actual "source code" of the DAS.

Current Directories

D:\USER\DA\VER_14

NOTE: Please, do not modify the original code of this directory (make a copy to your own directory...)

Running the DAS

Any project using the DSP Board has two software modules:

1. DSPMODULE

2. PCMODULE

that run in parallel. One primary function of the PCMODULE is to load the running code for the DSP into its RAM, since there is no ROM storage on the DSP Board. The other possible function is to provide a "man-machine" interface using the PC terminal and keyboard. Also data storage is facilitated using the Hard Drive.

In order to use the DAS, the DAS related files ("DAS.H" & "DAS.C") must be in the DSPMODULE. All the other software can be on the DSP side, PC side, or both sides according to the user's requirements.

The DSPMODULE for any generic application that used the DAS, should have the following files:

[make_dsp.bat]		[others "*.c"]
app_dsp.c	-> das.h	das.cmd
	[-> dsp_pc_comm.h]	lsiboot.obj
	[-> others "*.h"]	rts30.lib
das.c (or das.obj)		

and the files of the corresponding PCMODULE should be:

[make_pc.bat]	
app_pc.c	-> tms30.h
	[-> dsp_pc_comm.h]
	[-> others "*.h"]
[others "*.c"]	
30librar.obj	
load.obj	

Figure F-2: DAS User's Guide

where: CH2Read: amount of channels to read (1-9)

SampRateInMilisec: ex: .8, 1.0, 10

UdScaleFactors: pointer to a vector with the scale factors. NULL => use default ScaleFactors[27] vector (do nothing by default).

ud_SaveTo: pointer to a vector where all the unscaled inputs are saved NULL => use default SaveTo[9] vector

The user has access to the following global variables/vectors:

"intFlagDAS" FlagDAS=1 ==> data available & DAS disabled The Flag must be cleared (= 0) in order to proceed with the data aquisition.

"float SaveTo[9]" Default vector where the data from the DAS is stored as follows:

SaveTo[0] = data from CHB ;
SaveTo[1] = CH0 ;
SaveTo[2] = CH1 ;

.....
SaveTo[CH0_7] = CH0_7-1 ;
SaveTo[CH0_7+1] = CH0_7 ;

where CH0_7 (0<=CH0_7<=7) is the number of channels mapped from A

"float ScaleFactors[27]"

Default vector for the scale factors.

From the A/D converter a number "Num" is generated that is related to the actual input by:

MaxNum (32767) MaxVolt (ex: 2.5)

Num Volt

MinNum (-32768) MinVolt (ex: -2.5)

After manipulations we obtain:

$Volt = Fac2 + (Num - Fac0) * Fac1$

where Fac0 = MinNum

$Fac1 = (MaxVolt - MinVolt) / (MaxNum - MinNum)$

$Fac2 = MinVolt$

So, the vector with the scale factors is mounted as follows:

ScaleFactors[] = { Fac0, Fac1, Fac3, (factors from CHB)

Fac0, Fac1, Fac3, (CH0)

Fac0, Fac1, Fac3, (CH1)

....., (.....)

Fac0, Fac1, Fac3, (CH0_7 - 1)

Fac0, Fac1, Fac3, (CH0_7)

where CH0_7 (0<=CH0_7<=7) is the number of channels mapped from A

"OutA" & "OutB"

These variables are mapped to the output while the DAS is active.

This is a hardware related problem: the same register is used for inputs and outputs, so, any input is mapped to the respective output (CHA or CHB) unless something is written to that register before the next AC conversion. So, every time that something is read, OutA and OutB are mapped to the output. The data must be scaled and shifted (ex: OutA = mynum<<16)

Structure of an "app_dsp.c" that uses the DAS

```
#include das.h
main ()
{
    ...
    InitDAS( CH2Read, SampRate, myScale, mySaveTo );
    StartDAS();
    .....
    while(1)
    {
        .....
        if(FlagDAS==1)
        {
            .....
            read data from mySaveTo;
            FlagDAS=0; "clear the flag to enable DAS"
        }
    }
}
```

Figure F-2: (Continued) DAS User's Guide

tween holes. After this, the buffered samples with the rotor information are retrieved by the PC, where the data can be saved.

F.3 Transient Measurements

The DAS has been used to carry out measurements on a micro-alternator. The ratings and manufacturer's parameters of the generator under consideration have already been specified in Table D-1 and Table D-2 respectively.

F.3.1 General Setup

The general setup to carry out the measurements can be seen in Figure F-3. The SM is operated in steady state conditions when a local load is added to the system. During the disturbance, phase and field voltages and currents are measured as well as the rotor position.

Voltages and currents are available from the control panel of the SM and the rotor position is measured using the procedure described in the previous section. All the signals are raw inputs to the DAS, where some preprocessing takes place to account for scaling problems, before sending the data to the PC.

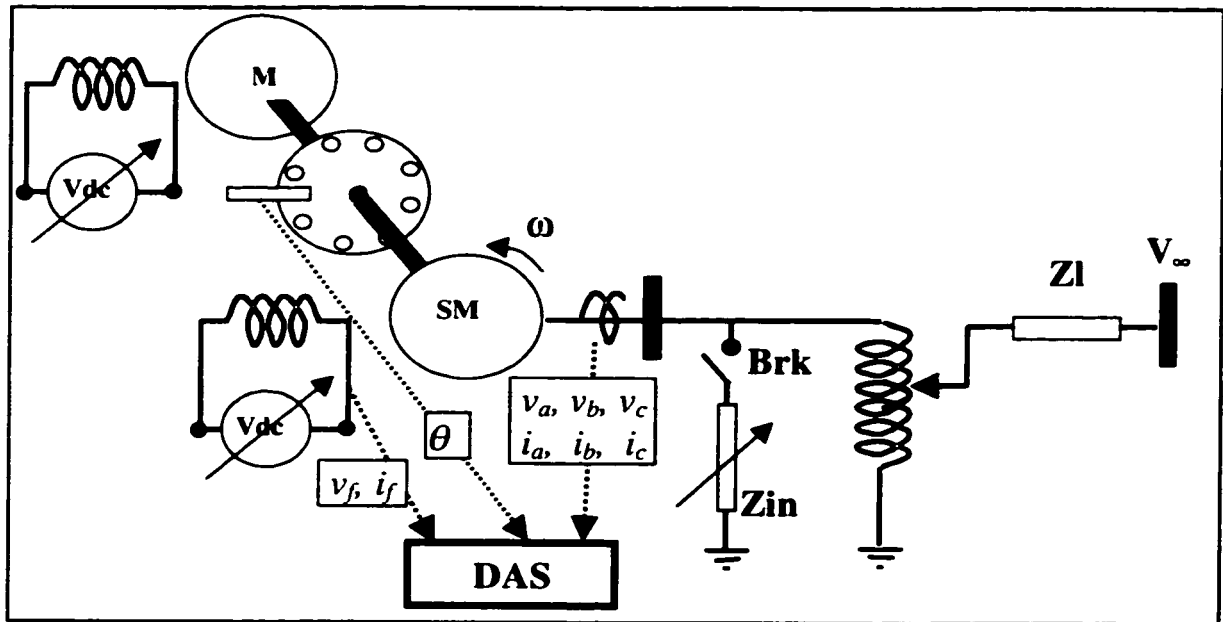


Figure F-3: Setup for the Transient State Measurements

F.3.2 Measurements

Two measurements have been done according to the amount of load that is inserted when the switch “Brk” is closed in Figure F-3. Table F-1 shows the initial conditions under which the experiments are carried out for both a load insertion equivalent to 10% and 67% of the machine ratings respectively.

When the load is inserted, armature and field voltages and currents as well as the rotor position are recorded at a frequency of 5000Hz. In order to be able to use the data, some preprocessing is required.

The instantaneous speed for each sample is derived from the rotor position. After filtering the speed with a low pass filter with a cut off frequency of 100Hz, the rotor position can be regenerated as follows. The initial rotor position (sample one) is obtained as the

average that the first 100 samples would have in sample one using the filtered speed. With the initial position and the filtered speed the different angles for all the samples are calculated.

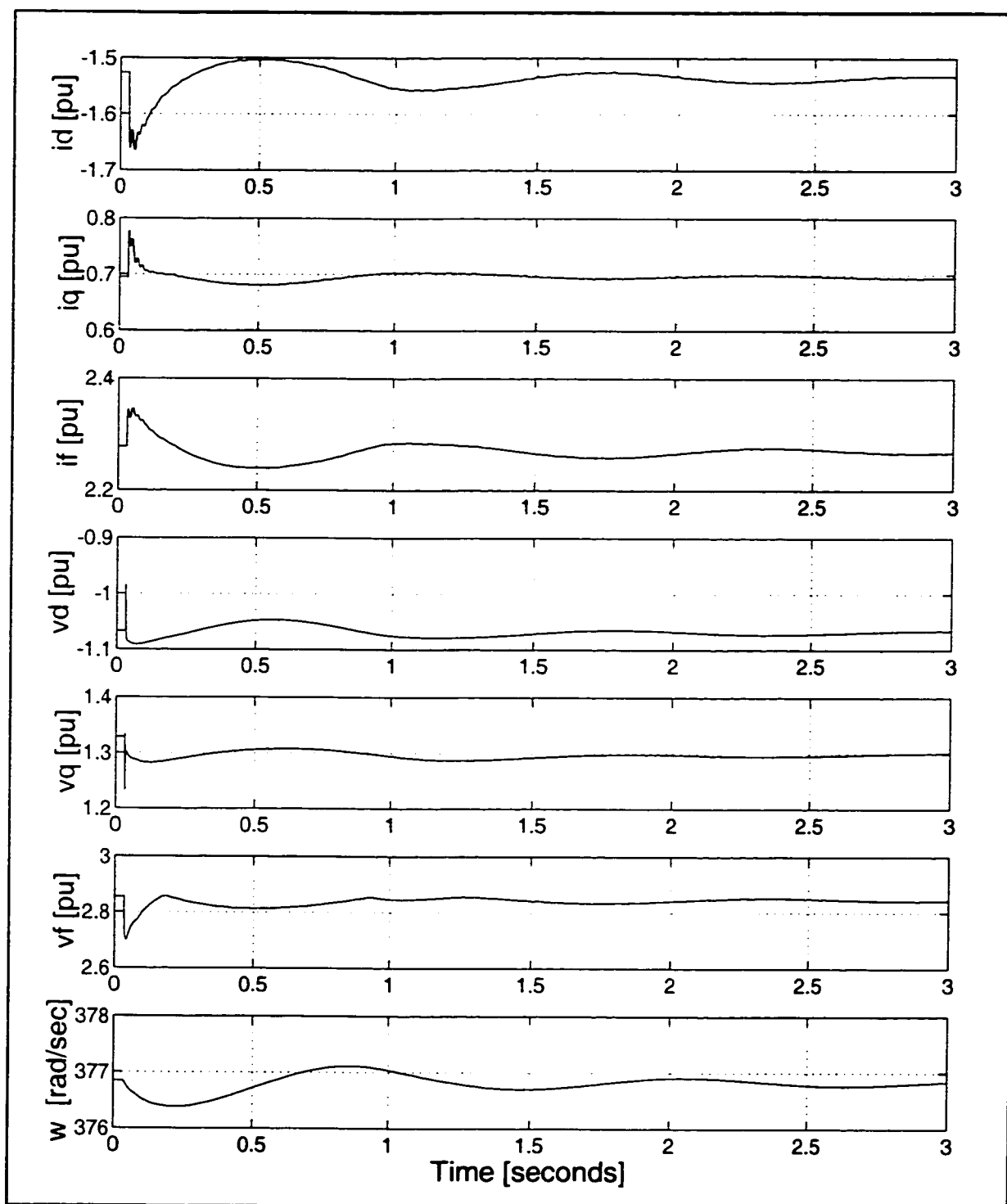
Table F-1: Transient Measurements					
Perturbation Name	Initial Steady State			Resistive Load Insertion	
	P [pu]	Q [pu]	V [pu]	Z_{in} [ohms]	p^a [pu]
LDIN10	0.862	0.427	1.001	168.1	0.096
LDIN67	0.661	0.001	0.999	24.2	0.667

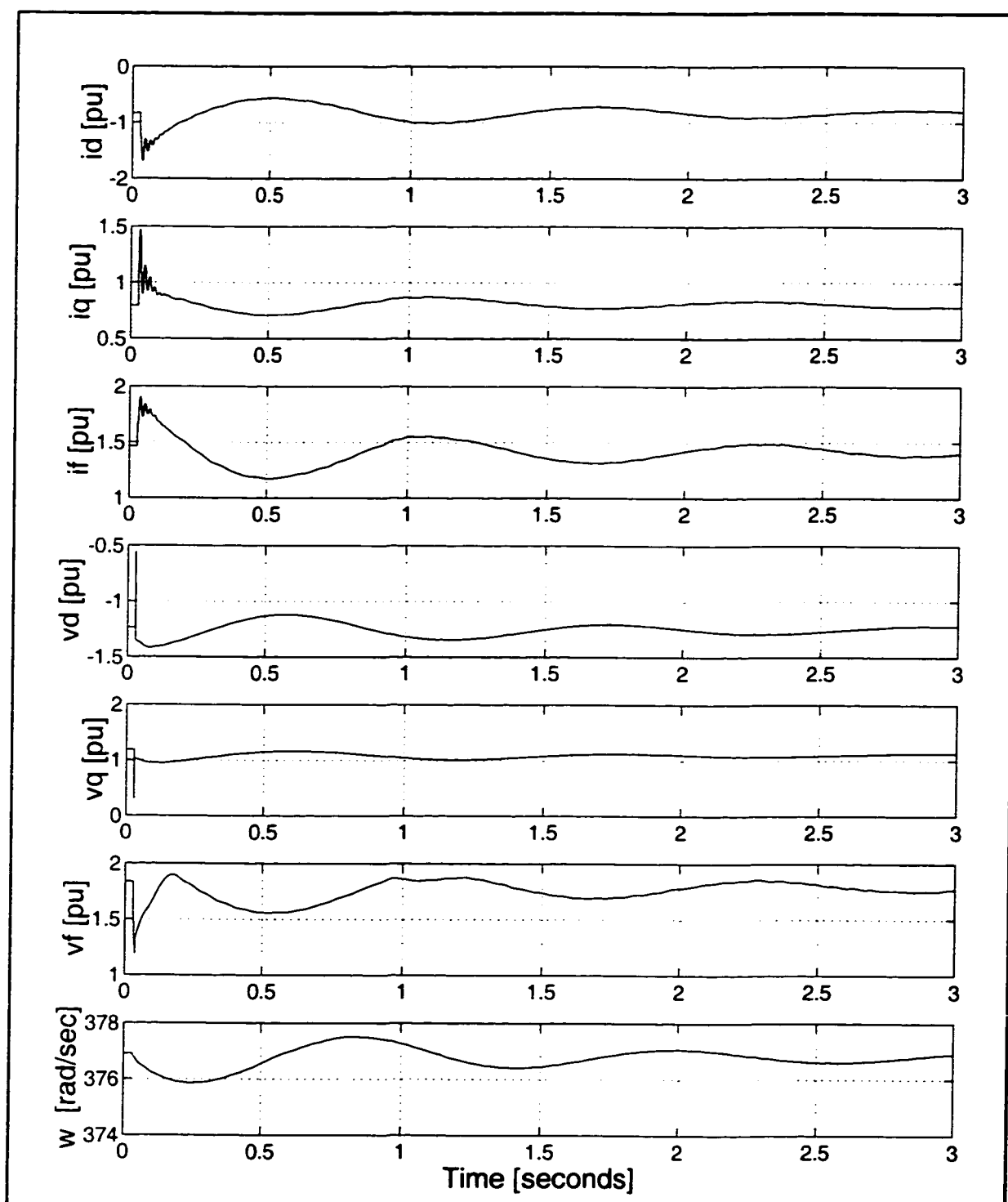
a. Based on machine ratings

Voltages and currents are normalized using the per unit system specified in Appendix C. Applying the Park transformation defined in equations (2-5) to the stator currents and voltages, it is possible to obtain the corresponding direct and quadrature axis components.

A sudden load insertion generates fast changes, specially in the voltages. Indeed, these changes exceed the sampling speed capacity of the DAS and are reflected as abrupt variations that occur in a few samples. Instead of having a wave form, these alterations are shown as a discontinuous signal. This presents a problem if the signal is to be filtered, because those peaks, far from being a noise component, will be eliminated during the filtering process. To avoid this problem, the very first 10 samples following the perturbation have not been filtered. The rest of the samples have been filtered using a low pass filter with a cut off frequency of 50 Hz.

The data, ready to be used in the estimation process, is plotted for each case in Figure F-4 and Figure F-5 where, for convenience, the speed is in radians per second.

**Figure F-4: LDIN10 Measurements**

**Figure F-5: LDIN67 Measurements**